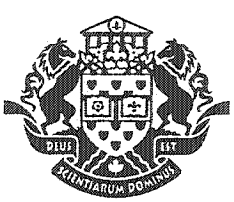

Université d'Ottawa · University of Ottawa

Université d'Ottawa · University of Ottawa

FACULTÉ DE ÉTUDES SUPÉRIEURES ET POSTDOCTORALES

FACULTY OF GRADUATE AND POSTDOCTORAL STUDIES

Rosa GUZZO

AUTEUR DE LA THÈSE - AUTHOR OF THESIS

Ph.D.(Pharmacology)

GRADE - DEGREE

Department of Cellular and Molecular Medicine

FACULTÉ, ÉCOLE, DÉPARTEMENT - FACULTY, SCHOOL, DEPARTMENT

TITRE DE LA THÈSE - TITLE OF THE THESIS

Sarcolemmal Membrane Associated Proteins:
Structure-function Analyses and Localization Studies

B. Tuana

DIRECTEUR DE LA THÈSE - THESIS SUPERVISOR

CO-DIRECTEUR DE LA THÈSE - THESIS CO-SUPERVISOR

EXAMINATEURS DE LA THÈSE - THESIS EXAMINERS

P. Albert

B. Allen

C. Kennedy

M. Sonnenfeld

J.-M. De Koninck, Ph.D.

LE DOYEN DE LA FACULTÉ DES ÉTUDES SUPÉRIEURES ET POSTDOCTORALES

SIGNATURE

DEAN OF THE FACULTY OF GRADUATE AND POSTDOCTORAL STUDIES

SARCOLEMMAL MEMBRANE ASSOCIATED PROTEINS:

STRUCTURE-FUNCTION ANALYSES AND LOCALIZATION STUDIES

Rosa M. Guzzo

Thesis submitted to the Faculty of Graduate and Postdoctoral Studies
In partial fulfillment of the requirements for the degree of
Doctor of Philosophy in Pharmacology

Department of Cellular & Molecular Medicine
Faculty of Medicine
University of Ottawa

Your file Votre référence
ISBN: 0-612-89995-0
Our file Notre référence
ISBN: 0-612-89995-0

Dedication

This thesis is dedicated to my family.

Acknowledgements

I am indebted to the many people who have influenced and inspired me both scientifically and personally. Foremost, I would like to thank Dr. Balwant Tuana for his guidance, encouragement and support during the course of my studies. I would also like to thank members of my advisory committee, Dr. Michael McBurney, Dr. Christine Pratt and Dr. William Staines, as well as other members of the department (Dr. Stephen Lee, Dr. David Park) for their advice, insightful discussions, time and effort. Maysoon Salih has been an excellent mentor in the lab as well as a wonderful friend, who always offered guidance, advice and assistance. Dr. Kevin Wong and Dr. John Leddy have somehow always managed to keep me relatively sane and were always available for great discussions (scientific and otherwise). There have been many people in the department, both past and present, who have helped to create a pleasant and fun working environment (George Chatzis, Dr. Serdal Sevinc, Paul Wielowieyski, Dr. Puneet Singh, Yalda Sedaghat, Vanessa Scanga, Swapna Doriswami, to name a few). Kim Wong and Rainy Tang have always been more than helpful by providing excellent technical assistance. Mary Anne Kent has been a great friend who on countless occasions has provided a shoulder to lean on. Stephen Crocker is a very important person in my life, and I am very fortunate for the strength, friendship and encouragement he continues to provide.

Abstract

Previous work from our lab identified a novel cDNA encoding a family of tail-anchored coiled-coil integral membrane proteins termed SLMAPs (sarcolemmal membrane associated proteins) (Wigle et al., 1997). Subsequent studies determined that SLMAPs are encoded by a single gene, and alternative splicing yields three SLMAP isoforms, including two muscle-specific variants (SLMAP1, SLMAP2) and a ubiquitously expressed isoform (SLMAP3). Here, I report a series of studies designed to examine putative novel and isoform specific functions of SLMAPs in striated muscle and fibroblast cells.

The tissue distribution and subcellular localizations of SLMAPs were examined in developing and adult mouse tissues in order to correlate SLMAP expression with specific physiological or developmental process(es). Immunohistochemical staining using polyclonal anti-SLMAP antibodies revealed that SLMAPs are highly expressed in developing somites and cardiac tissue. Confocal microscopy determined that SLMAPs localized within the discrete membrane structures (sarcoplasmic reticulum and T-tubules) of developing and mature skeletal and cardiac muscle, respectively. These localization studies suggest a correlative role for SLMAPs in excitation-contraction (EC) coupling mechanisms. In vivo expression of SLMAPs in pre-fusion myoblasts indicated a possible involvement in skeletal myogenesis. An additional SLMAP protein was expressed under conditions that promote differentiation in cultured myoblasts. Deregulation of SLMAPs by ectopic expression in myoblasts resulted in a potent inhibition of fusion without affecting the expression of muscle-specific genes.

Protein-protein interaction assays demonstrated that the leucine zipper motifs in SLMAPs mediate SLMAP homodimer formation. Proteomic analysis further revealed that a muscle-specific SLMAP variant binds a component of the contractile apparatus (cardiac myosin heavy chain). The expression of a cardiac-specific SLMAP isoform that resides in distinct membranes, self assembles and interacts with the contractile apparatus further suggest a unique role for this molecule in excitation-contraction coupling mechanisms.

Alternative splicing mechanisms generate SLMAP variants with divergent carboxyl-terminal hydrophobic segments, which target SLMAPs to different membrane compartments. Immunocytochemistry studies revealed that the expression of the first transmembrane domain directs a 6Myc-SLMAP fusion protein to the endoplasmic reticulum in COS7 cells. Alternatively, sequences encompassing the second transmembrane domain target 6Myc-SLMAP proteins to the mitochondria. These findings are consistent with the localizations of other tail-anchored membrane proteins that are inserted into the mitochondria or endoplasmic reticulum via post-translational mechanisms.

A novel SLMAP isoform with a previously uncharacterized N-terminal sequence is a core component of the centrosome. SLMAP sequences directed a green fluorescent protein to the microtubule organizing centre and deletions of the newly identified N-terminal sequence prevent targeting to centrosomes. Deletion-mutant analysis indicated that preservation of SLMAP secondary structure is required for centrosome targeting. Furthermore, elevated levels of SLMAPs inhibit cell growth suggestive of a role in cell cycle progression.

The molecular and cellular properties of SLMAPs indicate that these molecules provide diverse functions, including membrane assembly and function in striated muscle. The characterization of a novel SLMAP variant that localizes at the microtubule organizing center further suggests a role in cell proliferation.

Table of Contents

Chapter 2

Chapter 3

"SLMAPs Are Directed into Distinct Cellular Membranes by Alternative Splicing Mechanisms and May Serve Roles in Their Structural Arrangement in the Developing Cardiac Myocyte"

Chapter 4

Overview of the Structure, Composition and Function of the Microtubule Organizing Centre

Chapter 5

Chapter 6

Chapter 7

Chapter 8

List of Abbreviations

aa	Amino acid
AD	Activation domain
AKAP	A-kinase anchoring protein
AP	Action potential
ATPase	Adenosine triphosphatase
ATP	Adenosine triphosphate
BFA	Brefeldin A
β-gal	Beta-galactosidase
bHLH	Basic Helix-Loop Helix
BrdU	5-Bromo-2'-deoxyuridine
Ca^{2+}	Calcium ion
CAT	Chloramphenicol acetyl-CoA transferase
cDNA	Complementary DNA
DAP1	4'6'-Diamino-2-phenylindole
DHPR	Dihydropyridine receptor
DMEM	Dulbecco Minimal Essential Medium
DMSO	Dimethyl sulfoxide
DNA-BD	DNA binding domain
d.p.c.	days post coitum
E-C	Excitation-contraction
ECM	Extracellular matrix
E. coli	*Eschericia* coli

EDTA	Ethylenediaminetetracetic acid
EGTA	Ethyleneglycol-bis(B-aminoethyl ether)-N.N'-tetracetic acid
ER	Endoplasmic reticulum
ERGIC	Endoplasmic reticulum Golgi intermediate compartment
FBS	Fetal bovine serum
FHA	Forkhead associated
FITC	Fluorescein isothiocyanate
GAPDH	Glyceraldehyde-3-phosphate dehydrogenase
GFP	Green fluorescent protein
GST	Glutathione sepharose transferase
IgG	Immunoglobulin
IPTG	beta-D-Isopropyl-thiogalactopyranosine
JP	Junctophilin
JSR	Junctional sarcoplasmic reticulum
kb	Kilobase
kDa	Kilodalton
LB	Luria broth
LSR	Longitudinal sarcoplasmic reticulum
LZ	Leucine zipper
mRNA	Messenger RNA
MTOC	Microtubule organizing centre
MW	Molecular weight
NOC	Nocodazole

NP-40	Nonyl phenoxy polyethoxy ethanol
nt	Nucleotide
PAGE	Polyacrylamide gel electrophoresis
PBS	Phosphate-buffered saline
PCM	Pericentriolar matrix
PCR	Polymerase chain reaction
PFA	Paraformaldehyde
PKA	Protein kinase A
PKC	Protein kinase C
PM	Plasma membrane
PMSF	Phenylmethanesulfonyl fluoride
RIPA	Radioimmunoprecipitation assay
rpm	revolutions per minute
RT-PCR	Reverse transcriptase-PCR
RyR	Ryanodine receptor
SDS	Sodium dodecyl sulfate
SERCA	Sarco-endoplasmic reticulum Ca^{+2}-ATPase
SL	Sarcolemmae
SLMAP	Sarcolemmal-membrane associated protein
SNARE	Soluble N-ethylmaleimide-sensitive factor attachment protein receptor
SR	Sarcoplasmic reticulum
TBS	TRIS-buffered saline

TMD	Transmembrane domain
TRIS	Tris(hydroxymethyl)aminomethane
T-tubules	Transverse tubules
µL	microliter
µm	micrometer
VSV-G	Vesicular stomatitis virus glycoprotein

List of Figures

Chapter One

Chapter Two

Chapter Three

Chapter Four

Chapter Five

Chapter Six

List of Tables

Preface

The experimental results are presented in manuscript format, in accordance with the guidelines set forth by the University of Ottawa School of Graduate Studies and Research. Experimental findings are preceeded by an overview of cardiac and skeletal muscle development, the membrane organization of striated muscle and the role of membrane components in excitation-contraction coupling mechanism (Chapter one). The molecular and biochemical properties of the family of alpha-helical coiled-coil sarcolemmal membrane associated proteins are introduced in Chapter one. Subsequent Chapters demonstrate that: (i) regulated expression of SLMAPs are involved in myogenesis and are critical for myoblast fusion (Chapter two) and; (ii) that SLMAPs are directed to distinct cellular membranes by alternative splicing mechanisms and may serve roles in the structural arrangement of the cardiomyocyte (Chapter three). In Chapter five, a novel SLMAP isoform is described as a core component of the centrosome. This study is preceeded by an overview of the structure, composition and function of centrosomes. (Chapter four).

Chapter One.

General Introduction.

General Introduction

A. Cardiac and Skeletal Muscle.

In the developing embryo the two forms of striated muscle - cardiac and skeletal muscle - are derived from a common myogenic lineage. Cardiac and skeletal muscle systems arise from populations of mesodermal precursor cells within distinct regions of the embryo and are induced to become cardiac or skeletal muscle by local embryonic signaling molecules (Zaffran and Frasch, 2000; Kablar and Rudnicki, 2000; Brent and Tabin, 2002). Distinct networks of transcription factors further regulate cardiac and skeletal muscle specific gene expression. Despite such differences, there exist fundamental similarities related to the structural components of cardiac and skeletal muscle cells as well as the molecular mechanism underlying muscle contraction. In the proceeding sections, the commonalities and distinctions between these two muscle systems are reviewed and key concepts in muscle biology are introduced.

A.1. The Heart.

The mature four-chambered heart is a highly regulated, complex organ whose continuous cycles of contraction-relaxation drive blood through the circulatory system, deliver oxygen, nutrients and hormones to organs and remove carbon dioxide and wastes from organ systems (Katz and Katz, 1989). Normal development and performance of the heart depends upon the proper expression, assembly and regulation of the molecular components that make up cardiac cells. A vast amount of information about cardiac function has been acquired through the characterization of cardiac genes, including those

encoding contractile elements, ion channels and integral membrane proteins. Functional characterizations of the cardiac proteins that serve a key role in the molecular mechanisms of contraction, for instance, have greatly contributed to the understanding of cardiac function in normal and diseased states (Kamp and Hell, 2000; Scoote and Williams, 2002).

A.1.i. Cardiac Morphogenesis.

Initiated early in gestation, the heart is the first functional organ to develop in vertebrates and arises from bilaterally symmetric populations of cells within the anterior lateral plate mesoderm that are committed to a cardiogenic fate (Schultheiss et al., 1995; Olson and Srivastava, 1996). Paired populations of cardiogenic precursor cells migrate medially and coalesce along the ventral midline of the embryo to form a linear heart tube (Rosenquist and Dehaan, 1966; Rugh, 1968; Kaufman and Navaratnam, 1981; Lawson and Pederson, 1992). This simple contractile tubular structure then undergoes rightward looping, a morphogenetic process critical for the proper alignment of inflow and outflow tracts as well as the left-right positioning of the presumptive ventricles. Only after cardiac looping is complete do the individual heart chambers (atria and ventricles) become morphologically distinct. Progression from a looped heart to a four-chambered heart with separate pulmonary and systemic circuits entails an impressive transformation including chamber morphogenesis, septation, valvogenesis and specialization of the conduction tissue (Olson and Srivastava, 1996; Srivastava and Olson, 2000).

A.1.ii. Transcriptional Regulation of Cardiac Development.

Diverse families of spatially and temporally restricted cardiac enriched transcription factors regulate cardiac morphogenesis (Lyons, 1996; Srivastava and Olson, 2000; Bruneau, 2002). GATA4 zinc finger transcription factors and Nkx2.5 homeodomain transcription factors, two of the earliest known markers of precardiac cells, regulate various aspects of cardiac morphogenesis including heart tube formation, cardiac looping, chamber differentiation, and septation (Lyons et al., 1995; Tanaka et al., 1999; Heikinheimo et al., 1994; Lints et al., 1993; Crispino et al., 2001; Biben et al., 2000; Kuo et al., 1999; Molkentin et al., 1997). The molecular mechanisms underlying chamber morphogenesis, chamber maturation, septation and conduction system formation are regulated by several families of cardiac-enriched factors, including basic helix loop helix factors (dHAND, eHAND), MADS-box factors (MEF2c), homeodomain-containing factors (Irx4) and T-box factors (Srivastava and Olson, 2000). Many of these factors converge along common pathways in cardiac development to co-regulate cardiac-specific gene expression. Combinatorial interactions among cardiac-enriched transcription factors have thus emerged as a central mechanism for controlling cardiac-specific gene expression (Lee et al., 1998; Nemer and Nemer, 2001; Bruneau, 2002).

A.1.iii. Structural Organization of Cardiac Muscle Cells.

There are three functional classes of cardiac cells; the conducting cells, the pacemaker cells and the myocardial or contractile cells. Collectively, these cells are responsible for the circulatory and endocrine functions of the four-chambered mammalian heart (Opie, 1991). The myocardial cells, which comprise the majority of the heart mass, are responsible for filling the ventricles with blood and generating the

contractions necessary to constantly pump blood through the vascular system. A highly ordered assembly of cytoskeletal elements defines the contractile unit of the myocyte, referred to as the 'sarcomere'. Each sarcomere is composed of overlapping thin actin filaments, thick myosin filaments as well as several associated proteins (Katz, 2001). It is this assembly of contractile myofilaments, shown schematically in Figure 1, which confers the cross-striated appearance to cardiac and skeletal muscle cells. The entire region of the sarcomere that is filled by thick myosin filaments defines the 'A' (anisotropic) band; whereas the 'I' (isotropic) band represents the region in adjacent sarcomeres composed only of thin actin filaments. The 'Z' line marks the boundary between adjacent sarcomeres where actin and titin filaments are attached. Regulatory proteins, including tropomyosin and the calcium-binding protein troponin, mediate the interactions between actin and myosin cross-bridges during muscle contraction (Katz, 2001).

Situated adjacent to the contractile elements are three distinct forms of intracellular membrane structures. Localized between the myofibrils, the mitochondria fulfill the high metabolic demands of the heart by generating energy in the form of adenosine triphosphate (ATP). The cardiac mitochondria provide an additional role in the modulation of cytosolic calcium ion levels, which facilitate muscle contraction (Bers, 2002). A highly convoluted system of internal tubular membranes, the sarcoplasmic reticulum, forms a mesh-like lattice that surrounds the myofibrils and controls the availability of intracellular calcium to the contractile machinery for activation of contraction-relaxation cycles (Opie, 1991). Invaginations of the external membrane system, the sarcolemmal (SL) give rise to tubular structures known as transverse (T)-

Figure 1. Organization of the Muscle Sarcomere

Overlapping thin actin filaments and thick myosin filaments define the sarcomere of striated muscle. The 'A' band represents the entire region of the sarcomere that is filled by thick myosin filaments. Situated in the center of the 'A' band, the 'M' band consists of myosin filaments that are not overlapped by actin filaments. The region in adjacent sarcomeres composed only of thin actin filaments represents the 'I', whereas the 'Z' line marks the boundary between adjacent sarcomeres where actin and titin filaments are attached. Modified from Flucher (1992).

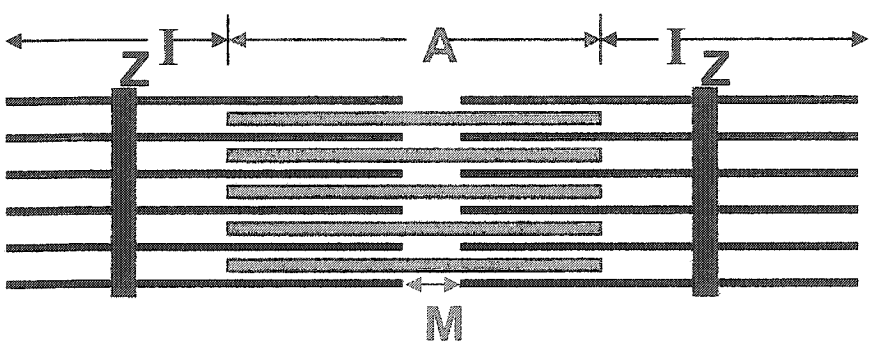
I
A
I
Z
Z
M

tubules. Localized at the T-tubule membrane system, ion channels regulate the influx of calcium that is necessary to induce muscle contraction. A more detailed overview of the structure and functions of the SR and T-tubules related to the regulation of muscle contraction-relaxation are provided in section A.4 of this Chapter.

A characteristic feature of the heart is that a wave of electrical activation is converted to an orderly spread of contraction (Bers, 2002). To achieve the synchronous, rapid contractile properties of the heart, the myocytes are adjoined to neighbouring cells through specialized regions of the plasma membrane known as intercalated discs. Cardiac gap junction channels, a component of intercalated discs are comprised of a complex organization of transmembrane connexin proteins. These proteins form channels at the SL of adjoining cells to allow the passage of ions and second messengers between cells, which are necessary for rapid propagation of action potentials from myocyte to myocyte (Van Veen et al., 2001).

The results of various studies using genetically modified mice have demonstrated that cardiac performance is greatly affected by the profile of expression, distribution and activity of the components present in cardiac membrane systems (as reviewed by Dulhunty et al., 2002). Further identification and characterization of the membrane components of cardiac muscle may thus advance our current level of understanding of cardiac function in the normal and diseased state.

A.2. Skeletal Muscle.

Skeletal muscle represents approximately forty percent of the six hundred and thirty muscles of the human body. This form of striated muscle is responsible for all

voluntary movement and respiration. Outlined in the following section are the morphogenetic and differentiation processes that are unique to skeletal muscle as well as the organization of skeletal muscle fibers.

A.2.i. Skeletal Muscle Morphogenesis and Differentiation.

Skeletal myogenesis is a highly regulated developmental process, whose hallmark features include the permanent withdrawal of determined muscle precursor cells from the cell cycle, the fusion of myoblasts to form elongated multinucleated myotubes and the synthesis of muscle specific proteins (Wakelam, 1985; Andres and Walsh, 1996; Walsh and Perlman, 1997). In vertebrates, skeletal body muscle is primarily derived from paraxial mesodermal tissue on either side of the notochord and neural tube, which condenses to form segmentally arranged somites (Buckingham, 2001). In response to local embryonic signals, muscle progenitor cells in somites undergo differentiation and mature to form the axial musculature and the muscles of the body wall and limbs (Blagden and Hughes, 1999; Buscher and Izpisua Belmonte, 1999).

In somites, the decision to proliferate or differentiate is coordinated by the balance of positive and negative cell cycle regulators (Walsh and Perlman, 1997). A complex network of muscle determination factors controls the differentiation of myogenic precursor cells to committed myoblasts. The MyoD family of basic helix loop helix (bHLH) transcription factors; whose members include MyoD, Myf5, myogenin and MRF4/Myf6/herculin is regarded as the master regulatory family coordinating the determination and differentiation of skeletal muscle precursor cells (Lassar et al., 1989 and 1994; Sabourin and Rudnicki, 2000). Functional inactivation of the MyoD family in

animal and cell culture models provided valuable insights regarding the regulatory role(s) of each family member in myogenesis; and have contributed to the understanding that the coordinate activation of MyoD and Myf5 is necessary for the commitment of proliferating somatic cells to the myogenic lineage (Davis et al., 1987; Rudnicki et al., 1993; Braun and Arnold, 1996). Furthermore, myogenin expression is essential for the fusion of myoblasts into mature myotubes (Edmondson and Olson, 1989; Wright et al., 1989; Hasty et al., 1993; Nebeshima et al., 1993; Rawls et al., 1998; Valdez et al., 2000); whereas MRF4/Myf6/herculin is a critical factor for the maintenance of the terminally differentiated state in fetal and adult skeletal muscles (Rhodes and Konieczny, 1989; Braun et al., 1990; Miner and Wold, 1990). The transcriptional activation of muscle-specific genes is mediated by the binding of myogenic bHLH proteins complexed with E-proteins (another class of the bHLH family) to consensus nucleotide sites referred to as E-boxes present in promoter regions (Lassar et al., 1994). The identification of the downstream target genes that are regulated by skeletal muscle-specific transcription factors is an active field of investigation; as such knowledge further contributes to our framework of understanding of skeletal muscle development and physiology.

A.2.ii. Organization of skeletal muscle.

a. Myoblast fusion.

An important process in skeletal muscle development, that does not occur during cardiac development, is the fusion of differentiating myoblasts to form multinucleated, elongated myotubes. Myoblasts have a well-organized cytoskeletal and membrane framework, whereby associations among cytoskeletal proteins and membrane

Figure 2. Myoblast fusion.

The schematic depicts the process of myoblast fusion, as previously described in *Drosophila* melangaster embryos. Precursor and myoblast cells must first recognize and adhere to fusion competent cells. Vesicles align at the apposed surface membranes to generate 'prefusion complexes'. A short-lived electron dense material that forms membrane 'plaques' then replaces these transient vesicles. Fusion competent cells align and plasma membrane breakdown is initiated in regions where the membranes of adjacent cells are tightly apposed, thus establishing cytoplasmic continuity and ultimately generating multinucleated myotubes. Modified from Doberstein et al. (1997).

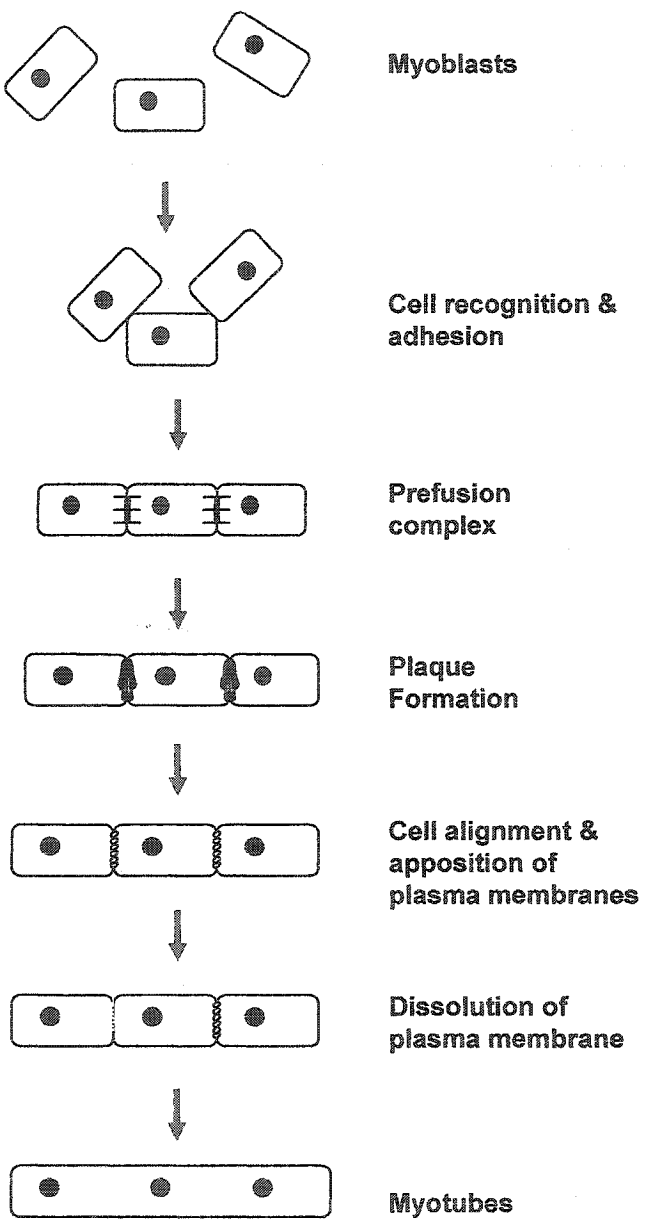
Myoblasts
Cell recognition & adhesion
Prefusion complex
Plaque Formation
Cell alignment & apposition of plasma membranes
Dissolution of plasma membrane
Myotubes

components regulate cell shape, interactions with neighbouring cells as well as interactions with components of the extracellular matrix (ECM) (Luna and Hitt, 1992). During the fusion process, these interactions are subjected to massive re-organization (Lassar et al., 1994; Buckingham et al., 1994; Barnoy et al., 1998). Morphologically, the fusion process is initiated at 13 days post coitum (d.p.c) in mouse embryos (Furst et al, 1989) and may be defined by a series of events including; (i) cell-cell alignment of fusion-competent cells; (ii) the generation of tightly apposed plasma membranes between neighbouring cells; (iii) the breakdown of apposed membranes; and (iv) the establishment of cytoplasmic continuity between aligned cells (Abmayr et al., 2003; Taylor, 2000 and 2002). Recent studies using *Drosophila* embryo models have provided a more comprehensive overview of key intermediate events leading to the generation of multinucleated myotubes and are depicted schematically in Figure 2 (Doberstein et al, 1997; Paululat et al., 1999; Dworak and Fink, 2002). At the level of the electron microscope, membrane vesicles have been seen to align along apposed membranes to generate prefusion complexes resembling electron-dense zipper-like plaque structures (Doberstein et al., 1997; Paululat et al., 1999). These vesicles are thought to form gap junction-like structures that precede the breakdown of the plasma membrane. While cytoplasmic vesicles resembling the prefusion complexes in flies have been identified in vertebrates, the molecular composition of these vesicles is not well understood (Engel et al., 1986; Robertson et al., 1990).

Several classes of molecules have been described to play essential roles in this morphological process. Galliano et al. (2000) have corroborated the significance of plasma membrane-cytoskeletal interactions in the fusion process by examining those

protein associations mediated by transmembrane metalloproteases. During myogenic differentiation in cultured cells, the cytoplasmic tail of ADAM12 ("a disintegrin and metalloprotease") specifically binds to muscle-specific α-actinin-2, an actin-binding and actin–crosslinking protein. This interaction is thought to be essential for myoblast fusion, as overexpression of the entire cytosolic ADAM12 tail containing the major α-actinin-2 binding site severely inhibited fusion in an *in vitro* model. The observed fusion defect was attributed to the physical disruption of the ADAM12-α-actinin interaction (Galliano et al., 2000). Other studies have shown that membrane associations with the microtubule network are critical for the alignment of pre-fusion myoblasts (Holtzer et al., 1985; Gunderson et al., 1989). Surface molecules belonging to a family of transmembrane calcium-dependent intercellular adhesion proteins have been implicated in formation of fusion-competent myoblasts, due in part to their associations with microtubules and cytoplasmic catenin proteins (Zeschnigk et al., 1995; Kaufmann et al., 1999; Kuch et al., 1997). Functional inhibition of the M-cadherin in myogenic cells by antagonistic peptides and antisense RNA inhibited the fusion process in cultured myoblasts (Zeschnigk et al., 1995) and it was postulated that cytoplasmic M-cadherin-catenin complexes linked to the microtubules are critical for the alignment of myoblasts during fusion. It remains unclear, however whether cadherin-dependent microtubule-associated factors (cdMAF) mediate the M-cadherin-catenin complex interaction with microtubules (Kaufmann et al., 1999). Continued research in the field of myoblast fusion may provide significant contributions to the understanding of muscle development and regeneration (Horsley et al. 2003; Charge and Rudnicki, 2003).

b. Myofibril development.

The sarcomeric assembly of contractile myofilaments in skeletal muscle cells is not unlike that of cardiac cells (Figure 1). Sarcomeric development requires the proper formation and assembly of the contractile myofilaments, the transformation of the vesicular SR into a tubular SR and the docking of T-tubule components at the sarcomeric Z-lines or the A-I junction (Fischman, 1970; Flucher, 1992; Crowe and Baskin, 1977; Peachey and Franzini-Armstrong, 1983). A morphological feature of mature striated muscle that is critical for mediating cycles of muscle contraction-relaxation is that a lattice-like distribution of specialized membrane systems (SR, T-tubules) surrounds the myofibrils (Porter and Palade, 1957; Peachey and Franzini-Armstrong, 1983; Franzini-Armstrong, 1994; Franzini-Armstrong and Jorgensen, 1994). In developing skeletal muscle, the faithful assembly of the contractile components relative to membrane structures is co-incident with the myotube to myofiber transition (16-17 d.p.c. in mouse) (Takekura et al., 2001). A key aspect of muscle physiology is the regulated assembly of protein complexes that link the myofibrils, cytoskeleton, membrane systems and the extracellular matrix (Franzini-Armstrong, 1994; Bagnato et al., 2003). For instance, the dystrophin complex and associated molecules constitute a structural scaffold that permits interactions among the myofibrils, the cytoskeleton, the plasma membrane and the extracellular matrix (Blake et al., 2002). The identity of the molecular components responsible for maintaining stable associations between membrane systems (SR, T-tubules) and the myofibrils are not well characterized.

A.3. Specialized Membranes Systems in Muscle.

Cardiac and skeletal muscles contain specialized membrane systems that play a central role in the contraction-relaxation process. These membrane systems consist of the SR and T-tubules, which are distributed as a convoluted network around and between the myofibrils (Opie, 1991; Flucher, 1992 and Flucher et al., 1993). An overview of their organization, function as well as the profile of proteins residing at these membranes systems is described.

A.3.i. The Sarcoplasmic Reticulum.

The sarcoplasmic reticulum (SR), a specialization of the endoplasmic reticulum, comprises an internal network of smooth surfaced endomembranes controlling the storage of calcium, the release of calcium to the cytoplasm and the re-uptake of calcium from the cytoplasm (Martonosi, 2000). To achieve these distinct roles, the SR is subdivided into two continuous membrane compartments: the 'longitudinal' SR and the 'terminal cisternae' (junctional) SR (Lompre et al., 1994). A primary function of the 'longitudinal' SR that surrounds the myofibrils involves the re-uptake of cytosolic calcium ions. This role is reflected by an enrichment of ATP-dependent Ca^{2+} pumps in the longitudinal SR membranes (Brandl et al., 1986; Zarain-Herzberg et al., 1990; Lytton et al., 1989 and 1992). SERCA (sarco-endoplasmic reticulum Ca^{+2}ATPases) genes encode a family of highly homologous ATP-dependent calcium pumps expressed in fast twitch skeletal muscle (SERCA1a, 1b; Brandl et al., 1986), cardiac and slow twitch skeletal muscle (SERCA2a; Zarain-Herzberg et al., 1990), smooth muscle (SERCA2b; Lytton et al., 1989) as well as in nonmuscle tissue (SERCA3; Lytton et al., 1992). The

activity of this family of Ca^{+2}ATPases is essential for the rapid removal of cytosolic calcium necessary for muscle relaxation (Tada et al, 1978; Lytton et al., 1992).

The main functions of the 'terminal cisternae' or 'junctional' SR involve the release and storage of calcium ions. Encoded by three distinct genes, tissue-specific ryanodine receptors constitute the primary ligand-gated calcium release channels residing in the terminal cisternae of cardiac (RyR2) and skeletal (RyR1, RyR3) muscle (Takeshima et al., 1989; Marks et al., 1989; Zorzato et al., 1990; Otsu et al., 1990; Hakamata et al., 1992; Giannini et al., 1992; Marziali et al., 1996; Tarroni et al., 1997). A homotetrameric assembly of RyR molecules creates a channel spanning the junction between the SR and the proximal T-tubules (Fleisher and Inui, 1989; Franzini-Armstrong and Jorgensen, 1994). Carboxyl-terminal transmembrane segments anchor the RyR molecules at the SR membrane, whereas the remaining cytoplasmic portion of the homotetramer creates a characteristic 'foot' structure (Takeshima et al., 1989). A pivotal step in the molecular mechanism of muscle contraction is the activation of the RyR, which subsequently triggers the release of calcium from the SR in skeletal and cardiac muscle. The RyR also serves as a scaffold for the assembly of regulatory proteins and other components participating in the modulation of calcium buffering and calcium release at the junctional SR in striated muscle (Zhang et al., 1997; Guo and Campbell, 1995; Guo et al., 1996; Marx et al., 2000 and 2001; Fruen et al., 2000; Bers, 2002). Calsequestrin, a moderate affinity, high capacity calcium binding protein residing in the lumen of the junctional SR is functionally linked to RyR (Ikemoto et al., 1991; Zhang et al, 1997). Dissociation of calcium ions from calsequestrin is induced upon activation of RyR, thus increasing the levels of free calcium ions for release from the SR (Ikemoto et

al., 1991). Integral membrane proteins, triadin and junctin provide the necessary stabilization of the RyR-calsequestrin complex (Guo and Campbell, 1995; Zhang et al., 1997). The terminal cisternae SR is further subdivided into the 'corbular' SR, which is also enriched in RyR and calsequestrin; however unlike the junctional SR this subcompartment of the SR does not reside in juxtaposition with the surface membranes (PM or T-tubules) (Jorgensen et al., 1988).

The appearance and distribution of the SR and myofibril components in mouse embryogenesis have been reported by several studies and described in the development of skeletal (ie. diaphragm) muscle (Takekura et al., 2001; Flucher, 1992 and Flucher et al., 1993). Early in development, the SR arises from the smooth-surfaced endoplasmic reticulum (ER) and displays a reticular distribution pattern relative to the myofibril components (Flucher et al., 1993). The nonjunctional SR membranes contact components of the Z-line early in myofibril development; whereas later in mouse development (17 d.p.c.) SR networks are observed as a banding pattern flanking the Z-line at the level of the I-band (Walker et al., 1968; Flucher et al., 1993). At 16-17 d.p.c., a periodic arrangement of RyR-positive clusters are evident by immunofluorescent labeling and electron microscopy along the A-I border flanking the Z-line of the sarcomere (Takekura et al., 2001). In contrast, the Ca^{+2}ATPase is typically distributed at cross-striated structures representing the longitudinal SR (Flucher, 1992). In cardiac tissue, the SR matures near birth and is detected as a sparse membrane network in the fetal heart. Consistent with these observations, the rate and level of Ca^{+2} uptake are significantly lower in the fetal SR relative to the neonatal and adult SR (Hoerter et al, 1981; Mahony and Jones, 1986).

A.3.ii. The Transverse (T)-Tubules.

Specialized invaginations of the surface membrane play a central role in the mechanism of excitation-contraction coupling in striated muscle. The EC-coupling mechanism is described in greater detail in the proceeding section. Invaginations of the sarcolemma and glycocalyx comprise the transverse tubule (T-tubules) system in both cardiac and skeletal muscle tissue. Whereas atrial cardiomyocytes, Purkinje cells and embryonic and neonatal ventricular myocytes do not have T-tubules, this membrane system is present in adult ventricular cells as well as in developing and adult skeletal muscle (Brette and Orchard, 2003). In adult cardiac ventricular cells, the T-tubules reside at the level of the Z-line, occurring at regular intervals (2 μm) along the longitudinal axis and have also been detected as longitudinal extensions (Sommer and Jennings, 1992; Brette and Orchard, 2003). The genesis of the T-tubule system has been closely examined in developing skeletal muscle and is characterized by a continuum of morphological changes that are completed only several weeks after birth in mammals (Edge, 1970; Flucher, 1992; Franzini-Armstrong, 1991). Immature T-tubules arise following the formation of SR elements in developing mouse embryos and first appear as longitudinally-arranged tubular invaginations or punctate structures occupying the spaces between myofibrils in skeletal muscle (Flucher, 1992; Flucher et al., 1993; Takekura et al. 2001). Couplings between the SR and T-tubules are initiated at 15 to 16 d.p.c. in mice, co-incident with appearance of spontaneous twitching in skeletal muscle (Takekura et al., 2001). A dramatic increase in the abundance and density of membrane invaginations occurs between 16 to 18 d.p.c. (Takekura et al., 2001), during which time the spatial overlap of immature T-tubules and the SR appear as longitudinally-orientated tubules

(Flucher et al., 1993). The transition from an immature longitudinal orientation to the mature transverse arrangement occurs gradually and is completed approximately three weeks after birth in the mouse, coinciding with increased ambulatory activity of the mouse (Edge, 1970; Franzini-Armstrong, 1991). In mature skeletal muscle, the T-tubule system acquires a final distribution at the A-I junction of the sarcomere (Martonosi, 2000).

A key component of T-tubule system in cardiac and skeletal muscle is the dihydropyridine (DHP) receptor, known otherwise as the voltage-activated L-type Ca^{+2} channel. Consisting of five distinct subunits ($\alpha 1$, $\alpha 2$, β, δ, γ) (Catarall, 1991a, 1991b and 1995), the DHP receptor shares structural similarities with the voltage-sensitive sodium (Na^{+}) channels and potassium (K^{+}) channels (Noda et al., 1986; Catterall, 1994). The $\alpha 1$ subunit of the DHP receptor serves as the calcium ion channel and also senses the voltage change caused by depolarization of the surface membrane (Dulhunty et al., 2002). The functional and structural couplings with the RyR are critical for DHP receptor activity in muscle contraction (further described in the proceeding section). The distribution and assembly of DHP receptors in striated muscle have been examined by immunolocalization studies and electron microscopy. Such studies have revealed significant differences in the arrangement of DHP receptors in cardiac and skeletal muscle (Sun et al., 1995; Bers and Stiffel, 1993; Franzini-Armstrong, 1999). In cardiac muscle, DHP receptors at the T-tubules form complexes with the SR terminal cisternae known as 'dyad' junctions. These structures demarcate a single sarcoplasmic reticulum cisternae flanking a T-tubule. In contrast, the SR-T-tubule couplings in skeletal muscle form a 'triad' structure, consisting of two sarcoplasmic reticulum cisternae facing a

central T-tubule (Porter and Palade, 1957; Franzini-Armstrong, 1999). Tetrad groups of DHP receptors appose the foot structure formed by tetramers of RyRs in skeletal muscle (Takekura et al., 1994a and 1994b; Franzini-Armstrong and Jorgensen, 1994). In contrast, cardiac DHP receptors do not form tetrads (Sun et al., 1995) and the ratio of RyR to DHP receptors is significantly higher in cardiac muscle (4-10) compared to skeletal muscle (0.5) (Bers and Stiffel, 1993).

A.4. The Excitation-Contraction Coupling Mechanism.

A change in the electric field across the muscle membrane generates a depolarization signal, which propagates along the length of the myofiber. To activate muscle contraction, the membrane depolarization signal elicits an elevation in the levels of cytoplasmic calcium ions. While many key components of the EC-coupling process are present in the two forms of striated muscle, several fundamental differences exist in cardiac and skeletal muscle. In cardiac muscle, the EC coupling mechanism has been described as a 'calcium-induced calcium release' process (Figure 3). In this respect, the DHP receptor functions as the primary pathway for calcium entry into the cell (Bers, 2002; Dulhunty, 2002). The cardiac DHP receptor and the RyR (RyR2) are not directly linked by protein-protein interactions; rather the plasma membrane depolarization signal causes a conformational change in the DHP receptor that allows an influx of extracellular calcium through the calcium channel. This rise in cytoplasmic calcium levels then triggers the activation of the cardiac RyR (RyR2), leading to calcium release from SR stores into the myofibrillar spaces (Endo et al., 1970; Bers, 2002; Brette and Orchard, 2003). It is this further release of calcium from the SR that constitutes the primary source

of calcium ions for muscle contraction (Wier and Balke, 1999; Brette and Orchard, 2003). In skeletal muscle, the DHP receptor functions as a voltage-gated calcium channel, whereby charge-dependent conformational changes in the DHP receptor promotes the direct physical coupling of the DHP receptor with the RyR (Block et al., 1988; Lu et al., 1994; Leong and MacLennan, 1998a and 1998b; Bers, 2002). This physical association is significant as it results in the activation of the RyR, thus permitting calcium release from the internal SR stores.

The proper expression and activity of the molecular components that regulate EC coupling in both cardiac and skeletal muscle are vital for survival, and mutations in the proteins involved in calcium handling cause serious conditions such as malignant hypothermia, central core disease and cardiac arrhythmias (Dulhunty et al., 2002). Proper assembly and activity of the DHP receptor and the RyR, for instance are essential criterions for the rapid propagation of the depolarization signal and calcium signaling in both cardiac and skeletal muscle (Adams et al., 1990; Takekura et al., 1994a; Tanabe et al, 1988 and 1990).

Figure 3. Excitation-Contraction Coupling in Cardiac Muscle.

Membrane depolarization activates the T-tubule localized L-type calcium channels, known also as the dihydropyridine (DHP) receptors. Activation of these ion channels serves as the primary route for the calcium influx into the cardiomyocyte. This influx of calcium ions in turn activates the calcium release channels (RyR) localized at the junctional SR, which induces calcium release from the SR. Elevated levels of cytosolic calcium promote the binding of calcium ions to troponin C, which subsequently activates the contractile machinery. Removal of calcium ions, necessary for muscle relaxation, is achieved by various mechanisms including; (i) SR Ca^{+2}ATPase activity; (ii) SL Na^{+}/Ca^{+2}-exchanger activity; (iii) SL Ca^{+2}ATPase activity; or (iv) mitochondrial Ca^{+2} uniport. Auxillary membrane proteins, such as junctophilins are thought to stabilize junctional membrane complexes. SL, sarcolemmae; SR, sarcoplasmic reticulum; JSR, junctional SR; LSR, longitudinal SR; AP, action potenial; TT, T-tubules; JP, junctophilin; SERCA, sarco(endo)plasmic reticulum Ca^{+2} ATPase; NCX, sodium-calcium exchanger; RyR, ryanodine receptors; DHPR, dihydropyridine receptors. Modified from Bers (2002).

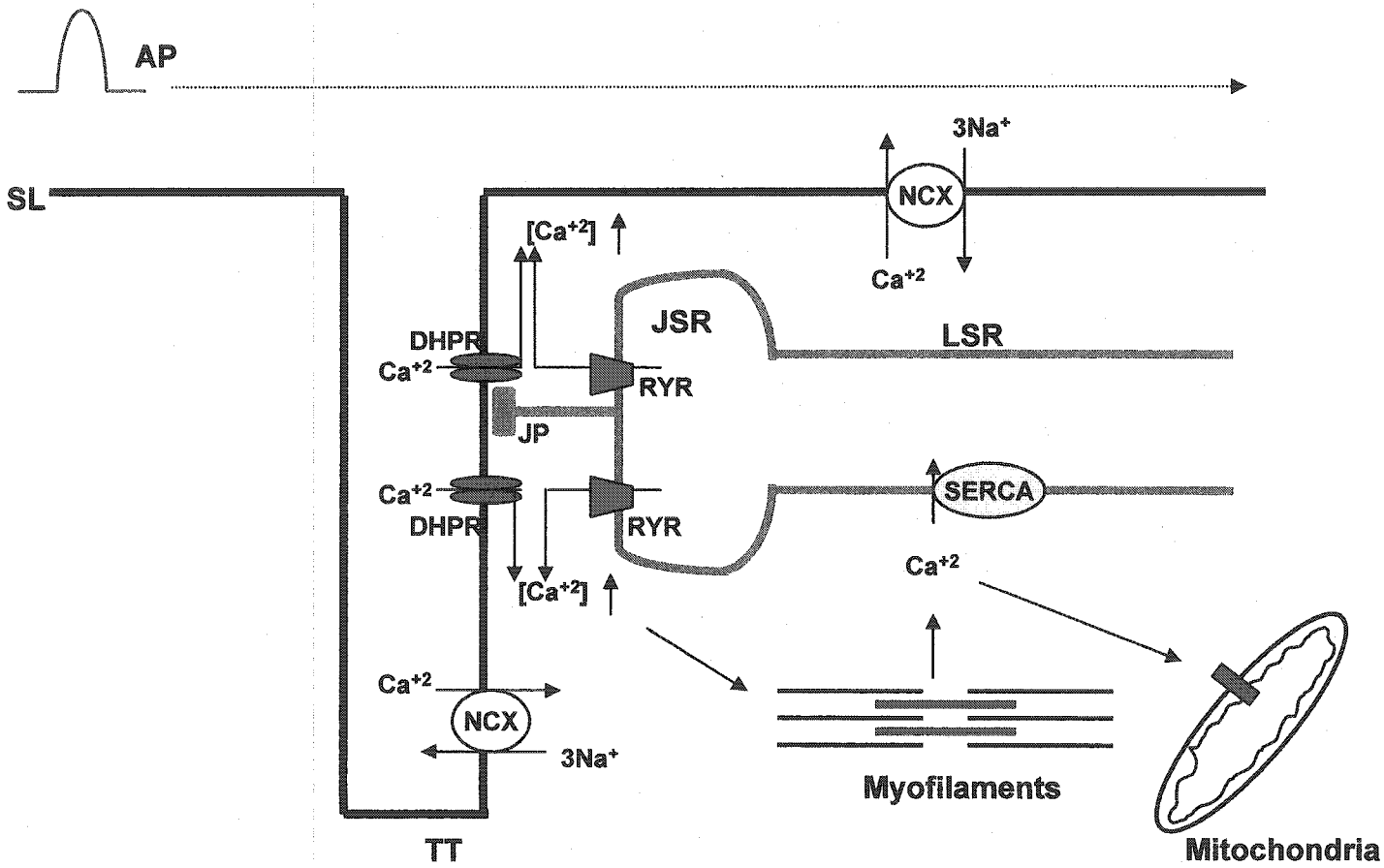
AP
SL
3Na+
NCX
Ca+2
[Ca+2]
JSR
LSR
DHPR
Ca+2
RYR
JP
Ca+2
DHPR
RYR
SERCA
[Ca+2]
Ca+2
Ca+2
NCX
3Na+
Myofilaments
Mitochondria
TT

A.5. Junctional Membrane Complexes.

Junctional membrane complexes create close membrane associations, thus facilitating crosstalk between ion channels localized at distinct membrane systems (Pozzan et al., 1994; Berridge 1998). The identities of the molecular components that couple the SR with the T-tubule system in striated muscle are unclear. Auxiliary molecules are thought to mediate such couplings since, in the absence of either DHP receptor or the RyR in mice, the formation of triad junctions are preserved in mutant skeletal muscle (Franzini-Armstrong, 1991; Ikemoto et al., 1997). Further support for the existence of additional junctional membrane complexes was provided by studies demonstrating that membrane depolarization does not elicit calcium release in a nonmuscle cell line transfected with DHPR and RyR, nor does the expression of these ion channels promote ER-PM associations (Takekura et al., 1995; Suda et al., 1997). Taken together these observations support the existence of additional junctional membrane-associated proteins; thus further identification of junctional components that would advance our understanding of EC coupling continues to be an active area of investigation.

A newly identified tail-anchored membrane protein designated junctophilin (JP), may provide stabilization of junctional membranes by associating with the terminal cisternae SR membrane and the T-tubule membrane system (Takeshima et al., 2000; Ito et al., 2001, Komazaki et al., 2002 and 2003). Three isoforms encoded by distinct JP genes include the skeletal muscle-specific JP-1, JP-2 expressed in skeletal, cardiac and smooth muscle and the brain-specific JP-3 isoform (Takeshima et al., 2000). A carboxyl-terminal transmembrane domain anchors JP within the junctional face of the SR membrane, whereas amino-terminal sequences direct interactions with sarcolemmal

phospholipids (Takeshima et al., 2000). Involvement of JP-1 and JP-2 in the formation of junctional membrane complexes in striated muscle was examined by deletion analysis in mice (Takeshima et al., 2000; Ito et al., 2001; Komazaki et al., 2002). Mutant mouse embryos lacking JP-2 died early in development (10.5 d.p.c.) due to cardiac arrest (Takeshima et al., 2000). A deficiency in periphery-couplings was observed by electron microscopic analysis of cardiac myocytes from 9.5 d.p.c. JP-$2^{-/-}$ embryos (Takeshima et al., 2000). Furthermore, JP-1 deficiency resulted in death shortly after birth, and consistent with its role in membrane junction formation, ultrastructural analysis of $JP^{-/-}$ mutant skeletal muscle revealed extremely sparse triad formation (Ito et al., 2001; Komazaki et al., 2002). Taken together, these observations support a role for junctophilin in stabilizing SR-T-tubule associations. It remains to be determined whether junctophilin mediates this stabilization by complex formation with other uncharacterized membrane proteins.

B. Sarcolemmal Membrane Associated Proteins (SLMAPs).

To identify novel components of cardiac membrane systems that may advance our understanding of the molecular components of E-C coupling, antibodies to highly purified canine sarcolemma were used to screen a rabbit heart cDNA library (Wigle et al., 1997). These studies, conducted in Dr. Tuana's lab, resulted in the identification of a cDNA encoding a novel family of sarcolemmal-membrane associated proteins (SLMAPs). Three distinct transcripts were subsequently identified, including a 5.9 kb transcript, a 4.5 kb transcript and a 3.5 kb transcript. Fluorescence in situ hybridizations confirmed that a single gene located on the short arm of human chromosome 3 (3p14.3-

21.2) encodes all three transcripts. The rapid amplification of cDNA ends (RACE) further indicated that the three transcripts share common carboxyl terminal sequences and have divergent amino-terminal sequences, as depicted in Figure 4.

B.1. Structural Features of SLMAPs: Unique Members of the Tail-Anchored Membrane Protein Superfamily.

Eludication of the amino acid composition of SLMAP revealed that SLMAPs possess several interesting structural features (Wigle et al., 1997). A central alpha-helical coiled-coil domain, two leucine zipper motifs and a carboxyl-terminal transmembrane domain constitute the primary structural features of SLMAPs. The topological properties of SLMAPs indicate that these molecules belong to the superfamily of tail-anchored (TA) membrane proteins that include various proteins serving diverse cellular functions such as vesicle targeting and fusion (soluble N-ethylmaleimide-sensitive factor attachment protein receptor: SNARES); electron transfer (cytochrome P450); apoptosis (Bax) and excitation-contraction coupling (junctophilin) (Kutay et al., 1993; Wattenberg and Lithgow, 2001; Ito et al, 2001).

B.1.i. Alpha Helical Coiled-Coil Structure.

Analysis of SLMAP secondary structure revealed that SLMAP isoforms have a propensity to form alpha-helical coiled-coil structure along the length of the molecule (Figure 4). The coiled-coil motif is a common structural feature, which confers protein

Figure 4. Structural Features of SLMAPs.

(A) Three distinct mRNA species (3.5 kb, 4.5 kb, 5.9 kb) encode SLMAP1, SLMAP2 and SLMAP3, respectively. Whereas SLMAP3 is widely expressed, SLMAP1 and SLMAP2 are muscle-specific variants. Previous in vitro transcription-translation experiments have confirmed that SLMAP3 may be generated by the utilization of two in-frame initiating methionines (M1 and M2), separated by 133 amino acids. These translation start sites are predicted to encode proteins of 91 kDa and 80 kDa, respectively. SLMAP2 and SLMAP1 are predicted to encode proteins of 47 kDa and 35 kDa, respectively. A PEST motif, which generally confers susceptibility to proteolysis, exists in SLMAP3 and SLMAP2 sequences. The common carboxyl sequences present in SLMAPs contain two leucine zipper motifs (LZ) and a transmembrane (TM) domain.

(B) SLMAPs are predicted to form coiled-coils throughout the length of the molecule, as predicted by the COILS program using a window of 28 amino acids (Lupas, 1996).

(C) An extreme carboxyl-terminal hydrophobic domain mediates the insertion of SLMAP into membrane systems. The bulk of the molecule is exposed to the cytoplasm, where it may form associations with cytoplasmic or cytoskeletal components via the extensive coiled-coil structure.

A.

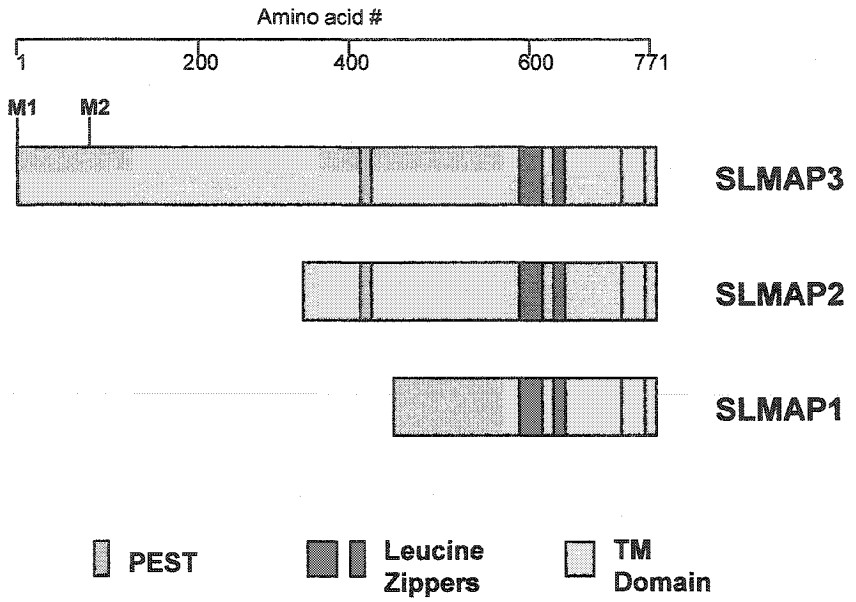
Amino acid #
1
200
400
600
771
M1
M2
SLMAP3
SLMAP2
SLMAP1
PEST
Leucine Zippers
TM Domain

B.

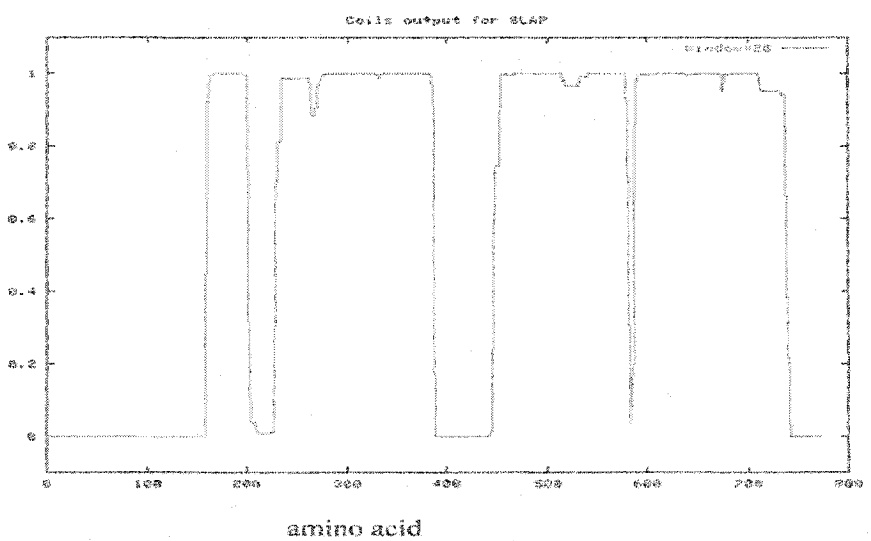
amino acid

C.

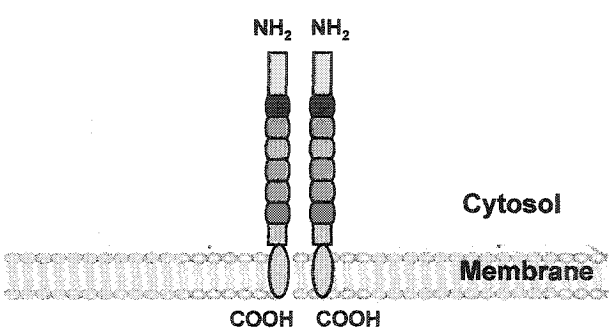
NH2
NH2
Cytosol
Membrane
COOH
COOH

stability by directing subunit oligomerization. Proteins that withstand considerable cellular stress such as motor proteins (myosin), extracellular proteins (laminin) and cytoskeletal components (α-keratin) harbor coiled-coil motifs (Burkhard et al., 2001). Intermolecular coiled-coil motifs are thought to mediate the assembly of integral membrane components involved in exocytotic membrane fusion events (Chapman et al., 1994; Canaves and Montal, 1998). In this respect, coiled-coil forming domains present in the plasmalemmal t-SNARE proteins, SNAP-25 and syntaxin as well as the synaptic vesicle-membrane associated protein, synaptobrevin direct complex formation that is required to merge the opposing vesicles with the plasma membrane (Chapman et al., 1994; Canaves and Montal, 1998; Freedman et al., 2003; Sutton et al., 1998). Coiled-coil structure has also emerged as a common structural feature predicted in the components of various organelles, including core regulatory and structural components of the centrosome. At the level of the centrosome, coiled-coil motifs are speculated to serve as structural scaffolds for the assembly of specific complexes required for proper cell cycle-cycle mediated activities (Doxsey et al., 1994; Fry et al., 1998b and 1999; Boukson-Castaing et al., 1996; Takahashi et al., 1999 and 2002; Li et al., 2001; Chevrier et al., 2002).

The predicted structure of the coiled-coil consists of two to five amphipathic α-helices wrapped around each other (Burkhard et al. 2001). Coiled-coils represent either parallel right-handed helices with an eleven residue periodicity (undecad repeat) or parallel left-handed helices with a seven residue periodicity (heptad repeat) (Burkhard et al., 2001). The residues of the heptad repeat are designated as amino acid residues '*abcdefg*' such that residues at 'a' (first residue) and 'd' (fourth residue) positions are

hydrophobic whereas, 'e' and 'g' position residues are predominantly polar (Poirier et al., 1998).

B.1.ii. Leucine Zipper Motifs.

Characterization of SLMAP sequences by Wigle et al. (1997) resulted in the identification of two leucine zipper motifs within the common carboxyl core of SLMAPs (Figure 4). These motifs represent an 11-heptad coiled-coil structure and are thought to provide a scaffold for the assembly of other unidentified proteins. Alternatively, these regions of the molecules may direct SLMAP-SLMAP interactions, as has been described for the function of leucine zippers in other proteins (Fry et al., 1999; Nomura et al., 1993). The structure of the leucine zipper motif consists of an amphipathic α-helix with hydrophobic residues along one face of the helix. Hydrophobic leucine residues reside at the innermost overlapping point of the coils at every seventh position (Landshulz et al., 1988). This arrangement creates a straight line of leucine residues that are capable of associating with other coiled-coil helices in a parallel orientation.

Protein oligomerization represents a fundamental mechanism for modulating activity and for targeting complexes to specific destinations within the cell. Leucine zippers, specialized forms of coiled-coil structure mediate the homo- and hetero-dimerization of various classes of proteins representing nuclear transcription factors, cytoskeletal proteins, kinases and integral membrane ion channels (Marx et al, 2001 and 2002; Hulme et al, 2002; Fry et al., 1999). The leucine zipper motifs present in the ion channels controlling calcium signaling in striated muscle, direct the assembly of macromolecular signaling complexes onto the channel (Marx et al., 2002; Marx et al.,

2001; Hulme et al., 2002). Leucine heptad repeats within the carboxyl-terminus of the skeletal muscle L-type calcium channel (Cav1.1) directly bind the leucine zipper motifs present in the A-kinase anchoring protein, thus creating a structural template for the association of regulatory proteins (Marx et al., 2001; Hulme et al., 2002). Such protein-protein interactions exert significant effects on muscle physiology as the associated signaling molecules (kinases, phosphatases) modulate channel activity (Marx et al., 2001; Hulme et al., 2002). In a similar respect, the leucine zipper motifs in the cardiac calcium release channel (RyR), direct the formation of macromolecular signaling complexes through associations with the leucine zipper motif of adaptor proteins (Marx et al., 2001). The fundamental role of leucine zippers as protein-protein interaction modules is supported by their prevalence in components localized to various organelles, including centrosomes or the microtubule organizing center (MTOC) of the cell (Bouckson-Castaing et al., 1996; Wittmann et al., 1998; Fry et al., 1999; Hong et al., 2000). In this respect, a mammalian centrosomal serine-threonine kinase, Nek2 kinase requires leucine-zipper mediated homodimer formation for its activity on centrosomal substrates. Phosphorylation of a centrosomal Nek2-associated protein (C-Nap1) by Nek2 kinase homodimers results in the dissociation of C-Nap from mitotic centrosomes (Fry et al., 1998a, 1998b and 1999; Mayor et al., 2002). Dissociation of C-Nap from the centrosome results in loss of cohesion between duplicated centrosomes, which represents a necessary event for subsequent mitotic phase progression (Fry et al., 1995 and 1998b; Mayor et al., 2002). The interactions mediated by leucine zipper motifs in SLMAPs as well as the functional significance of these interactions, remains to be defined.

B.1.iii. Carboxyl-Terminal Transmembrane Domain.

An important aspect in cell biology concerns the molecular mechanisms that direct the targeting of newly synthesized proteins, such as SLMAPs to their proper subcellular localizations. Based on immunolocalization studies, SLMAPs were shown to form associations with membrane structures in cardiac cells as well as in cultured cells, and as such are speculated to serve a role in membrane processes (Wigle et al., 1997; Wielowieyski et al., 2000). Genomic sequence analysis combined with RT-PCR studies revealed that SLMAPs possess two mutually exclusive transmembrane domains (TMD; TMD1 and TMD2) at the extreme carboxyl terminus, consistent with the topology of tail-anchored membrane proteins (Wielowieyski et al., 2000) (Figure 4). Detergent-extraction studies have further confirmed that SLMAPs are integral membrane proteins, with the bulk of the polypeptide oriented within the cytosol (Wigle et al., 1997). The transmembrane domains identified in SLMAPs are encoded by alternative exon X (TM1) and exon XI (TM2) of the SLMAP1 genomic sequence (Figure 5) (Wielowieyski et al., 2000). Splicing of the alternative exon encoding TM1 introduces an in frame stop codon which renders the second transmembrane domain (TM2) nonfunctional. SLMAP variants are therefore predicted to express a single transmembrane domain, either TM1 or TM2.

Several distinct mechanisms have been defined for protein insertion into membrane systems. The signal recognition particle (SRP)-dependent pathway is perhaps the best-characterized mechanism that mediates the co-translational insertion of proteins into phospholipid bilayers. As the polypeptide is released from the ribosome, a hydrophobic signal sequence encoded near the amino terminus of the polypeptide is

exposed and is recognized by a soluble signal recognition particle (SRP) (Walter and Johnson, 1994; Meacock et al., 2000). The SRP cognate receptor, localized at the membrane of the endoplasmic reticulum, specifically binds to the ribosome-nascent chain-SRP complex. Protein integration into the membrane is then directed by an ER membrane localized translocon (Sec61) (Meacock et al., 2000; Johnson and van Waes, 1999; Matlack et al., 1998).

SRP-independent post-translational mechanisms are used for the membrane insertion of a distinct class of proteins designated 'tail-anchored membrane proteins'. Integral membrane proteins belonging to this class of proteins reside in distinct organelles including the endoplasmic reticulum, mitochondria and peroxisomes (Wattenberg and Lithgow, 2001). The topology of tail anchored membrane proteins is defined by a stretch of hydrophobic residues at the extreme carboxyl-terminus that inserts into the phospholipid bilayer while the remainder of the molecule resides in the cytosol (Wattenberg and Lithgow, 2001). During protein synthesis, the nascent polypeptide folds co-translationally within the cytoplasm and upon its release from the ribosome, the hydrophobic tail associates with molecular chaperones (Wattenberg and Lithgow, 2001). Translocation across the target phospholipid bilayer is accomplished via a translocon-independent process described by Kutay et al. (1995).

Residues immediately adjacent to the transmembrane domain in tail-anchored membrane proteins confer membrane-selective sorting (Kuroda et al., 1998; Wattenberg and Lithgow, 2001). Studies by Borgese et al. (2001) have supported this concept by demonstrating that charged residues at the extreme carboxyl-terminus dictate targeting of the mammalian tail-anchored cytochrome b5 to either the mitochondrial outer membrane

or the endoplasmic reticulum. In addition to the presence of positively charged residues adjacent to the transmembrane domain segment, the length of the transmembrane domain also constitutes an important determinant for compartment-specific targeting of tail-anchored membrane proteins. Whereas a twenty-one amino acid hydrophobic anchor targets VAMP-1A splice isoform to the endoplasmic reticulum; a seventeen amino acid hydrophobic segments inserts VAMP-1B splice isoform to the mitochondria (Isenmann, et al., 1998). It is apparent from SLMAP structure that SLMAPs likely belong to this class of membrane proteins (Figure 4). The functional significance of the two TMDs present in SLMAP is not well understood. Whether alternate splicing of the SLMAP gene represents a mechanism for differential targeting of the polypeptide to distinct membrane systems remains to be determined (Wielowieyski et al., 2000).

B.2. Tissue Specific SLMAP Expression.

The three SLMAP isoforms are expressed in a tissue specific manner and likely confer functions related to the development and molecular physiology of specific tissues and organ systems. Broad tissue expression was shown for the SLMAP3 (5.9 kb) transcript as this mRNA was detected in cardiac tissue, fast and slow twitch skeletal muscle, smooth muscle, liver, pancreas, kidney, spleen and brain (Wigle et al., 1997). In contrast, the SLMAP1 (3.5 kb) transcript and the SLMAP2 (4.5 kb) transcript exhibited muscle-specific expression and were exclusively expressed in cardiac tissue (atria, ventricles), slow twitch skeletal muscle and smooth muscle tissue isolated from aorta, uterus, esophagus and stomach (Wigle et al., 1997). In view of the tissue-specific nature of SLMAP isoform expression, several mechanisms are postulated to give rise to SLMAP

isoform heterogeneity including alternative splicing and differential promoter usage. Although the molecular mechanism responsible for generating tissue-specific SLMAP expression remains to be resolved, the abundance of SLMAP transcripts in muscle prompted us to speculate that SLMAPs fulfill essential functions in muscle physiology. The subcellular distribution of this family of integral membrane proteins in developing and mature cardiac, skeletal and smooth muscle may provide valuable insights regarding potential functions in the structural and functional organization of muscle tissue. In addition, the ubiquitously expressed SLMAP isoform (SLMAP3) may serve a fundamental role in cell biology.

Figure 5. Carboxyl-terminal exons encode two distinct membrane anchors.

(A) Genomic characterization of the 3' sequences common to all three SLMAP variants revealed that alternative exon X and exon XI encode two distinct carboxyl-terminal transmembrane domains, designated TMD1 and TMD2 respectively (Wielowieyski et al., 2000).

(B) Seventeen amino acid residues are predicted to encode either TMD1 or TMD2 (underlined). The transmembrane domain segments were predicted using the PSORT prediction tool available from the PSORT www server (Klein et al., 1985; Nakai and Kanehisa, 1992). A BLAST search for either TMD did not reveal homology to other known membrane proteins.

A.

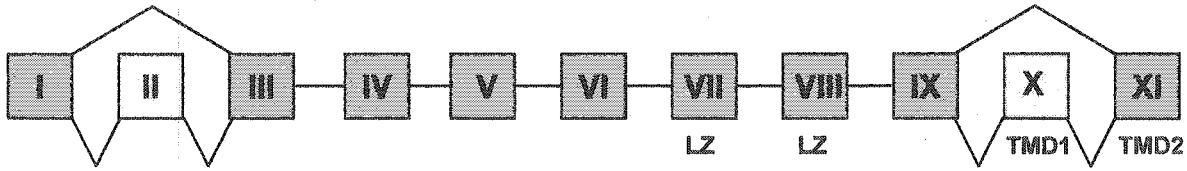

B.

Exon X P S I L Q P V P A V F I G L F L A F L F W C F G P L W ^

Exon XI K P W P W M P M L A A L V A V T A I V L Y V P G L A R A S P ^

C. Statement of the Problem

Previous characterization of the SLMAP gene has provided valuable information regarding the genomic organization of SLMAP, the expression profile of SLMAPs as well as biochemical and structural features of the molecule. Taken together, these data suggest that SLMAPs represent a unique family of tail-anchored integral membrane proteins with an extensive coiled-coil structure exposed to the cytoplasm. The biological functions provided by this family of proteins however remain largely undefined. Studies were thus designed to gain insight into the potential roles of SLMAPs in muscle as well as nonmuscle systems. Based on the initial examination of SLMAP tissue distribution and analysis of its molecular properties, I hypothesized that SLMAP isoforms are targeted to distinct subcellular structures via alternative splicing mechanisms and may serve a role in organizing membrane as well as cytoskeletal systems. To gain insight regarding the potential biological roles of SLMAPs in striated muscle as well as in proliferating cells, I examined the subcellular distributions of SLMAPs via immunocytochemical and immunohistochemical studies. Pharmacological, biochemical and molecular biological studies further employed to characterize SLMAP-associations and the effects of changing their cellular levels were also examined. The results of my studies have demonstrated that:

(i) SLMAPs are enriched in developing and mature skeletal muscle and localize in muscle membrane systems that control excitation-contraction coupling mechanisms. The induction of a novel SLMAP isoform correlated with myotube

formation and the regulated expression of SLMAP was critical for myoblast fusion (Chapter Two).

(ii) SLMAPs are directed into distinct cellular membrane systems by unique carboxyl-terminal domains generated by alternative splicing mechanisms and may serve roles in the structural arrangement of cardiac membrane systems through homodimerization and interactions with the cytoskeleton (Chapter Three).

(iii) A novel SLMAP isoform having an amino-terminal extension was ubiquitously expressed and found to be a component of the cell's microtubule organizing center. This SLMAP isoform may serve to regulate mitosis and cellular proliferation (Chapter Five).

Chapter Two.

Guzzo et al. (2003). Regulated Expression and Temporal Induction of the Tail-anchored Membrane Protein SLMAP is Critical for Myoblast Fusion (Submitted to the Journal of Biological Chemistry).

The following outlines the experimental contributions of the authors of this manuscript. Embryo isolations, cryostat sectioning, immunohistochemistry (with the exception of Figure 1B and Figure 3D), microscopy and image analyses, northern and western blot analyses, immunoprecipitations, determination of fusion indices and protein-protein interaction assays were performed by R.M. Guzzo. Immunohistochemistry presented in Figure 1B was performed by Dr. Jeffrey Wigle. Dr. Edwin Moore performed the deconvolution confocal microscopy (Figure 3D). Maysoon Salih and R.M. Guzzo generated the mammalian expression constructs and the stable transfectants. R.M. Guzzo wrote the manuscript, under the guidance of Dr. Balwant Tuana.

Regulated Expression and Temporal Induction of the Tail-anchored Membrane Protein SLMAP is Critical for Myoblast Fusion.

Rosa M. Guzzo, Jeffery Wigle, Maysoon Salih, Edwin D. Moore* and Balwant S. Tuana

Department of Cellular and Molecular Medicine, 451 Smyth Rd, University of Ottawa, Ottawa, Ontario, Canada K1H 8M5.
*Department of Physiology, University of British Columbia, Vancouver, British Columbia, Canada V6T 1Z3

Telephone (613) 562-5800 ext. 8578

Fax (613) 562-5434

email: btuana@uottawa.ca

Corresponding author: Balwant S. Tuana, Ph.D.

Abbreviations: *SLMAP*, sarcolemmal membrane-associated protein; *PCR*, polymerase chain reaction; *PFA*, paraformaldehyde; *TM*, transmembrane domain; *LZ*, leucine zipper; *d.p.c.*, days post coitum; *SR*, sarcoplasmic reticulum; *T-tubules*, transverse tubules; *EC*, excitation-contraction.

Abstract

The sarcolemmal-membrane associated proteins (SLMAPs) define a new class of coiled-coil tail anchored membrane proteins generated by alternative splicing mechanisms (Wigle, J.T., Demchyshyn, L., Pratt, M.A., Staines, W.A., Salih, M. and Tuana, B.S. (1997) *J. Biol. Chem.* **272**. 32384-32394; Wielowieyski, P.A, Sevinc, S., Guzzo, R., Salih, M., Wigle, J.T. and B.S. Tuana (2000) *J. Biol. Chem.* **275**. 38474-38481). *In vivo* expression analysis indicated that SLMAPs are present in somites (11 d.p.c.) and in fusing myotubes. Subcellular SLMAP was distributed in a disordered fashion and acquired a distinct pattern of localization coincident with the organization of the sarcoplasmic reticulum and T-tubules. Skeletal muscle myoblasts were found to express a single 5.9 kb transcript which encodes the full length ~91 kDa SLMAP3 isoform. Myoblast differentiation was accompanied by the stable expression of the ~ 91 kDa SLMAP protein as well as the appearance of an ~80 kDa isoform. Deregulation of SLMAPs by ectopic expression in myoblasts resulted in a potent inhibition of fusion without affecting the expression of muscle-specific genes. Membrane targeting of the deregulated SLMAPs was not critical for the inhibition of myotube development. Protein-protein interaction assays indicated that SLMAPs are able to self assemble and the deregulated expression of mutants that were unable to form SLMAP homodimers also inhibited myotube formation. These data imply that regulated levels and the temporal induction of SLMAP isoforms are important for normal muscle development.

Introduction.

Early in development, mesodermal cells are committed to a muscle cell fate in response to locally derived embryonic differentiation signals (1,2). The withdrawal of determined myoblasts from the cell cycle is coordinated by the repression of growth promoting genes coupled with simultaneous induction of muscle-specific genes. A family of basic helix loop helix myogenic regulatory factors (MRFs) including MyoD, Myf5, myogenin and MRF4 predominantly control skeletal muscle specification and differentiation (3-5). A hallmark feature of normal skeletal muscle development is the fusion of mononucleated myoblasts to form fully differentiated elongated multinucleated myotubes (6-8). Morphologically, this process has been examined extensively in Drosophila, as myoblast fusion is complete in a matter of hours (9-13). The process of myoblast fusion consists of various steps including: (i) cell-cell recognition of fusion competent cells; (ii) cell-cell adhesion for close contact between fusion competent cells; (iii) cell alignment and formation of prefusion complexes; and, (iv) the breakdown of membranes to remove excess membrane material (10, 14). Several protein classes play pivotal roles in this process, including cell adhesion and cell surface proteins (N-cadherins, M-cadherin, neural cell adhesion molecule (N-CAM), integrins, disintegrins), cytoskeletal components and cytosolic signaling molecules (15-20). The identification of the molecular components necessary for myoblast fusion would promote our understanding of skeletal muscle formation in development and in regenerating adult skeletal muscle.

A key aspect in muscle differentiation is the formation of specialized membrane systems that serve a central role in calcium regulation. These specialized membrane

systems consist of sarcolemmal invaginations known as the Transverse-tubules (T-tubules) and the sarcoplasmic reticulum (SR), an extensive internal membrane compartment controlling intracellular calcium storage, release and uptake. Structural analyses have revealed that components of the SR and T-tubules are expressed early in development within muscle precursors at the prefusional stage (21-25). Proper organization of these specialized membrane systems is essential for normal muscle development and function (26,27).

In an effort to identify novel membrane components involved in EC-coupling, we previously cloned cDNAs encoding a family of α-helical coiled-coil proteins referred to as sarcolemmal associated proteins (SLAPs) (renamed SLMAPs) (28,29). The SLMAPs comprise a unique family of tail-anchored membrane proteins, which exhibit developmental and tissue specific expression (28,29). Structural heterogeneity among SLMAP variants arise as a result of a combination of alternative splicing and alternative start site usage of a single gene assigned to human chromosome 3p14.3-21.2. Detailed sequence analyses revealed that SLMAPs share common carboxyl-terminal sequences characterized by extensive coiled-coil structure containing two leucine zippers motifs speculated to serve roles in protein-protein interactions. Alternative splicing at the carboxyl terminus generates SLMAP variants having unique transmembrane domains, which target SLMAPs to cellular membranes (29). In our current study, we have investigated the developmental expression of SLMAP in skeletal muscle and have used an *in vitro* model of skeletal muscle differentiation to examine whether SLMAP serves a role in myogenesis. Our results suggest that SLMAP is expressed in early somites and

may serve roles in myoblast fusion and in the membrane biology of EC-coupling in developing muscle.

Experimental Procedures

Cell Culture and Transfection.

Proliferating C2C12 myoblast cells were maintained at 37°C in Dulbecco's modified Eagle medium (DMEM) supplemented with 10% heat inactivated fetal bovine serum, 50 units/mL penicillin, 50 μg/mL streptomycin and gentamycin. For differentiation studies, C2C12 cells were plated on gelatin or Matrigel coated plates. Confluent C2C12 cultures were induced to differentiate by replacing growth medium with DMEM containing 2% horse serum. For stable expression of 6Myc-SLMAP fusion proteins, C2C12 cells were transfected using Lipofectamine Plus™ (GIBCO BRL) or Fugene (Roche) transfection reagents according to the manufacturers' specifications. Myoblasts transfected with 6Myc-pcDNA3 served as controls. G418 resistant clones were subsequently assayed for expression of exogenous SLMAP protein by immunoblot analysis. The level of exogenous SLMAP protein was quantified relative to endogenous SLMAP by densitometery.

Immunohistochemistry.

Timed-pregnant mice were sacrificed by lethal injection of sodium pentobarbital. Embryos (11-15 d.p.c.) were removed, rinsed briefly in PBS, and then immediately fixed in 4% paraformaldehyde in 0.1 M phosphate buffer, pH 7.4. Embryos were incubated

overnight in cryoprotectant (20% sucrose in PBS) at 4°C. Fixed embryos were embedded in Tissue-Tek O.C.T. compound, frozen and stored at –80°C. Cryosections (6-10 μm) were collected on gelatin coated microscope slides and stored at –80°C. Older embryos (18 d.p.c.) and adult tissues were isolated, rinsed in PBS, embedded in Tissue-Tek O.C.T. compound and then frozen. Cryosections were mounted onto slides and fixed overnight in 4% paraformaldehyde. Immunohistochemistry was performed by first prewarming slides to 37°C. PFA-fixed sections were washed in PBS then treated with 50 mM ammonium chloride in PBS for 5 minutes to reduce nonspecific staining of blood proteins. Sections were blocked in PBS containing 10% goat serum, 1% Triton-X-100 and 10% bovine serum albumin for 20 minutes at room temperature before being exposed to primary antibodies (1 hour at room temperature). Following several washes in PBS, sections were incubated in PBS containing 5% goat serum, 1% Triton-X-100 and the appropriate fluorochrome-linked secondary antibodies for one hour at room temperature. After several washes in PBS, sections were mounted with antifading solution (Molecular Probes) and examined by either conventional microscopy or confocal microscopy.

In a series of experiments, coverslips were covered with ten microlitres of a solution composed of 90% glycerol, 10% 10X PBS (composition of PBS in mM; 137 NaCl, 8 NaH_2PO_4, 2.7 KCl, 1.5 K H_2PO_4, pH 7.4) 2.5% triethylenediamine, and 0.02% NaN_3, to which fluorescent microspheres (0.2 μm diameter, Molecular Probes) labeled with FITC and Texas Red had been added. The microspheres are fiduciary markers and permit accurate alignment of the 3D data sets. A series of two-dimensional images were acquired through the cells at 0.25 μm spacing using a Nikon Diaphot 200 microscope and a Planapo 60/1.4 objective (pixel dimensions 100x100 nm). Other details of the

microscope and optics can be found in Scriven et al (52). The point spread function of the microscope was measured using fluospheres of the appropriate color (0.1 μm diameter, Molecular Probes). The images were prepared, deconvolved and analyzed as previously reported (51).

Antibodies.

Anti-SLMAP(C) rabbit antibodies were raised against the carboxyl 370 amino acids of SLMAP, as previously described (28). Antibodies used in this study included: anti-myogenin monoclonal antibody (Pharmingen); anti-α-tubulin monoclonal antibody (clone DM 1A; Sigma-Aldrich); anti-myosin heavy chain monoclonal antibody MF20 (Dr. David Parry, University of Ottawa); anti-caveolin 3 monoclonal antibody (Transduction Laboratories); anti-α-actinin2 monoclonal antibody (Sigma-Aldrich); anti-α1 DHP receptor monoclonal antibody (Chemicon); and anti-Ca^{2+}-ATPase monoclonal antibody (Developmental Studies Hybridoma Bank, University of Iowa). Rhodamine-RedX-conjugated mouse secondary antibody (Jackson Laboratories), Alexa-Fluor 594-conjugated mouse secondary antibody (Molecular Probes) and Alexa-Fluor 488-conjugated rabbit secondary antibodies (Molecular Probes) were used in immunohistochemistry studies. Secondary antibodies used in immunoblotting experiments included anti-rabbit IgG peroxidase linked whole antibody (Amersham Pharmacia Biotech) and peroxidase conjugated AffiniPure goat anti-mouse IgG (Jackson ImmunoResearch Laboratories, Inc.).

Immunofluorescence Microscopy.

Samples were visualized using Axiophot (Carl Zeiss Inc) microscope equipped with a 3CCD colour video camera. An Olympus IX70 laser-scanning inverted microscope was used for observation with a 63x oil immersion objective. Images were acquired using the BioRad MRC 1024 confocal. Acquired images were digitally processed using Northern Eclipse (Version 5.0, Empix Imaging Inc.) acquisition software as well as the Confocal Assistant 40 software. Images were further processed using Adobe Photoshop™ 5.0 (Adobe Systems Inc.).

Northern Blot Analysis.

Total RNA was extracted from proliferating C2C12 cells or from C2C12 cells at various days after differentiation using Trizol Reagent (Roche Molecular Biochemicals) according to the manufacturer's specifications. Equivalent amounts of total RNA was electrophoresed through 1% agarose and 2.2% formaldehyde denaturing gel then transferred to a positively charged nylon membrane (Roche Molecular Biochemicals). The blot was prehybridized in 1% blocking reagent in maleic acid at 65°C for one hour and then hybridized overnight with PCR-generated digoxigenin-labeled (Roche Molecular Biochemicals) cDNA probes. SLMAP cDNA used for probing corresponded to the common carboxyl terminus sequences present in SLMAPs (28). cDNAs for rat myogenin and glyceraldehyde-3-phosphate dehydrogenase (GAPDH) cDNA were also digoxigenin-labeled for hybridization. After several washes (2X-0.5X SSC; 0.2% SDS), the membrane was incubated in blocking solution (Roche Molecular Biochemicals), and then incubated with anti-digoxigenin alkaline phosphatase antibody (1:10 000 in blocking solution). Blots were washed several times in 0.1 M maleic acid; 0.15 M NaCl, pH 7.5;

0.3% Tween20, and then incubated in detection buffer (10 mM Tris-HCl; 0.1 M NaCl, pH 9.5) for 5 minutes, prior to detection of DIG labeled probes using the CSPD reagent (Roche Biochemicals). Membranes were subsequently exposed to Kodac MR film.

Immunoblot analysis.

Cultured cells were lysed in modified RIPA buffer (10 mM Tris-HCl, pH 7.4, 1 mM EDTA, 300 mM NaCl, 1% Nonidet P-40, 0.1% SDS, 1% sodium deoxycholate) supplemented with protease inhibitor cocktail (Sigma-Aldrich). Particulate material and unbroken cells were removed by centrifugation at 10,000xg for ten minutes at 4°C. Clarified lysates were retained and the protein content was determined using the BCA protein assay kit (Pierce). Protein extracts were resolved by electrophoresis on 10% SDS-polyacrylamide gels and electrotransferred to PVDF membranes (Roche Molecular Biochemicals). Membranes were blocked with 5% skim milk powder (SMP) in TRIS-buffered saline containing 0.05% Tween-20 (TBS-T), and then incubated at room temperature for one hour in the relevant primary antibodies. After several washes in TBS-T, membranes were incubated in the appropriate peroxidase-linked secondary antibodies in 5% SMP/TBS-T for one hour. Membranes were washed in TBS-T and antibody detection was performed using the enhanced chemiluminescent detection system (Renaissance, NEN). Membranes were exposed to x-ray films (Kodac MR film).

Densitometry.

Densitometric analysis was performed using the Scion Image software (Scion Corp.) based on the NIH Image program.

SLMAP expression plasmids.

SLMAP3M1 (nt 1-2337) was PCR generated from the SLMAP rabbit cDNA clone (Accession #U21157) using forward primer SLMAPN-F (GGAATTCGATGCC GTCAGCCTTGGC) and reverse primer SLMAPN-R (GATGCCAGCTTCTAGAGGGA GGACG). PCR products were inserted into the EcoR1 and Xba1 sites of pcDNA3 mammalian expression plasmid (Invitrogen), in frame with the 6Myc epitope tag. Sites of ligations were confirmed by DNA sequencing. 6Myc-tagged ΔNSLMAP expression construct encompassing the BglIII/Xba1-digested SLMAP3 restriction fragment (lacking first 315 amino acids of SLMAP3) was generated as described by Wigle *et al.* (28). 6MYC-tagged SLMAP1 expression constructs encoding transmembrane domain 2 (TM2) or the construct lacking both TM domains were generated according to Wielowieyski *et al.* (29). The leucine zipper mutant (SLMAPΔLZ) was generated by digesting 6Myc-SLMAP1-pcDNA3 with BamH1. This digestion removed the segment of SLMAP that encoded the leucine zippers (nucleotides 1790-2001). Nucleotides 2001-2314 of SLMAP3M1 (designated SLMAP3') in pcDNA3 were retained for subsequent ligation. A PCR amplicon of 6Myc-SLMAP1 lacking the leucine zippers was PCR-generated from the 6Myc-SLMAP1-pcDNA3 template using the 5' primer (GAATTCAATGGATGAGCAAGACCT; 6Myc-SLP15') and the 3' primer (CGGATCCCTCTTTCTGCTGGTCCTCACACTGC; LZ-less). The PCR product (lacking the leucine zippers) was restriction digested (BamH1) and then ligated into SLMAP3'. The GFP-tagged SLMAP (GFP-ΔNSLMAP) construct, which lacked the

first 315 amino acids of SLMAP3 was generated using a BglIII/Xba1-digested SLMAP3 restriction fragment inserted into GFP-pcDNA3.

Determination of Fusion Indices.

Fusion indices were determined for stable transfectants and control cells following six days in differentiation media. Each clone was initially seeded at 8.0×10^5 cells per 60 mm plate and induced to differentiate when confluent. Cells were fixed in 4% paraformaldehyde then stained with Harris Haematoxylin / 0.2% acetic acid and counterstained in Eosin solution. A minimum of 12 random fields was assayed. The total number of nuclei per field and the number of nuclei (3 or more) per myotube were counted and fusion indices were calculated as: (number of nuclei in myotubes / total nuclei in each field) x 100. The fusion index for each clone was taken as average ± standard error of the mean fusion index and the significance of the results relative to control cells was determined using ANOVA.

Immunoprecipitations.

C2C12 cells transiently transfected with GFP and 6Myc expression constructs were lysed thirty-six hours post-transfection with RIPA buffer as described above. To eliminate nonspecific interactions, clarified cell lysates were precleared with Protein A/G Plus agarose-conjugated beads (Santa Cruz) for 15 minutes at 4°C with constant rotation. Precleared lysates were retained and protein contents were measured. For each immunoprecipitation condition, 350 µg of total protein was used and samples were diluted 1:1 in PBS. Immunoprecipitations were performed by incubating lysates with

anti-myc 9E10 monoclonal antibodies (1:100), purified rabbit IgG's or beads only overnight at 4°C with constant rotation. Immune complexes were captured with the addition of equivalent amounts of prewashed Protein A/G Plus agarose-conjugated beads to each sample for four hours at 4°C. Immunoprecipitated proteins bound to the protein A/G-agarose beads were washed extensively and then resuspended in 2X SDS-PAGE loading buffer. Immune complexes were eluted from the protein A/G-agarose beads by boiling, resolved by SDS-PAGE and then subjected to immunoblot analysis.

In vivo interaction assay.

Sequences encoding the first 454 amino acids of SLMAP (SLMAPN) was generated by PCR amplification of full length SLMAP rabbit clone (Accession # U21157) using primers 5'-GGAATTCATGCCGTCAGCCTTGGCCATC and 3'-CGAATTCACAG AAGGGACAAGCTGAG. Primers 5'-GGAATTCGATGCCGTCAGCCTTGGC and 3'-GATGCCAGCTTCTAGAGGGAGGACG were used to PCR amplify the SLMAP sequence encoding amino acids 454-775 (SLMAPC). SLMAPC cDNA with leucine zipper deletions (aa 597-667; SLMAPCΔLZ) was amplified from template SLMAP3M1ΔLZ using primers 5'-GGGAATTCATGGATGAGCAAGACCTG and 3'-CCGTCTAGATCATTGGAGCAGCTTCAGGTTGTC. SLMAPN PCR product was EcoR1/BamH1 digested and the SLMAP-C and SLMAP-CΔLZ PCR products were EcoR1/Xba1 digested. Digested SLMAP products were used for insertion into the same sites of (i) pM in frame with the GAL4 DNA-binding domain (DND-BD) or (ii) pVP16 activation domain (AD) vector (Mammalian Matchmaker Two Hybrid Assay Kit, Clontech).

Subconfluent C2C12 myoblasts grown on 60 mm plates were co-transfected with 1 μg of mammalian CAT reporter vector (pG5CAT) containing five consensus GAL4 binding sites, 1 μg of the β-galactosidase expression plasmid (pCMV-LacZ) and 2 μg of recombinant plasmids derived from pM and pVP16 (Clontech) using the Lipofectame Plus™ transfection reagent (Gibco BRL). For a positive control (sample 14), cells were co-transfected with 1 μg of pG5CAT, 1 μg pCMV-LacZ, 1 μg of pVP16-T (VP16 AD to SV40 target antigen known to interact with p53) and 1 μg of pM53 (fusion of GAL4 DNA-BD to mouse p53 protein). Forty-eight hours after transfection, cells were lysed in 0.25 M Tris-HCl, pH 7.8 by two rounds of freeze-thaw and then centrifuged at 10,000xg for 10 minutes. Samples were heated to 65°C for 10 minutes, cooled on ice then combined with CAT assay buffer (135 mM TRIS pH 7.8, 1.6 mM chloramphenicol, 0.74 μCi ^{3}H-acetyl CoA). Mixtures were heated to 37°C for 1 hour then extracted with ice-cold ethyl acetate. Extracts were centrifuged at 10,000 xg for 10 minutes and the aqueous phase was retained for quantification of radioactivity (^{3}H) using a liquid scintillation counter. The levels of CAT activity were normalized to the β-galactosidase activity in the respective cell extracts. Basal CAT activity (sample #1 control) was set as 1 and the fold induction of CAT activity was calculated as cpm (samples #2-14)/ basal CAT activity.

Results.

SLMAP expression in developing skeletal muscle.

As a first step toward understanding the function of SLMAPs in skeletal muscle, we examined the *in vivo* distribution of SLMAP in developing and mature skeletal

muscle. Fusion protein antibodies generated to the carboxyl-terminal sequences of SLMAP (28) were used to detect SLMAP localization in cryosections of tissue from developing mice (11-18 days post coitum; d.p.c.) as well as in adult skeletal muscle (Figure 1). As illustrated in Figure 1A (a) SLMAP expression was detected in developing somites at 11 d.p.c. Early in development (11-13 d.p.c), SLMAP labelling was primarily observed at punctate clusters along the length of the myotube (Figure 1A; a,b). Prior to the myotube to myofiber transition (15 d.p.c.), SLMAP distribution became increasingly well organized and was abundant at reticular formations and fine longitudinal structures (Figure 1A; c), consistent with the organization of the developing SR and T-tubules (21, 22). This SLMAP-specific staining pattern was clearly evident in skeletal muscle examined at later stages in development (18 d.p.c.; Figure 1A; d,e) and was also observed in cryosections of adult tibialis anterior muscle (Figure 1B, a-c).

To more closely examine the subcellular localization of SLMAPs in developing and skeletal muscle, double immunofluorescent labelling was performed using various muscle-specific antibodies. We first examined the arrangement of SLMAPs relative to myofibril components by co-staining with α-actinin 2, an actin filament crosslinking molecule present at the Z-line of myofibrils. Staining with the Z-line marker clearly revealed a striated pattern at 11 d.p.c. and at 13 d.p.c. (Figure 2A; b, e). In view of the punctate SLMAP-specific labelling, the distribution of SLMAP relative to α-actinin 2 was difficult to resolve by confocal microscopy at 11 d.p.c. (Figure 2A; a, c) and 13 d.p.c. (Figure 2A; d, f). The observed punctate SLMAP labelling is thought to reflect the immature organization of SLMAP in developing somites, as later in development (18 d.p.c.) SLMAP (Figure 2B; a, c, d, f) was shown to clearly associate with distinct

structures flanking the myofibril Z-line (Figure 2B; b, c, e, f). In skeletal muscle analyzed at 18 d.p.c. as well as mature adult skeletal muscle (Figure 2C), the majority of SLMAP labeling was distinct from that of α-actinin and was primarily detected as a continuous network around and between the myofibrils as well as fine longitudinal structures oriented perpendicular to the Z-line.

SLMAP labelling appeared to extend to peripheral structures in skeletal muscle, indicative of SLMAP association with the plasma membrane (Figure 2B; d). Caveolin 3 belongs to a family of integral membrane proteins, which constitute a subcompartment of the plasma membrane known as caveolae. Immunolocalization studies have reported that caveolin 3 coincides with the distribution of dystrophin at the skeletal muscle fiber surface (31); thus monoclonal caveolin 3 antibodies were used in our studies to demarcate these surface membrane regions. As illustrated in Figure 3A, caveolin 3-specific antibodies revealed a distinct labeling pattern at the peripheral membrane, without labeling internal membrane structures in developing muscle at 15 d.p.c. (Figure 3A; b), 18 d.p.c. (Figure 3A; e) or adult soleus muscle (Figure 3A; h). In contrast, SLMAP antibodies labelled internal reticular structures in developing and adult skeletal muscle (Figure 3A; a, d, g) and revealed some co-distribution with caveolin 3 at the plasma membrane sub-domains (Figure 3A; c, f, i). Since the reticular-like distribution of SLMAPs appeared consistent with the distribution of components associated with developing SR and T-tubules, skeletal muscle of older embryos (18 d.p.c.) and adult soleus muscle were co-stained with SLMAP antibodies and markers of these membrane systems. In longitudinal and transverse cryosections of developing skeletal muscle (18 d.p.c.) and adult skeletal muscle, SLMAP co-localized with the Ca^{+2}ATPase, a marker of

longitudinal SR membrane system (Figure 3B; a-i). This codistribution with the SR marker was observed within clusters in transverse cryosections of developing skeletal muscle (18 d.p.c.) (Figure 3B; d-f) and adult soleus muscle (Figure 3B; g-i). In longitudinal cryosections (18 d.p.c.), SLMAP and the Ca^{+2}-ATPase were co-localized at cross striations along the length of the myofibres (Figure 3B; a-c). To determine the localization of SLMAP relative to the T-tubules, dual immunostaining was performed using antibodies that specifically recognize the α-1 subunit of the dihydropyridine (DHP) receptor (Figure 3C). Under various experimental conditions, a clear signal for the DHPR α-1 subunit could not be resolved in developing skeletal muscle by confocal microscopy, thus immunostaining of mature skeletal muscle is presented. Consistent with the mature organization of T-tubules, the α-1 DHP receptor antibody labelled membrane clusters in transverse cryosections of adult muscle (Figure 3C; b, e). Some co-localization of the DHP receptor was evident with SLMAP as yellow staining (Figure 3C; c, f). The combination of deconvolution and three-dimensional image analyses of muscle sections labelled with SLMAP antibodies and the surface membrane markers, anti-caveolin-3 and the DHP receptor (Figure 3D), demonstrated that SLMAP localized to discrete regions in the cellular interior, and at the cell's periphery. By deconvolution microscopy, there is some co-localization of SLMAP with caveolin-3 (Figure 3D, panel A), and with the DHP receptor (Figure 3D, panel B) as indicated by the white voxels. Taken together, the above data indicates that SLMAP is a component of both the surface membrane and the SR.

Induction of ~ 80kDa SLMAP isoform during muscle differentiation.

In view of the observation that SLMAP is expressed early in developing skeletal muscle, we assessed whether SLMAP transcript and protein levels are regulated during skeletal muscle differentiation. The C2C12 myoblast cell line derived from mouse femoral muscle satellite cells is a well established *ex vivo* model of skeletal muscle differentiation (31, 32). In mitogen rich media, C2C12 cells proliferate as myoblasts and can be induced to differentiate by withdrawing serum from the culture media. Following mitogen depletion, myoblasts undergo biochemical and morphological differentiation as confirmed by the induction of muscle-specific gene expression and myoblast fusion to produce elongated multinucleated myotubes.

By immunoblot analysis, undifferentiated C2C12 myoblasts exclusively expressed a 91 kDa SLMAP protein (Figure 4B; lane 0). The previously characterized anti-SLMAP rabbit antibodies used were specific for the detection of SLMAP proteins by immunoblot analysis since no signal was observed following immunoabsorption of SLMAP antibodies with bacterially synthesized SLMAP proteins (Figure 4C; lane 0). We investigated whether SLMAP transcript (Figure 4A) and protein (Figure 4B) levels are altered during the time course of myogenic differentiation. By Northern blot analysis, the biochemical differentiation of C2C12 cells was monitored based on the induction of myogenin mRNA expression as this bHLH transcription factor myogenin is expressed early in skeletal muscle differentiation program and is critical for myoblast fusion (33-36). Induction of myogenin mRNA expression was detected as early as 24 hours following removal of mitogens from the culture media and its expression level increased as the differentiation program progressed (Figure 4A). Morphological differentiation was verified on the basis of myotube formation, which occurred approximately two days

following the removal of mitogens from the media. A 5.9 kb SLMAP transcript was expressed in undifferentiated C2C12 myoblasts and corresponds to the transcript encoding SLMAP3 (Figure 4A). No discernible change in the level of SLMAP transcript expression was detected during the course of differentiation, nor were other SLMAP transcripts expressed as differentiation progressed in these cells.

SLMAP protein levels were next examined to determine whether SLMAP undergoes post-transcriptional regulation during differentiation. Whereas MyoD was expressed in differentiating myoblasts as well as in undifferentiated cells committed to the myogenic lineage (data not shown), myogenin protein expression was observed only following induction of myotube formation (Figure 4B). The ubiquitous 91 kDa SLMAP isoform was expressed in both proliferating myoblasts and in differentiated myotubes. Interestingly, SLMAP antibodies also recognized a differentiation-induced ~80 kDa protein (Figure 4B, lanes 1-7). Immunoabsorption of SLMAP antibodies with bacterially expressed SLMAP fusion proteins further established the antibody specificity for the ~80 kDa SLMAP variant (Figure 4C; lane 7). Densitometric analysis confirmed that the expression level of the ~80 kDa SLMAP protein increased as differentiation progressed, whereas expression of the 91 kDa protein remained relatively constant (Figure 4D). To address the question of a specific link between the induction of the ~80 kDa SLMAP protein and cell cycle withdrawal, SLMAP protein expression was examined in two nonmyogenic cell lines. Withdrawal from the cell cycle was induced in HeLa and NIH 3T3 fibroblast cells by culturing these cells under serum-starvation conditions (0.5% FBS in DMEM, 48 hours). The ~80 kDa SLMAP protein was not detected by immunoblot analysis of protein extracts from serum starved cells (data not shown).

Forced expression of SLMAP in myoblasts affects morphological differentiation.

In order to assess whether the temporal induction of the SLMAP isoform was critical for myotube formation, we ectopically expressed SLMAP in C2C12 myoblasts and examined their ability to undergo biochemical and morphological differentiation. Expression plasmids containing full-length SLMAP sequences fused to the 6Myc epitope tag (6Myc-SLMAP3; Figure 5A) was transfected into C2C12 cells and selected in G418 for stable expression. Interestingly, C2C12 myoblasts overexpressing SLMAP3 cultured for six days in differentiation promoting conditions showed a significant reduction in the number of myotubes relative to the control transfectants (Figure 5B,C). To further the effect of SLMAP overexpression on myoblast fusion, additional 6Myc-SLMAP variants were generated including a variant lacking amino acids 1-315 of SLMAP3 (6Myc- ΔN SLMAP), SLMAP1 expressing the constitutively active transmembrane domain (TM; 6Myc-SLMAP1-TM) as well as a transmembrane domain mutant (6Myc-SLMAP1ΔTM) (Figure 5A). Consistent with the overexpression of the full-length molecule in myoblasts, forced expression of both the membrane associated SLMAP variants (6Myc-ΔNSLMAP; 6Myc-SLMAP1-TM) and the transmembrane domain mutant (6Myc-SLMAP1ΔTM) elicited a significantly reduced (>90% inhibition) capacity for myotube formation (Figure 5B, C). The level of ectopically expressed SLMAP protein was quantified for each transfected myoblast and it`s level relative to endogenous SLMAP varied from 0.5 to 1.5-fold for the full length SLMAP to 1 to over 5-fold for the shorter deletion mutants. Irrespective of the level of SLMAP expression, each transfectent gave the same degree of inhibition of myoblast fusion. It should be noted that the control for

these experiments represented myoblasts transfected with the 6Myc-pcDNA3 vector and that Myc-epitope tagged proteins have also been used by others to study myoblast fusion and differentiation (53).

To determine whether the effect on fusion observed with SLMAP overexpression was attributed to defective biochemical differentiation, we monitored the expression of skeletal muscle specific proteins by immunoblot analysis. Expression of the early differentiation marker, myogenin and muscle-specific myosin heavy chain (MyHC) was induced in each of the SLMAP over-expressing clones (Figure 6). The relative level of expression of these polypeptides in fusion defective myoblasts with respect to the mock transfected clones after day 5 of differentiation was 1.28 for MyHc and 0.99 for myogenin as quantified by densitometery. The fusion defects observed due to inappropriate induction of SLMAPs were therefore not a consequence of inhibition of biochemical differentiation of myoblasts, rather these findings suggest that regulated levels of SLMAPs are critical for the proper fusion of membranes.

SLMAP homodimerization is mediated by the leucine-rich coiled-coils

Coiled-coil motifs, are known to mediate protein oligomerizations and constitute a primary structural feature of the SLMAP polypeptides (28, 29). To assess the potential for SLMAP oligomerization, we performed co-immunoprecipitation experiments using C2C12 cells transfected with GFP- and 6Myc-epitope tagged SLMAP polypeptides (Figure 7A). C2C12 were co-transfected with constructs encoding 6Myc-SLMAP3 (102 kDa) and the GFP-ΔNSLMAP variant (72 kDa) (Figure 7B); or were co-transfected with constructs encoding the 6Myc-SLMAP1 variant (49 kDa) and the GFP-

ΔNSLMAP variant (72 kDa) (Figure 7C). Immunoblotting with monoclonal anti-myc antibodies were used to confirm the presence of the 102 kDa 6Myc-SLMAP3 protein (Figure 7B; second panel, red star) as well as the 49 kDa 6Myc-SLMAP1 (Figure 7C; second panel, orange star) in lysates (L) of transfected cells. In lysates of transfected cells, SLMAP antibodies recognized the 6Myc-tagged SLMAP proteins and the GFP-ΔNSLMAP variant (Figure 7B and C; first panel; lane L). Immunoblot analysis demonstrated each of the 6Myc-SLMAP variants were specifically immunoprecipitated by anti-myc monoclonal antibodies (Figure 7B and C; second panel, lane M). Association of the 6Myc-SLMAP3 protein with the GFP-ΔNSLMAP protein was confirmed by immunoblot analysis using SLMAP antibodies (Figure 7B; first panel; lane M). The carboxyl terminal sequences present in SLMAP are responsible for this interaction as 6Myc-SLMAP1 specifically precipitated the GFP-ΔNSLMAP protein (Figure 7C, first panel; lane M). These results demonstrate that SLMAPs are able to self-assemble and this association is mediated by carboxyl terminal SLMAP sequences.

Previous sequence analyses of the carboxyl sequences conserved in each of the SLMAP isoforms have identified a leucine-rich coiled-coil motif (28). As this specialized form of coiled-coil structure is known to serve as an oligomerization motif, which can modulate protein activity in various proteins (37-40), we reasoned that the leucine-rich coiled-coil present in SLMAPs mediate SLMAP-SLMAP interactions. An *in vivo* interaction assay was therefore used to address this issue, whereby myoblasts were co-transfected with the chloramphenicol acetyl-CoA transferase (CAT) reporter construct and SLMAP variants encompassing amino-terminal (SLMAP(N)) or carboxyl-terminal sequences (SLMAP(C)) fused to either the VP16 activation domain or the GAL4 DNA-

binding domain (DNA-BD) (Figure 8A). CAT gene expression was monitored forty-eight hours post-transfection and basal levels were determined in lysates from control transfectants (Figure 8B; lanes 1-4). The level of CAT induction was similar to basal levels in cells co-transfected with either: SLMAP(C) and SLMAP(N) constructs (Figure 8B; lane 6) fused to either the AD or DNA-BD; or SLMAP(N) and SLMAP(N) fused to the AD or DND-BD (Figure 8B; lane 5). A significant induction of CAT activity above basal levels (104 fold) was measured in the lysates of cells co-transfected with SLMAP(C)-AD construct and the SLMAP(C)-DNA-BD construct, confirming that the SLMAP carboxyl terminal containing sequence information is essential for SLMAP homodimerization (Figure 8B, lane 8). Since the leucine-rich coiled coil motifs are encoded within this region of SLMAP, leucine-rich coiled coil mutants fused to the AD and DNA-BD constructs were generated (SLMAPΔLZ). The leucine-rich coiled coil mutant (SLMAPCΔLZ) failed to activate expression of the CAT reporter gene above basal levels (Figure 8B; lanes 9-11). The leucine-rich coiled coil motifs of an unrelated protein, ninein (Accession No. NM008697) were fused to the GAL4 DNA binding domain and cotransfected with carboxyl-terminal SLMAP sequences fused to the VP16 activation domain (Figure 8B; lane 12). These conditions did not result in activation of CAT reporter expression and suggest that the leucine-rich coiled coil in SLMAP specifically mediate SLMAP-SLMAP associations. On the basis of these results, we have concluded that the leucine-rich coiled coil motifs constitute the physical interaction sites necessary for SLMAP homodimer formation.

We next assessed whether the defective fusion phenotype observed in cells overexpressing SLMAP was attributed to inappropriate SLMAP homodimer formation.

To address this issue, myoblasts were stably transfected with a SLMAP mutant lacking the leucine-rich coiled-coil and induced to differentiate as previously described. Fusion indices were calculated for the mutant and control cells after six days in differentiation media. In the absence of SLMAP-SLMAP interactions, a fusion defective phenotype was also observed in these (Figure 9), thus indicating that the deregulation of SLMAP oligomerization is not responsible for the defective myotube formation.

Discussion

The data presented indicate that SLMAP is expressed in a developmentally regulated manner and may serve a role in myoblast fusion and membrane function during myogenesis. The studies here reveal that the expression of SLMAP is initiated early during in vivo skeletal myogenesis and SLMAP proteins become distributed within specialized membrane systems involved in calcium signalling as development progressed. SLMAP expression was detected within somites at 11 d.p.c., when myogenic cells elongate and immature myofibrils appear (41). SLMAP expression levels increased as the fusion process was initiated in the developing embryo (13 d.p.c.) (41); thus suggesting that regulated SLMAP levels may be required for this crucial morphological process in skeletal muscle development. We observed that the morphological differentiation of myoblasts correlated with the induction of a novel ~80 kDa SLMAP isoform. There appeared to be a direct link between the onset of myotube formation and the induction of the ~80kDa SLMAP isoform. The appearance of the ~80kDa SLMAP variant was observed only upon initiation of myotube formation and is not a consequence of cell cycle withdrawal as it was not expressed in nonmyogenic cell lines forced to exit

the cell cycle. These data indicate that the temporal appearance of SLMAP isoforms during skeletal myogenesis appears to be specific for the differentiation process. SLMAP mRNA expression levels remained unchanged during the course of differentiation and both myoblasts and myotubes were found to express a single 5.9 kb mRNA transcript. Post-transcriptional regulation of SLMAP may provide the specificity of expression required during differentiation. In this regard, two initiating methionines have previously been identified within SLMAP mRNA which may account for the expression of the two different SLMAP isoforms observed during myotube formation (28).

The de-regulation of SLMAP by ectopic expression in myoblasts seriously compromised the ability of these cells to fuse into myotubes under differentiation promoting conditions. In spite of the impaired ability of SLMAP overexpressing myoblasts to form multinucleated myotubes, these cells remained permissive for biochemical differentiation since markers of skeletal muscle differentiation (myogenin, myosin heavy chain) were expressed under differentiation-promoting conditions. The fusion defect appeared to be independent of SLMAP association with membranes since the expression of mutants lacking the carboxyl terminal transmembrane domain also impaired the ability of myoblasts to fuse. The primary structure of SLMAP revealed that it has extended coiled-coil regions that may be ideal for protein-protein interactions. Protein-protein interaction assays demonstrated that SLMAP proteins can self assemble and that these interactions are mediated by the leucine-rich coiled coil motifs. Overexpression of SLMAP deletion mutants defective in the homodimerization domain also compromised the fusion of myoblasts. Thus the fusion-defective phenotype caused by deregulated expression of SLMAP in myoblasts strongly suggests that normal levels

of the polypeptide and the temporal induction of SLMAP isoforms may serve critical roles in the fusing of myoblasts.

The organized assembly of specialized membrane components (SR, T-tubules) relative to components of the contractile apparatus is a hallmark feature of differentiated muscle structure and function (46, 27). The distribution of SLMAP relative to the myofibrils and muscle membrane systems in developing and adult skeletal muscle indicated that it is a major component of the continuous membrane network around and between the myofibrils, consistent with the distribution of the SR and T-tubules. By confocal microscopy, SLMAPs were distributed along longitudinal structures perpendicular to the Z-line and were largely co-distributed with the SR Ca^{+2}ATPase in developing and adult muscle. Immunohistochemical labelling with anti-SLMAP and anti-α1-DHP receptor antibodies also showed that SLMAPs reside at the T-tubular membrane system. The observation that SLMAPs are distributed to SR and T-tubules suggests that SLMAPs may function as junctional membrane components that provide structural integrity, as has been recently described for junctophilin, another carboxyl-terminal anchored protein of the SR membrane, which binds the lipid moeties of the T-tubule membrane to organize junctional membrane complexes (47-50). The ability of SLMAPs to reside in different membrane systems and to homodimerize may allow this molecule to serve a role in membrane organization. The structural features of SLMAP indicate that these molecules belong to a superfamily of tail-anchored membrane proteins and share structural features with the syntaxins and synaptobrevins, which function in membrane fusion and regulate excitation-secretion coupling (42, 44, 45). By analogy our data imply that SLMAPs may serve to regulate myoblast fusion and EC coupling based on their

cellular locations and interactions. Topological studies suggest that the SLMAP molecule is oriented in the cytoplasm, thus providing the opportunity to assemble with other cytoplasmic, cytoskeletal and membrane components. Protein-protein interactions among membrane and cytoskeletal components represent an important feature of myoblast fusion. For instance, Galliano et al. (43) showed that the interactions between cytosolic portion of the transmembrane metalloprotease ADAM12 ("a disintegrin and metalloprotease) and α-actinin are necessary for myoblast fusion. Similarly, the cytoplasmically oriented coiled-coil SLMAP sequences may participate in association with other yet unidentified components of the sarcomeric cytoskeleton or signalling molecules participating in the fusion process. In this regard, our recent data suggests SLMAP may interact with microtubules and myosin (Guzzo et al., manuscript in preparation) and studies are in progress to determine the functional consequences of this interaction in fusing myoblasts and in the membrane biology of EC coupling.

Acknowledgements

This work was supported by the Heart and Stroke Foundation of Ontario (awarded to BST) and the Canadian Institutes of Health Research studentship (awarded to RMG). We would like to thank Dr. Andrew Ridsdale of the Loeb Research Institute (Ottawa, Canada) for his expert technical assistance in confocal microscopy; Carl MacIntosh and Dr. Jackie Vanderluit (University of Ottawa) for their guidance in isolating mouse embryos and Kim Wong (University of Ottawa) for technical assistance with cryostat sectioning.

References.

1. Bailey P, Holowacz T, Lassar AB. (2001). *Curr Opin Cell Biol.* **13**, 679-89.

2. Buckingham, M. (2001) *Curr. Opin. Genet. Develop.* **11**, 440-448.

3. Lassar, A.B., Skapek, S.X. and Novitch, A.F. (1994) *Curr. Opin. Cell Biol.* **6**, 788-794.

4. Sabourin, L.A. and Rudnicki, M.A. (2000) *Clin. Genet.* **57**, 16-25.

5. Pownall, M.E., Gustafsson, M.K. and Emerson, C.P. (2002) *Ann. Rev. Cell and Develop. Biol.* **18**, 747-783.

6. Wakelam, M.J. (1985) *Biochem. J.* **228**, 1-12.

7. Andres, V. and Walsh, K. (1996) *J. Cell Biol.* **132**, 657-66.

8. Walsh, K. and Perlman, H. (1997) *Curr. Opin. Genet. Dev.* **7**, 597-602.

9. Bate, M. (1990) *Develop.* **110**, 791-804.

10. Paululat, A., Holz, A. and Renkawitz-Pohl, R. (1999) *Mech. Develop.* **83**, 17-26.

11. Taylor, M.V. (2000) *Curr. Biol.* **10**, R646-R648.

12. Taylor, M.V. (2002) *Curr. Biol.* **12**, R224-R228.

13. Dworak, H.A. and Sink, H. (2002) *BioEssays* **24**, 591-601.

14. Doberstein, S.K., Fetter, R.D., Mehta, A.Y. and Goodman, C.S. (1997) *J. Cell Biol.* **136**, 1249-1261.

15. MacDonald, K.A., Lakonishok, M. and Horwitz, A.F. (1995) *J. Cell Sci.* **108**, 2573-2581.

16. Yagami-Hiromasa, T., Sato, T., Kurisaki, T., Kamijo, K., Nabeshima, Y. and Fujisawa-Sehara A. (1995) *Nature* **377**, 625-656.

17. Knudsen, K.A., Myers, L. and McElwee, S.A. (1990a) *Exp. Cell Res.* **188**, 175-184.

18. Knudsen, K.A. (1990b) *Curr. Opin. Cell Biol.* **2**, 902-906.

19. Zeschnigk, M., Kozian, D., Kuch, C., Schmoll, M. and Starzinski-Powitz, A. (1995). *J. Cell Sci.* **108**, 2973-2981.

20. Mege, R.M., Goudou, D., Diaz, C., Nicolet, M., Garcia, L., Geraud, G. and Rieger, F. (1992) *J. Cell Sci.* **103**, 897-906.

21. Franzini-Armstrong, C. (1991) *Develop. Biol.* **146**, 353-363.

22. Flucher, B.E., Phillips. J.L., Powell, J.A., Andrews, S.B. and Daniels, M.P. (1992) *Develop. Biol.* **150**, 266-280.

23. Flucher, B.E., Takekura, H. and Franzini-Armstrong, C. (1993) *Develop. Biol.* **160**, 135-147.

24. Takekura, H., Flucher, B.E. and Franzini-Armstrong, C. (2001) *Dev. Biol.* **239**, 204-214.

25. Seigneurin-Venin, S., Parrish, E., Marty, I., Rieger, F., Romey, G., Villaz, M. and Garcia, L. (1996) *Exp. Cell Res.* **223**, 301-307.

26. Franzini-Armstrong, C. and Jorgensen, A.O. (1994). *Ann. Rev. Physiol.* **56**, 509-534.

27. Flucher, B.E. and Franzini-Armstrong, C. (1996) *Proc. Natl. Acad. Sci. U.S.A.* **95**, 8101-8106.

28. Wigle, J.T., Demchyshyn, L., Pratt, M.A., Staines, W.A., Salih, M. and Tuana, B.S. (1997) *J. Biol. Chem.* **272**. 32384-32394.

29. Wielowieyski, P.A, Sevinc, S., Guzzo, R., Salih, M., Wigle, J.T. and B.S. Tuana (2000) *J. Biol. Chem.* **275**. 38474-38481.

30. Song, K.S., Scherer, P.E., Tang, Z.L., Okamoto, T., Li, S., Chafel, M., Chu, C., Kohtz, D.S. and Lisanti, M.P. (1996) *J. Biol. Chem.* **271**, 15160-15165.

31. Yaffe, D. and Saxel, O. (1977) *Nature* **270**, 725-727.

32. Blau, H.M., Chin, C.-P. and Webster, C. (1983) *Cell* **32**, 1171-1180.

33. Edmondson, D.G. and Olson, E.N. (1989) *Genes and Develop.* **3**, 628-40.

34. Wright, W.E., Sassoon, D.A. and Lin, V.K. (1989) *Cell* **56**, 607-617.

35. Hasty, P., Bradley, A., Morris, J.H., Edmondson, D.G., Venuti, J.M., Olson, E.N. and Klein, W.H. (1993) *Nature* **364**, 501-506.

36. Nabeshima, Y., Hanaoka, K., Hayasaka, M., Esumi, E., Li, S., Nonaka, I. and Nabeshima, Y. (1993) *Nature* **364**, 532-535.

37. Landshultz, W.H., Johnson, P.F. and McKnight, S.L. (1988) *Science* **240**, 1759-1764.

38. Adamson, J.G., Zhou, N.E. and Hodges, R.S. (1993) *Curr. Opin. Biotechnol.* **4**, 428-437.

39. Marx, S.O., Reiken, S., Hisamatsu, Y., Gaburjakova, M., Gaburjakova, J., Yang, Y.M., Rosemblit, N. and Marks, A.R. (2001) *J. Cell Biol.* **153**, 699-708.

40. Hulme, J.T., Ahn, M., Hauschka, S.D., Scheuer, T. and Catterall, W.A. (2002) *J. Biol. Chem.* **277**, 4079-4087.

41. Furst, D.O., Osborn, M. and Weber, K. (1989) *J. Cell Biol.* **109**, 517-527.

42. Hay, J.C. and Scheller, R.H. (1997) *Curr. Opin. Cell Biol.* **9**, 505-12.

43. Galliano, M.F., Huet, C., Frygelius, J., Polgren, A., Wewer, U.M. and Engvall, E. (2000) *J. Biol. Chem.* **275**, 13933-13939.

44. Jahn, R. and Sudhof, T.C. (1999) *Ann. Rev. Biochem.* **68**, 863-911.

45. Jahn R, Lang T, Sudhof T.C. (2003) *Cell* **112**, 519-533.

46. Franzini-Armstrong, C. (1994) *In* Myology. A.E. Engel and C. Franzini-Armstrong, editors. McGraw-Hill Inc., New York, 176-199.

47. Takeshima, H., Komazaki, S., Nishi, M., Iino, M. and Kangawa, K. (2000) *Mol. Cell* **6**, 11-22.

48. Ito, K., Komazaki, S., Sasamoto, K., Yoshida, M., Nishi, M. and Kitamura, K. (2001) *J. Cell Biol.* **154**, 1059-1067.

49. Komazaki, S., Ito, K., Takeshima, H. and Nakamura, H. (2002) *FEBS Lett.* **524**, 225-229.

50. Komazaki, S., Nishi, M. and Takeshima, H. (2003) *FEBS Lett.* **542**, 69-73.

51 Dan, P., Cheung, J.C.Y., Scriven, D.R.L. and Moore, E.D.W. (2003) *Am. J. Physiol. Heart Circ. Physio.l* 284, H1295-H1306.

52. Scriven, D.R.L., Dan, P. and Moore E.D.W. (2000) *Biophys. J.* **79**, 2682-2691.

53. Martin, B., Schneider, R., Janetzky, S., Waibler, Z., Pandur, P., Kuhl, M., Behrens, J., von der Mark, K., Starzinski-Powitz, A. and Wixler, V. (2002) *J Cell Biol.* **159**, 113-122

Fig. 1. SLMAP expression in developing and adult skeletal muscle. **(A)** Formalin-fixed frozen sections (6-10 μm) of mouse embryos at stages 11 d.p.c.(a); 13 d.p.c. (b) 15 d.p.c. (c); and 18 d.p.c. (d, e) were labelled with rabbit polyclonal antibodies to SLMAP (28). SLMAP-specific antibodies labelled developing somites (a) as well as punctate structures in longitudinal sections of skeletal muscle at 13 d.p.c. (b). Later in development (d-e), SLMAPs staining revealed a more prominent and increasingly organized distribution within reticular formations in both longitudinal (c,d) and transverse (e) sections. **(B)** Confocal images showed SLMAP to be distributed along transverse bands in longitudinal cryosections of adult rat tibialis anterior muscle stained with SLMAP antibodies. Scale bar = 25 μm.

Figure 1 Chapter 2

A.

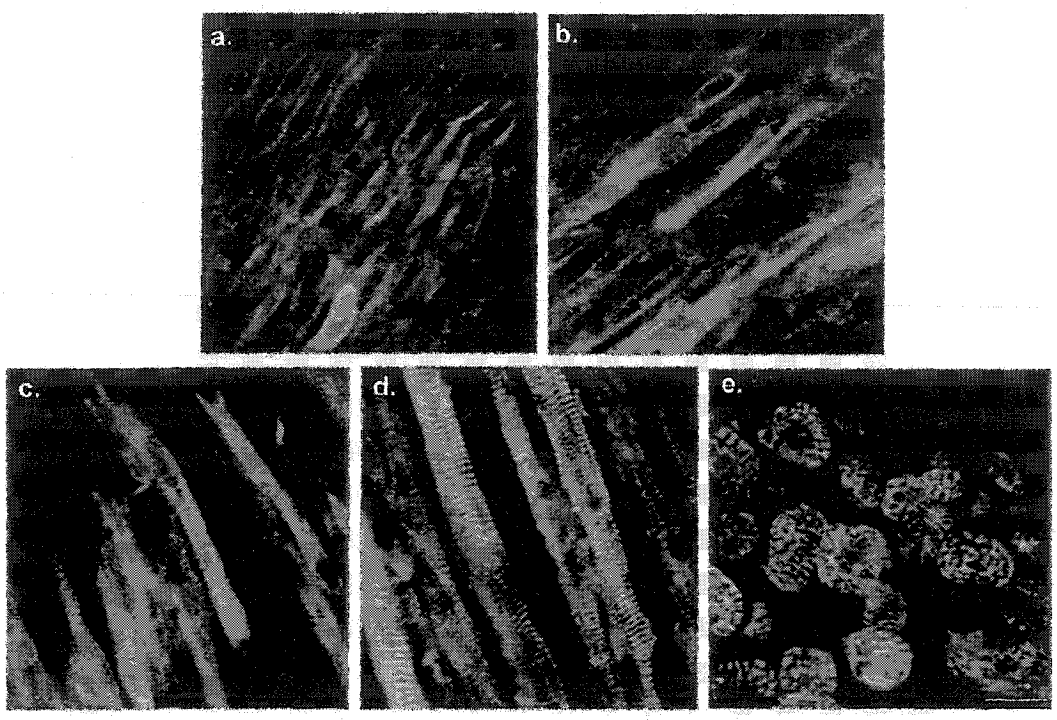

B.

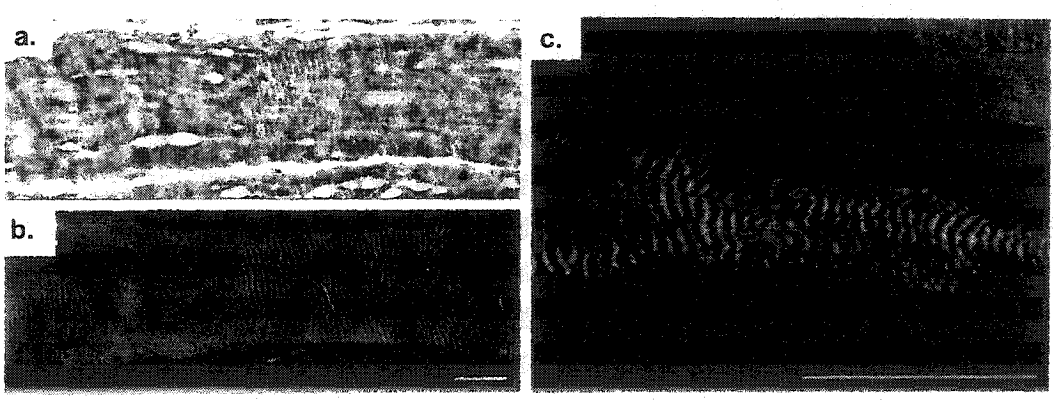

Fig. 2. Distribution of SLMAP relative to myofibril arrangement in developing and adult skeletal muscle. Cryosections of whole mouse embryos were simultaneously stained for SLMAP and the myofibril marker α-actinin. **(A)** At 11 d.p.c. (a-c) and 13 d.p.c. (d-f), α-actinin (b, e) was clearly distributed along striated structures demarcating the Z-lines of developing skeletal myofibrils. In contrast, punctate SLMAP labelling was observed in skeletal muscle at 11 d.p.c. (a) and 13 d.p.c. (d). At this stage, the overlap of the SLMAP signal with the α-actinin signal (c, f) is attributed to the immature organization of SLMAP. **(B)** At 18 d.p.c., SLMAP antibodies (a, d) predominantly stained structures flanking the α-actinin stained Z-line (b, e). When images were overlaid, it was evident that SLMAPs are largely distributed in structures surrounding the myofibrils (c, f). **(C)** In transverse cryosections of adult soleus muscle, SLMAP antibodies (a) consistently labelled structures flanking the Z-line stained by α-actinin (b). A merge of SLMAP (a) and α-actinin (b) signals is shown in (c). Scale bar = 10 μm.

A.

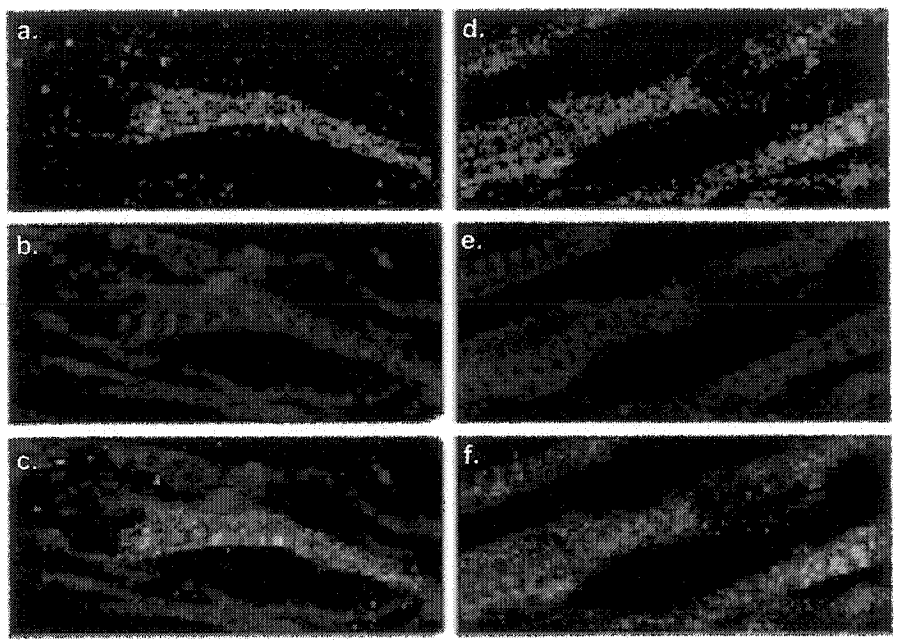

B.

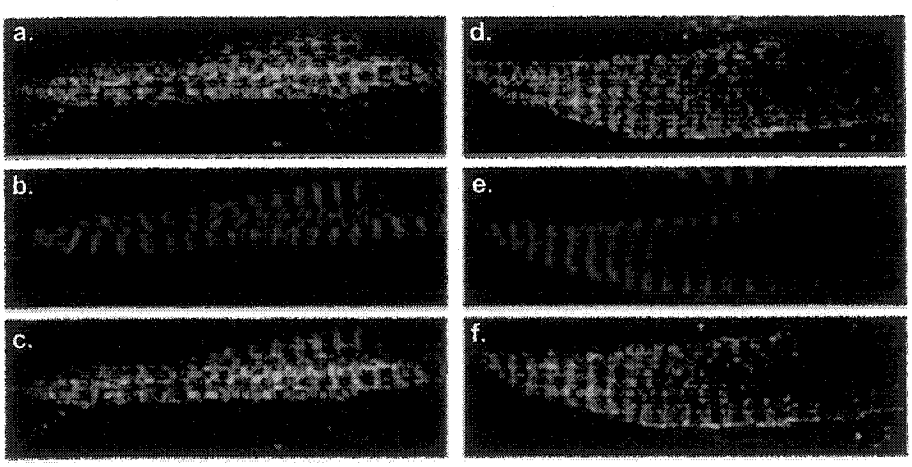

C.

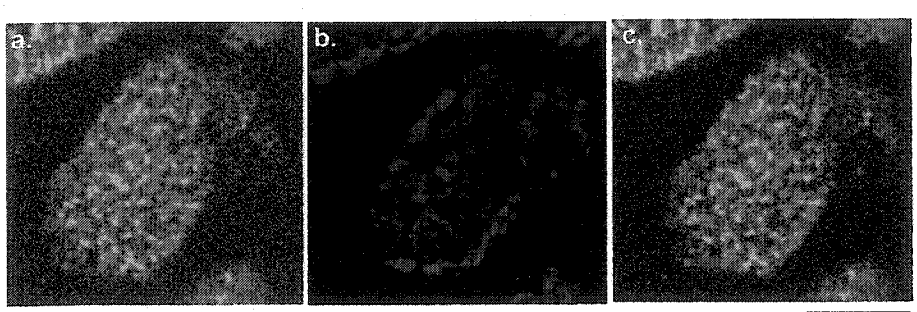

Fig. 3. SLMAP localization relative to membrane structures. (A) Caveolin 3 specific labelling (b, e, h) is associated with the subcompartment of the skeletal muscle surface membranes at 15 d.p.c. (a-c), 18 d.p.c. (d-f) as well as in mature soleus muscle (g-i). SLMAP distribution (a, d, g) was distinct from that of caveolin 3 as evidenced by SLMAP staining at sub-sarcolemmal membrane associated structures. Merged images of SLMAP and caveolin 3 stained sections are shown in (c, f, i).

Figure 3A

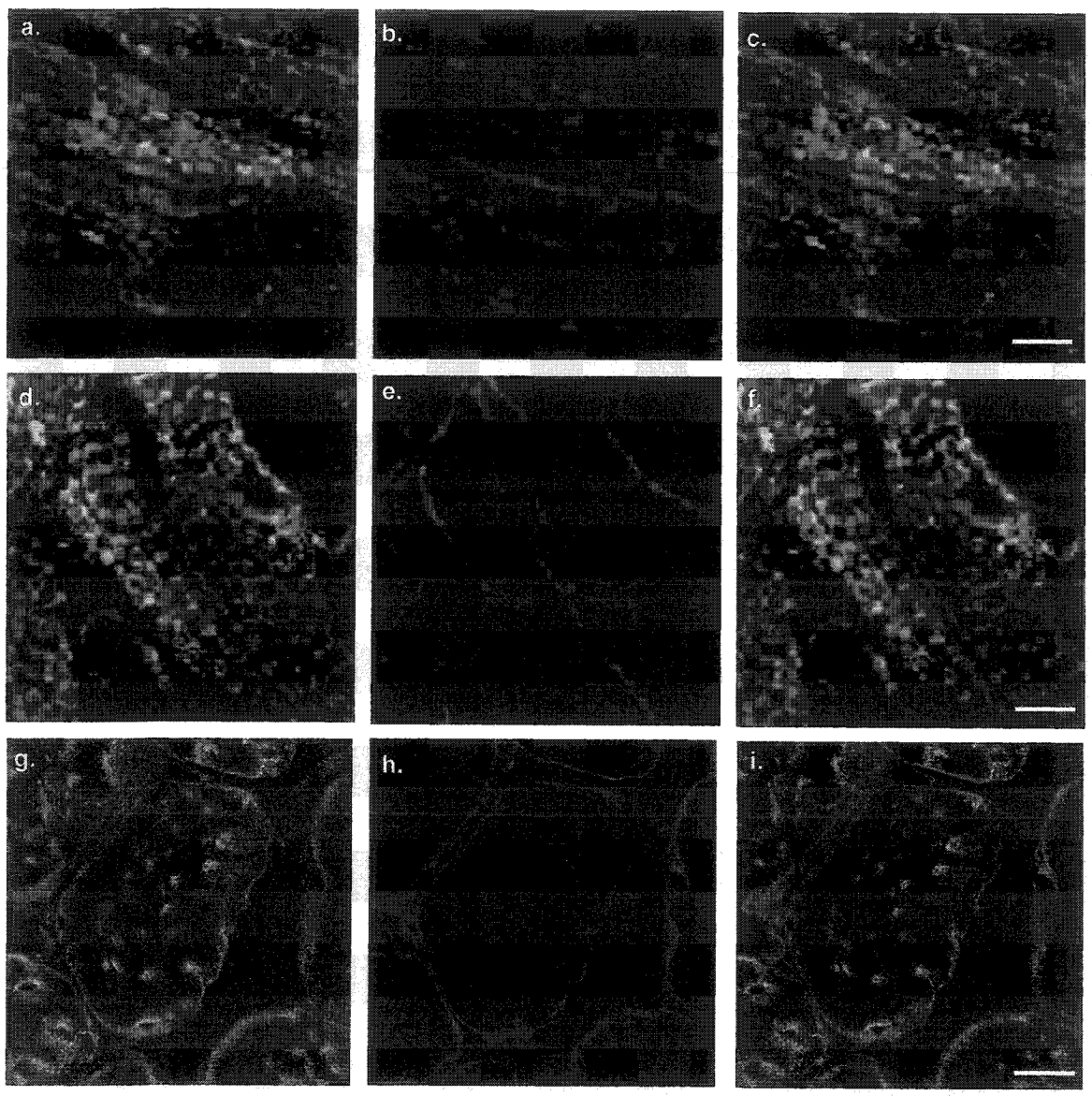

Fig. 3. SLMAP localization relative to membrane structures. (B) Co-localization (c, f, i) of SLMAP (a, d, g) with the sarcoplasmic reticulum Ca^{2+} ATPase (b, e, h) was consistently observed in developing skeletal muscle (18 d.p.c.; a-f) as well as in adult soleus muscle (g-i).

Figure 3B

Chapter 2

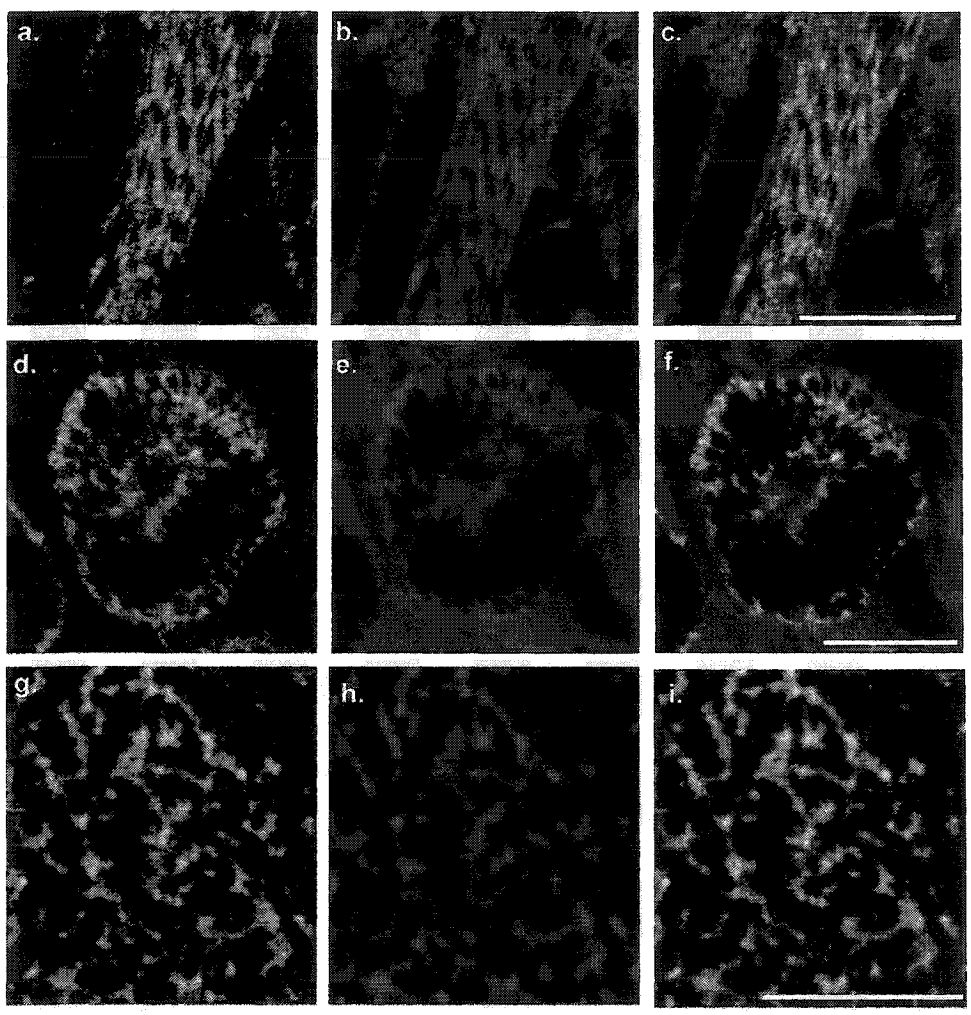

Fig. 3. SLMAP localization relative to membrane structures. **(C)** The α1-subunit of the DHP receptor (b, e) was used to identify T-tubules in adult soleus muscle. Regions of DHP receptor co-localization with SLMAP (a, d) are shown in yellow (c, f). Scale bar = 10 μm.

Figure 3C

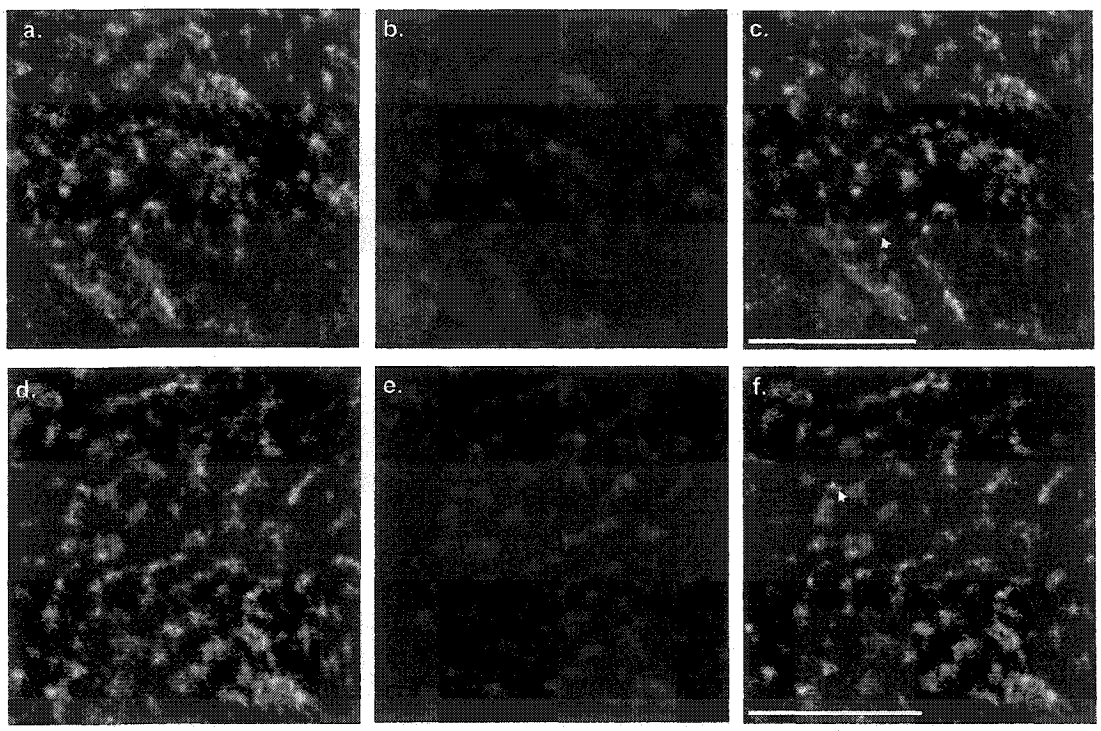

Fig. 3. SLMAP localization relative to membrane structures. **(D)** Three dimensional reconstruction of confocal images are presented for embryonic skeletal muscle (18 d.p.c.) co-stained with SLMAP and caveolin (panel A) or SLMAP and DHP receptor (panel B). Each image is a three-dimensional reconstruction of the indicated depth and colocalized voxels are shown in white. (a) Staining for caveolin-3 is shown in red and SLMAP staining is shown in green. The image is 8 μm deep. (b) DHP receptor staining is shown in red and SLMAP staining is shown in green. The image is 7.75 μm deep. Scalebar = 5 μm in each dimension.

Figure 3D **Chapter 2**

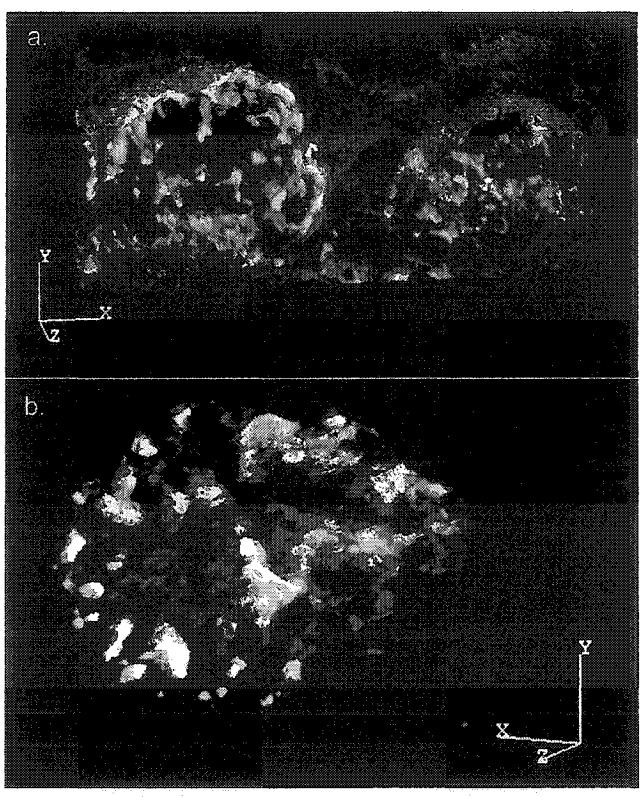

Fig. 4. SLMAP transcript and protein expression during myogenic differentiation. **(A)** SLMAP mRNA expression was assessed in C2C12 myoblasts (lane 0) and differentiating C2C12 myotubes at various days (lanes 1-5) following the removal of mitogens from the culture media. The 5.9kb SLMAP transcript was expressed in undifferentiated (lane 0) and in differentiating C2C12 myotubes (lanes 1-5). Myogenin mRNA expression is induced upon initiation of the myogenic differentiation program (lanes 1-5). To indicate the integrity of the RNA samples and equivalent loading, the expression of the GADPH transcript is shown. **(B)** Western blot analysis demonstrated that undifferentiated C2C12 cells (myoblasts) express a 91kDa SLMAP isoform (lane 0). An 80 kDa SLMAP isoform is induced upon C2C12 differentiation (lanes 1-7). Myogenin and MF20 (myosin heavy chain) antibodies were used as markers of skeletal muscle differentiation and α-tubulin antibodies were used to control for equivalent loading. The 91 kDa SLMAP isoform is expressed in undifferentiated myoblasts and at all timepoints following onset of differentiation; whereas the 80 kDa SLMAP isoform was detected only in differentiating cells. **(C)** Immunoabsorption of SLMAP antibodies with bacterially expressed SLMAP-maltose binding protein was performed to confirm the specificity of the antibody for the 91kDa SLMAP protein in undifferentiated C2C12 myoblasts (lane 0). Antibody specificity for the 80 kDa SLMAP protein expressed in differentiating C2C12 cells (lane 7) was also demonstrated. **(D)** Densitometric analysis of SLMAP expression levels during differentiation. Western blots represented in (B) were analyzed using the SCION software. Densitometry values (y-axis, arbitrary units) were normalized against α-tubulin levels measured for each day in differentiation media (x-axis). Increased expression of the differentiation-specific 80kDa SLMAP isoform was observed with increased time in differentiation media.

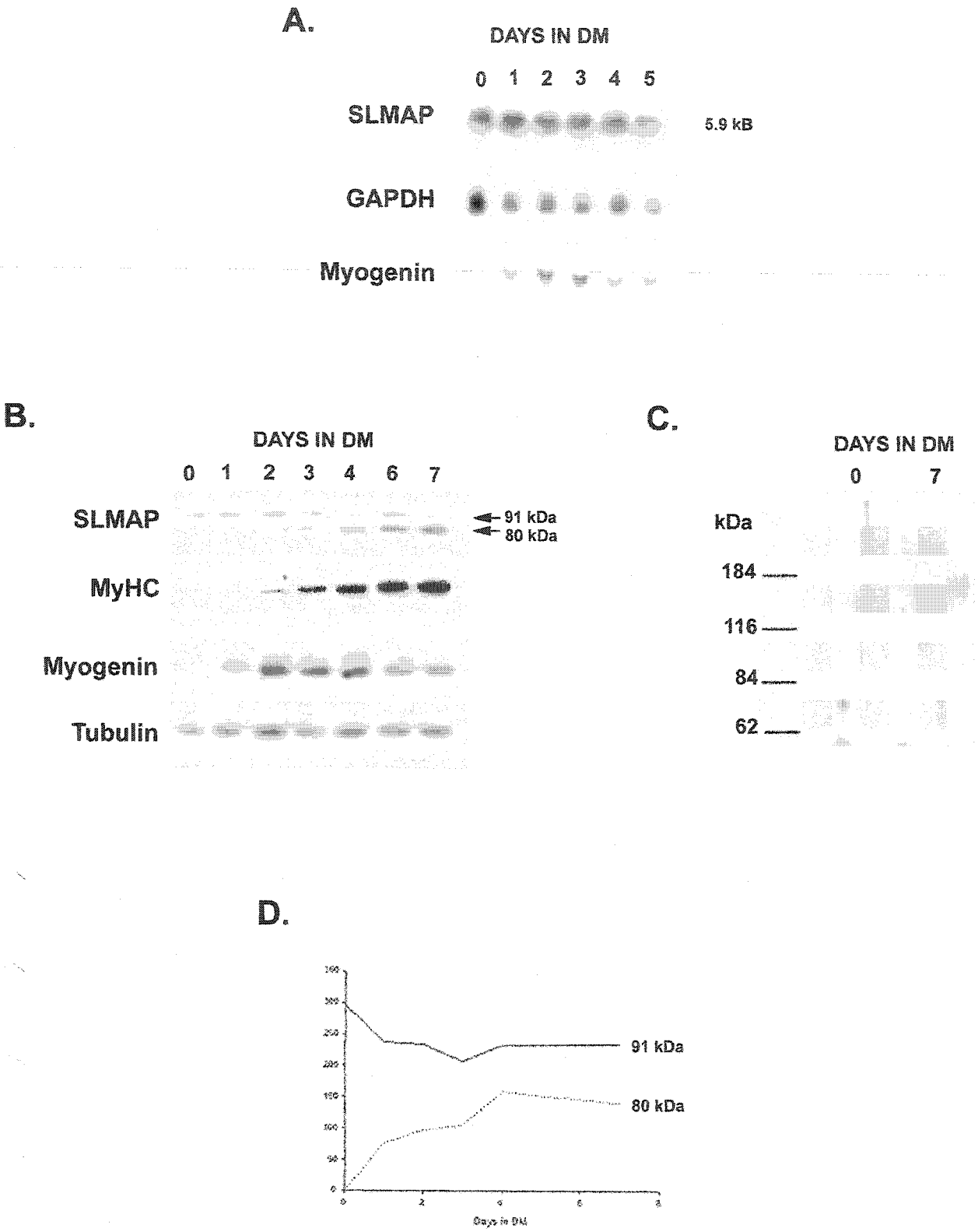
A.
DAYS IN DM
0 1 2 3 4 5
SLMAP
5.9 kB
GAPDH
Myogenin
B.
DAYS IN DM
0 1 2 3 4 6 7
SLMAP
91 kDa
80 kDa
MyHC
Myogenin
Tubulin
C.
DAYS IN DM
0 7
kDa
184
116
84
62
D.
91 kDa
80 kDa

Fig. 5. SLMAP overexpression affects the morphological differentiation of C2C12 myoblasts. **(A)** Schematic representation of the 6Myc-tagged SLMAP expression constructs used for stable transfections in C2C12 myoblasts. M1 and M2 refer to the two divergent initiating methionines identified in SLMAP3 (28). **(B)** Morphology of differentiating C2C12 myoblasts stably transfected with control 6Myc-pcDNA3 (a); 6Myc-SLMAP3 (b), 6Myc-SLMAP1 (c) and 6Myc-SLMAP1ΔTM (d). 6Myc-positive C2C12 clones were differentiated for 6 days in differentiation medium, fixed with 4% paraformaldehyde, stained with haematoxylin and eosin and then photographed. **(C)** Reduced myotube formation was observed in C2C12 myoblasts that were stably transfected with 6Myc-SLMAP variants. Fusion indices were calculated as described in Experimental Procedures. Error bars represent standard deviation for each clone.

Figure 5

A.

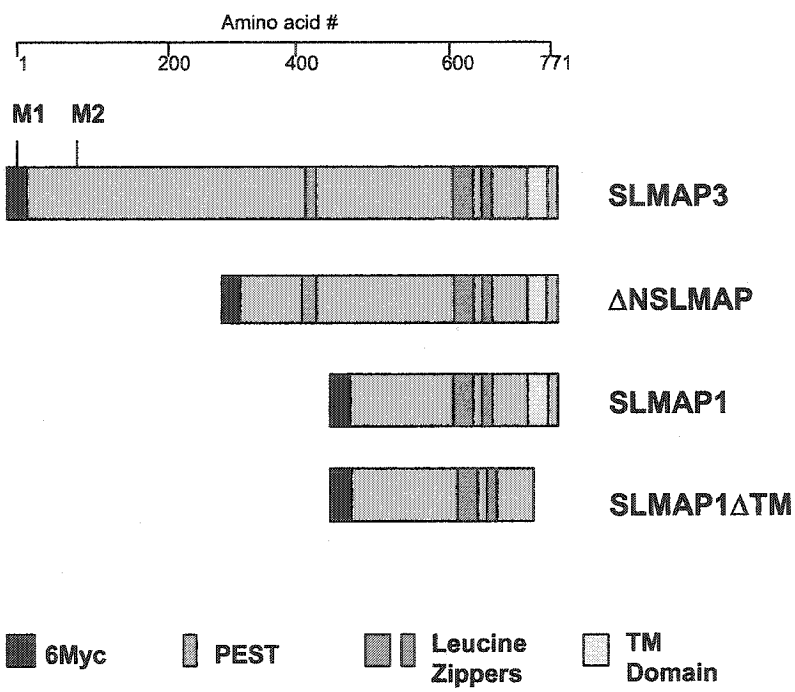
Amino acid #
1
200
400
600
771
M1
M2
SLMAP3
ΔNSLMAP
SLMAP1
SLMAP1ΔTM
6Myc
PEST
Leucine Zippers
TM Domain

B.

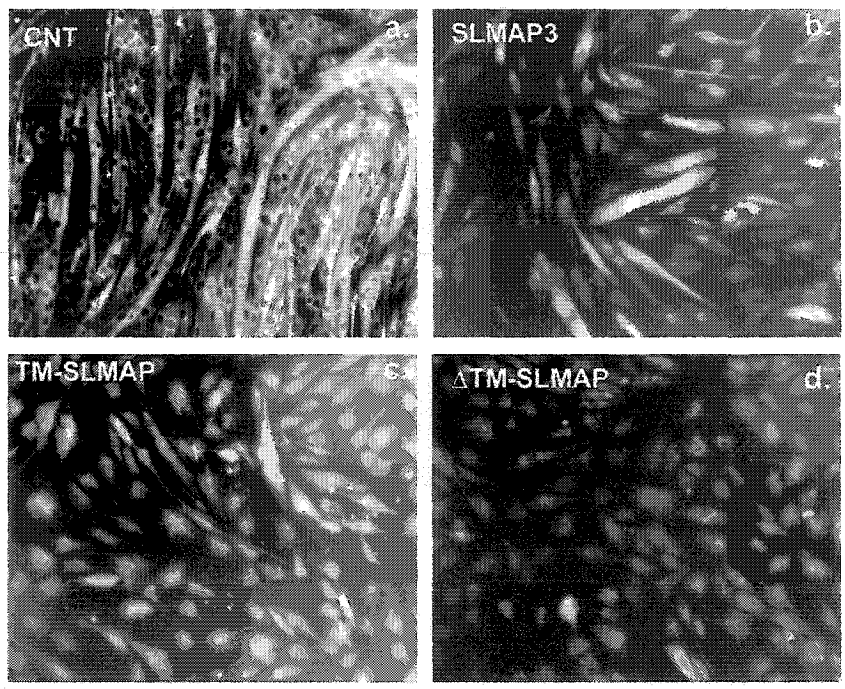
CNT
a.
SLMAP3
b.
TM-SLMAP
c.
ΔTM-SLMAP
d.

C.

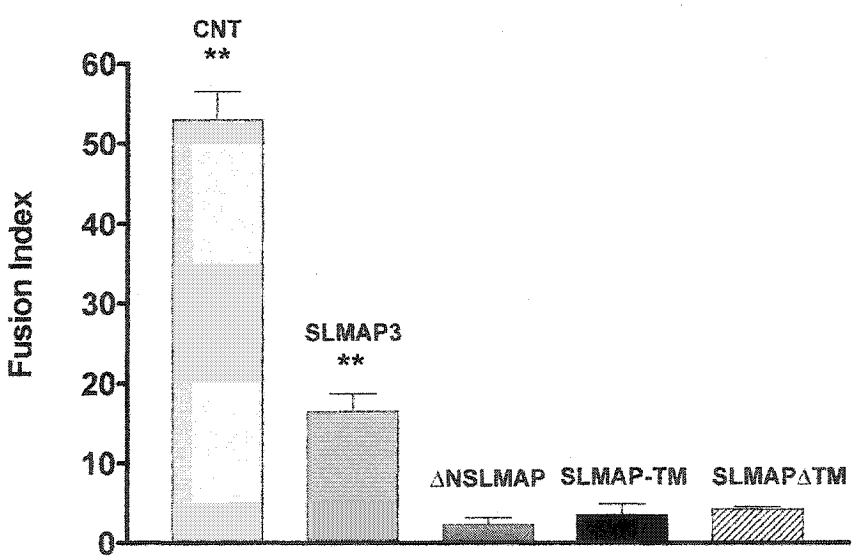
CNT
**
SLMAP3
**
Fusion Index
60
50
40
30
20
10
0
ΔNSLMAP
SLMAP-TM
SLMAPΔTM

Fig. 6. SLMAP overexpression does not affect biochemical differentiation. Stable C2C12 cells that ectopically express 6Myc-SLMAP variants were monitored for the expression of differentiation markers at 0 and 5 days following the removal of mitogens. The ectopic expression of 6Myc-SLMAP3 (102 kDa), 6Myc-ΔNSLMAP (72 kDa), 6Myc-SLMAP-TM (47 kDa) or 6Myc-ΔTM-SLMAP1 (42 kDa) was assayed by immunoblotting experiments using anti-myc monoclonal antibodies. Anti-myogenin monoclonal antibodies and anti-MF20 monoclonal antibodies were used to detect the expression of these differentiation markers. Anti-α-tubulin antibodies were used as a control for equal loading.

Figure 6 Chapter 2

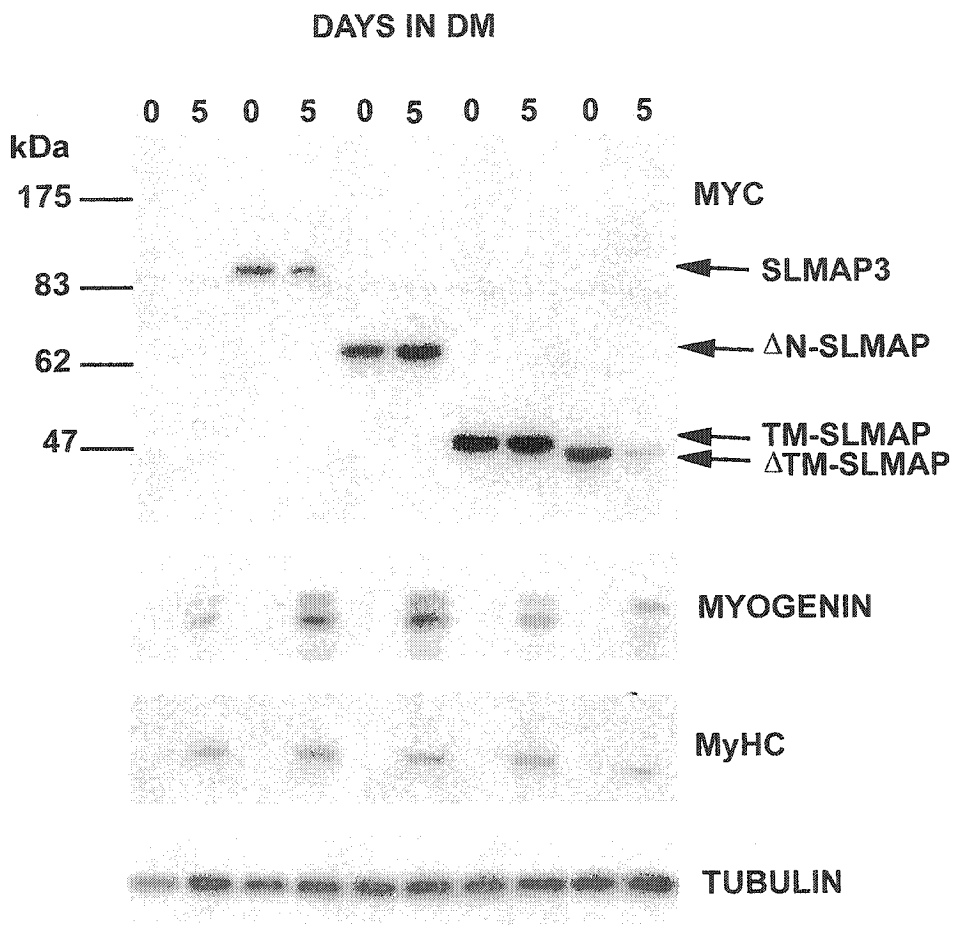

Fig. 7. Carboxyl-terminal SLMAP sequences direct SLMAP-SLMAP interactions. **(A)** Schematic representation of the 6Myc and GFP-tagged expression constructs used for transient transfections and immunoprecipitation studies. **(B)** C2C12 cells were transfected with 6Myc-SLMAP3 (MYC-M1; *) or co-transfected with 6Myc-SLMAP3M1 (MYC-M1; *) and GFP-ΔNSLMAP (GFP-SLP; +). The membrane blot shown in the first panel was immunoblotted with anti-SLMAP rabbit antibodies. In C2C12 lysate (L), SLMAP antibodies detected the 91 kDa endogenous SLMAP as well as the ectopically expressed 6Myc-SLMAPM1 (*; 103 kDa) and the GFP-ΔNSLMAP (+; 72 kDa) variant. In the second panel, myc antibodies detected only the 6Myc-SLMAP3 variant in lysates (L; *) of transfected cells. Immunoprecipitations with myc antibodies specifically purified the 6Myc-SLMAP3 variant (second panel, lane M; *). Western blot analysis using SLMAP antibodies (panel A) further showed that the immunoprecipitated 6Myc-SLMAP3 (*) protien complexed with the GFP-ΔNSLMAP (+) protein (lane M, first panel). **(C)** C2C12 cells were co-transfected with 6Myc-pcDNA3 and GFP-pcDNA3 (controls) or were co-transfected with 6Myc-SLMAP1 (MYC-SLP1; *) and GFP-ΔNSLMAP (GFP-SLP; +). The membrane shown in the first panel was immunoblotted with anti-SLMAP rabbit antibodies. In lysates lanes (L) of control cells, SLMAP antibodies detected only the 91 kDa endogenous SLMAP. SLMAP antibodies detected both the 6Myc-SLMAP1 (*; 47 kDa) and the GFP-ΔNSLMAP (+; 72 kDa) variant in lysates of transfected cells. In the second panel, myc antibodies detected only the 6Myc-SLMAP1 variant (*) in lysates (L) of transfected cells. Immunoprecipitation with myc antibodies specifically purified the 6Myc-SLMAP1 variant (second panel, lane M; *). Western blot analysis using SLMAP antibodies (panel A) also showed that the immunoprecipitated 6Myc-SLMAP1 (*) complexed with the GFP-ΔNSLMAP (lane M, first panel; +). L, lysate; B, mock immunoprecipitation with protein A/G-agarose beads only; M, immunoprecipitation with anti-myc monoclonal antibody; C, control immunoprecipitation with rabbit IgGs.

Figure 7

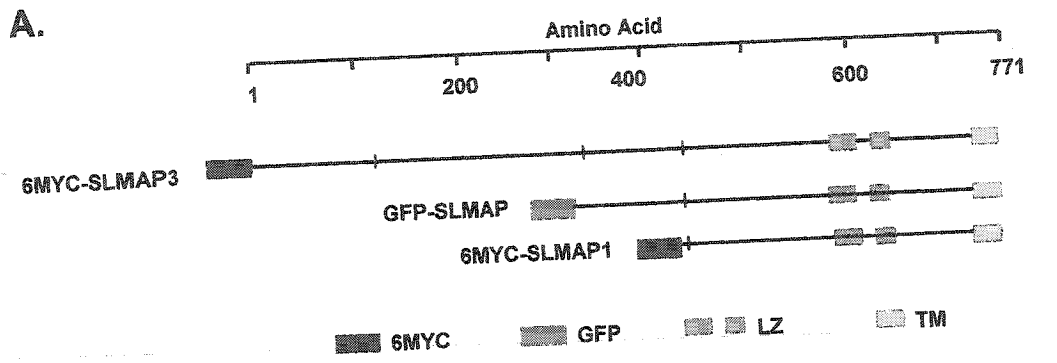
A.
Amino Acid
1
200
400
600
771
6MYC-SLMAP3
GFP-SLMAP
6MYC-SLMAP1
6MYC
GFP
LZ
TM

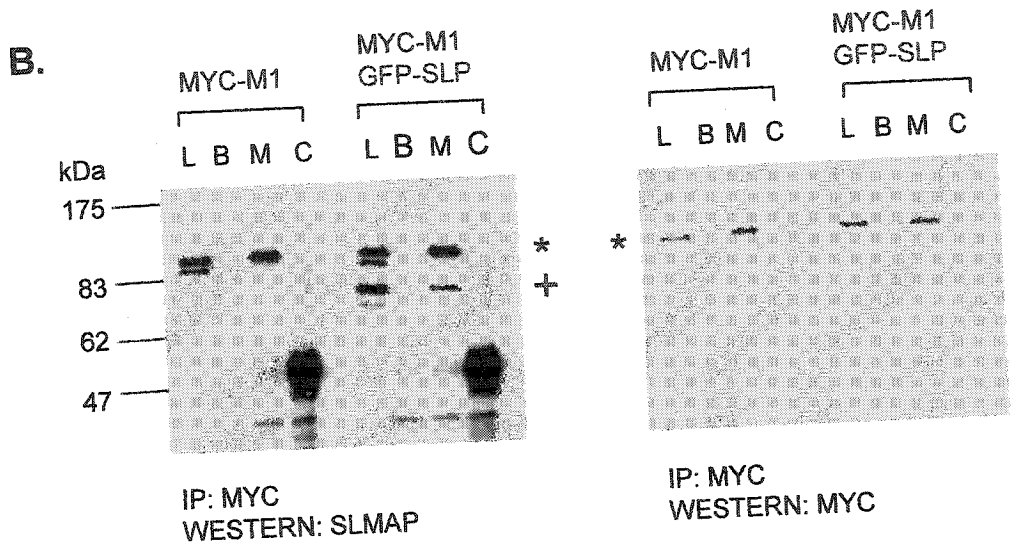
B.
MYC-M1
MYC-M1
GFP-SLP
L B M C
L B M C
kDa
175
83
62
47
*
+
IP: MYC
WESTERN: SLMAP
MYC-M1
MYC-M1
GFP-SLP
L B M C
L B M C
*
IP: MYC
WESTERN: MYC

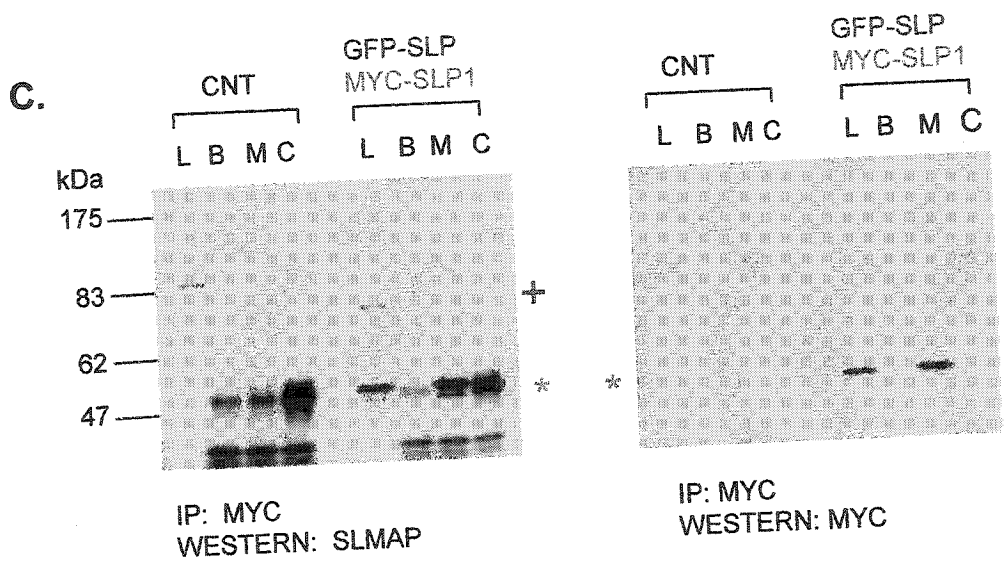
C.
CNT
GFP-SLP
MYC-SLP1
L B M C
L B M C
kDa
175
83
62
47
+
*
IP: MYC
WESTERN: SLMAP
CNT
GFP-SLP
MYC-SLP1
L B M C
L B M C
*
IP: MYC
WESTERN: MYC

Fig. 8. Leucine zipper motifs mediate SLMAP homodimer formation. **(A)** SLMAP3 sequences encoding amino acids 1-450 (SLMAPN) or 450-771 (SLMAPC) were fused in frame with either the GAL4 DNA binding domain (DNA-BD) or activation domain (AD) derived from VP16 protein of herpes simplex virus. **(B)** C2C12 myoblasts were co-transfected with CAT reporter plasmid pCMV-LacZ, DNA-BD recombinant plasmid or AD recombinant plasmid: Lane (1) DNA-BD + AD; (2) SLMAPN- (DNA-BD) + AD; (3) DNA-BD + SLMAPC-(AD); (4) SLMAPC-(DNA-BD) + AD; (5) SLMAPN-(DNA-BD) + SLMAPN-(AD); (6) SLMAPN-(DNA-BD) + SLMAPC-(AD); (7) SLMAPC-(DNA-BD) + SLMAPN-(AD); (8) SLMAPC-(DNA-BD) + SLMAPC-(AD); (9) SLMAPCΔLZ-(DNA-BD) + SLMAPCΔLZ-(AD); (10) SLMAPCΔLZ-(DNA-BD) + SLMAPC- (AD); (11) SLMAPC-(DNA-BD) + SLMAPCΔLZ (AD); (12) Ninein-LZ-(DNA-BD) + SLMAPC-(AD); and (14) positive control. Forty-eight hours after transfection, cells were lysed and then assayed for CAT activity. The level of CAT activity measured for each sample was normalized based on transfection efficiency as described in Experimental Procedures. SLMAP homodimer formation was mediated by carboxyl sequences (8) encompassing the leucine zipper motifs. Deletion of the leucine zippers (9-11) failed to activate CAT reporter expression above basal levels.

Figure 8

A.

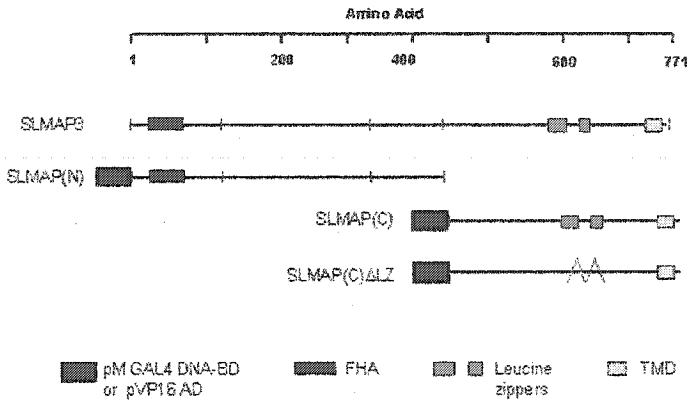
Amino Acid
1
288
480
680
771
SLMAP3
SLMAP(N)
SLMAP(C)
SLMAP(C)ΔLZ
pM GAL4 DNA-BD or pVP16 AD
FHA
Leucine zippers
TMD

B.

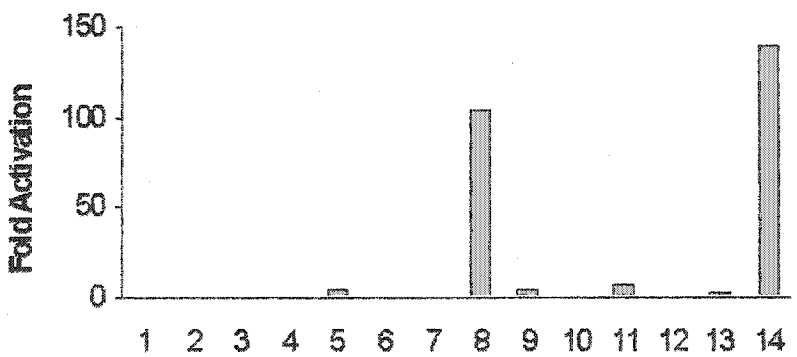
Fold Activation
150
100
50
0
1 2 3 4 5 6 7 8 9 10 11 12 13 14

Fig. 9. Fusion defects are not attributed to aberrant SLMAP-SLMAP associations. **(A)** Morphology of differentiating C2C12 myoblasts stably transfected with 6Myc-SLMAP1ΔLZ (b) or the control 6Myc-pcDNA3 vector (a). **(B)** Cells stably expressing either 6Myc-SLMAP1ΔLZ or the control vector (6Myc-pcDNA3) were cultured in differentiation media for 6 days, fixed with 4% paraformaldehyde and stained with haematoxylin and eosin. Fusion indices were calculated as described in Experimental Procedures. Error bars represent standard deviation.

A.

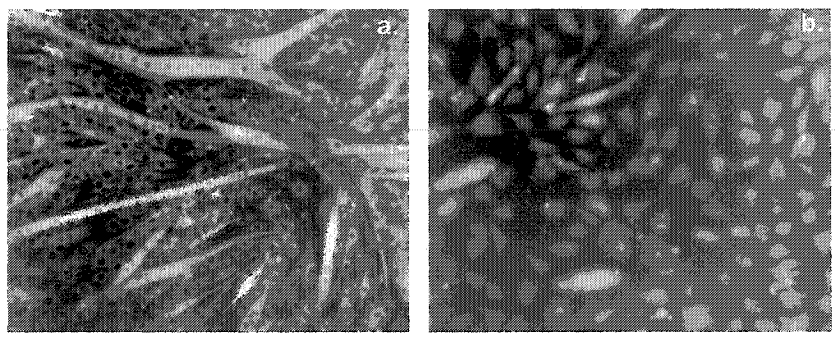

B.

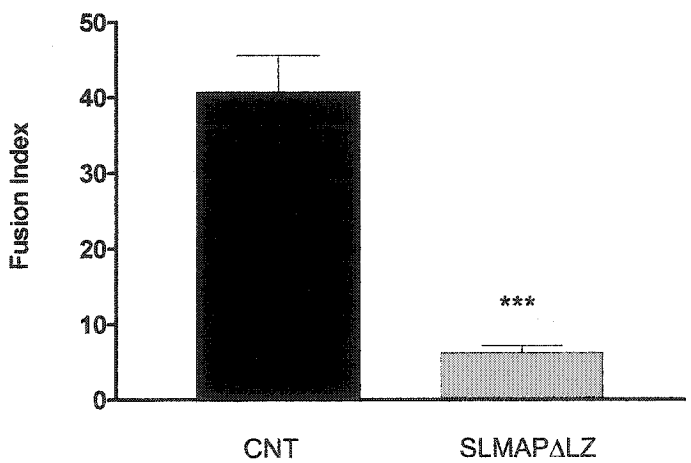

Chapter Three.

Guzzo et al. (2003). SLMAPs Are Directed into Distinct Cellular Membranes by Alternative Splicing Mechanisms and May Serve Roles in the Structural Arrangement of the Cardiac Myocyte (manuscript formatted for the Journal of Cell Science).

The following outlines the experimental contributions of the authors of this manuscript. Immunocytochemistry, immunohistochemistry (with the exception of Figure 3B), embryo sectioning, microscopy, image analyses, transient transfections and cell culture were performed by R. Guzzo. Deconvolution confocal microscopy (Figure 3D) was performed by Dr. Edwin Moore. The generation and purification of the GST-SLMAP proteins, pull down assays and silver staining were performed by R.Guzzo. Dr. John Kelly (National Research Council of Canada) and his colleagues performed the gel extraction, digestion and mass spectrometric analysis. Culture adult rat cardiomyocytes were provided by Dr. G.N. Pierce (Institute of Cardiovascular Sciences, St. Boniface Hospital Research Centre, Winnipeg). Maysoon Salih and R. Guzzo generated the mammalian expression constructs and R. Guzzo wrote the manuscript.

SLMAPs Are Directed into Distinct Cellular Membranes by Alternative Splicing Mechanisms and Serve Potential Roles in the Structural Arrangement of the Cardiac Myocyte

Rosa M. Guzzo[*], Maysoon Salih[*], John F. Kelly[‡], Edwin D. Moore[+] and Balwant S. Tuana[*]

[*]Department of Cellular and Molecular Medicine, 451 Smyth Rd, University of Ottawa, Ottawa, Ontario, Canada K1H 8M5

[‡] Institute for Biological Sciences, National Research Council, 100 Sussex Drive, Ottawa, Ontario, Canada, K1A 0R6

[+]Department of Physiology, University of British Columbia, Vancouver, British Columbia, Canada V6T 1Z3

Corresponding author:

Abbreviations:

SLMAP, sarcolemmal membrane-associated protein; *ER*, endoplasmic reticulum; *SR*, sarcoplasmic reticulum; *TMD*, transmembrane domain; *LZ*, leucine zipper; *EC-coupling*, excitation-contraction coupling; *GST*, glutathione sepharose transferase; *GFP*, green fluorescent protein.

SUMMARY

In cardiac myocytes, the ordered arrangement of cell surface membranes (sarcolemmal and transverse (T)-tubules) and internal membranes of the sarcoplasmic reticulum (SR) relative to the contractile apparatus is essential for excitation-contraction coupling. The molecules involved in maintaining this structural arrangement remain to be defined. Here we ascribe molecular and cellular properties to the tail-anchored sarcolemmal-membrane associated proteins (SLMAPs) that are consistent with a role in the membrane arrangement of the cardiomyocyte. The expression of SLMAP was developmentally regulated appearing predominantly in the ventricle at 9 days post coitum (d.p.c) and uniformly distributed throughout the myocardium at 13 d.p.c. The localization of SLMAP became increasingly well organized as development progressed and was seen to coincide with the organization of the various membrane systems in the adult myocyte. Proteomic analysis indicated that SLMAPs could self assemble and bind cardiac myosin. In nonmuscle cells, the targeting of the SLMAPs to different membrane systems was found to be dependent on the distinct C-terminal membrane anchors generated by alternative splicing mechanisms. SLMAP was also shown to be a component of the ER membrane but was not involved in vesicle transport. The cardiac specific expression of SLMAP isoforms that can reside in distinct membranes, self assemble and interact with the contractile apparatus suggest a unique role for this molecule in EC coupling.

INTRODUCTION

Protein-lipid and protein-protein interactions are of critical importance for the integrity and function of membrane-bound organelles in eukaryotic cells (Ezerman and Ishikawa, 1967; Sitia and Meldolesi, 1992; Volpe et al., 1992). Muscle cells have evolved a specialized membrane architecture that is necessary for the regulation of ion channel communication underlying the process of excitation-contraction (EC) coupling. The sarcoplasmic reticulum (SR), derived from the smooth surfaced endoplasmic reticulum, constitutes an abundant internal membrane system comprised of two molecularly distinct membrane domains: the longitudinal (nonjunctional) SR and the terminal cisternae (junctional) SR (Villa et al., 1993; Franzini-Armstrong, 1999). Situated in close apposition to the junctional or terminal cisternae SR is a system of sarcolemmal invaginations, known as transverse (T)-tubules. Localized entry of calcium ions through the L-type calcium channel situated at the T-tubules is induced upon depolarization of the sarcolemma and triggers the release of calcium to the cytosol from SR-localized calcium release channels (Endo et al., 1970 and 1977; Fabiato, 1989; Verkhratsky and Shmigol, 1996). This increase in intracellular calcium levels activates the closely situated contractile units to facilitate myocyte shortening; thus the proper spatial distribution of membrane systems relative the contractile myofilament proteins are pivotal for the EC coupling mechanism (Atar et al., 1995; Bers, 2002). Subsequent removal of the intracellular calcium ions is necessary for the relaxation of the myocyte and is achieved by the activities of the longitudinal SR-localized Ca^{+2} adenosine triphosphatase (ATPases) SERCA pumps and the Na^{+}-Ca^{+2} exchanger present at the T-

tubules and sarcolemma (Kiriazis and Kranias, 2000; Reuter et al., 2003; McDonough et al., 2002; Bers, 2002).

Mouse genetic models with mutations introduced in cardiac SR proteins or with alterations in the expression levels of SR proteins that function in calcium release (ryanodine receptor 2), calcium storage (calsequestrin, phospholamban) and calcium reuptake (SERCA2) have further advanced our understanding of the molecular physiology of the normal and diseased heart (Takeshima et al., 1998; Sato et al., 1998; Jones et al., 1998; Schmitt et al., 2003; Luo et al., 1994, 1996 and 1998; He et al., 1997; Kiriazis and Kranias, 2000). The mechanisms that organize the cardiac myocyte membrane architecture, so that the appropriate targeting of the EC coupling apparatus can be achieved and maintained on a beat to beat basis, remain poorly understood. Identification of the molecular components necessary for the organization and stabilization of the cardiac membrane architecture would not only advance the understanding of cardiomyocyte function but may also offer insights into heart disease where the deregulation of membrane components has been correlated with cardiac dysfunction (Marx and Marks, 2002; Scoote and Williams, 2002). Recent studies indicate that a family of proteins designated the junctophilins (JPs) may contribute to the formation of the dyadic couplings between the SR/ER and the T-tubules in cardiomyocytes (Takeshima et al., 2000: Komazaki et al., 2003). A carboxyl-terminal hydrophobic segment targets the molecule to the ER/SR membrane, while the cytoplasmic domain interacts with lipid moieties of the plasma membrane (Takeshima et al., 2000). Targeted disruption of the cardiac/skeletal JP subtype (JP-2) resulted in early embryonic lethality (10.5 d.p.c.) and structural and functional analysis of cardiac

myocytes from mutant embryos (9.5 d.p.c.) revealed deficiencies in peripheral couplings as well as defects in EC coupling (Takeshima et al., 2000).

In an effort to identify novel components of cardiac membrane systems, a heart cDNA library was screened with purified sarcolemmal antibodies. These previous studies resulted in the isolation of cDNAs encoding a novel family of coiled-coil integral membrane proteins termed the SLMAPs (sarcolemmal membrane associated proteins) (Wigle et al., 1997). The overall structure of SLMAPs indicates that these molecules, consisting of muscle specific variants (SLMAP1, SLMAP2) and a ubiquitously expressed isoform (SLMAP3), belong to a class of integral membrane proteins known as tail-anchored (TA) membrane proteins (Kutay et al., 1993). Consistent with the topology of tail-anchored membrane proteins, a carboxyl-terminal hydrophobic domain inserts SLMAPs into membrane systems with the amino-terminal domain exposed to the cytoplasm (Wigle et al., 1997; Wielowieyski et al., 2000). SLMAPs do not possess an amino-terminal signal sequence, thus a post-translational targeting mechanism that operates independent of the signal-recognition particle (SRP) is predicted to mediate SLMAP-membrane insertion (Borgese et al., 1993; Kutay et al., 1993; Wattenberg and Lithgow, 2001). Genomic characterization of the carboxyl sequences of the SLMAP gene further confirmed the presence of two hydrophobic segments encoded by either alternative exon X or exon XI (Wielowieyski et al., 2000). It is speculated that these two divergent transmembrane domains target SLMAPs to distinct membrane systems and contribute to the membrane scaffold in cardiac muscle cells.

Whereas SLMAP1 and SLMAP2 are abundantly expressed in cardiac membrane fractions, the SLMAP3 variant has previously been shown to display wide tissue

distribution (Wigle et al., 1997). The SLMAPs share several structural features with proteins known to mediate intracellular communication among eukaryotic membrane-bound organelles of the secretory system, including components of the vesicular trafficking machinery. In this regard, the SNAREs (soluble N-ethylmaleimide-sensitive factor attachment protein receptor) define a class of coiled-coil tail anchored membrane proteins that regulate the docking and fusion of cargo-containing transport vesicles to their target organelles (Rothman and Warren, 1994; Kutay, 1993). By virtue of their molecular properties and broad tissue expression, we hypothesize that SLMAPs are ubiquitous membrane components of nonmuscle systems.

In the current study, we have defined the pattern of SLMAP localization in developing and adult cardiomyocytes. Affinity chromatography studies using recombinant SLMAP were employed to identify SLMAP-associated proteins in cardiac tissue. Furthermore, we have examined the SLMAP-membrane associations that are mediated by the two divergent carboxyl-terminal transmembrane domains.

MATERIALS AND METHODS

Immunohistochemistry

Timed-pregnant mice were sacrificed by lethal injection of sodium pentobarbital. Embryos (9-15 days post coitum) were removed, rinsed briefly in PBS, and then immediately fixed in 4% paraformaldehyde in 100 mM phosphate buffer, pH 7.4. Embryos were incubated in cryprotectant consisting of 20% sucrose in PBS. Fixed embryos were embedded in Tissue-Tek O.C.T. compound, frozen and stored at –80°C. Cryosections (6-10 um) were collected on gelatin coated microscope slides and stored at

–80°C. Older embryos (18 d.p.c.) and adult tissues were isolated, rinsed in PBS, embedded in Tissue-Tek O.C.T. compound and then frozen. Cryosections were mounted onto slides and fixed overnight in 4% paraformaldehyde. Immunohistochemistry was performed by first prewarming slides to 37°C. PFA-fixed sections were washed in PBS then treated with 50 mM ammonium chloride in PBS for 5 minutes to reduce nonspecific staining of blood proteins. Sections were blocked in PBS containing 10% goat serum, 1% Triton-X-100 and 10% bovine serum albumin for 20 minutes at room temperature before being exposed to primary antibodies (1 hour at room temperature). Following several washes in PBS, sections were incubated in PBS containing 5% goat serum, 1% Triton-X-100 and the appropriate fluorochrome-conjugated secondary antibodies for one hour at room temperature. After several washes in PBS, sections were mounted with antifade solution (Molecular Probes).

Ventricular myocytes were isolated from adult male Wistar rats and fixed using methods previously described (Scriven et al., 2000). Fixed cells were adhered to acid washed coverslips using poly-L-lysine (Sigma), rinsed in phosphate buffered saline and permeabilized in a PBS solution containing 0.1% Triton X-100 for 10 minutes. Cells were then incubated with the relevant primary antibodies overnight in a humidified environment at room temperature. Antibodies were diluted in buffer consisting of 75 mM NaCl, 18 mM Na_3citrate, 2% goat serum, 1% BSA, 0.05% Triton X-100 and 0.02% NaN_3. After several rinses in wash solution (75 mM NaCl, 18 mM Na_3citrate, 0.05% Triton X-100), cells were incubated with highly cross adsorbed fluorescein isothiocyanate (FITC) conjuated anti-rabbit and Texas Red conjugated anti-mouse secondary antibodies (Jackson Immunobiologicals) for two hours at room temperature.

Cells were then rinsed in antibody wash solution and coverslips were mounted onto frosted slides in a solution composed of 90% glycerol, 10% 10X PBS, 2.5% triethylenediamine, and 0.02% NaN_3. Fluorescent microspheres (0.2 μm diameter, Molecular Probes) labeled with FITC and Texas Red were added to the mounting medium to act as fiduciary markers and permit accurate alignment of the 3D data sets.

Antibodies

The following antibodies were used for immunofluorescence staining: monoclonal anti-Golgi 58K antibody (1:50) (Sigma-Aldrich); rabbit anti-calnexin carboxyl terminus polyclonal antibody (1:300) (Stressgen); monoclonal anti-ERGIC-53 antibody (1: 1000) (Dr. H.P. Hauri, University of Basle, Switzerland); monoclonal anti-α-tubulin antibody (1:500) (clone DM1A; Sigma-Aldrich); monoclonal anti-myc 9E10 monoclonal antibody (1:50) (Dr. J. Bell, University of Ottawa); monoclonal anti-α-actinin2 antibody (1:800) (clone EA-53, Sigma-Aldrich), monoclonal anti-caveolin 3 antibody (1 μg/mL) (BD Transduction Laboratories); monoclonal anti-ryanodine receptor 2 C3-33 antibody (1:1000) (Dr. D.W. MacLennan, University of Toronto); anti-ryanodine receptor (1 μg/ml, Affinity Bioreagents) and rabbit anti-Tom20 polyclonal antibody (1:500) (Dr. H. McBride, Ottawa Heart Institute). Filamentous actin was stained using a 1:1000 dilution of FITC-conjugated phalloidin (Sigma-Aldrich). Anti-SLMAP(C) rabbit antisera was raised against the carboxyl 370 amino acids of SLMAP, as previously described (Wigle et al., 1997) and used at 1:400 for immunofluorescent staining and at 1:5000 for immunoblotting. Rabbit anti-α-mannosidase II antibody (Dr. M.G. Farquhar, University of California San Diego) was used at 1:100 for

immunoblotting experiments. The secondary antibodies used in these studies included Alexa-Fluor 488-conjugated anti-rabbit immunoglobulins (Molecular Probes) and Alexa Flour 594-conjugated anti-mouse immunoglobulins (Molecular Probes). Secondary antibodies used in immunoblotting experiments included anti-rabbit IgG peroxidase linked whole antibody (Amersham Pharmacia Biotech) and peroxidase conjugated AffiniPure goat anti-mouse IgG (Jackson ImmunoResearch Laboratories, Inc.).

Microscopy, Image Acquisition and Deconvolution

Samples were visualized using an Axiophot (Carl Zeiss Inc) microscope equipped with a 3CCD colour video camera. An Olympus IX70 laser-scanning inverted microscope with a 63x oil immersion objective was also used for observation. Images were acquired using the BioRad MRC 1024 confocal. Acquired images were digitally processed using Northern Eclipse (Version 5.0, Empix Imaging Inc.) acquisition software as well as the Confocal Assistant 40 software. Images were further processed using Adobe Photoshop™ 5.0 (Adobe Systems Inc.).

A series of two-dimensional images were acquired through the cells at 0.25 μm spacing using a Nikon Diaphot 200 microscope and a Planapo 60/1.4 objective. This configuration produced voxel dimensions of 100 x 100 x 250 nm and satisfied the Nyquist criteria for sampling and prevented aliasing. The image detector was a thermo-electrically cooled CCD camera with a SiTe S1502AB chip with a peak quantum efficiency of 80%. Other details of the microscope can be found in Scriven et al. (2000). The point spread function of the microscope was measured using fluospheres of the

appropriate color (0.1 μm diameter, Molecular Probes). The images were prepared, deconvolved and analyzed as previously reported (Dan et al., 2003).

Generation of GST-fusion proteins

Rabbit SLMAP1 cDNA was PCR amplified from full length SLMAP3 cDNA using the forward primer (GEXSL15': cgGAATTCaaagcagtgacgacac) and reverse primer (GEX3': cgGAATTCgtgtacggactcaagaaa). PCR conditions consisted of: (i) 3 minutes at 94°C; (ii) 30 cycles at 94°C for 40 seconds (denaturing); 60°C for 30 seconds (annealing); 72°C for 2.5 minutes (extension); followed by (iii) one last step at 72°C for 10 minutes. PCR products were EcoRI digested and ligated into the EcoRI site of pGEX-2TK vector (Amersham Pharmacia Biotech) to yield pGEX-SLMAP1. Insert orientation was verified by restriction site mapping and sequencing.

pGEX-2TK or pGEX-SLMAP1 were used to transform BL21 Codon Plus (Stratagene) competent cells. Transformed cells were plated on LB agar plates supplemented with ampicillin (1000 ug/mL), chloramphenicol (40 μg/mL) and 2% glucose. Overnight bacterial cultures for each transformant were grown at 37°C until an optical density reading (A_{600nm}) of 0.5-0.6 was reached. Fusion protein synthesis was induced with 0.1 mM IPTG for 4 hours at room temperature. Cells were collected by centrifugation for 10 minutes at 5,000 rpm and resuspended in lysis buffer (PBS pH 7.4, 1% Triton-X-100, 0.8% NaCl, 5% glycerol) supplemented with protease inhibitor cocktail (Sigma-Aldrich). To lyse the cells, 0.1 mg/ml of lysozyme was added and the bacterial cell lysates were incubated on ice for 30 minutes, followed by brief sonication. Sonicated material was centrifuged for 20 minutes at 20,000 xg and collected

supernatants were then incubated with glutathione sepharose 4B (Amersham Pharmacia Biotech) beads with constant rotation at 4°C. Beads were separated from the lysate by brief centrifugation (4,000 rpm; 10 seconds) and the protein-linked beads were washed several times with lysis buffer. Two additional washes were performed with purification buffer (PBS pH 7.4, 0.5% NP-40, 0.8% NaCl, 5% glycerol).

GST-pull down assays

H9c2 cells, maintained at 37°C in Dulbecco modified essential media (DMEM) supplemented with 10% heat inactivated fetal bovine serum and antibiotics, were lysed in RIPA buffer (1% Nonidet P-40, 0.5% sodium deoxycholate, 0.1% SDS in PBS pH 7.4, protease inhibitors). Unbroken cells and debris were removed by centrifugation and protein contents were determined using the BCA Protein Assay Kit (Pierce). The H9c2 cell lysate was precleared with glutathione sepharose 4B (Amersham Pharmacia Biotech) beads linked to GST (30 minutes rotation at 4°C). 6 mg of precleared cell lysate was incubated overnight at 4°C with equivalent amounts of purified GST or GST-SLMAP1 bound to glutathione sepharose 4B (GST) beads. After binding, the beads were extensively washed with 1X RIPA, 0.5X RIPA or PBS, then resuspended in 2X sample buffer. Captured proteins were eluted from the beads by boiling and then separated on 7.5% SDS-PAGE gels (Laemmli, 1970).

Crude microsomes were isolated from adult rabbit ventricles by homogenization in buffer consisting of 50 mM Tris-HCl pH 7.8; 20 mM sodium tetraphosphate and 1 mM EDTA supplemented with protease inhibitor cocktail (Sigma-Aldrich). The homogenate was cleared of debris by centrifugation at 10,000 xg for ten minutes at 4°C, then filtered

through cheesecloth. KCl was added to a final concentration of 0.6M and the cleared homogenate was further centrifuged at 100,000 xg for 45 minutes at 4°C. The pellet was retained and solubilized overnight with constant rotation in buffer consisting of 12.5 mM MOPS pH 7.2, 0.8% CHAPS, 0.5% NP-40, 450 mM NaCl, 150 mM sucrose and 25 uM EGTA. Solubilized membranes were then subjected to high speed centrifugation (190,000 xg; 1 hour). The supernatant was retained as the solubilized crude microsome fraction. Protein contents were determined using the BCA Protein Assay kit (Pierce) and GST-pull downs were performed as described above for H9c2 cells.

Silver Staining

SDS-polyacrylamide gels were fixed in 50% ethanol; 5% acetic acid solution for 30 minutes at room temperature. Gels were then washed for 10 minutes in 50% ethanol followed by two washes (20 minutes total) in double distilled water. Gels were subsequently incubated in silver staining sensitizer solution (0.02% sodium thiosulphate) for 5 minutes, then washed twice in double distilled water prior to staining in 0.1% silver nitrate for 30 minutes. Gels were briefly rinsed in double distilled water, and then exposed to developer solution (0.04% formalin in 2% sodium carbonate). The reaction was stopped by the addition of 5% acetic acid solution upon visualization of bands. Gels were stored in 1% acetic acid solution.

Digestion Protocol and Mass Spectrometry

Gel slices were destained (15 mM potassium ferricyanide; 50 mM sodium thiosulfate) and incubated at room temperature with shaking. Gel pieces were then

washed (3 x 10 minutes) in deionized water and acetonitrile was added to shrink the gel pieces. Gel pieces were rehydrated with buffer consisting of 0.01 μg/ul of trypsin in 50 mM ammonium bicarbonate and digested overnight at 37°C. The buffer containing the digested peptides was transferred to a mass spectrometer analysis plate and analyzed on the Q-tof ultima instrument (Micro Mass). Samples were analyzed using a nano-LC-MS/MS method with runs of 45 minutes/sample and a gradient of acetonitrile ranging from 5 to 55%.

Subcellular fractionation of the Golgi and ER

Stacked golgi fractions (SGF) and endoplasmic reticulum fractions were isolated from rabbit liver according to the method described by Taylor et al. (1997). All procedures were performed on ice in the presence of protease inhibitors (PMSF, leupeptin, aprotonin, pepstatin A). Freshly removed livers were minced and then homogenized (0.5M phosphate buffered sucrose, 100 mM KH_2PO_4 / K_2HPO_4 pH 6.5 and 5 mM $MgCl_2$). The homogenate was centrifuged at 1500 xg for 10 minutes to remove unbroken cells, debris and nuclei. Postnuclear supernatant (PNS) was loaded onto a sucrose step gradient (1.3 M sucrose, 0.86 M sucrose, PNS in 0.5 M sucrose, 0.25 M sucrose) and centrifuged at 100,000 xg for one hour. Fractions collected from the gradient included SI (0.25-0.5 M interface); A (0.5 M layer); SII (0.5-0.86 M interface); B (0.86 M layer); SIII (0.86-1.3 M interface); C (1.3 M layer) and pellet. SII fraction was adjusted to 1.15 M sucrose, and then overlaid with 1.0 M sucrose, 0.86 M sucrose and 0.25 M sucrose. This sucrose gradient was centrifuged at 76,000 xg for 3 hours. Fractions collected included: SGFA (0.25 M layer); SGF1 (0.26-0.86 M interface);

SGFB (0.86 M layer); SGF2 (0.86-1.0 M interface); SGFC (1.0 M layer); SGF3 (1.0-1.15 M interface); and SGFL (1.15 M layer). Protein content of each fraction was determined via the BCA protein assay (Pierce). Equal amounts (10 μg) of each fraction were loaded onto a 10% SDS polyacrylamide gel.

Cell culture, transfections and cytoskeletal disruptions

COS7 African green monkey kidney cells and H9c2 cells (CRL-1446, ATCC) were maintained at 37°C in Dulbecco modified essential media (DMEM) supplemented with 10% heat inactivated fetal bovine serum and antibiotics. Transient transfection experiments were performed using the Fugene™ (Roche Biochemicals) transfection reagent according to the manufacturers' specifications. Disruption of microtubules was induced in COS7 cells with 10 μM nocodazole (Sigma-Aldrich) for two hours at 37°C. Filamentous actin was disrupted in COS7 cells with 1 μM cytochalasin D (Sigma Aldrich) for 2 hours at 37°C. Ventricular cardiomyocytes were isolated from adult rat hearts as described by Liu and Pierce (1993).

SLMAP expression constructs

6Myc-tagged SLMAP1 expression constructs encoding transmembrane domain 1 (TMD1), transmembrane domain 2 (TMD2) or the construct lacking both TM (ΔTM) domains were generated according to Wielowieyski et al. (2000). The leucine zipper mutant (SLMAPΔLZ) contained TMD2 sequences and was generated by digesting 6Myc-SLMAP1-pcDNA3 with BamH1. This digestion removed the segment of SLMAP that encoded the leucine zippers (nucleotides 1774-1984). Nucleotides 2001-2314 of

SLMAP3M1 (designated SLMAP3') in pcDNA3 were retained for subsequent ligation. A PCR amplicon of 6Myc-SLMAP1 lacking the leucine zippers was generated from the 6Myc-SLMAP1-pcDNA3 template using the 5' primer (6MYC-SLP15') and the 3' primer (CGGATCCCTCTTTCTGCTGGTCCTCACACTGC; LZ-less). The PCR product (lacking the leucine zippers) was restriction digested (BamH1) and then ligated into SLMAP3'. The GFP-SLMAP1-TMD2 construct was PCR generated using the 5' primer GGGAATTCAATGGATGAGCAAGACCTG and 3' primer SLMAPN-R (GATGCCAGCTTCTAGAGGGAGGACG). EcoR1/Xba1 digested PCR products were inserted into the EcoR1/Xba1 sites of pcDNA3 mammalian expression plasmid (Invitrogen), in frame with a 6Myc epitope tag or into the EcoR1/XbaI sites of pcDNA3, in frame with a GFP tag. Sites of ligations were confirmed by DNA sequencing.

Immunocytochemistry

Cells grown on sterile glass coverslips were fixed in either 4% paraformaldehyde (PFA) in phosphate buffer for 15 minutes at room temperature or in ice-cold methanol for five minutes. Following either fixation method, coverslips were mounted onto glass slides and cells were incubated with the relevant antibody(s) diluted in 10 mM PBS containing 0.3% Triton-X-100 (PBS-T) for 2 hours at room temperature. After several washes in PBS, cells were incubated in the appropriate fluorochrome-conjugated secondary antibody(s) for 45 minutes at 37°C. Cells were washed extensively in PBS, and then mounted with antifade media (Molecular Probes).

ER-Golgi protein transport assays

The ts045-VSVG-GFP expression plasmid was donated by Dr. Lippincott-Schwartz (Presley et al., 1997). The plasmid was co-transfected with 6Myc-tagged SLMAP-pcDNA3 constructs into COS7 at 40°C for 15 hours. Cells were then shifted to either 32°C for one hour or 15°C for three hours to monitor the transport of ts045-VSVG-GFP from the ER to the ERGIC, Golgi and plasma membrane.

RESULTS

SLMAP expression in the developing myocardium and adult cardiomyocytes.

In view of the abundant SLMAP transcript expression in cardiac muscle (Wigle et al., 1997; Wielowieyski et al., 2000), we investigated the temporal and spatial pattern of SLMAP expression in developing cardiac tissue. At nine days post coitum (d.p.c.), the primitive mouse heart exists as a tubular structure with presumptive atrial and ventricular chambers. SLMAP-antibody labelling of formalin-fixed sagital cryosections of mouse embryos revealed that SLMAPs were expressed in both the atria and ventricles at this early stage developmental stage, with more robust staining observed in the ventricular myocardium (Fig. 1A). At 13 d.p.c., the developing heart is divided by septa into a four-chambered heart (Epstein and Buck, 2000) and SLMAPs were uniformly expressed in the atrial and ventricular myocardium, as well as the interventricular and interatrial septum (Fig. 1B; a,c,d). An immunofluorescent signal was not observed in sections incubated in pre-immune rabbit serum (Fig. 1B; c), nor was a signal obtained in sections where the primary antibody was omitted (secondary antibody control, not shown). Confocal images of ventricular myocytes stained for SLMAPs at 13 d.p.c. revealed diffuse SLMAP-localization (Figure 2a). A distinct distribution of SLMAPs relative to the myofibrils was

not observed at this developmental stage (Fig. 2a-c). In older embryos (18 d.p.c.), a clear striated pattern of SLMAP expression was apparent and SLMAP localization was primarily distinct from that of the Z-line marker, α-actinin (Fig. 2d-f).

Immunostaining and confocal microscopy was used to further examine the subcellular localization of SLMAPs in cultured adult rat ventricular myocytes. In contrast to the disordered SLMAP distribution in early embryonic ventricular myocytes, a regular cross-striated pattern of SLMAP distribution was observed in adult cardiac cells (Fig. 2 g-i). SLMAP labelling of the Z-line was apparent by confocal and deconvolution microscopy (Fig. 2i and Fig. 3A, parallel arrows in panel a); however SLMAPs were also seen to reside between the Z-lines (Fig. 3B, panel A, u) as well as in longitudinal structures oriented parallel to the Z-line (Fig. 2i). This staining pattern is consistent with the network-like distribution of the SR and T-tubules that surrounds the myofibrils (Opie et al., 1991). The reticular staining pattern acquired with SLMAP antibodies was also reminiscent of the longitudinal SR.

In adult ventricular cardiomyocytes, SLMAP-specific staining was shown to extend toward the periphery of the cell and also labelled invaginations of the plasma membrane, thus we examined whether SLMAPs are associated with external membrane systems in mature myocytes. Caveolin 3 proteins are expressed in cardiac, skeletal and smooth muscle and reside at the vesicular invaginations of the plasma membrane known as caveolae (Song et al., 1996). Caveolin 3 antibodies clearly labelled a subcompartment of the surface cardiac membrane as well as plasma membrane invaginations (Fig. 3A, b and Fig. 3B, panel b), consistent with the distribution of caveolin 3 in the transverse tubular membrane system in cardiac cells (Liu et al., 2003). SLMAP co-localization with

caveolin 3 at the cell surface, membrane invaginations and along the Z-lines was well resolved by deconvolution microscopy (Fig 3B, panel b; Fig. 3A, c). Regional differences in the SLMAP-caveloin 3 co-localization were apparent as cavolin 3 along the Z-lines was more heavily co-localized with SLMAP than the cell surface (Fig. 3A, c; Fig. 3B, panel B).

The ryanodine receptors (RyR) or the calcium release channels are essential components of the EC-coupling machinery in muscle localized at the terminal cisternae SR membranes. By immunofluorescent microscopy, RyRs are typically detected as a series of regularly spaced doublets in developing and adult cardiomyocytes (Fig. 3e and Fig. 3B, panel C in red) (Carl et al., 1995). Dual staining with SLMAP and RyR2-specific antibodies revealed that SLMAPs labelled extensive reticular formations in isolated ventricular myocytes, in addition to the RyR-stained doublets (Fig. 3d, f and Fig. 3B, panel C).

Identification of SLMAP-associated proteins.

To gain insight regarding the biological role(s) of SLMAPs in cardiac cells, affinity chromatography assays using bacterially expressed recombinant glutathione sepharose transferase linked SLMAP proteins (GST-SLMAP1) were performed to identify SLMAP-associated proteins. GST-SLMAP1 fusion proteins were immobilized on glutathione-Sepharose beads (Fig. 4A) and incubated with detergent extracts of H9c2 cells or crude microsomal fractions isolated from adult rabbit ventricles. Following extensive washing to remove non-specific and weakly bound proteins, the proteins bound to recombinant SLMAPs were eluted, separated by SDS-PAGE and visualized by silver

staining. A protein band with an apparent molecular weight of 35 kDa and a less abundant protein band of 70 kDa expressed in H9c2 cells were found to consistently bind GST-SLMAP1 (Fig. 4B). In addition, a band with an apparent molecular weight of over 200 kDa was eluted from the immobilized GST-SLMAP1 proteins incubated with the cardiac fractions (Fig. 4C). Each of the recovered proteins specifically interacted with the GST-SLMAP fusion proteins, since none of the protein bands were recovered by GST alone (Fig. 4B, C). In addition, the protein bands were not identified in other control experiments where GST or GST-SLMAP recombinant proteins were incubated with lysis buffer alone. The 200 kDa, 70kDa and 35kDa proteins were excised from the silver stained gels, trypsin digested and further analyzed for peptide composition by mass spectrometry. Database comparisons of the tryptic peptide sequences of the 70 kDa and 35 kDa proteins matched Accession No. 790240, 790238 and 20870858, each representing SLMAP. The ability SLMAPs to self assemble has been corroborated by additional studies (immunoprecipitations, in vitro protein-protein interactions) conducted in our laboratory (manuscript in preparation). The peptide sequences acquired from the mass spectrometric analysis of the 200 kDa protein corresponded to the cardiac alpha and beta subunits of myosin heavy chain. These findings suggest that SLMAPs may provide a structural link between the cardiac membrane systems and the contractile myofilaments.

SLMAP3 associates with intracellular membranes in nonmuscle cells.

The SR is derived from the smooth endoplasmic reticulum, an extensive membrane-bound organelle, which contributes to general intracellular calcium regulation in eukaryotic cells (Baumann and Walz, 2001). In view of the abundant SLMAP

expression in the SR of cardiac cells and the ubiquitous distribution of the SLMAP3 variant (Wigle et al., 1997), we sought to determine whether SLMAP3 is also a component of membrane systems (ER, Golgi) in nonmuscle cells such as liver. Total membranes were prepared from the postnuclear supernatant of rat liver homogenates and further separated into ER and golgi fractions by sucrose gradient centrifugation (Fig. 5) (Taylor et al., 1997). Protein fractions from each gradient were collected, separated by SDS-PAGE and subject to immunoblot analysis using anti-SLMAP antibodies as well as specific markers of the ER (calnexin) and a cis-golgi marker (α-mannosidase). A 91 kDa SLMAP isoform, consistent with the molecular size of the full length SLMAP3 protein, co-purified with calnexin in fractions enriched in the ER. The SLMAP3 protein was not identified in a highly enriched stacked golgi fraction where α-mannosidase was purified (Fig. 5).

Immunocytochemistry and biochemical fractionation studies have previously revealed that SLMAPs are targeted to intracellular membrane systems by sequences at the extreme carboxyl terminal region of the molecule (Wielowieyski et al., 2000). The membrane targeting regions of SLMAPs were confined to sequences encompassing transmembrane domain 1 (TMD1) encoded by alternative exon V in SLMAP1 and sequences encompassing transmembrane domain 2 (TMD2) encoded by exon VI (Wielowieyski et al., 2000). To further elucidate whether TMD1 or TMD2 target SLMAPs to distinct membrane systems, SLMAP constructs encoding either TMD1 or TMD2 sequences fused to the 6Myc epitope tag were transfected into COS7 cells (Fig. 6). When expressed in COS7 cells, the 6Myc-pcDNA empty vector exhibited a nonspecific distribution throughout the cytoplasm as well as in the nucleus (data not

shown). Transient expression of SLMAP sequences encompassing TMD1 generated a pronounced perinuclear localization, which also extended throughout the cytoplasm in a diffuse reticular pattern consistent with the distribution of ER proteins (Fig. 7A; a). The ectopic expression of SLMAP sequences encompassing TMD2 targeted the 6Myc-tagged fusion protein to distinct reticular formations as well as filament-like projections throughout the cell that were not observed in cells expressing TMD1 (Fig. 7A; b). Extraction with Triton-X-100 prior to fixation resulted in lack of myc staining in paraformaldehyde fixed cells expressing 6Myc-SLMAP-TMD2, thus confirming this SLMAP variant associates with detergent soluble complexes such as membrane structures (data not shown). Recent studies conducted in our laboratory have indicated that the leucine zipper motifs in SLMAPs specifically direct SLMAP homodimerization (manuscript in preparation). Thus, to assess whether SLMAP oligomerization could affect SLMAP targeting to membrane systems, mutants lacking the leucine zipper motifs were expressed in COS7 cells. In the absence of the leucine zipper motifs, the expression of TMD2 sequences retained the ability to direct the 6Myc-SLMAPΔLZ fusion protein to the filament-like membrane structures (Fig. 7A; c). Notably, in the absence of either transmembrane domain, the 6Myc-SLMAPΔTM fusion protein was not targeted to reticular or filament-like membrane structures, rather was diffusely distributed throughout the cytosol (Figure 7A; d).

To further examine whether the expression of the two transmembrane segments mediate differential SLMAP-membrane associations, co-transfection experiments were performed using (i) SLMAP cDNA encompassing TMD1 fused to 6Myc (6Myc-SLMAP-TM1); and (ii) SLMAP cDNA encompassing TMD2 fused to GFP (GFP-

SLMAP-TM2). The subcellular distribution of the 6Myc-SLMAP-TM1 fusion protein as well as the GFP-SLMAP-TM2 fusion proteins were monitored by visualizing GFP fluorescence relative to myc immunolabeling in those cells which co-expressed the SLMAP fusion proteins (Fig. 7B). While some overlap in the GFP and myc signal by immunocytochemistry in cells co-expressing TMD1 and TMD2 (Figure 7B; c, yellow signal), the localizations were predominantly distinct (Fig. 7B; a-c). Inclusion of the GFP tag did not appear to affect membrane targeting since cells that were co-transfected with GFP-SLMAP and 6Myc-SLMAP fusion proteins encompassing the same TMD (TMD2) showed completely overlapping distribution profiles (Fig. 7B; d-f).

SLMAP transmembrane domains target SLMAPs to distinct membrane systems in COS7 cells.

In view of the observation that the two carboxyl-terminal transmembrane domains target SLMAPs to distinct membrane structures in COS7, we monitored SLMAP localization relative to various components of intracellular membrane-bound organelles. Co-staining with the ER marker calnexin demonstrated significant co-distribution with 6Myc-SLMAP-TMD1 variant at reticular formations (Fig. 8A; a-c); however limited co-distribution was observed in cells expressing 6Myc-SLMAP-TMD2 (Fig. 8A; d-f) or 6Myc-SLMAP-TMD2ΔLZ (Fig. 8A; g-i). Anti-ERGIC-53 monoclonal antibodies, which were used to detect the ER-golgi intermediate compartment, consistently labelled fine punctate structures concentrated at perinuclear sites in COS7 cells (Schindler et al., 1993; Itin et al., 1995). This distribution pattern was distinct from that of either 6Myc-SLMAP-TMD1 (Fig. 8B; a-c) or 6Myc-SLMAP-TMD2 (Fig. 8B; d-f). Whereas myc staining

demonstrated that TMD1 and TMD2 direct SLMAPs to perinuclear sites, neither TMD1 nor TMD2 sequences target SLMAPs to the golgi as assessed by co-staining with the anti-Golgi58K monoclonal antibody (Fig. 8C; a-i). Consistent with these observations, the fungal metabolite Brefeldin A, a widely used agent that disrupts the structure of the Golgi apparatus (Lippincott-Schwartz et al., 1989 and 1990) did not alter the distribution of membrane-associated SLMAPs (data not shown).

SLMAP membrane associations require an intact microtubule system.

The importance of cytoskeleton for the organization of the membrane-bound organelles such as the ER has been demonstrated by the pharmacological disruption of microtubules (Baumann and Walz, 2001). In cells treated with the microtubule depolymerizing agent nocodazole, the ER membrane collapses and forms aggregates around the nucleus (Terasaki et al., 1986; Lee et al., 1989; Presley et al., 1997). In our studies, the effect of nocodazole on microtubule assembly was confirmed by staining with α-tubulin, which illustrated a distinct redistribution of the cytoplasmic microtubules (Fig. 9A; d-f). Under conditions that disrupt microtubules, the distribution of the ectopically expressed ER-membrane associated SLMAP variant (6Myc-SLMAP1-TMD1) was altered from a reticular-like distribution (Fig. 9A; a) to an aggregate-like distribution (Fig. 9A; b). These nocodazole-induced structures were not however observed in COS7 expressing the transmembrane domain mutant (6Myc-SLMAPΔTM) (Fig. 9A; c). These observations imply that SLMAP-membrane associations are dependent upon an intact microtubule network, which is consistent with the distribution of SLMAP-TMD1 at the ER network.

To determine whether SLMAPs are associated with the actin cytoskeleton, COS7 cells expressing 6Myc-SLMAP fusion proteins were treated with cytochalasin D, an actin myofilament disrupting agent (Cooper, 1987). In the presence of cytochalasin D, actin-containing microfilaments in COS7 cells were transformed from filamentous (Figure 9B; e, g) to punctate structures (Fig. 9B; f, h). Depolymerization of the actin filament system did not however appear to alter the localization of 6Myc-SLMAP fusion proteins expressing either TMD1 (Fig. 9B; a, b) or TMD2 (Fig. 9B; c ,d).

ER-Golgi transport studies.

Comparisons of the predicted SLMAP protein sequence with sequences deposited in the Genbank database were performed using the BLAST program to identify proteins sharing overall homology with SLMAPs that may provide insight to SLMAP function. The results of BLAST searches revealed that SLMAPs share similarity (24% similarity over 261 amino acids) (Fig. 10) with the *Saccharomyces cerevisiae* coiled-coil protein Uso1p (Accession No. NP 010225). This coiled-coil yeast protein is necessary for the transport of vesicles from the ER and the docking of vesicles at the golgi (Sapperstein et al., 1996; Cao et al., 1998). Analysis of the amino acid sequences encoding SLMAPs (Accession No. AAA65597) also indicated the presence of a putative di-acidic sorting signal upstream of the carboxyl-terminal TM domain (Fig. 10; in red). Di-acidic motifs, defined by Asp/Glu residues separated by a variable residue (D/E)X(D/E), are often located in close proximity to tyrosine-based sorting motifs (YXXϕ) and are thought to mediate the efficient export from the ER by interacting with the vesicular transport machinery (Nishimura and Balch 1997; Bannykh et al., 1998).

In view of these features, we investigated whether SLMAPs are involved in vesicular transport from the ER to the golgi. Previous studies have shown that overexpression of coiled-coil membrane proteins involved in vesicle trafficking from the ER to golgi inhibit protein export from the ER (Hatsuzawa et al., 2000). To examine this possibility, COS7 cells were co-transfected with an ER-localized 6Myc-SLMAP variant and the GFP-tagged glycoprotein of the temperature sensitive strain of vesicular stomatitis virus (ts045-VSV-G-GFP), which serves as a marker of ER to golgi transport. When maintained at the restrictive temperature (39.5°C), the viral glycoprotein could not be exported from the ER due to a thermoreversible-folding defect (Fig. 11; d) and consequently co-distributed with 6Myc-SLMAP (Fig. 11; a). Proper folding and subsequent transport out of the ER to the golgi and cell periphery was achieved when the ts045-VSV-G transfected cells were incubated at the permissive temperature (32°C) (Fig. 11; e). Whereas the GFP-labeled viral glycoprotein was transported out the ER to the golgi and plasma membrane under conditions that promote vesicular transport, the 6Myc-SLMAP fusion protein did not appear to exit the ER (Fig. 11; b). Expression of the SLMAP mutants lacking either the transmembrane domain or the leucine zipper motifs did not affect the ability of the viral glycoprotein to exit the ER at the permissive temperature (data not shown). COS7 cells co-expressing ts045-VSV-G-GFP and 6Myc-SLMAP were also incubated at reduced temperatures to monitor whether SLMAPs cycle from the ER to the ERGIC (Tang et al., 1995). At 15°C the membrane associated SLMAP was retained in the ER (Fig. 11; c), whereas the GFP-labeled viral glycoprotein was visualized as vesicular clusters concentrated at perinuclear sties (Fig. 11; f) consistent with localization at the ERGIC. Collectively, these studies indicate that

SLMAP do not exit the ER, nor do altered levels of expression inhibit vesicular transport processes.

TMD2 sequences target SLMAP to mitochondria.

The subcellular localization of the ectopically expressed SLMAP variant encoding TMD2 (Fig.7A; b, c) was reminiscent of the distribution of mitochondrial proteins. To address this issue further, immunostaining was performed using antibodies directed against a well-characterized component of the outer mitochondrial membrane, Tom20 (Kanaji et al., 2000). A distinct pattern of Tom20 distribution was observed relative to the localization pattern of the 6Myc-SLMAP-TMD1 variant in COS7 cells (Fig. 12; a-c). Striking co-distribution of Tom20 with either the 6Myc-SLMAP-TMD2 variant (Fig. 12; d-f) or the 6Myc-SLMAP1ΔLZ-TMD2 (Fig. 12; g-i) were observed by dual immunostaining, thus indicating that TMD2 sequences direct SLMAPs to the mitochondria.

DISCUSSION

The data reported here demonstrate that SLMAPs can homodimerize, reside in distinct membrane systems and form associations with the microtubule cytoskeleton and myosin. These molecular properties of SLMAPs are consistent with a role in organizing the membrane architecture with respect to the cytoskeleton and the contractile apparatus of the cardiomyocyte. Immunoconfocal imaging revealed that SLMAPs are highly expressed early in the developing myocardium and are primarily distributed within the SR membranes of ventricular myocytes, in accordance with our

previous biochemical studies (Wigle et al., 1997). Confocal imaging of SLMAPs expression in mature cardiomyocytes indicates that SLMAPs co-distribute with markers of the junctional and nonjunctional SR membrane. Immunolocalization studies using caveolin 3 and α-actinin antibodies further indicated that a pool of SLMAPs are distributed at the Z-line and membrane invaginations that are consistent with the distribution of the T-tubular membrane system. Although the transmembrane domain-mediated targeting of SLMAPs in cardiac myocytes warrants further investigation, the immunolocalization studies presented here suggest that SLMAPs reside in distinct membrane components that serve a primary function in EC-coupling mechanisms. Previous RT-PCR studies have also indicated that fetal, neonatal and adult heart mutually express SLMAP transcripts encoding exon IX (TMD1) and exon V (TMD2) (Wielowieyski et al., 2000). Taken together, these observations suggest that divergent carboxyl-terminal transmembrane domains may target SLMAPs to junctional membrane domains of the SR-T-tubule system as well as nonjunctional SR membrane domains. The distribution of SLMAPs in various cardiac membrane domains in adult myocytes, in addition to their ability to self assemble (manuscript in preparation) further suggests that SLMAPs may regulate membrane function through homodimer formation. These polypeptides may be ideally situated to organize the specialized membrane junctions involving the sub-cisternal SR as well as the dyad structures.

Immunolocalization studies presented in COS7 cells support the hypothesis that SLMAPs possess mutually exclusive transmembrane domains responsible for directing SLMAPs to specific membrane systems. These hydrophobic carboxyl-terminal segments are essential for anchoring SLMAPs within intracellular membrane systems, as 6Myc-

SLMAP fusion proteins lacking either transmembrane domain failed to target the heterologous protein (myc) to reticular formations in COS7 cells. SLMAP homodimerization was nonessential for membrane localization since the removal of the SLMAP dimerization motifs (leucine zippers) did not influence targeting of SLMAPs to intracellular membrane structures. Interestingly, the carboxyl-terminal TMD1 primarily directed SLMAPs to the ER, whereas sequences encompassing TMD2 targeted SLMAP to the mitochondria in COS7 cells. Tail-anchored integral membrane proteins such as SLMAP, are typically inserted post-translationally into either the endoplasmic reticulum or the mitochondria (Wattenberg and Lithgow, 2001). Several studies have examined the molecular basis for this differential targeting, and have revealed that important targeting information may be conferred within the amino acid residues of the carboxyl-terminal TMD itself, as well as within the residues flanking the TMD (Kanaji et al, 2000; Wattenberg and Lithgow, 2001). Further analysis of the divergent TMD sequences present in SLMAPs, as well as the upstream cytoplasmic-oriented residues may expose information that is necessary and sufficient for the differential membrane targeting of SLMAPs.

Analysis of the amino acid sequences encoding SLMAPs have indicated that SLMAPs possess several structural features that are consistent with those of proteins involved in intracellular transport mechanisms. For instance, extensive regions of coiled-coiled structure and carboxyl-terminal membrane anchoring domains are common features of various ER resident proteins, as well as golgi localized proteins (Jakymiw et al., 2000). A BLAST search revealed that SLMAPs share identity with the yeast coiled-coil protein required for ER to golgi transport (Sapperstein *et al*, 1996). In light of this

homology and the localization of SLMAPs at the ER, we investigated whether SLMAPs are involved in the transport of vesicles from the ER to the Golgi. The presence of a di-acidic sorting motif upstream of the TMD (within the cytoplasmic region of the molecule) further suggested that SLMAPs may serve a role in ER export. Overexpression of SLMAPs did not affect ER to golgi transport of the viral glycoprotein. Consistent with these observations, immunocytochemistry studies using specific markers for the golgi and ERGIC revealed that SLMAPs are not targeted to other membrane systems along the secretory pathway of COS7 cells. Collectively these studies confirm that SLMAPs are excluded from vesicular transport along the secretory pathway and retained in the ER. Whereas SLMAPs do not possess ER retention or retrieval signals, the presence of hydrophobic membrane anchors as well as the ability to form homodimers may serve to retain SLMAPs within the ER (Sitia and Meldolesi, 1992; Nilsson et al., 1991; Munro, 1991 and 1995; Colley et al., 1992; Tang et al., 1992; Weisz et al., 1993).

There is evidence to suggest that SLMAPs provide a molecular link between the intracellular membranes and the microtubule-based cytoskeleton. Under conditions that disrupt microtubules (nocodazole), the cellular distribution of the ectopically expressed SLMAP-TMD1 variant was altered from a reticular-like distribution to a punctate-like distribution. Several membrane-associated proteins provide a link between intracellular membranes and the microtubule cytoskeleton, including the cytoplasmic linker proteins (CLIPs) and the ER integral membrane protein, p63 (Scheel and Kreis, 1991; Pierre et al., 1992; Klopfenstein et al., 1998). Such interactions, which may also involve SLMAPs, are crucial for the positioning and the structural maintenance of the ER (Terasaki et al, 1986; Lee and Chen, 1988). Interestingly, affinity chromatography studies presented in

this study indicate that a muscle-specific SLMAP variant (SLMAP1) associates with the beta and alpha subunit of the myosin heavy chain in cardiac muscle. Deconvolution microscopy further revealed that SLMAPs are localized at regions between the Z-lines in adult cardiac myocytes, consistent with the distribution of myosin. These findings are significant and warrant further investigation, as little is known regarding the molecular mechanisms that mediate interactions among components of the SR membrane and myofibril proteins. In this respect, a splice variant of the ankyrin 1 gene (ankyrin 1.5) was recently proposed to provide a molecular link between the SR membrane and contractile elements based on its binding to a large sarcomeric protein, termed obscurin (Bagnato et al., 2003; Kontrogianni-Konstantopoulos et al., 2003). SLMAP and other yet unidentified accessory proteins may provide a similar role as the ankyrin by establishing a scaffold that links the SR membrane domains with the contractile cytoskeleton. Additional studies are required to better define these associations. Furthermore, whether the assembly of SLMAPs within the membrane aids in the transmission of the calcium signal to the contractile apparatus during EC coupling remains to be explored.

REFERENCES

Atar, D., Gao, W.D. and Marban E. (1995). Alterations of excitation-contraction coupling in stunned myocardium and in failing myocardium. *J. Mol. Cell. Card.* **27**, 783-791.

Bagnato, P., Barone, V., Giacomello, E., Rossi, D. and Sorrentino, V. (2003). Binding of an ankyrin-1 isoform to obscuring suggests a molecular link between the sarcoplasmic reticulum and myofibrils in striated muscles. *J. Cell Biol.* **160**, 245-253.

Bannykh, S.I., Nishimura, N. and Balch, W.E. (1998). Getting into the Golgi. *Trends Cell Biol.* **8**, 21-25.

Baumann, O. and Walz, B. (2001). Endoplasmic reticulum of animal cells and its organization into structural and functional domains. *Int. Rev. Cytol.* **205**, 149-214.

Bers, D.M. (2002). Cardiac excitation-contraction coupling. *Nature* **415**, 198-205.

Borgese, N., D'Arrigo, A., De Silvestris, M. and Pietrini, G. (1993). NADH-cytochrome b_5 reductase and cytochrome b_5 – The problem of posttranslational targeting to the endoplasmic reticulum. In: Subcellular Biochemistry, eds. N. Borgese and J.R. Harris, vol 21, New York: Plenum Press 313-341.

Cao, X., Ballew, N. and Barlow, C. (1998). Initial docking of ER-derived vesicles requires Uso1p and Ypt1p but is independent of SNARE proteins. *EMBO J.* **17**, 2156-2165.

Carl, S.L., Felix, K., Caswell, A.H., Brandt, N.R., Ball, W.J., Vaghy, P.L., Meissner, G. and Ferguson, D.G. (1995). Immunolocalization of sarcolemmal dihydropyridine receptor and sarcoplasmic reticular triadin and ryanodine receptor in rabbit ventricle and atrium. *J. Cell Biol.* **129**, 672-682.

Colley, K.J., Lee, E.U. and Paulson, J.C. (1992). The signal anchor and stem regions of the beta-galactoside alpha 2,6-sialyltransferase may each act to localize the enzyme to the Golgi apparatus. *J. Biol. Chem.* **267**, 7784-7793.

Cooper, J.A. (1987). Effects of cytochalasin and phalloidin on actin. *J. Cell Biol.* **105**, 1473-1478.

Dan, P., Cheung, J.C.Y., Scriven, D.R.L., and Moore, E.D.W. (2003). Epitope-dependent localization of estrogen receptor-α, but not -β, in en face arterial endothelium. *Am. J. Physiol. Heart Circ. Physiol.* 284, H1295-H1306.

Endo, M., Tanaka, M. and Ogawa, Y. (1970). Calcium induced calcium release of calcium from the sarcoplasmic reticulum of skinned skeletal muscle. *Nature* **228**, 34-36.

Endo, M. (1977). Calcium release from the sarcoplasmic reticulum. *Physiol. Rev.* **57**, 71-108.

Epstein, J.A. and Buck, C.A. (2000). Transcriptional regulation of cardiac development: implications for congenital heart disease and DiGeorge syndrome. *Ped. Res.* **48**, 717-724.

Ezerman, E.B. and Ishikawa, H. (1967). *J. Cell Biol.* **35**, 405-420.

Fabiato, A. (1989). Appraisal of the physiological relevance of two hypotheses for the mechanism of calcium release from the mammalian cardiac sarcoplasmic reticulum: calcium-induced calcium release versus charge-coupled release. *Mol. Cell. Biochem.* **89**, 135-140.

Franzini-Armstrong, C. (1999). The sarcoplasmic reticulum and the control of muscle contraction. *FASEB J.* **13**, S266-S270.

Hatsuzawa, K., Hirose, H., Tani, K., Yamamot, A., Scheller, R.H. and Tagaya, M (2000). Syntaxin 18, a SNAP receptor that functions in the endoplasmic reticulum, intermediate compartment and cis-Golgi vesicle trafficking. *J. Biol. Chem.* **275**, 13713-13720.

He, H., Giordano, F.J., Hilal-Dandan, R., Choi, D.I., Rockman, H.A., McDonough, P.M., Bluhm, W.F., Meyer, M., Sayen, M.R., Swanson, E. and Dillmann, W.H. (1997). Overexpression of the rat sarcoplasmic reticulum Ca^{+2} ATPase gene in the heart of transgenic mice accelerates calcium transients and cardiac relaxation. *J. Clin. Invest.* **100**, 380-389.

Itin, C., Foguet, M., Kappeler, F., Klumperman, J. and Hauri, H.P. (1995). Recycling of the endoplasmic reticulum/Golgi intermediate compartment protein ERGIC-53 in the secretory pathway. *Biochem. Soc. Trans.* **23**, 541-544.

Jakymiw, A., Raharjo, E., Rattner, J.B., Eystathioy, T., Chan, E.K. and Fujita, D.J. (2000). Identification and characterization of a novel Golgi protein, golgin-67. *J. Biol. Chem.* **275**, 4137-4144.

Jones, L.R., Suzuki, Y.J., Wang, W., Kobayashi, T.M., Rarnesh, V., Franzini-Armstrong, C., Cleemann, L. and Morad, M. (1998). Regulation of Ca^{2+} signaling in transgenic mouse cardiac myocytes overexpressing calsequestrin. *J. Clin. Invest.* **101**, 1385-1393.

Kanaji, S., Iwahashi, J., Kida, Y., Sakaguchi, M. and Mihara, K. (2000). Characterization of the signal that directs Tom20 to the mitochondrial outer membrane. *J. Cell Biol.* **151**, 277-288.

Kiriazis, H. and Kranias, E.G. (2000). Genetically engineered models with alterations in cardiac membrane calcium-handling proteins. *Ann. Rev. Physiol.* **62**, 321-351.

Klopfenstein, D.R., Kappeler, F. and Hauri, H.P. (1998). A novel and direct interaction of endoplasmic reticulum with microtubules. *EMBO J.* **17**, 6168-6177.

Komazaki, S., Nishi, M. and Takeshima, H. (2003). Abnormal junctional membrane structures in cardiac myocytes expressing ectopic junctophilin type I. *FEBS Lett.* **542**, 69-73.

Kontrogianni-Konstantopoulos, A., Jones, E.M., van Rossum, D.B. and Block, R.J. (2003). Obscurin is a ligand for small ankyrin 1 in skeletal muscle. *Mol. Biol. Cell* **14**, 1139-1148.

Kutay, U., Hartmann, E. and Rapoport, T.A. (1993). A class of membrane proteins with C-terminal anchor. *Trends Cell Biol.* **3**, 72-75.

Laemmli, U.K. (1970). Cleavage of structural proteins during the assembly of the head of bacteriophage T4. *Nature* **227**, 680-685.

Lee, C. and Chen, L.B. (1988). Dynamic behaviour of endoplasmic reticulum in living cells. *Cell* **54**, 37-46.

Lee, C., Ferguson, M. and Chen, L.B. (1989). Construction of the endoplasmic reticulum. *J. Cell Biol.* **109**, 2045-2055.

Lippincott-Schwartz, J., Yuan, L.C., Bonifacino, J.S. and Klausner, R.D. (1989). Rapid redistribution of Golgi proteins into the ER in cells treated with brefeldin A: evidence for membrane cycling from the Golgi to ER. *Cell* **56**, 801-813.

Lippincott-Schwartz, J., Donaldson, J.G., Schweizer, A., Berger, E.G., Hauri, H.P., Yuan, L.C. and Klausner, R.D. (1990). Microtubule-dependent retrograde transport of proteins into the ER in the presence of brefeldin A suggests an ER recycling pathway. *Cell* **60**, 821-836.

Liu, K. Z. and G. N. Pierce. (1993). The effects of low density lipoprotein on Ca^{2+} transients in isolated cardiomyocytes. *J. Biol. Chem.* **268**, 3767-3775.

Liu, L., Mohammadi, K., Aynafshar, B., Wang, H., Li, D., Liu, J., Ivanov, A.V., Xie, Z. and Askari, A. (2003). Role of caveolae in signal-transducing functions of cardiac Na^+/K^+-ATPase. *Am. J. Cell. Physiol.* **284**, C1550-1560.

Luo, W., Grupp, I.L., Harrer, J., Ponniah, S., Gropp, G., Duffy, J.J., Doetschman, T. and Kranias, E.G. (1994). Targeted ablation of the phospholamban gene is associated with markedly enhance myocardial contractility and loss of β-agonist stimulation. *Circ. Res.* **75**, 401-409.

Luo, W., Wolska, B.M., Grupp, I.L., Harrer, J.M., Haghighi, K., Ferguson, D.G., Slack, J.P., Grupp, G., Doetschman, T., Solaro, R.J. and Kranias, E.G. (1996). Phospholamban gene dosage effects in the mammalian heart. *Circ. Res.* **78**, 839-847.

Luo, W., Chu, G., Sato, Y., Zhou, Z., Kadambi, V.J. and Kranias, E.G. (1998). Transgenic approaches to define the functional role of dual site phospholamban phosphorylation. *J. Biol. Chem.* **273**, 4734-4739.

Marx, S.O. and Marks, A.R. (2002). Regulation of the ryanodine receptor in heart failure. *Basic Res. Card.* **97** Supplement 1, I49-I51

McDonough, A.A., Velotta, J.B., Schwinger, R.H., Philipson, K.D. and Farley, R.A. (2002). The cardiac sodium pump: structure and function. *Basic Res. Card.* **97** Suppl 1:119-124

Munro, S. (1991). Sequences within and adjacent to the transmembrane segment of alpha-2,6-sialyltransferase specify Golgi retention. *EMBO J.* **10**, 3577-3588.

Munro, S. (1995). An investigation of the role of transmembrane domains in Golgi protein retention. *EMBO J.* **14**, 4695-4704.

Munro, S. (1998). Localization of proteins to the Golgi apparatus. *Trends Cell Biol.* **8**, 11-15.

Nilsson, T., Lucocq, J.M., Mackay, D. and Warren, G. (1991). The membrane-spanning domain of beta-1,4-galactosyltransferase specifies trans Golgi localization. *EMBO J.* **10**, 1367-1375.

Nishimura, N. and Balch, W.E. (1997). A di-acidic signal required for selective export from the endoplasmic reticulum. *Science* **252**, 556-58.

Opie, L.H. (1991). The heart: physiology and metabolism. Second Edition. Raven Press Ltd. New York.

Pierre, P., Scheel, J., Rickard, J.E. and Kreis, T.E. (1992). CLIP-170 links endocytic vesicles to microtubules. *Cell* **70**, 887-900.

Presley, J.F., Cole, N.B., Schroer, T.A., Hirschberg, K., Zaal, K.J. and Lippincott-Schwartz, J. (1997). ER-to-Golgi transport visualized in living cells. *Nature* **389**, 81-85.

Reuter, H., Henderson, S.A., Han, T., Mottino, G.A., Frank, J.S., Ross, R.S., Goldhaber, J.I. and Philipson, K.D. (2003). Cardiac excitation-contraction coupling in the absence of Na^{+}-Ca^{2+} exchange. *Cell Calcium* **34**, 19-26.

Sapperstein, S.K., Lupashin, V.V., Schmitt, H.D. and Waters, M.G. (1996). Assembly of the ER to golgi SNARE complex requires uso1p. *J. Cell Biol.* **132**, 755-767.

Sato, Y., Ferguson, D.G., Sako, H., Dorn, G.W. II, Kadambi, V.J., Yatani, A., Hoit, B.D., Walsh, R.A. and Kranias EG. (1998). Cardiac-specific overexpression of mouse cardiac calsequestrin is associated with depressed cardiovascular function and hypertrophy in transgenic mice. *J. Biol. Chem.* **273**, 28470-28477.

Scheel, J. and Kreis, T.E. (1991). Motor protein independent binding of endocytic carrier vesicles to microtubules in vitro. *J. Biol. Chem.* **266**, 18141-18148.

Schindler, R., Itin, C., Zerial, M., Lottspeich, F. and Hauri, H.P. (1993). ERGIC-53, a membrane protein of the ER-Golgi intermediate compartment, carries an ER retention motif. *Eur. J. Cell Biol.* **61**, 1-9.

Schmitt, J.P., Kamisago, M., Asahi, M., Li, G.H., Ahmad, F., Mende, U., Kranias, E.G., MacLennan, D.H., Seidman, J.G. and Seidman, C.E. (2003). Dilated cardiomyopathy and heart failure caused by a mutation in phospholamban. *Science* **299**, 1410-1413.

Scoote, M. and Williams, A.J. (2002). The cardiac ryanodine receptor (calcium release channel): emerging role in heart failure and arrhythmia pathogenesis. *Card. Res.* **56**, 359-372.

Scriven, D.R.L., Dan, P. and Moore, E.D.W. (2000). Distribution of proteins implicated in excitation-contraction coupling in rat ventricular myocytes. *Biophys. J.* **79**, 2682-2691.

Sitia, R. and Meldolesi, J. (1992). Endoplasmic reticulum: a dynamic patchwork of specialized subregions. *Mol. Biol. Cell* **3**, 1067-1072.

Song, K.S., Scherer, P.E., Tang, Z.L., Okamoto, T., Li, S., Chafel, M., Chu, C., Kohtz, S. and Lisanti, M.P. (1996). Expression of caveolin-3 in skeletal, cardiac and smooth muscle cells. *J. Biol. Chem.* **271**, 15160-15165.

Takeshima, H., Komazaki, S., Hirose, K., Nishi, M., Noda, T. and Iino, M. (1998). Embryonic lethality and abnormal cardiac myocytes in mice lacking ryanodine receptor type 2. *EMBO J.* **17**, 3309-3316.

Takeshima, Hl, Komazaki, S., Nishi, M., Iino, M. and Kangawa, K. (2000). Junctophilins: a novel family of junctional membrane complex proteins. *Mol. Cell* **6**, 11-22.

Tang, B.L., Wong, S.H., Low, S.H. and Hong, W. (1992). The transmembrane domain of N-glucosaminyltransferase I contains a Golgi retention signal. *J. Biol. Chem.* **267**, 10122-10126.

Tang, B.L., Low, S.H., Hauri, H.P. and Hong W. (1995). Segregation of ERGIC53 and the mammalian KDEL receptor upon exit from the 15°C compartment. *Eur. J. Cell Biol.* **68**, 398-410.

Taylor, R.S., Jones, S.M., Dahl, R.H., Nordeen, M.H. and Howell, K.E. (1997). Characterization of the Golgi complex cleared of proteins in transit and examination of calcium uptake activities. *Mol. Biol. Cell* **8**, 1911-1931.

Terasaki, M., Chen, L.B. and Fujiwara, K. (1986). Microtubules and the endoplasmic reticulum are highly interdependent structures. *J. Cell Biol.* **103**, 1557-1568.

Verkhratsky, A. and Shmigol, A. (1996). Calcium-induced calcium release in neurones. *Cell Calcium* **19**, 1-14.

Villa, A., Podini, P., Nori, A., Panzeri, M.C., Martini, A., Meldolesi, J. and Volpe, P. (1993). The endoplasmic reticulum-sarcoplasmic reticulum connection. *Exp. Cell Res.* **209**, 140-148.

Volpe, P., Villa, A., Podini, P., Martini, A., Nori, A., Panzeri, M.C. and Meldolesi, J. (1992). The endoplasmic reticulum-sarcoplasmic reticulum connection: distribution of endoplasmic reticulum markers in the sarcoplasmic reticulum of skeletal muscle fibers. *Proc. Natl. Acad. Sci. U.S.A.* 89, 6142-6146.

Wattenberg, G., and Lithgow, T. (2001). Targeting of C-terminal (Tail)-anchored proteins: understanding how cytoplasmic activities are anchored to intracellular membranes. *Traffic* **2**, 66-71.

Weisz, O.A., Swift, A.M. and Machamer, C.E. (1993). Oligomerization of a membrane protein correlates with its retention in the Golgi complex. *J. Cell Biol.* **122**, 1185-1196.

Wielowieyski, P.A, Sevinc, S., Guzzo, R., Salih, M., Wigle, J.T. and Tuana, B.S. (2000). Alternative Splicing, Expression, and Genomic Structure of the 3' Region of the Gene Encoding the Sarcolemmal-associated Proteins (SLAPs) Defines a Novel Class of Coiled-coil Tail-anchored Membrane Proteins. *J. Biol. Chem.* **275**, 38474-38481.

Wigle, J.T., Demchyshyn, L., Pratt, M.A., Staines, W.A., Salih, M. and Tuana, B.S. (1997). Molecular cloning, expression, and chromosomal assignment of sarcolemmal-associated proteins. A family of acidic amphipathic alpha-helical proteins associated with the membrane. *J. Biol. Chem.* **272**, 32384-32394.

Fig. 1. SLMAPs are expressed in the developing mouse myocardium. (A) Sagital sections (6 μm) of formalin-fixed mouse embryos were eosin-hematoxlyin stained (A; a, b) or subject to immunohistochemical analysis using anti-SLMAP rabbit polyclonal antibodies (A; c, d). At embryonic day nine, SLMAP-specific labelling (A; c, d) was observed within both the presumptive atrial (A) and ventricular (V) chambers, with greater expression observed in the ventricle. Scale bar = 250 μm. **(B)** At 13 d.p.c. SLMAPs were uniformly expressed in the atrial and ventricular myocardium, as well as the interventricular septum (IVS) and interatrial septum (IAS) (B; a, c, d). An immunofluorescent signal was not observed within the myocardium of 13 d.p.c. hearts using pre-immune rabbit serum in sequential (transverse) sections (B; b).

Figure 1 **Chapter 3**

A.

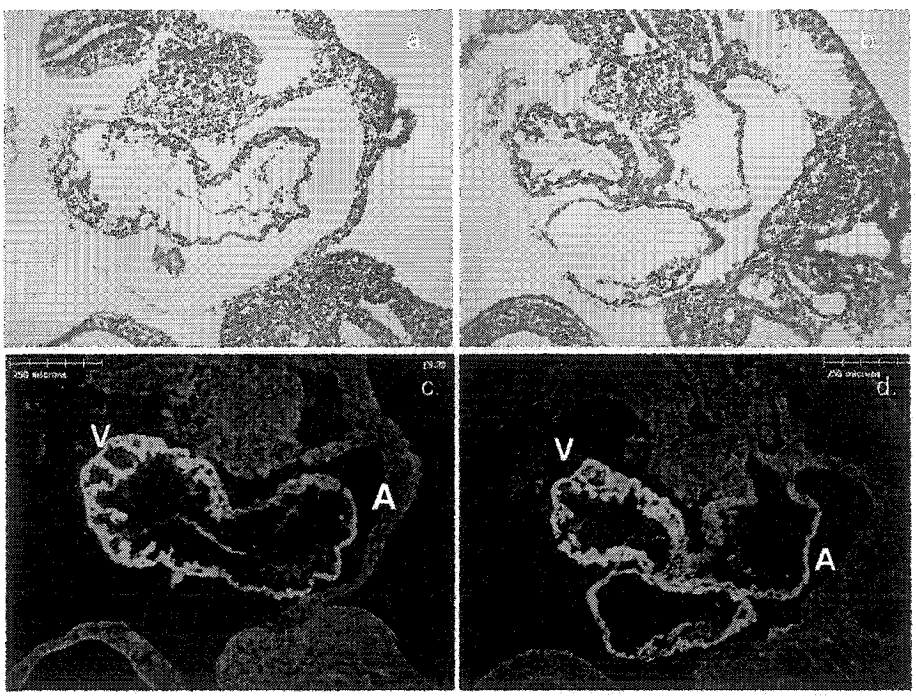

B.

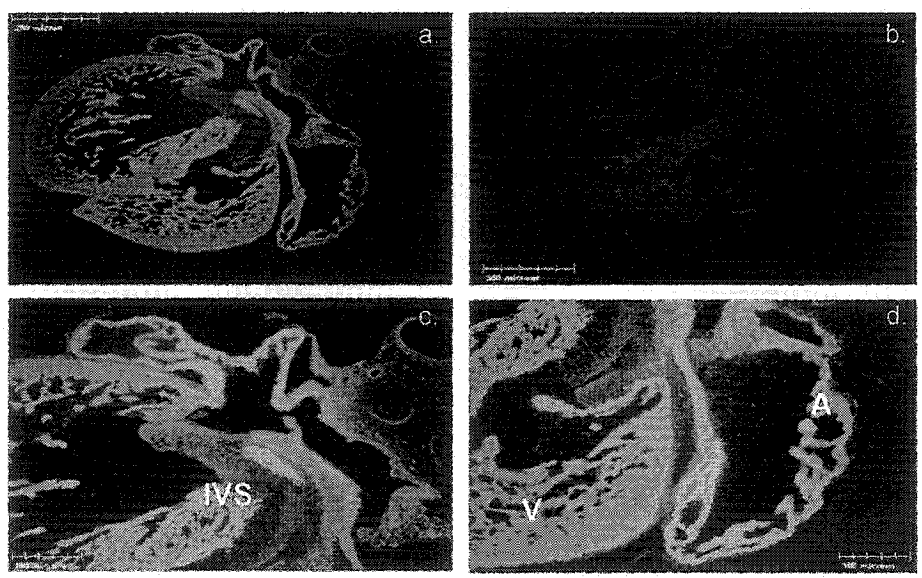

Fig. 2. SLMAP localization relative to myofibril contractile elements in developing and adult ventricular myocytes. Ventricular myocytes from 13 d.p.c. mouse embryos (a-c), 18 d.p.c. mouse embryos (d-f) and adult rats (g-i) were stained for SLMAP (a, d, g) and the myofibril marker protein, α-actinin (b, e, h). The merge of the SLMAP and the α-actinin immunofluorescent signals are shown in (c, f, i). α-actinin proteins were visualized by confocal imaging at striated formations demarcating the Z-line of the myofibril in ventricular myocytes at 13 d.p.c. (b) SLMAP-specific labelling was displayed throughout the myocyte at this stage (a). SLMAP antibodies stained reticular formations (d) in older embryos (18 d.p.c.) and showed limited overlap with the z-line marker α-actinin (e, f). In isolated adult rat ventricular myocytes co-stained for SLMAP (g) and α-actinin (h), immunoconfocal images showed areas of co-localization (yellow) (i) as well as distinct SLMAP labelling at structures perpendicular to the α-actinin-labelled striations. Scale bar = 10 μm.

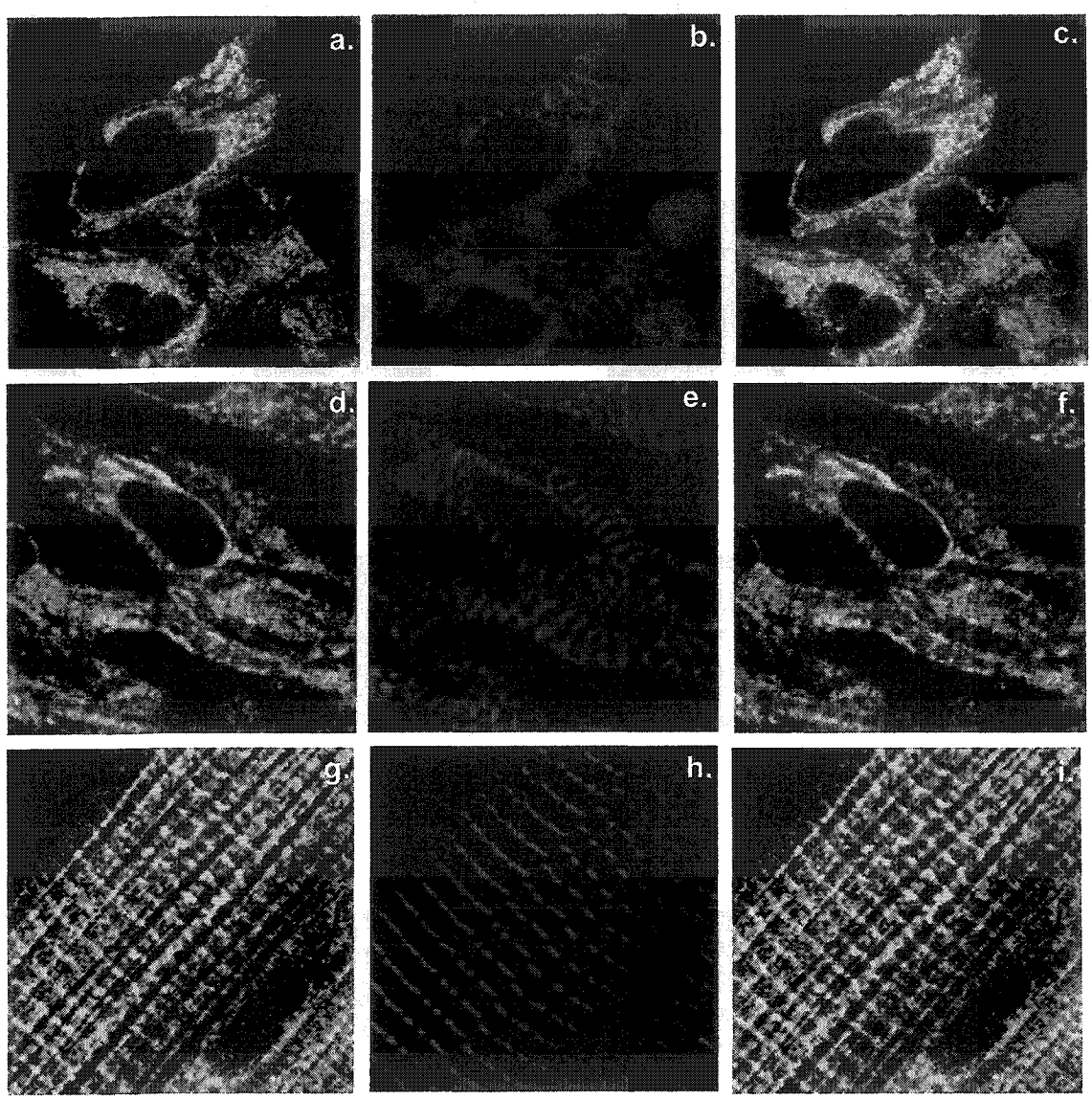
a.
b.
c.
d.
e.
f.
g.
h.
i.

Fig. 3. SLMAP distribution in cardiac membrane systems of cultured adult ventricular myocytes. (A) Caveolin 3 antibodies labelled peripheral structures representing a subdomain of the plasma membrane (A; b). SLMAP antibodies (A; a) primarily labelled internal structures (A; a). Overlay of the caveolin 3 and SLMAP staining showed that the two immunofluorescent signals coincided at membrane invaginations (A; c). Consistent with the distribution of membrane components of the terminal cisternae SR, the monoclonal anti-RyR2 antibody labelled regularly spaced doublets (A; e). SLMAP antibodies (A; d) stained similar structures as the RyR2 antibody as well as tubular-like structures that were distinct from RyR2 labelling (A; c). Scale bar = 10 μm. **(B)** Deconvolution microscopy was used to examine cells stained with SLMAP (green, panel A-C), caveolin-3 (red, panel B) and the ryanodine receptor (red, panel C). Areas of co-localization are indicated in white. The two parallel arrows in panel A point to the surface of the cell, which is heavily labeled by SLMAP antibodies, and to a pair of Z lines. Scale bar = 2 μm in each dimension and image is 0.5 μm thick (two Z planes). np, nuclear poles; m, M-line; *, nucleus; u = 'patchy' SLMAP labelling.

Figure 3

A.

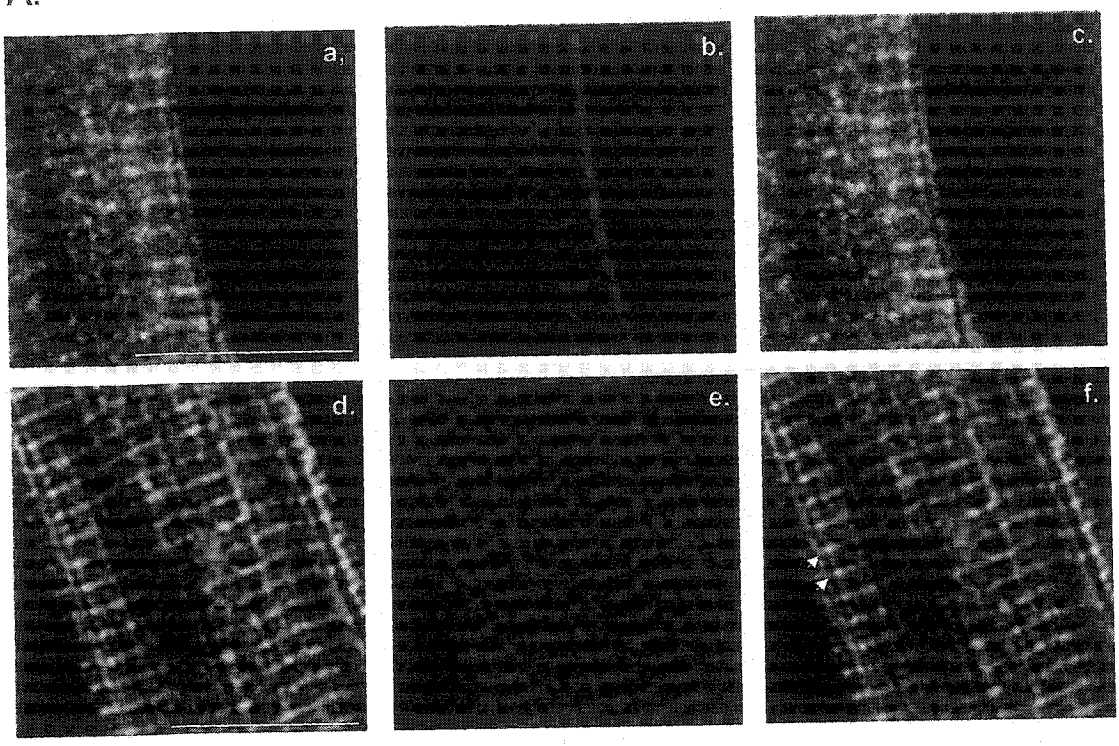

B.

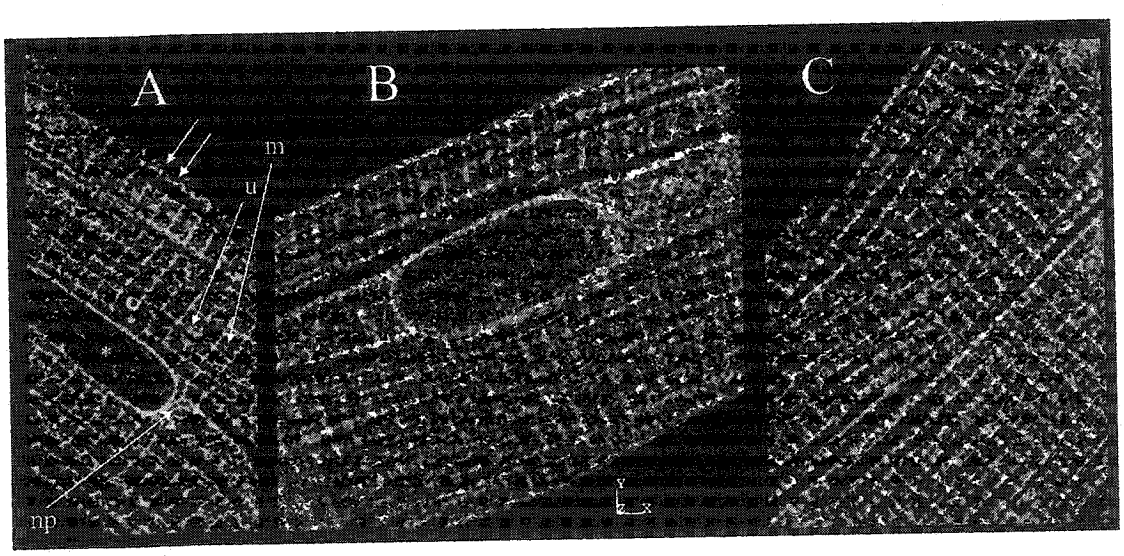

Fig. 4. Identification of the SLMAP-binding partners. **(A)** A Coomassie stained gel shows the purified GST (26 kDa) and GST-SLMAP1 fusion protein (GST-SLP1; 60 kDa) used in the 'pull-down' assays. **(B)** The electrophoretic profile of proteins isolated from the H9c2 lysate that associated with GST or GST-SLP1 proteins immobilized on glutathione sepharose beads is shown. A 35 kDa and 70 kDa protein specifically bound the GST-SLP1 proteins (lane 5). These bands were not recovered in H9c2 lysates incubated with GST alone (lane 4) or in buffer controls (no lysate) incubated with either GST (lane 2) or GST-SLP1 (lane 3). **(C)** Electrophoretic profile of proteins recovered from a rabbit heart microsomal lysate that associated with GST or GST-SLP1 proteins. A 220 kDa protein specifically associated with GST-SLP1 (lane 4). This protein did not interact with GST alone (lane 5); nor was this band identified in buffer controls (no lysate) incubating with GST (lane 2) or GST-SLP1 (lane 3).

Figure 4

A.

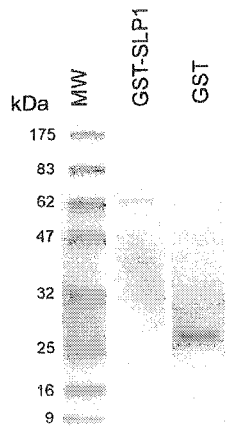
kDa
MW
GST-SLP1
GST
175
83
62
47
32
25
16
9

B.

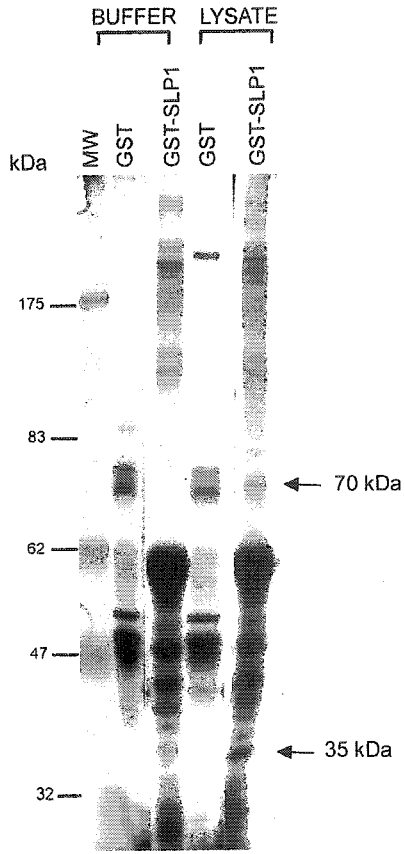
BUFFER
LYSATE
kDa
MW
GST
GST-SLP1
GST
GST-SLP1
175
83
62
47
32
70 kDa
35 kDa

C.

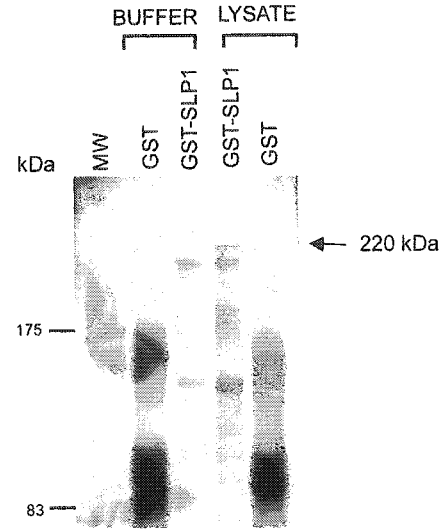
BUFFER
LYSATE
kDa
MW
GST
GST-SLP1
GST-SLP1
GST
175
83
220 kDa

Fig. 5. Endogenous SLMAP3 is expressed in purified ER fractions from rat liver. Rat liver was fractionated by sucrose gradient centrifugation as described in Materials and Methods. Western blot analysis demonstrated that the cis-Golgi marker, α-mannosidase resides in the stacked golgi fraction 1 (lane SGF1). Anti-SLMAP polyclonal antibodies did not detect SLMAPs in this fraction. Endogenous SLMAP3 (91 kDa) proteins are distributed among fractions where the ER marker calnexin is expressed (lanes B1; S3; SGF3). H (homogenate); PNS (postnuclear supernatant); SGF (stacked golgi fraction); P (pellet).

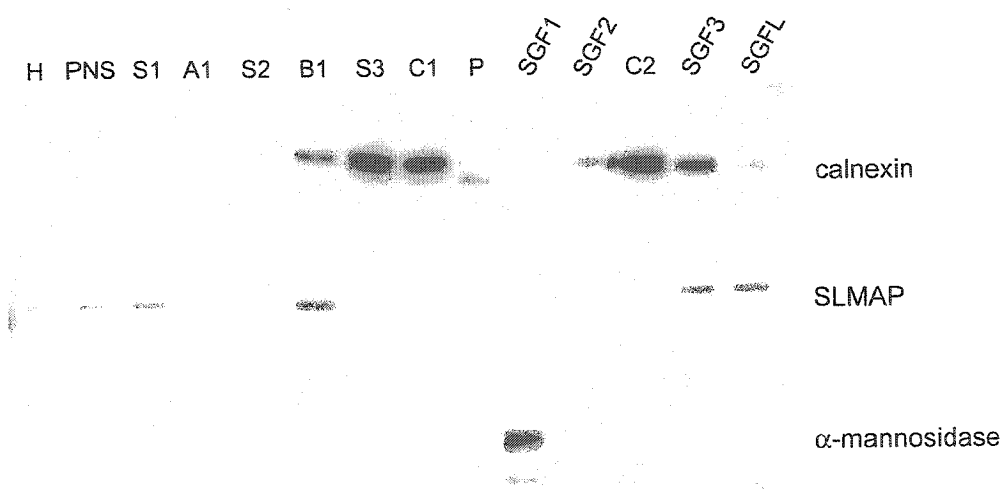
H
PNS
S1
A1
S2
B1
S3
C1
P
SGF1
SGF2
C2
SGF3
SGFL
calnexin
SLMAP
α-mannosidase

Fig. 6. Schematic representation of 6Myc-tagged SLMAP expression constructs. Sequences encoding the 6Myc-epitope tag were fused in frame with: SLMAP1 sequences encompassing TMD1 (6Myc-SLMAP-TMD1); SLMAP1 sequences encompassing TMD2 (6Myc-SLMAP-TMD2); SLMAP1 sequences lacking either TMD (6Myc-SLMAP1ΔTM); and SLMAP1 sequences encompassing TMD2, yet lacking the leucine zipper motifs (6Myc-SLMAP1ΔLZ-TMD2). Sequences encoding GFP were also fused in frame with amino-terminal sequences of SLMAP1 encompassing TMD2 (GFP-SLMAP1-TMD2). These constructs were used for transient transfection studies in COS7 cells.

Figure 6

Chapter 3

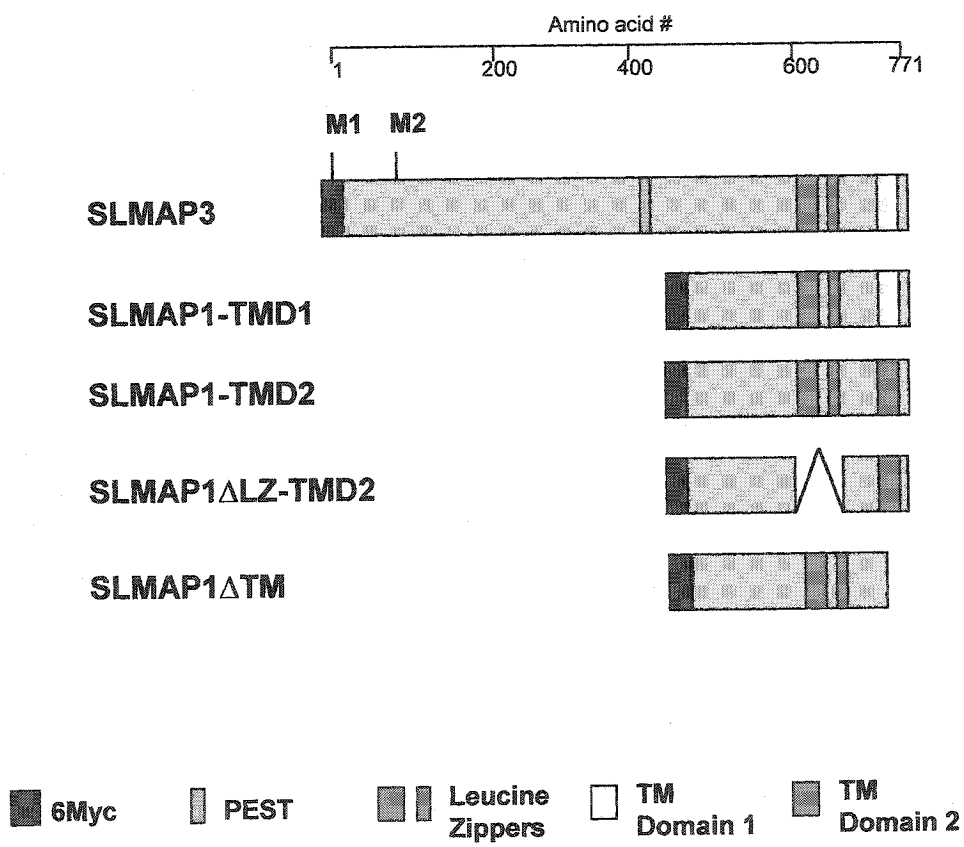

Fig. 7. Divergent carboxyl-terminal transmembrane domains mediate SLMAP membrane targeting. (A) Myc antibody staining of cells expressing 6Myc-SLMAP1-TMD1 revealed targeting to juxtanuclear sites and reticular formations extending throughout the cytoplasm (A; a). The 6Myc-SLMAP1-TMD2 fusion protein was ectopically expressed at filamentous-like structures in COS7 cells (A;b). A similar pattern of localization was observed in cells expressing 6Myc-SLMAP1ΔLZ-TMD2 (A; c). In the absence of either transmembrane domain (6Myc-SLMAP1ΔTM), myc labeling was observed throughout the cell and membrane associations were not detected (A; d). **(B)** COS7 cells were co-transfected with 6Myc-SLMAP-TMD1 and GFP-SLMAP-TMD2 (B; a-c) to confirm that the two transmembrane domains did not target SLMAPs to the same intracellular membrane sites. Myc labelled cells are shown in red and GFP labelled cells are shown in green. Cells co-transfected with 6Myc-SLMAP-TMD2 and GFP-SLMAP-TMD2 (B; d-f) showed complete overlap (yellow) of the myc and GFP signals. The merge of the myc and GFP signal are shown in (B; c, f). Scale bar = 10 μm

A.

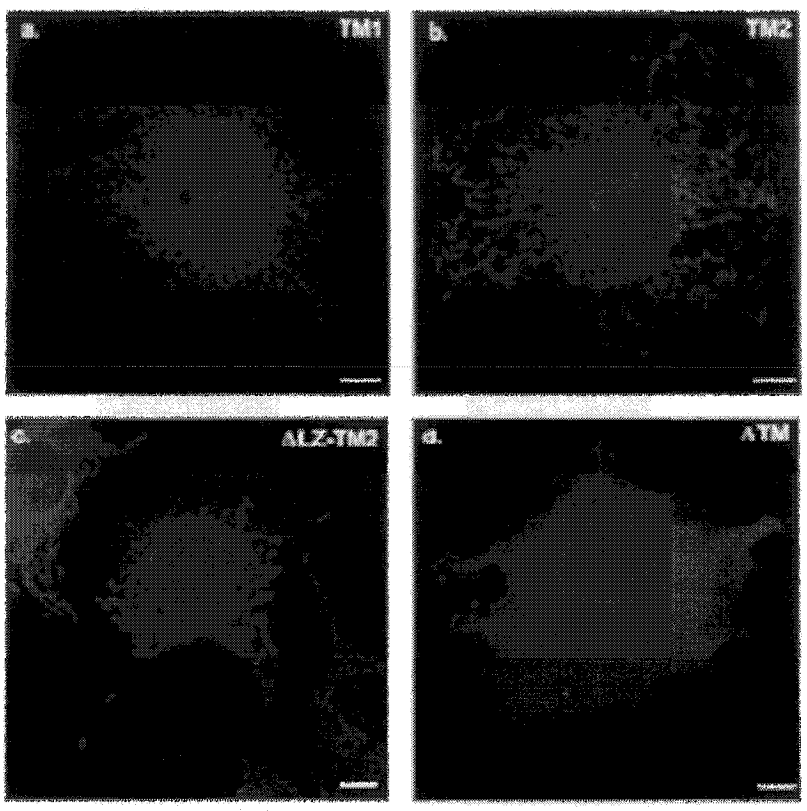

B.

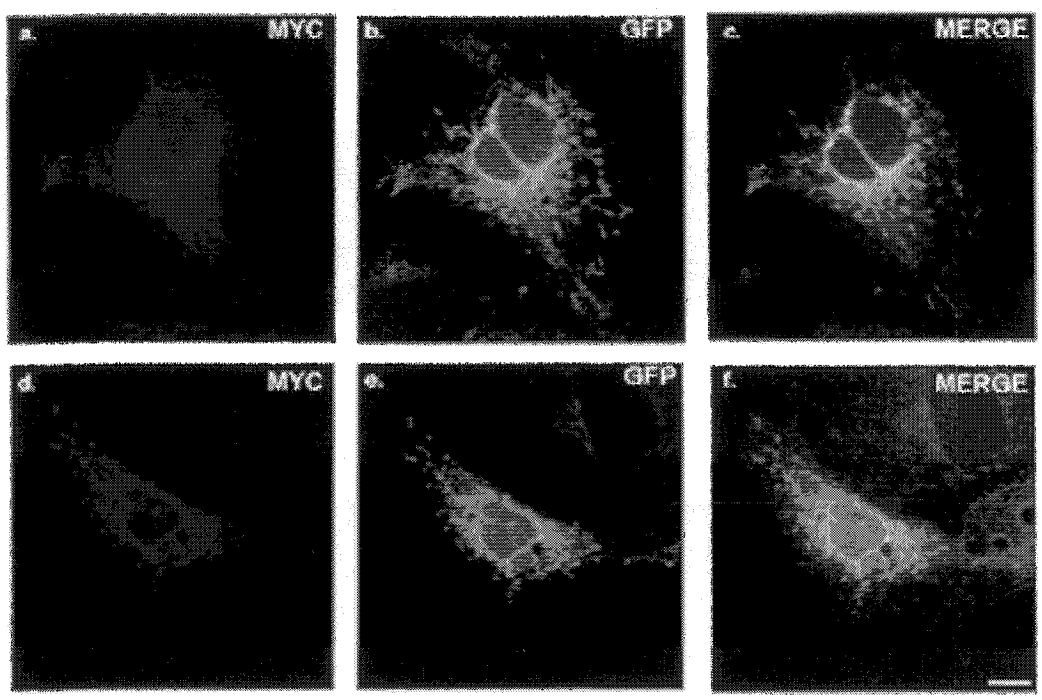

Fig. 8. SLMAP co-staining with markers of membrane bound organelles of the secretory system. **(A)** COS7 cells transiently transfected with 6Myc-tagged SLMAP variants encompassing either TMD1 (A; a-c), TMD2 (A; d-f) or ΔLZ-TMD2 (g-i) were stained with anti-calnexin polyclonal antibodies (b, e, h). Significant co-distribution of the myc (A; a) and calnexin signal (A; b) was observed at perinuclear sites as well as at reticular formations extending throughout the cytoplasm in cells expressing the SLMAP-TMD1 variant (A; a-c). The overlay of the myc and calnexin signal in these cells is shown in (A; c). Whereas considerable overlap (yellow) of the calnexin signal (A; e) and the myc signal (A; d) was observed in COS7 cells expressing TMD2 (A; d-f), regions where the two signals remained distinct were also notable (A; f, merge). The distinction between the calnexin signal (h) and the myc signal (g) was also apparent in cells expressing the SLMAPΔLZ-TMD2 (A; i, merge). Scale bar = 10 μm

Figure 8A

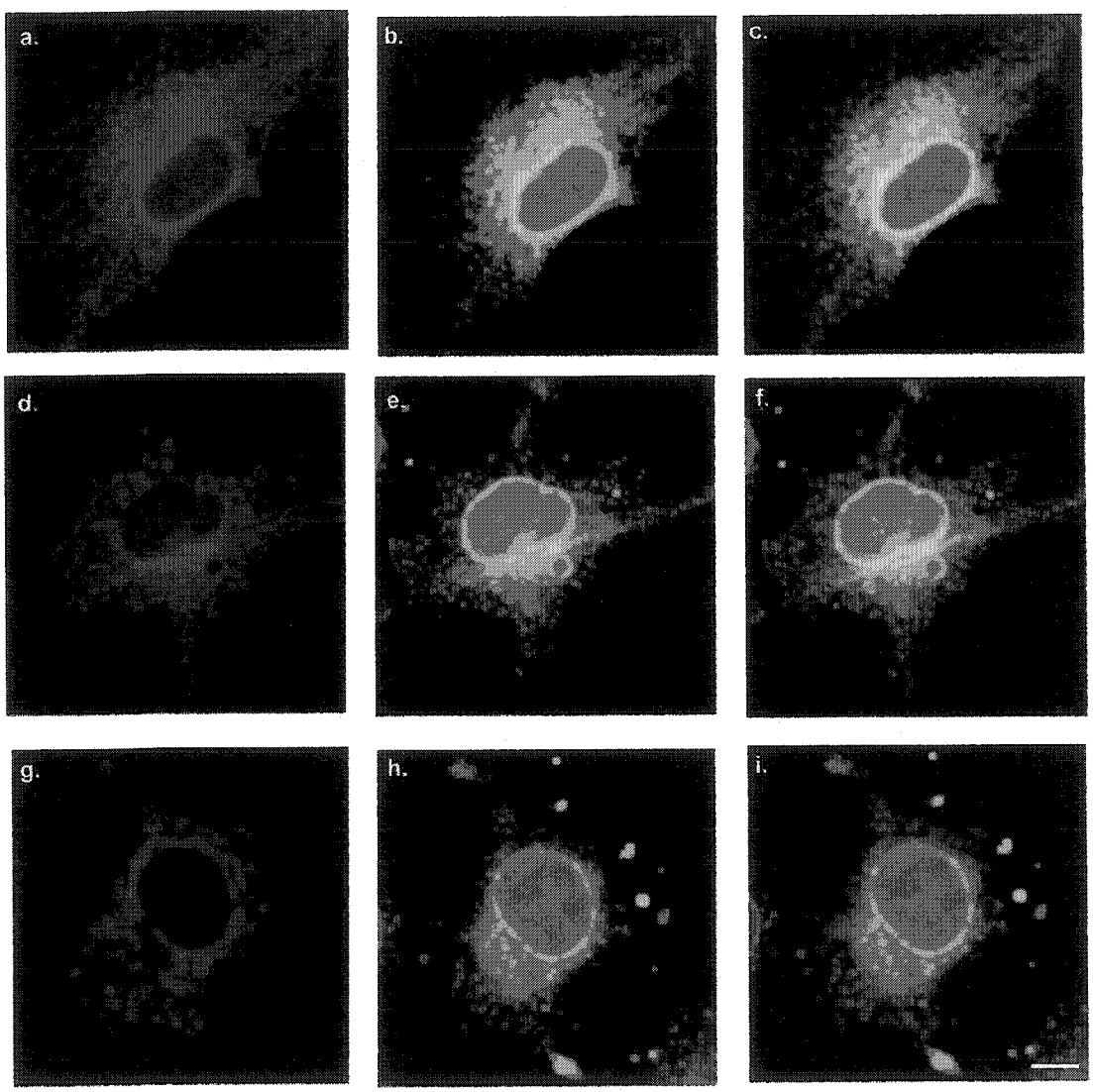

Fig. 8. SLMAP co-staining with markers of membrane bound organelles of the secretory system. (B) The ERGIC of cells transfected with either 6Myc-SLMAP-TMD1 (B; a-c) or 6Myc-SLMAP1-TMD2 (d-f) was detected by immunofluorescent labeling with anti-ERGIC-53 monoclonal antibodies (B; b, e). Co-staining with anti-SLMAP polyclonal antibodies (B; a, d) revealed that 6Myc-SLMAP-TMD1 and 6Myc-SLMAP1-TMD2 extended beyond the boundaries of the ERGIC (B; c, f). Scale bar = 10 μm

Figure 8B

Chapter 3

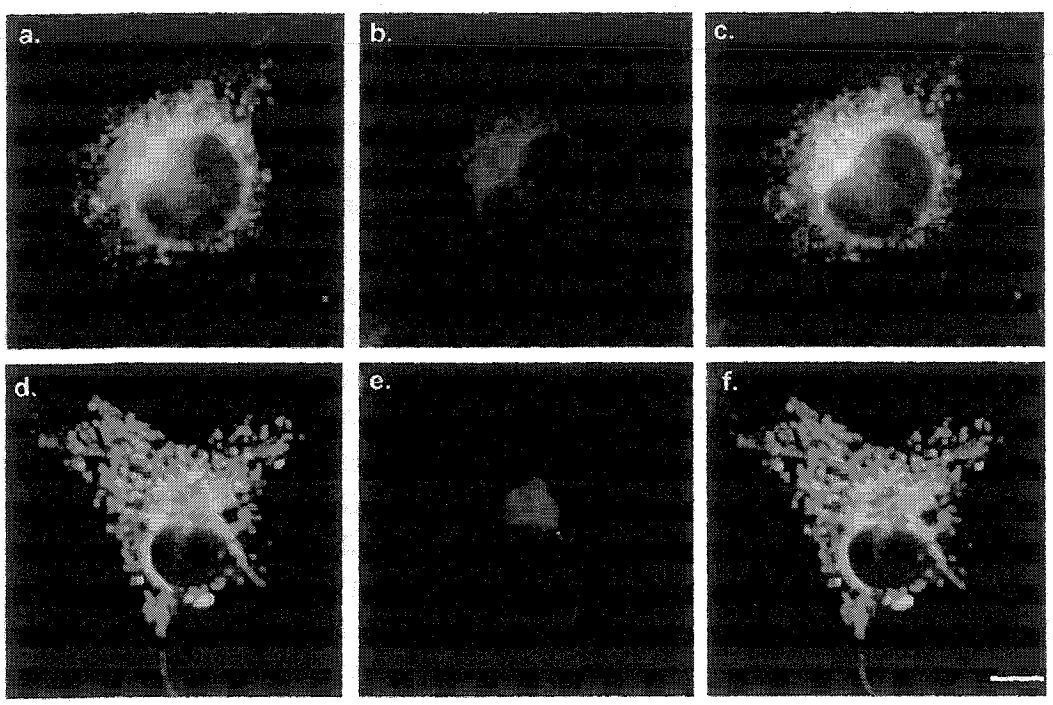

Fig. 8. SLMAP co-staining with markers of membrane bound organelles of the secretory system. (C) The golgi was labelled by anti-golgi 58K monoclonal antibodies (C; b, e, h) in cells expressing either 6Myc-SLMAP-TMD1 (C; a-c); 6Myc-SLMAP-TMD2 (C; d-f) or 6Myc-SLMAPΔLZ-TMD2 (g-i). Anti-SLMAP antibodies were used to detect the localizations of the 6Myc-tagged fusion proteins (a, d, g). The ectopically expressed SLMAP variants were not shown to co-distribute with the golgi marker protein, as the two signals remained distinct in overlays of the two images (C; c, f, i). Scale bar = 10 μm.

Figure 8C

Chapter 3

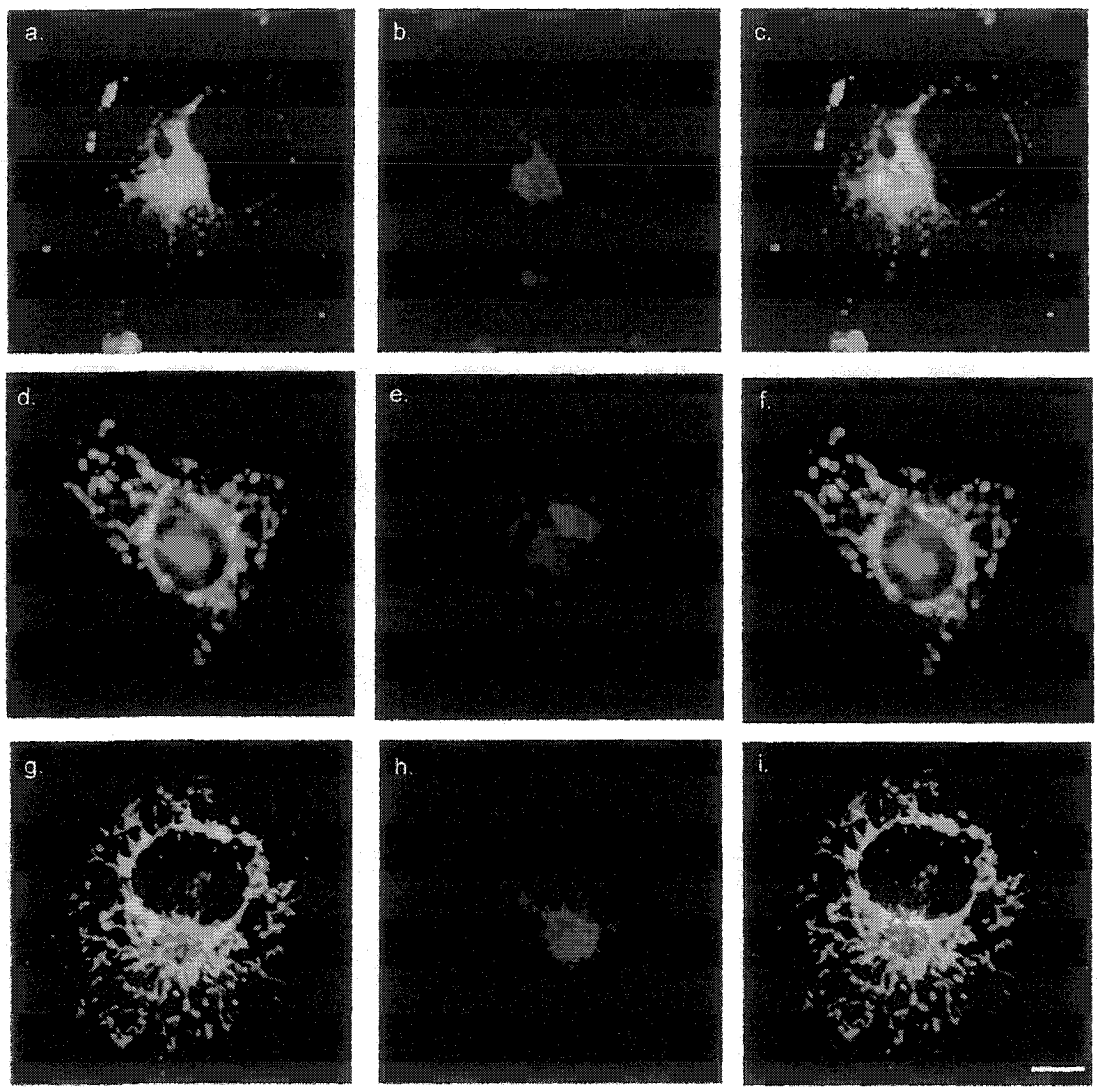

Fig. 9. SLMAP-TMD1 membrane associations are microtubule dependent. (A) COS 7 cells were transfected with the ER-localized 6Myc-SLMAP-TMD1 variant (A; a, b, d, e) or the transmembrane domain mutant (6Myc-SLMAPΔTM) (A; c, f). In control cells, SLMAP antibodies detected the ectopically expressed 6Myc-SLMAP-TMD1 proteins at reticular formations (A; a). Anti-α-tubulin antibodies labelled a filamentous microtubule network in control cells (A; d). In cells treated with nocodazole (A; b, c, e, f), the distribution of α-tubulin was transformed from a filamentous to a diffuse pattern (A; e, f). Disruption of microtubules induced the formation of punctate structures in cells expressing 6Myc-SLMAP-TMD1 (A; b). Treatment with nocodazole did not alter the distribution of the transmembrane domain mutant (A;c). **(B)** Disruption of the actin cytoskeleton with cytochalasin D did not affect SLMAP-membrane associations. The filamentous actin cytoskeleton (B; e, g) was detected by phalloidin staining in cells transfected with either 6Myc-SLMAP-TMD1 (B; a, b, e, f) or 6Myc-SLMAP-TMD2 (B; c, d, g, h). Treatment with cytochalasin D caused the depolymerization of the actin filaments as shown in (B; f, h). The distributions of 6Myc-SLMAP-TMD1 (C; a, b) or 6Myc-SLMAP-TMD2 (C; c,d) was unaffected by cytochalasin D treatment, as assessed by myc labeling (C; b,d). Scale bar = 10 μm.

A.

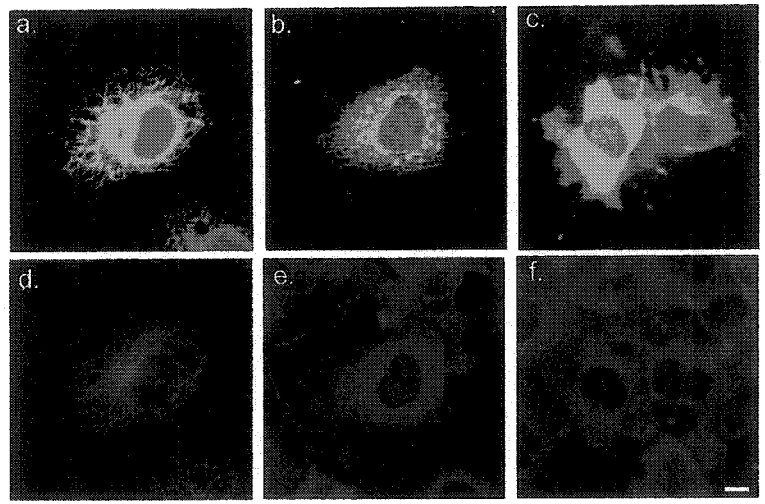

B.

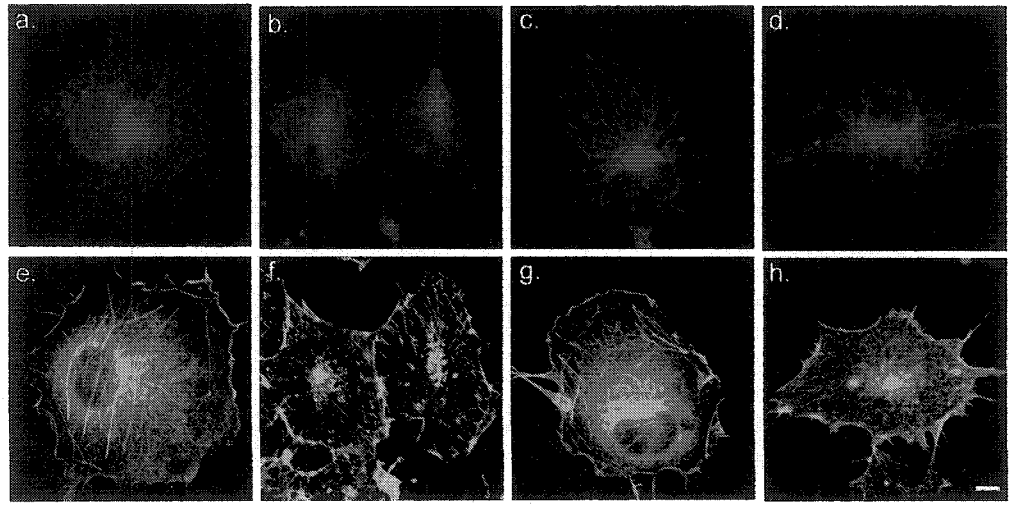

Fig. 10. SLMAPs share similarity with Uso1p. A BLAST homology search was performed to identify proteins that share identity with SLMAP. SLMAP amino acid sequences (Accession No. AAA65597) showed 24% similarity over 261 amino acids with the yeast protein Uso1p (Accession No. NP 010225). A putative di-acidic sorting signal {(D/E)X(D/E)} (in red) was identified within SLMAP sequence. A tyrosine-based motif (underlined) was also identified upstream of the di-acidic sorting motif.

Identities = 63/261 (24%), Positives = 133/261 (50%), Gaps = 6/261 (2%)

```
SLAMP: 30   QVEESSKQIQVLQAQLQRLHMDIENLREEKDNEITSTRDELLSARDEILLLHQAAEKAAS 89
           Q+E  S +  +   QL++   D+E  +EE  ++  S++DE  S    +    + A  A
USO1p: 1014 QIERGSIEKNI--EQLKKTISDLEQTKEEIISKSDSSKDEYESQISLLKEKLETATTAND 1071

SLMAP: 90   ERDTDIASLQEELKKVRAELERWRKAASEYEKEVTSLQSSFQLRCQQCEDQQKEEATRLQ 149
           E     I+ L +  +++ AEL  ++   +E E ++ + + + +   ++ E+  KEE  +L+
USO1p: 1072 ENVNKISELTKTREELEAELAAYKNLKNELETKLETSEKALK-EVKENEEHLKEEKIQLE 1130

SLMAP: 150  GELEKLRKEWNVLETECHSLKKENVLLSSELQRQEKELHNSQKQSLELTSDLSILQMTRK 209
            E  + +++ N L     SL+KE+  L+++L++ E+++ N ++Q  E  S L+  ++T
USO1p: 1131 KEATETKQQLNSLRANLESLEKEHEDLAAQLKKYEEQIANKERQYNEEISQLND-EITST 1189

SLMAP: 210  ELENQMGSLKEQHLRDSADLKILLSKAENQAKDVQKEYEKTQTVLSELKLKFEMTEQEKQ 269
           + EN+  S+K+++     ++K + S +E Q+   + E +     + ELK K E  E
USO1p: 1190 QQENE--SIKKKNDELEGEVKAMKSTSEEQSNLKKSEIDALNLQIKELKKKNETNEASLL 1247

SLMAP: 270  SITDELKQCKDNLKLLQEKGN 290
                ++     +K LQ++ N
USO1p: 1248 ESIKSVESETVKIKELQDECN 1268
```

Fig. 11. Overexpression of SLMAP does not affect VSV-G transport from the ER. COS7 cells were co-transfected with 6Myc-SLMAP and ts045-VSV-G-GFP. When maintained at 40°C (a, d, g), the GFP-tagged viral glycoprotein was retained in the ER (d) and co-distributed with the myc-labelled SLMAP protein (a). At 32°C, ts045-VSV-G-GFP exited the ER and was observed at perinuclear structures as well as at the cell periphery (e); whereas the 6Myc-SLMAP (b) appeared to remain in the ER. In cells incubated at reduced temperatures (15°C), the GFP-tagged viral glycoprotein is redistributed to perinuclear punctate-like structures indicative of the ERGIC (f). The localization of the 6Myc-SLMAP (c) remained unaltered in these cells. Overlay of the myc and GFP signals are shown in (g, h, i).

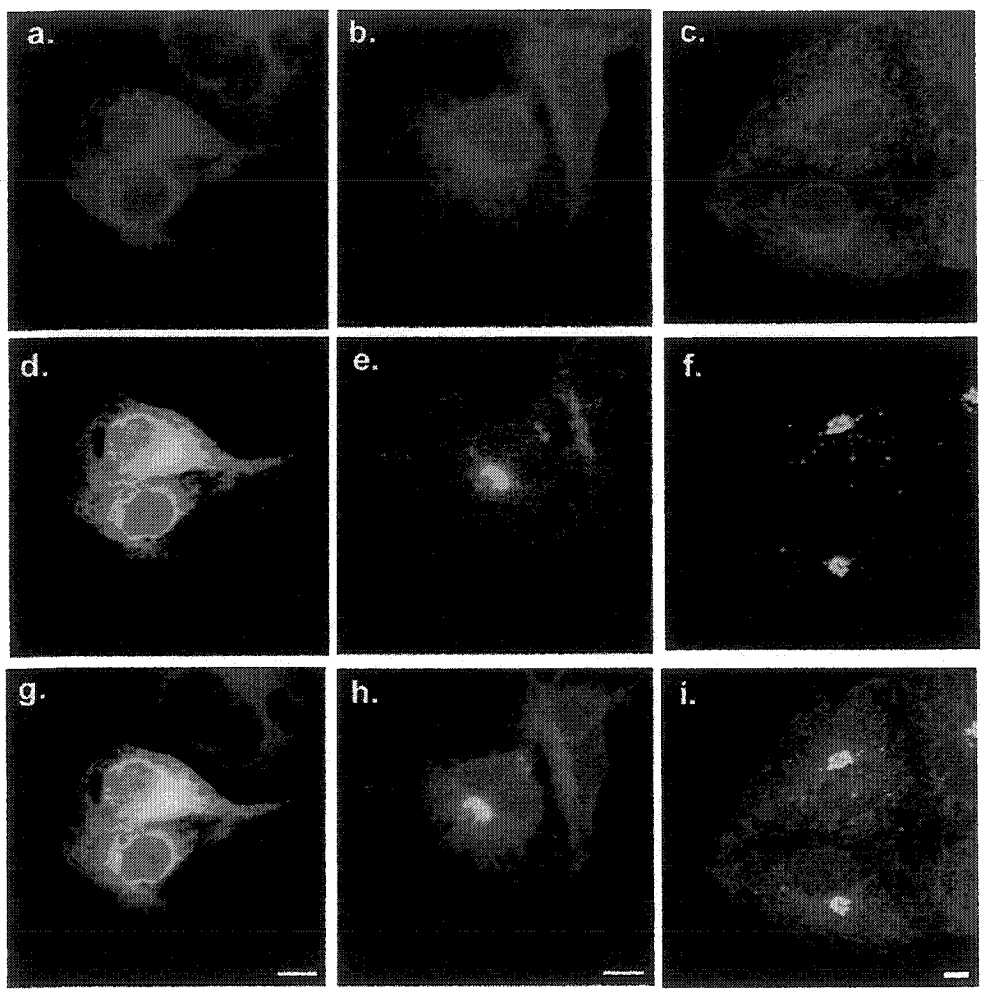
a.
b.
c.
d.
e.
f.
g.
h.
i.

Fig. 12. TMD2 sequences direct SLMAPs to the mitochondria in COS7 cells. COS7 were transiently transfected with 6Myc-SLMAP-TMD1 (a-c); 6Myc-SLMAP-TMD2 (d-f); or 6Myc-SLMAPΔLZ-TMD2 (g-i). Cells were co-stained with anti-myc monoclonal antibodies (a, d, g) and anti-Tom20 polyclonal antibodies (b, e, h). The overlay of the two signals is shown in (c, f, i). Whereas the myc and Tom20 signals in 6Myc-SLMAP-TMD1 expressing cells were largely distinct (c); the myc and Tom20 signals were found to coincide at filamentous-like structures representing the mitochondria in those cells expressing either 6Myc-SLMAP-TMD2 (f) or 6Myc-SLMAPΔLZ-TMD2 (i). Scale bar = 10 μm

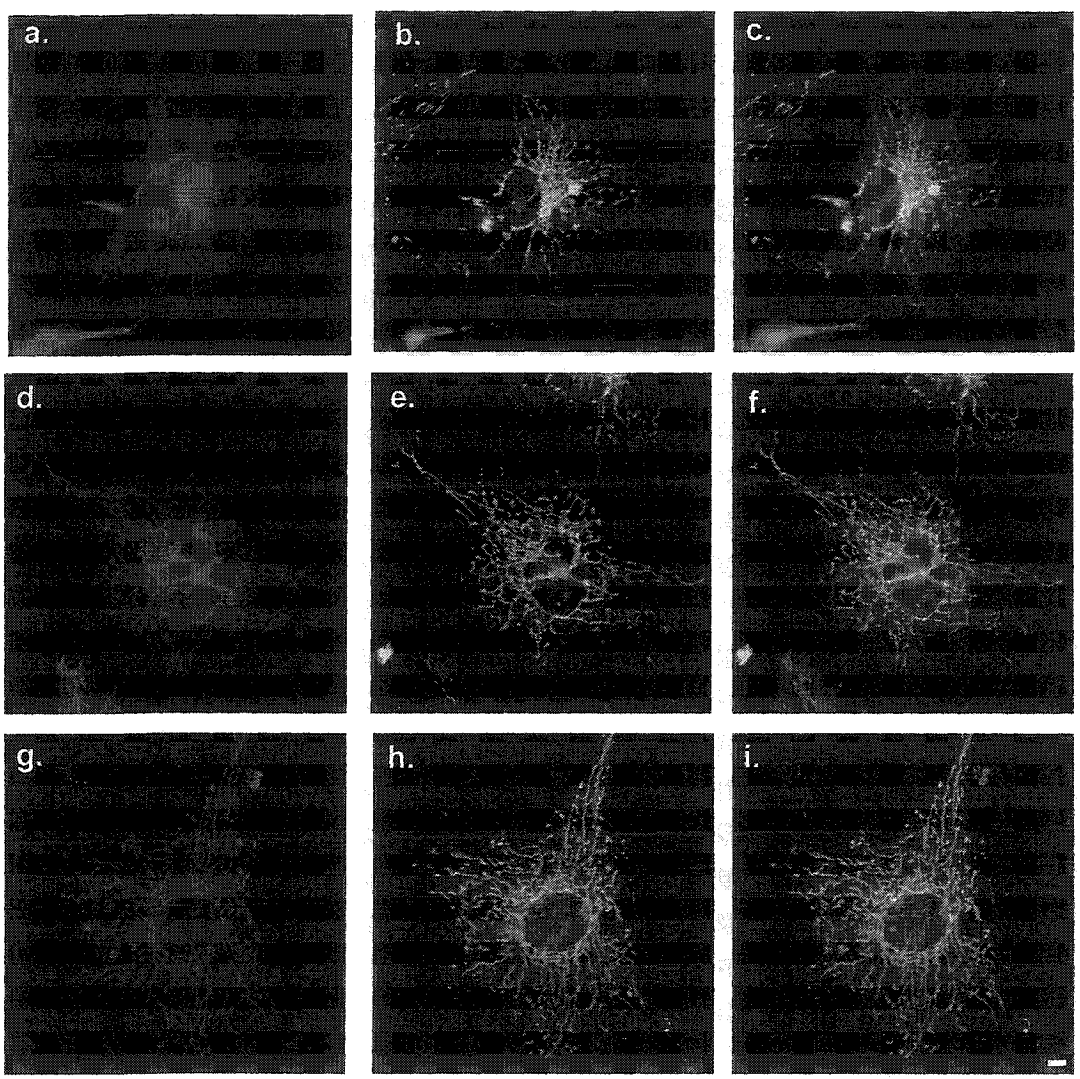
a.
b.
c.
d.
e.
f.
g.
h.
i.

Chapter Four.

Overview of the structure, composition and function of the microtubule organizing centre.

Examination of the subcellular localizations of endogenous SLMAPs by immunocytochemistry resulted in the identification of a novel variant that localizes at centrosomes. The genomic organization of the 5' sequences which encode this novel isoform as well as the structural features that dictate targeting of SLMAPs to centrosomes are described in the appended manuscript (Chapter Five). The following provides an overview of the functional significance of this organelle in cell biology as well as a description of various structural and regulatory components necessary for proper centrosome activity.

A. Genomic Stability: Faithful segregation of sister chromatids.

In proliferating cells, the cell's complement of nuclear DNA is duplicated once every cell cycle during S phase and must be subsequently partitioned to incipient daughter cells to ensure genomic stability. To accomplish this, the cell must properly assemble a bipolar microtubule-based structure known as the mitotic spindle. As depicted in Figure 1, spindle microtubules are anchored by a dynamic structure termed the centrosome, otherwise known as the microtubule organizing center (MTOC) of the cell.

Almost a century ago, Theodore Boveri (1914) proposed that defects in centrosome dynamics might give rise to the chromosomal abnormalities characteristic of cancer cells. The link between centrosome function and cancer has been further corroborated by the observations that malignant tumours and tumour-derived cell lines exhibit several structural and numerical centrosome abnormalities (Salisbury et al., 1999; Kramer and Ho, 2001; Nigg, 2002). Defects in centrosome activities may result in the

Figure 1. Aberrant mitotic spindle formation in centrosome defective cells.

(A) Centrosomes (red) are positioned at the poles of the mitotic spindle apparatus. The plus-ends of mitotic microtubules emanating from centrosomes make contact with the duplicated chromosomes aligned at the center of the spindle. A bipolar mitotic spindle is required for equal partitioning of the duplicated chromosomes to the two incipient daughter cells.

(B) Defects in centrosome duplication or separation may give rise to monopolar spindles, which are incapable of chromosome segregation (modified from Doxsey, 1998).

(C) In the event of excessive centrosome duplication, multipolar spindles are generated and result in the distribution of chromosomes to more than two daughter cells.

A.

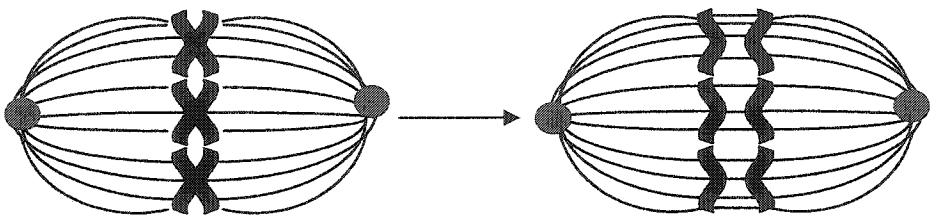

B.

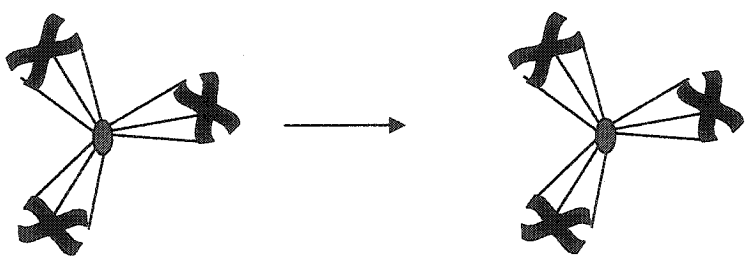

C.

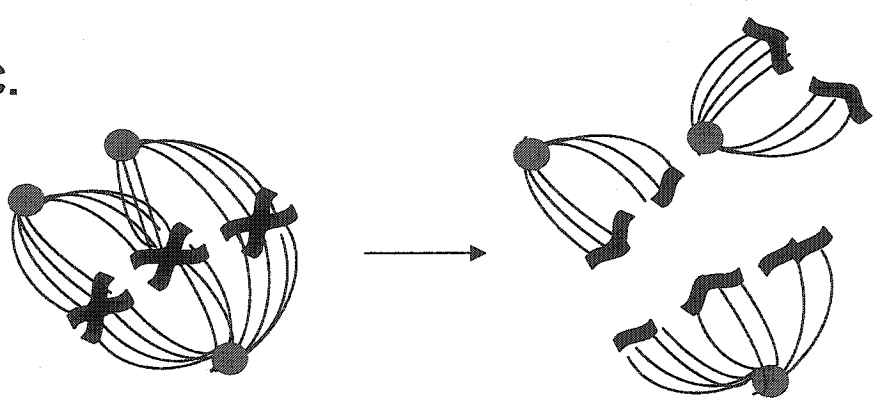

formation of monopolar spindles, incapable of chromosome segregation, or conversely may generate multipolar spindles that distribute the chromosomes to more than two daughter cells (Doxsey, 1998; Kramer and Ho, 2001) (Figure 1). Such defects ultimately present serious implications in the maintenance of genomic stability. In a recent review, Nigg (2002) emphasizes that whether defects in centrosome function directly cause tumorgenesis or arise as a consequence of the disease remains to be clearly established.

B. Centrosomes: Microtubule Organizing Centres.

Centrosomes are dynamic organelles responsible for controlling the organization and nucleation of the interphase and mitotic microtubule (MT) cytoskeleton. Structurally, each centrosome consists of two orthogonally positioned cylindrical centrioles composed of nine triplet microtubule bundles (Robbins et al., 1968; Kuriyama and Borisy, 1981; Albrecht-Buehler, 1992) (Figure 2). Several studies have demonstrated that centrioles play a pivotal role in the recruitment and organization of centrosome components as well as in the execution of cytokinesis (Karsenti, 1991; Piel et al., 2001). Surrounding these centrosomal substructures is an electron dense pericentriolar matrix (PCM) containing various structural and enzymatic components necessary for MT nucleation (Andersen, 1999; Whitehead and Salisbury, 1999).

The 'centrosome cycle', occurring once every cell cycle, is a complex process involving stages of duplication, separation, maturation and segregation (Doxsey, 2001). These events must be well coordinated with DNA replication to ensure proper cell cycle progression and the faithful segregation of sister chromatids to progeny cells (Fisk et al, 2002). In interphase cells, the minus ends of MT's are anchored

Figure 2. Centrosome structure.

Centrosomes are composed of two orthogonally positioned, barrel shaped centrioles, including a maternal centriole and a daughter centriole. Each centriole is made up of nine sets of radially positioned triplet microtubules. The structure of the maternal centriole differs from that of the daughter centriole in the presence of appendages, which anchor microtubules. Interconnecting fibers link the two centrioles at their proximal ends. Surrounding the centrioles is a proteinaceous material known as the pericentriolar material (PCM), which contains the components necessary for microtubule nucleation (modified from Doxsey, 2001).

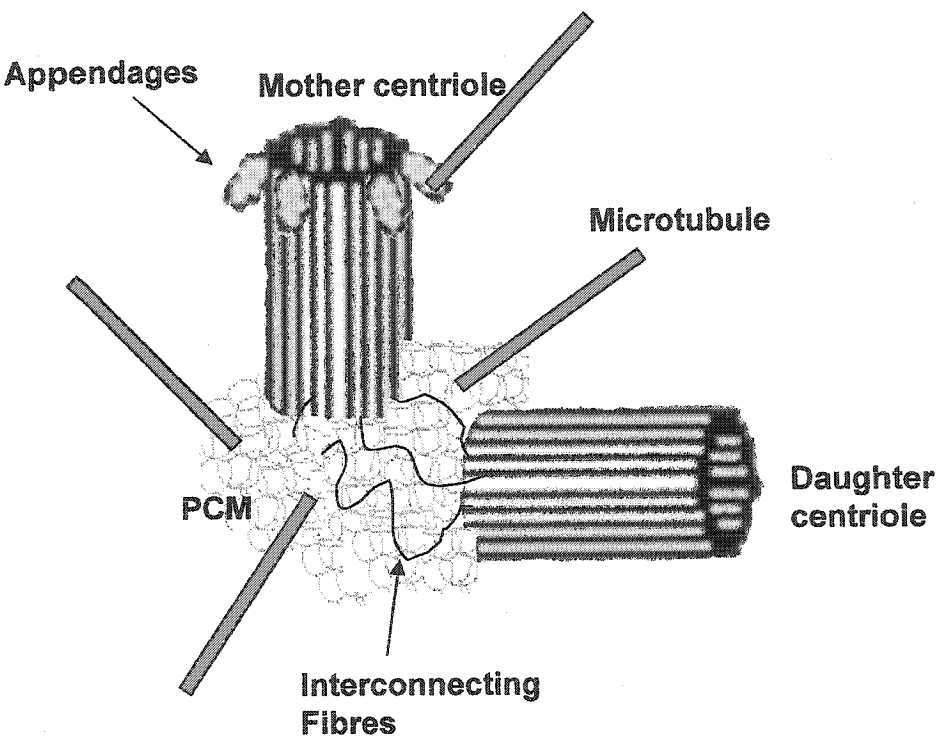
Appendages
Mother centriole
Microtubule
PCM
Daughter centriole
Interconnecting Fibres

at a single perinuclear centrosome composed of two centrioles. Initiated at G1 of the cell cycle, the link between the two centrioles is lost, which leads to splitting of the two centrioles. At S phase, the centrioles are duplicated thus generating four centrioles per cell, which are subject to elongation and maturation during the subsequent G2 phase. A sudden increase in the MT nucleating potential of centrosomes occurs concomitantly with the recruitment of extra pericentriolar material peaking at late G2 after centrosome maturation is complete (Khodjakov and Rieder, 1999). The two newly duplicated centrosomes separate at the onset of mitosis and migrate to opposite poles of the cell to establish the mitotic spindle. The plus-ends of the spindle MT's contact the sister chromatids by associating with sites at the chromosomes referred to as kinetochores. A critical event in mitotic exit and cell cleavage is the repositioning of the maternal centriole to the intercellular bridge linking the daughter cells (Piel et al., 2001).

C. Profile of Centrosome Components.

Several approaches have been used to identify novel molecular components of centrosomes. Serum from individuals with autoimmune disorders contain autoantibodies that specifically stain centrosomes (Tuffanelli et al., 1983; Mack et al., 1998; Gavanescu et al., 1999). Integral components of centrosomes have been identified by screening cDNA libraries with sera from individuals with autoimmune disorders, such as scleroderma (Doxsey et al., 1994). Homology searches, yeast-two hybrid screens, advanced microscopy and biochemical purification of centrosomes coupled with proteomic applications have further facilitated the identification of novel centrosome proteins (Wigge et al., 1998). As a result, over a hundred proteins have been identified as

integral proteins of the MTOC, representing diverse classes of structural and regulatory components.

C.1. Structural Components.

γ-tubulin is a highly conserved integral centrosome protein that associates with several other proteins to form the γ-tubulin ring complex (γ-TuRC) (Joshi et al., 1992; Felix et al., 1994; Stearns and Kirschner, 1994; Zheng et al., 1995; Fuller et al., 1995; Murphy et al., 1998). Assembly of γ-tubulin at the γ-TuRC is thought to provide the structural template for MT nucleation at centrosomes (Felix et al, 1994; Joshi et al, 1992; Stearns and Kirschner, 1994). There is additional evidence to suggest that the γ-TuRC complex functions by capping the minus ends of MT's (Wiese and Zheng, 2000; Keating and Borisy, 2000; Moritz et al., 2000).

Screening of a cDNA library with autoimmune sera resulted in the identification of a cDNA encoding a large coiled-coil centrosome protein, known as pericentrin (Doxsey et al., 1994). This integral component of the PCM provides several roles including a structural scaffold for the recruitment and assembly of protein complexes at centrosomes, the nucleation of MT's and the organization of the mitotic spindle (Doxsey et al., 1994; Dictenberg et al., 1998). Biochemical fractionation and advanced microscopy using *Xenopus* egg extracts revealed that pericentrin participates in MT nucleation by assembling with γ-tubulin in a highly-ordered reticular lattice structure, which makes contact with the ends of nucleated MT's (Dictenberg et al., 1998). In studies using Chinese hamster ovary cells, Dictenberg et al. (1998) demonstrated that as the MT nucleating activity increased from G1 to mitosis, pericentrin and γ-tubulin

progressively assemble onto the soluble reticular lattice in a centriole-independent manner. Exit from mitosis in these cells culminates in the dissolution of the γ-tubulin-pericentrin lattice, leading to the redistribution of pericentrin and γ-tubulin to the cytoplasm. These observations support the view that pericentrin, in complex with γ-tubulin constitutes the general architectural framework of the PCM necessary for MT nucleation. It should be noted, however that the complex formed by pericentrin and γ-tubulin is not part of the γ-TuRC. The transport of γ-tubulin-pericentrin complexes along the MT's to the centrosome is mediated by the pericentrin's association with the MT motor protein, dynein (Purohit et al., 1999; Young et al., 2000).

Structural components of centrosomes further function as molecular anchors of regulatory components at the MTOC. The centrosome and Golgi-localized PKN-associated protein (CG-NAP), for example assembles key signaling enzymes at centrosomes including various kinases and phosphatases (Takahashi et al., 1999; Sillibourne et al., 2002). Similarly, pericentrin functions as a structural anchor by directly interacting with the type II regulatory subunit (RII) of protein kinase A (PKA) as well as the PKA catalytic subunit (Diviani et al., 2000). This direct physical association tethers the PKA holoenzyme to the MTOC, thus maintaining PKA in close proximity to its centrosomal substrates (Diviani et al., 2000; Diviani and Scott, 2001). Thus the sequestration of multivalent signal transduction complexes at centrosomes aids in integrating signaling events required for cell cycle progression and centrosome function (Diviani and Scott, 2001).

C.2. Regulatory Components.

In earlier studies, Vandre et al. (1984) used monoclonal antibodies recognizing a class of mitotic phosphoproteins to demonstrate that phosphorylated proteins are abundant at centrosomes. Results of these studies suggested that protein phosphorylation at centrosomes is an important mechanism for regulating centrosome dynamics during mitosis. Various kinases and phosphatases have since been identified at that MTOC and several of these regulatory enzymes influence key aspects of centrosome function (Brinkley and Goepfert, 1998; Whitehead and Salisbury, 1999; Mayor et al., 1999).

Nek2, a mammalian serine-threonine kinase related to the *Aspergillus nidulans* NIMA kinase plays a pivotal role in the separation of centrosomes required for mitotic phase progression. Evidence of the role of Nek2 kinase in centrosome splitting was provided by studies demonstrating that the ectopic expression of active Nek2 at any phase of the cell cycle induces centrosome splitting and centriole separation (Fry et al., 1995 and 1998a). In contrast, expression of the inactive mutant has no effect in somatic cells (Fry et al.. 1998a). Subsequent studies have provided explanation of the molecular mechanism via which Nek2 kinase activity causes centrosome splitting. Nek2-mediated phosphorylation of C-Nap1 (centrosomal Nek2-associated protein) localized at the proximal ends of centrioles causes the dissociation of C-Nap1 from mitotic centrosomes, leading to a loss of cohesion between duplicated centrosomes (Fry et al., 1998b; Mayor et al., 2002).

As several other serine-threonine mitotic kinases are known to localize at the MTOC, an in-depth understanding of the functions provided by the various centrosomal

regulatory proteins is contingent upon the further identification of kinase-associated proteins and their physiological centrosomal substrates. (Giet and Prigent, 1999).

D. Future Directions in Centrosome Research.

The ability of the centrosome to nucleate MT has important consequences for the regulation of cell shape, cell polarity, the positioning of MT-dependent organelles, chromosome segregation and cytokinesis. The further identification and characterization of novel centrosomal components and centrosome-associated proteins may promote an improved understanding of the assembly and function of this important organelle.

Chapter Five.

Guzzo et al. (2003). A Novel Isoform of the Sarcolemmal Membrane-Associated Protein (SLMAP) is a Core Component of the Cell's Microtubule Organizing Centre (submitted to the Journal of Cell Science).

The following outlines the experimental contributions of the authors of this manuscript. R.M. Guzzo performed the immunoblotting experiments, transient transfections, drug treatments, immunocytochemistry studies, microscopy and image analysis, biochemical isolation of centrosomes, FACS analysis and cell proliferation assays. The genomic studies were performed by Maysoon Salih and Dr. Serdal Sevinc. Expression constructs were generated by Maysoon Salih and R.M. Guzzo. The manuscript was written by R.M. Guzzo, under the guidance of Dr. Balwant Tuana.

A Novel Isoform of the Sarcolemmal Membrane-Associated Protein (SLMAP) is a Core Component of the Cell's Microtubule Organizing Centre.

Rosa M. Guzzo, Serdal Sevinc, Maysoon Salih and Balwant S. Tuana

Correspondence to:

Abbreviations:

SLMAP, sarcolemmal membrane-associated protein; *MTOC*, microtubule organizing centre; *GFP*, green fluorescent protein; *PCR*, polymerase chain reaction; *PFA*, paraformaldehyde; *TM*, transmembrane domain; *LZ*, leucine zipper; *MTSB*, microtubule stabilization buffer; *PBS*; phosphate buffered saline; *DAPI*, 4',6-diamidino-2-phenylindole dihydrochloride; *FHA*, forkhead associated domain; *nt*, nucleotides; *aa*, amino acids.

SUMMARY

The microtubule organizing centre (MTOC) or the centrosome serves a critical role in the establishment of cellular polarity, organization of interphase microtubules and the formation of the bipolar mitotic spindle. We have elucidated the genomic structure of a gene encoding the sarcolemmal-membrane associated protein (SLMAP) which encodes a 91 kDa polypeptide with a previously uncharacterized N-terminal sequence encompassing a forkhead associated (FHA) domain that resides at the centrosome. Antibodies directed against SLMAPs demonstrated co-localization with γ-tubulin at the centrosomes at all phases of the cell cycle. Agents that specifically disrupt microtubules did not affect SLMAP association with centrosomes. Furthermore, SLMAP sequences directed a reporter green fluorescent protein to the centrosome and deletions of the newly identified N-terminal sequence from SLMAP prevented the centrosomal targeting. Deletion-mutant analysis concluded that overall structural determinants in SLMAPs were responsible for centrosomal targeting. Elevated levels of centrosomal SLMAP were found to be lethal while mutants that lacked centrosomal targeting inhibited cell growth accompanied by an accumulation of cells at G2/M phase of the cell cycle.

INTRODUCTION

The microtubule organizing centre (MTOC) of the cell is the centrosome, a complex organelle that fulfills multiple functions including the nucleation of interphase microtubules; the establishment of cellular polarity; the formation and positioning of the bipolar mitotic spindle; and the segregation of chromosomes (reviewed in Kellog et al., 1994; Doxsey, 2001; Nigg, 2002). Failure to preserve the integrity of centrosome structure and activity has severe consequences on cell cycle progression and genomic stability (Whitehead and Salisbury, 1999; Kaiser et al., 2002; Doxsey 2001). Deregulated centrosome activity has been shown to promote the missegregation of chromosomes, which may lead to aneuploidy, a common feature of tumors (Doxsey, 2002; Nigg, 2002). In view of the pivotal role of the MTOC in ensuring genomic stability, various kinases and phosphatases anchored at centrosomes function as central regulators of centrosome activity (Meraldi et al., 1999; Hinchcliffe et al. 1999; Sluder and Hinchcliffe, 2001; Nigg 2002). Examples include, $cdc2^{p34}$, cAMP dependent kinase II (PKA), Polo kinase, Cdc14A phosphatase, STK15 (BTAK) and Nek2 kinase (reviewed in Major et al., 1999; Meraldi and Nigg, 2001; Mailand et al., 2002; Whitehead and Salisbury, 1999). While the functional roles of many centrosomal kinases and phosphatases continue to be further defined, the repertoire of centrosome-associated substrates remains to be uncovered.

In recent years, considerable progress has been made in elucidating the protein composition of centrosomes. In this regard, proteins localized to the MTOC have been classified as: (i) integral components of centrosomes; (ii) proteins associated with centrosomes in a transient, cell cycle regulated manner; and/or (iii) proteins that require microtubules for centrosomal associations (Urbani and Stearns, 1999). Coiled-coil

structure has emerged as a common structural motif predicted in several proteins localized at the MTOC, among which include pericentrin, Nek2 protein kinase, ninein, CG-NAP, kendrin and p160-Rho-associated coiled-coil-containing protein kinase (ROCK) (Doxsey et al., 1994; Fry et al., 1998, 1999; Boukson-Castaing et al., 1996; Takahashi et al., 1999; Takahashi et al., 2002; Li et al., 2000; Chevrier et al., 2002). Further characterization of novel structural and regulatory components localized at the MTOC will foster an improved understanding of the complex mechanisms defining centrosomal processes.

Sarcolemmal membrane-associated proteins (SLMAPs) comprise a unique family of alpha-helical coiled-coil proteins encoded by a single gene mapped to human chromosome 3p14.3-21.2 (Wigle et al., 1997; Wielowieyski et al., 2000). Elucidation of the genomic organization of the 3` region of the SLMAP gene indicated the presence of several splice variants, which exhibit developmental and tissue specific expression (Wielowieyski et al., 2000). A central coiled-coil region encompassing two leucine zipper motifs constitutes the core structural feature of all SLMAP isoforms together with a single transmembrane domain at the carboxyl terminus that can be alternatively spliced to target these polypeptides to cellular membranes (Wielowieyski et al., 2000). In the present study we elucidated the genomic organization of the entire SLMAP gene which was found to be composed of 24 exons spread over ~122 kilobases of DNA. The genomic structure of the SLMAP gene predicted the presence of several splice variants, one of which was found to be a core component of the MTOC.

MATERIALS AND METHODS

Isolation and sequence analysis of genomic clones.

Genomic clones corresponding to the SLMAP gene were isolated by direct screening of two mouse genomic libraries (λFIXII and λDASH II; Stratagene). SLMAP cDNA probes used for library screening were PCR generated (Table I) and digoxigenin labeled, according to the manufacturer's directions (Roche Applied Science) for subsequent use in Southern blotting experiments. Positive phage DNA clones were digested and resolved by electrophoresis. The SLMAP exons in the restriction enzyme digest fragments of the phage genomic DNA clones were analyzed by Southern blotting. Genomic DNA for each of the eight clones was isolated (Table II), subcloned into pBlueScript KS (Stratagene) and subsequently sequenced using AmpliTaw sequencing methodology (ABI). Sequencing of the identified exons enabled the identification of exon-intron junctions by PCR using forward and reverse primers designed to span successive exons (Table I). PCR conditions consisted of the following step: (i) 3 minutes at 94°C; (ii) 30 cycles consisting of denaturation at 94°C for 30 seconds, annealing at 50-55°C for 30 seconds, extension at 72°C for 1-3 minutes; and (iii) 10 minutes at 72°C. Amplicons were resolved by electrophoresis, and the isolated DNA cloned into the pCR4-TOPO cloning vector (Invitrogen), for subsequent sequence analysis. Computer assisted alignment of SLMAP cDNA sequence (Accession #AF304451) with genomic sequences facilitated the identification of putative exons. The exon-intron organization of SLMAP3 was verified by aligning the mouse cDNA sequence of SLMAP3 (Accession AF304451) with mouse genomic sequences (NW 000090.1) deposited in GenBank. Consensus phosphorylation,

N-glycosylation and N-myristoylation sites were identified using PROSITE database available on the EMBL server (Falquet et al., 2002).

Cell Culture, Transfections and Drug Treatments.

NIH 3T3 fibroblast cells were grown in Dulbecco's modified Eagle's medium (DMEM) supplemented with 10% heat inactivated fetal bovine serum, 50 units/mL penicillin, 50 ug/mL streptomycin and gentamycin at 37°C in a humidified 5% CO_2 atmosphere. Transient transfection experiments were performed using the LIPOFECTAMINE PLUS™ (Gibco BRL) transfection reagent according to the manufacturers' specifications. For experiments where microtubules were disrupted, NIH 3T3 cells grown on sterile glass coverslips were treated with either nocodazole (Sigma Chemical Co., 6 ug/mL) or paclitaxel (Sigma Chemical Co., 4 uM) in growth media (DMEM) for 3 hours at 37°C.

Antibodies.

Two polyclonal antibodies against SLMAP were generated by injecting rabbits with two synthetic SLMAP specific peptides. Anti-SLMAP(C) rabbit antiserum was raised against the carboxyl 370 amino acids of SLAP, as previously described (Wigle et al., 1997). A second antibody, designated anti-SLMAP(N) was raised against the peptide RLSRGEESPPCEI which corresponds to the extreme amino terminus of SLMAP3, within the region separating two different initiating methionines M1 and M2 (Fig. 2A). Monoclonal anti-γ-tubulin (clone GTU-88, Sigma Chemical Co.) was used to identify

centrosomes and monoclonal anti-α-tubulin (clone DM 1A, Sigma Chemical Co.) was used to visualize cytoplasmic microtubules in immunocytochemical studies. The DNA stain 4',6-diamidino-2-phenylindole dihydrochloride (DAP1) was purchased from Molecular Probes. Secondary antibodies used in immuno-cytochemistry studies included FITC-conjugated anti-rabbit immunoglobulins (Amersham Pharmacia Biotech) and CY3-conjugated anti-mouse immunoglobulins (Jackson ImmunoResearch Laboratories, Inc.). Secondary antibodies used in immunoblotting experiments included anti-rabbit IgG peroxidase linked whole antibody (Amersham Pharmacia Biotech) and peroxidase conjugated AffiniPure goat anti-mouse IgG (Jackson ImmunoResearch Laboratories, Inc.).

Immunoblot analysis.

NIH 3T3 cells were solubilized by RIPA lysis buffer (1% Nonidet P-40, 0.5% sodium deoxycholate, 0.1% SDS in PBS pH 7.4) and centrifuged at 10,000xg (15 minutes, 4°C). Protein content of clarified supernatants was determined using the BCA Protein Assay Kit (Pierce). Proteins (15 ug) were resolved by electrophoresis on 10% SDS-polyacrylamide gels, according to Laemmli (1970). Separated proteins were electrophoretically transferred onto PVDF membranes (Amersham Pharmacia Biotech) and blocked in 5% skim milk powder (SMP) in TRIS-buffered saline containing 0.05 % Tween-20 (TBS-T), then incubated at room temperature for one hour with anti-SLMAP rabbit antibodies (1:4500) in 5% SMP/TBS-T. After four washes with TBS-T, blots were incubated with anti-rabbit IgG peroxidase linked whole antibody (Amersham Pharmacia

Biotech) in 5% SMP in TBS-T for one hour. Antibody detection was carried out using the enhanced chemiluminescent detection system (Amersham Pharmacia Biotech).

Isolation of centrosomes.

Centrosomes were isolated from NIH 3T3 cells using sucrose density gradients according to the method of Moudjou and Bornens (1998).

Mammalian expression plasmids.

SLMAP3M1 (nucleotides 1-2314) was PCR generated from the original full length SLMAP rabbit cDNA clone (Wigle et al., 1997) using the forward primer SLMAPN-F (GGAATTCGATGCCGTCAGCCTTGGC) and reverse primer SLMAPN-R (GATGCCAGCT TCTAGAGGGAGGACG). Forward primer SLMAPN-F and reverse primer (SLMAP+3') CCTCTAGAGCTCAGCTCTCACCTTCTTAAGC were utilized to produce carboxyl truncation mutant (nucleotides 1-1674), designated SLMAP3M1ΔC. Generation of amino terminal/ carboxyl terminal truncation mutant SLMAP3M2ΔC (nucleotides 389-1674) was accomplished using forward primer (ATG2M5') GGAATTCAGATGGTATGGAAGCC and the reverse primer (SLMAP+3'). The PCR products were each inserted into the EcoR1 and Xba1 sites of vector pcDNA3 (Invitrogen), in frame with the open reading frame of the green fluorescent protein (GFP). Sites of ligation were confirmed by DNA sequencing. To generate the leucine zipper mutant (GFP-SLMAP3M1ΔLZ), the GFP-SLMAP3M1 construct was digested with BamH1 to release the segment of SLMAP that included the leucine zippers (nucleotides 1-1994). We retained the vector which included nucleotides 2001-2314 of

SLMAP3M1 (designated SLMAP3') for subsequent subcloning of a PCR amplicon of SLMAP3M1 lacking the leucine zippers. This amplicon was generated using GFP-SLMAP3M1 template and employing primers GFP-5' (GGGATCCATGGAC AAAGGAGAAGAACTCTTCAC) and antisense primer LZ-less 3' (CGGATCCCTCTTTCT GCTGGTCCTCACACTGC) which both incorporated BamH1 sites. The PCR product (lacking the leucine zippers) was restriction digested (BamH1) and then subcloned into SLMAP3'. SLMAP amino terminal constructs were PCR generated using forward primer SLMAPN-F and the following reverse primers T3' (CCTGAGTCTAGATACTTGGAGTGTTAGC; nucleotides 1-490); U3' (CTTCTTCTAGAACATCTGTTCCCG; nucleotides 1-549); and V3' (TGCTCTAGATCAAGC CTGCCAACTGGT; nucleotides 1-603). PCR products were each subcloned into GFP-pcDNA3 and sites of ligation were confirmed by DNA sequencing.

Immunocytochemistry.

Cells grown on sterile glass coverslips were fixed by two methods. The first method involved a 10 minute exposure to 4% paraformaldehyde (PFA) in phosphate buffer at room temperature. The second method consisted of a one minute incubation in microtubule stabilization buffer (MTSB: 4M glycerol, 100 mM PIPES pH 6.9, 1 mM EGTA, 5 mM $MgCl_2$), followed by a two minute incubation in MTSB containing 0.5% Triton-X-100 to extract soluble cellular components, then an additional 2 minute exposure to MTSB. Detergent extracted cells were then fixed with 4% PFA as described. Following either fixation method, coverslips were mounted onto glass slides and cells

were incubated with relevant antibody(s) diluted in PBS containing 0.3% Triton-X-100 (PBS-T) for 3 hours at room temperature. After several washes in PBS, cells were incubated in the appropriate fluorochrome-conjugated secondary antibody(s) for 45 minutes at 37°C. DNA was stained with 4',6-diamidino-2-phenylindole dihydrochloride (DAPI, 1 ug/mL) for 15 minutes at room temperature.

Microscopy and Image Analysis.

Live cells were visualized with Axiovert S100 TV (Carl Zeiss Inc.) microscope equipped with SensiCam digital camera (PCO CCD Imaging). For immunocytochemistry studies, cells were visualized using Axiophot (Carl Zeiss Inc) microscope equipped with a 3CCD colour video camera. Acquired images were digitally processed using Northern Eclipse (Version 5.0, Empix Imaging Inc.) acquisition software. Images were further processed using Adobe Photoshop™ 5.0 (Adobe Systems Inc.).

BrdU Incorporation.

GFP-pcDNA3 or the SLMAP expression plasmids (GFP-SLMAP3M1; GFP-SLMAP3M1ΔC; GFP-SLMAP3M2ΔC) were transiently transfected into NIH 3T3 cells grown on glass coverslips. 5'-Bromo-2'-deoxyuridine (BrdU, 10 umol/L, Boehringer Mannheim) was added to the culture media at 36 hours post transfection for 2, 8, 12 or 24 hours. At the end of each labeling period, cells were washed in PBS and fixed in 70% ethanol (in 50 mM glycine, pH 2) for 30 minutes at -20°C. Cells were then covered with anti-BrdU monoclonal antibody (1:10, Boehringer Mannheim) and anti-GFP rabbit antibody (1:10, Clontech) in incubation buffer (66 mM TRIS buffer, 0.66 mM $MgCl_2$, 1

mM β-mercaptoethanol) for 30 minutes at 37°C. Following several washes in PBS, cells were incubated in secondary antibodies (in PBS) for 30 minutes at 37°C. Nuclei were stained with DAPI as previously described. Cells were then covered with mounting media and processed for immunofluorescence microscopy.

Fluorescence activated cell sorting (FACS analysis).

Transfected cells were harvested and analyzed 48 hours after removal of DNA precipitates and prepared for FACS analysis as described by Pestov et al. (1999). DNA content of propidium iodide (Molecular Probes, 10 ug/mL) stained GFP positive cells was measured by a Becton Dickinson FACScan cytometer using an argon laser (488nm) and analyzed with MulticycleAV (Phoenix Flow System) program.

RESULTS

Genomic Organization of the SLMAP Gene.

We previously reported that the 3' region of the SLMAP gene is composed of eleven exons and encodes a 47 kDa SLMAP (SLMAP2) polypeptide which is expressed in a tissue specific manner (Wielowieyski et al., 2000). The elucidation of the genomic structure of the complete SLMAP gene may offer valuable insights to gene function. In the current study SLMAP genomic sequences were analyzed by a combination of approaches involving direct screening of mouse genomic libraries using SLMAP cDNAs, a PCR-based cloning strategy as well as the alignment of SLMAP cDNA with GenBank deposited genomic sequences. By direct screening of the genomic library or the PCR-

based cloning strategy, eight genomic clones were isolated as outlined in Table II. The genomic clones ranged in size from 2 kb to 20 kb. Characterization of these genomic clones revealed that the SLMAP gene, spans over 122 kb of genomic DNA, and consists of twenty four exons (I-XXIV), including five alternative exons (XI, XII, XIII, XVII and XXIII) (Table III, Fig. 1). Sequence data for each intron-exon boundary conformed to the canonic consensus donor (GT) and acceptor (AG) splice sites described by Mount (1982) and is depicted in Fig 1A. Intron sizes varied from 87 bp to over 50.5 kb of genomic DNA, whereas SLMAP exons ranged in size from 51 bp to over 1.8 kb (Table III). Furthermore, each class of intron (0, 1 and 2) was represented within SLMAP genomic sequences (Mount, 1982).

As a result of our analysis, three additional alternative exons were identified in SLMAP. These novel alternative exons are exons XI (51 bp), XII (51 bp) and XIII (63 bp) (Table III, Fig. 1). Each alternative exon is flanked by either class 1 introns (introns 10, 11, 13) which interrupt the coding between the first and second base of the codon or a class 0 intron (intron 12) which occurs between codons (Mount, 1982). Notably, splicing of any of the alternative exons maintains the open reading frame of the predicted polypeptides. A PROSITE sequence scan did not predict the presence of conserved functional domains in alternative exons XI, XII or XIII, however consensus sites for casein kinase 2 phosphorylation, protein kinase C phosphorylation, N-glycosylation and N-myristoylation were identified (Fig. 1B; Falquet et al., 2002).

Leucine zipper motifs, two regions of specialized coiled-coil structure in the common carboxyl portion of SLMAPs are encoded by exons XX and XXI, corresponding to exons VII and VIII in SLMAP2 (Wielowieyski et al., 2000). Two distinct

transmembrane domains, TM1 and TM2 were previously identified within the extreme carboxyl terminus of SLMAPs and are encoded by alternative exon XXIII and exon XXIV of SLMAP3, known as alternative exon X and exon XI in SLMAP2 (Wielowieyski et al., 2000). Expression of TM1 and TM2 has previously been described as mutually exclusive. Splicing of alternative exon TM1 introduces an in frame stop codon which renders the second transmembrane domain (TM2) nonfunctional.

Two in-frame start codons (ATG1; M1) and (ATG2; M2) were previously reported in the full length cDNA sequence of the rabbit SLMAP3 isoform (Accession #U21157; Wigle et al., 1997) and have since been found to be conserved in mouse SLMAP cDNA. Analysis of the mouse SLMAP genomic sequences revealed that the first initiating methionine (ATG1; M1) is encoded by exon I, whereas the second initiating methionine (ATG2; M2) resides in exon II. Computer-assisted sequence analysis of exon I resulted in the identification of a consensus forkhead associated domain (FHA) corresponding to amino acid 24-58 within the region spanning M1 and M2 (Fig. 2A; bold print). FHA domains exist in proteins of diverse function and have been recognized as phosphoserine / threonine-specific protein-protein interaction motifs involved in phosphopeptide recognition (Durocher et al., 2000; Sun et al., 1998).

Endogenous Expression and Subcellular Distribution of SLMAP.

In vitro transcription-translation experiments revealed the presence of two SLMAP products whose molecular masses were similar to those predicted by the utilization of M1 (91 kDa) or M2 (80 kDa) (Wigle et al., 1997). To test whether a 91 kDa protein is produced in vivo, implying the utilization of M1 as the initiating methionine, antibodies

were generated against a peptide sequence in the M1-M2 region at the N-terminus of SLMAP (anti-SLMAP-N) or against a fusion protein encompassing the C-terminal region of SLMAP (anti-SLMAP-C). Both antibodies recognized a 91 kDa protein in NIH 3T3 cell extracts (Fig. 2B, lanes 1 and 2). Immunoadsorption of the anti-SLMAP(N) antibodies with purified SLMAP fusion protein confirmed the specificity of the antiserum (Fig. 2B; lane 3). These results suggest that a 91 kDa polypeptide is produced from M1 of SLMAP3 mRNA in NIH 3T3 cells.

The use of M1 as a translation initiation codon is predicted to add 132-residues to the N-terminal region of the previously identified SLMAP3 isoform. We then examined if these residues confer different biochemical and subcellular properties to SLMAP3M1 not previously described for other SLMAP isoforms. Immunocytochemical analysis of NIH 3T3 cells which exclusively express the 91 kDa isoform revealed that SLMAP3M1 resides in several subcellular compartments. While diffuse cytoplasmic SLMAP staining was evident, SLMAP proteins could also be detected in one or two foci generally situated adjacent to the nuclear membrane (Fig. 3A; a). The foci staining pattern, but not the diffuse cytoplasmic staining pattern were resistant to detergent extraction suggesting that SLMAP3M1 is tightly assembled with detergent-insoluble structures (Fig. 3A; b). The N-terminal directed peptide antibody (anti-SLMAP(N); Fig.3A; c), but not the control preimmune serum (Fig. 3A; d), detected SLMAP proteins at perinuclear foci in detergent extracted COS-7 cells as well. Peptide competition experiments abolished the staining pattern observed with anti-SLMAP(C) (Fig. 3A; e) and incubation with the preimmune antisera also abolished staining (Fig. 3A; f) thus confirming the antibody specificity for SLMAP proteins. The subcellular distribution of SLMAP was similar in other cells that

express the 91 kDa SLMAP isoform, including murine myoblasts (C2C12) and embryonic stem cells (data not shown).

SLMAP is a Core Component of the Centrosome.

The perinuclear foci staining of SLMAP is reminiscent of proteins that localize to the centrosome. To determine if SLMAP is associated with centrosomes, co-localization experiments were performed with γ-tubulin, a well characterized core centrosomal component (Stearns et al., 1991). As illustrated in Figure 3B, SLMAP labelling was co-incident with the γ-tubulin signal at each stage of the cell cycle as determined by DAPI staining. Interphase (G1) cells (Fig. 3B; a,f,k) contained one centrosome stained by both anti-SLMAP and anti-γ-tubulin. In mitotic cells SLMAP (Fig. 3B; b-e) co-localized with γ-tubulin (Fig. 3B; g-j) from prophase to anaphase (Fig. 3B; l-o). The SLMAP protein appears to have a symmetrical distribution during centrosome division since anti-SLMAP appeared to stain each centrosome with equal intensity.

Many proteins reside at the minus ends of microtubules and are thus dependent upon microtubules for their associations with the MTOC. These proteins can be distinguished from integral centrosomal proteins by treatments with agents that specifically disrupt microtubules. The fungal toxin, nocodazole causes depolymerization of the cytoplasmic microtubule network whereas taxol (paclitaxel) acts to stabilize cytoplasmic microtubules by binding tubulin directly along the length of the microtubule (De Brabander et al., 1986). Upon treatment with either drug, integral centrosomal proteins remain bound to centrosomal components whereas microtubule dependent

centrosome-associated proteins are no longer retained at the MTOC (De Brabander et al., 1986). Under control conditions (untreated) SLMAP3M1 was found to co-localize with γ-tubulin (Fig. 4A; a, d, g, j). The effects of taxol (Fig. 4A; k) and nocodazole (Fig. 4A; l) on microtubules were confirmed by staining with α-tubulin, which illustrated a distinct re-distribution of cytoplasmic microtubules. Treatment with taxol (Fig. 4A; b, e, h, k) or nocodazole (Fig. 4A; c, f, i, l) did not alter the localization of SLMAPs at centrosomes. These findings confirm that SLMAP localization at the centrosome is independent of microtubule assembly.

To demonstrate biochemically that SLMAP is a component of centrosomes, these subcellular structures were purified from NIH 3T3 cell extracts by fractionation on a sucrose density gradient (Moudjou and Bornens, 1998). The sucrose gradient fractions were resolved by SDS-PAGE and examined by immunoblotting with anti-γ-tubulin and anti-SLMAP (Fig. 4B). The centrosomal marker, γ-tubulin was present in the cell lysate (lane 1), and enriched in the crude centrosome preparation (lane 2), and even further concentrated in fraction 2 (lane 5) from the sucrose density gradient. The 91 kDa SLMAP3M1 protein was found to co-enrich with the γ-tubulin peak in fraction 2 (lane 5) of the purified centrosome preparation.

Centrosomal Targeting is Mediated by the Novel N-Terminal Region of SLMAPM1.

The data presented indicates that SLMAP3M1 is an integral component of centrosomes. These observations led us to hypothesize that the newly identified sequences from the M1 initiating codon might play a role in targeting SLMAP to the MTOC. To test this

hypothesis SLMAP3M1 cDNA (Fig. 5A) and a series of SLMAP deletion mutants (Fig. 6A-C) were fused in frame to the green fluorescent protein (GFP) to produce GFP-SLMAP fusion proteins. The GFP-SLMAP fusion constructs were used for transient expression studies in NIH 3T3 cells. Fig. 5B (a) shows that SLMAP3M1 cDNA encodes information that is sufficient to target the heterologous reporter GFP to the centrosome in live cells. This localization pattern was not observed in live mitotic cells expressing GFP alone (Fig. 5B; c). GFP-SLMAP3M1 co-localized with γ-tubulin at the centrosome (Fig. 5B; b, d), consistent with the localization of endogenous SLMAP3M1 (Fig. 3, 4). Deletion of the two leucine zipper regions did not affect GFP targeting to the centrosome (Fig. 6A; a), and the C-terminal truncation mutant (SLMAP3M1ΔC) also retained the ability to target GFP to centrosomes (Fig. 6A; b). A cDNA encoding SLMAP initiated from the second methionine (GFP-SLMAP3M2ΔC) lacking the transmembrane domain was unable to target GFP to centrosomes (Fig. 6A; c). It is notable that C-terminal mutants lacking the putative transmembrane domain resulted in the exclusion of SLMAP from the perinuclear membranes and reticular formations (Fig. 6C; b, c) consistent with the observation that C-terminal sequences play a role in membrane targeting of SLMAP (Wielowieyski et al., 2000). These results suggest that the newly described N-terminal sequences encompassing the FHA domain of SLMAP contain information that is required for centrosomal localization.

In order to identify the minimal sequences present in SLMAP sufficient for targeting to the MTOC, a series of SLMAP amino-terminal fragments fused to GFP were utilized in transient expression studies in NIH 3T3 fibroblast cells. Diffuse cytosolic and nuclear localization was observed in cells expressing the GFP-SLMAP mutant expressing

amino acids 1-163 (Fig. 6B, a); while GFP-positive detergent-insoluble aggregates were detected in cells transfected with SLMAP mutants expressing amino acids 1-183 and 1-201 (Fig. 6B; b, c). Based on observations by live microscopy and co-staining with the centrosome marker protein, γ-tubulin (data not shown), GFP fluorescence was not detected at centrosomes in cells overexpressing these extreme N-terminal SLMAP3M1 mutants. These observations suggest that, amino terminal sequences in addition to preservation of the overall structure of SLMAP or SLMAP-mediated protein interactions may be important determinants for targeting SLMAPs to centrosomes.

SLMAP Overexpression Affects Cell Proliferation.

The demonstration that SLMAP3M1 is localized at the centrosome raised the question as to whether SLMAPs serve a role in mitosis and cell growth. We observed that a large proportion of cells expressing the GFP-SLMAP3M1 variant were rounded (Fig. 6D; b) and detached from the coverslips within thirty-six hours following transfection. In contrast, cell viability did not appear to be affected by the expression of either the carboxyl-terminal mutant (GFP-SLMAP3M1ΔC; Fig. 6D; c) or the GFP-tagged SLMAP mutant lacking both the amino and carboxyl-terminal sequences (GFP-SLMAP3M2ΔC; Fig. 6D; d). To address this issue further we examined the effect of an overproduction of SLMAP3M1, SLMAP3M2 and SLMAP3M2ΔC on cell proliferation. A greater than two fold reduction in the level of BrdU incorporation was observed in cells expressing GFP-SLMAP3M1 fusion protein relative to GFP transfected control cells for labeling periods of two to eight hours (Fig.7A). Approximately 60% of cells expressing either SLMAP3M1, SLMAP3M2 or SLMAP3M2ΔC displayed BrdU

incorporation after a 24 hour pulse whereas essentially all of the control cells were positive for BrdU. These results indicate that regulated levels of SLMAPs are important for normal cell growth.

We sought to determine whether overexpression of SLMAPs altered cell proliferation by interfering in a cell cycle phase-specific manner. Fluorescence activated cell sorting (FACS) was used to identify GFP-expressing cells and thereby identify changes in cell cycle progression induced by SLMAP (Fig. 7B). Overproduction of GFP-SLMAP3M1 was toxic to NIH 3T3 cells as the majority of cells died within thirty-six hours post transfection. However, cells expressing the deletion mutant GFP-SLMAP3M2 remained viable for the time required for FACS analysis and overproduction of this deletion mutant caused about a 4-fold increase in G2/M (4N DNA; Fig. 7B; ii.) content compared to control cells (Fig. 7B; i.). These results suggest that deregulated levels of SLMAP3 in NIH 3T3 cells alter proliferation by interfering at the G2/M phase of the cell cycle.

DISCUSSION

In the present study, we show that a novel SLMAP isoform is a component of the MTOC and may serve a role in centrosomal function. The SLMAP gene is encoded by twenty-four exons that span over approximately 122 kb of continuous DNA sequence. Analysis of the sequences defined the presence of three additional regions of alternative splicing (exons XI, XII, XIII) in SLMAP. A new SLMAP variant (SLMAP3M1) containing an N-terminal extension of 132 amino acid residues that are encoded in exon I was identified to be a component of the MTOC. Using anti-peptide antibodies to the N-

terminal sequences, a protein of ~ 91 kDa was identified in various cell extracts. These findings confirm that SLMAP3M1 represents a ubiquitously expressed SLMAP isoform. Indirect immunofluorescence studies using fixation procedures known to aid visualization of the cytoskeleton localized SLMAP3M1 to the centrosome. SLMAP3M1 was detected at the centrosome at all stages of the cell cycle (therefore not a transient association) and co-localized with γ-tubulin. Treatments with reagents that specifically disrupt cytoplasmic microtubules did not affect SLMAP association at centrosomes indicating that SLMAP-centrosome association occur independent of microtubules. Thus SLMAP is a core component of the MTOC.

SLMAPM1 sequences were found to contain the information required to target the heterologous protein GFP to centrosomes. Large C-terminal deletions eliminating much of the coiled-coil structure including the leucine zipper motifs did not affect targeting of GFP to centrosomes. However, removal of the newly identified N-terminal residues from SLMAP abolished the targeting of GFP to the centrosome, indicating that the 132 N-terminal amino acid residues are required for centrosomal targeting. Further analysis of SLMAP deletion mutants encoding N-terminal sequences revealed that this region of SLMAP is not alone sufficient for centrosome targeting. While the N-terminus of SLMAP may serve a critical role in mediating SLMAP-centrosome associations, the preservation of the overall structure of SLMAP may constitute an additional determinant for ensuring faithful targeting at the MTOC. Conserved motifs for protein targeting to and retention within organelles such as the ER and Golgi have been characterized (Pelham, 1988; Jackson et al., 1990; Kjer-Nielsen et al., 1999; Munro and Nichols, 1999; Brown et al., 2001), yet little is known of conserved sequences directing proteins to

centrosomes. Recent studies have highlighted a conserved region of approximately 90 amino acids encoded in pericentrin and AKAP450 that confers targeting to centrosomes (Gillingham and Munro, 2000). This motif, known as the PACT domain, was not identified within the N-terminal sequences of SLMAP3 or within any other region of SLMAP. Thus our results indicate that structural motifs in addition to motifs such as the PACT domain are critical in targeting components to centrosomes.

Amino acid sequence analysis of the new SLMAP N-terminal sequences revealed the presence of a conserved motif known as the forkhead associated (FHA) domain. FHA domains have been characterized in a number of proteins of diverse function, including kinases, phosphatases, kinesins, transcription factors, DNA and RNA-binding proteins as well as metabolic enzymes (Hofmann and Bucher, 1995; Durocher and Jackson, 2002) and are known to serve as phosphoserine / threonine-specific protein-protein interaction motifs (Durocher et al., 2000; Sun et al., 1998). In this regard, FHA-interacting proteins such as Hklp2, a human homolog of Xklp2, a Xenopus kinesin-like motor protein which serve roles in centrosome separation and spindle bipolarity are known to reside at the MTOC (Boleti et al., 1996; Sueishi et al., 2000). The FHA domain in SLMAP may thus mediate associations with phospho-proteins present at MTOC. In this regard, the Aurora family of mitotic serine-threonine kinases is required for MTOC functions (Kimura et al., 1997; Kimura et al., 1999; Giet and Prigent, 1999). The presence of the FHA domains in SLMAP raises the possibility that it may interact with phosphorylated substrates of this kinase to affect centrosome activity and cell viability.

SLMAP shares several features inherent to other centrosomal proteins including a net negative charge (pI 4.9) and extensive regions of coiled-coil structure (Doxsey et al.,

1994; Boukson-Castaing et al., 1996; Balczon et al., 1994; Errabolu et al., 1994). The alternative exons XI, XII and XIII were predicted to introduce posttranslational modifications sites including phosphorylation for casein kinase 2 and protein kinase C, as well as N-glycosylation and N-myristoylation. Such modifications may impose significant consequences with respect to the biological function and regulation of SLMAPs. In view of the extensive splicing predicted in SLMAP, we speculate that alternative splicing may represent a fundamental mechanism that confers functional diversity among SLMAP variants as has been reported for other coiled-coil proteins. While we do not know the precise function of SLMAP at centrosomes, the deregulation of SLMAP expression had a marked effect on cell viability. It is notable that overexpression of full length SLMAP that targets to the centrosome (SLMAP3M1) was lethal to the cell suggesting that regulated levels of this centrosomal component are critical for normal cell viability. Increased levels of SLMAP mutants that did not target to centrosomes (GFP-SLMAP3M2) caused a significant number of cells to have a longer time of residency at the G2/M stage of the cell cycle. We speculate that increased synthesis of this SLMAP mutant may affect cell progression independent of SLMAP-centrosome associations. While the mechanism(s) mediating the observed SLMAP-induced effects on cell growth requires further investigation, the findings imply that the new SLMAP isoform is a core component of the centrosome whose regulated levels are critical for cell viability.

ACKNOWLEDGEMENTS

This work was supported by the Heart and Stroke Foundation of Ontario (awarded to BST) and a Canadian Institutes of Health Research studentship (awarded to RMG). We also thank Dr Jeff Wigle (University of Manitoba) for insightful comments and Dr. Stephen Lee (University of Ottawa) for providing the GFP-pcDNA vector.

REFERENCES

Andersen, S.S.L. (1999). Molecular characteristics of the centrosome. *Int. Rev. Cytol.* **187**. 51-109.

Boukson-Castaing, V., Moudjou, M., Ferguson, D.J.P., Mucklow, S., Belkaid, Y., Milon, G. and Crocker, P.R. (1996). Molecular characterization of ninein, a new coiled-coil protein of the centrosome. *J. Cell Sci.* **109**. 179-190.

Boleti, H., Karsenti, E. and Vernos, I. (1996). Xklp2, a novel Xenopus centrosomal kinesin-like protein required for centrosome separation during mitosis. *Cell* **84**. 49-59.

Brown, D.L., Heimann, K., Lock, J., Kjer-Nielsen, L., van Vliet C., Strow, J.L. and Gleeson, P.A. (2001). The GRIP domain is a specific targeting sequence for a population of trans-Golgi network derived tubulo-vesicular carriers. *Traffic* **2**. 336-344.

Chevrier, V., Piel, M., Collomb, N., Saoudi, Y., Frank, R., Paintrand, M., Narumiya, S., Bornens, M. and Job D. (2002). The Rho-associated protein kinase p160ROCK is required for centrosome positioning. *J. Cell Biol.* **157**. 807-817

De Brabander, M., Geuens, G., Nuydens, R., Willebrords, R., Aerts, F. and DeMey, J. (1986). Microtubule dynamics during the cell cycle: the effects of taxol and nocodazole on the microtubule system of Pt K2 cells at different stages of the mitotic cycle. *Int. Rev. Cytol.* **101**. 215-274.

Dictenberg, J.B., Zimmerman, W., Sparks, C.A., Young, A., Vidair, C., Zheng, Y., Carrington, W., Fay, F.S. and Doxsey S.J. (1998). Pericentrin and gamma-tubulin form a protein complex and are organized into a novel lattice at the centrosome. *J. Cell Biol.* **141**. 163-174.

Doxsey, S.J., Stein, P., Evans, L., Calarco, P.D. and Kirschner, M. (1994). Pericentrin, a highly conserved centrosome protein involved in microtubule organization. *Cell* **76**. 639-650.

Doxsey, S.J. (2001). Re-evaluating centrosome function. *Nat. Rev. Mol. Cell Biol.* **2**. 688-698.

Doxsey, S.J. (2002). Duplicating dangerously: linking centrosome duplication and aneuploidy. *Mol. Cell* **10**. 439-440.

Durocher, D., Taylor, I.A., Sarbassova, D., Haire, L.F., Westcott, S.L., Jackson, S.P., Smerdon, S.J. and Yaffe, M.B. (2000). The molecular basis of FHA domain: phosphopeptide binding specificity and implications for phospho-dependent signaling mechanisms. *Mol. Cell* **6**. 1169-1182.

Durocher, D and Jackson, S.P. (2002). The FHA domain. *FEBS Lett.* **513**. 58-66.

Errabolu, R., Sanders, M.A. and Salisbury, J.L. (1994). Cloning of a cDNA encoding human centrin, an EF-hand protein of centrosomes and mitotic spindle poles. *J. Cell Sci.* **107**. 9-16

Falquet, L., Pagni, M., Bucher, P., Hulo, N., Sigrist, C.J., Hofmann, K. and Bairoch, A. (2002). The PROSITE database, its status in 2002. *Nucleic Acids Res.* **30**. 235-238

Fry, A.M., Meraldi, P. and Nigg, E.A. (1998). A centrosomal function for the human Nek2 protein kinase, a member of the NIMA family of cell cycle regulators. *EMBO J.* **17**. 470-481.

Fry, A.M., Arnaud, L. and Nigg, E.A. (1999). Activity of the human centrosomal kinase, Nek2, depends on an unusual leucine zipper dimerization motif. *J. Biol. Chem.* **274**. 16304-16310.

Giet, R. and Prigent, C. (1999). Aurora/Ipl1p-related kinases, a new oncogenic family of mitotic serine-threonine kinases. *J. Cell Sci.* **112**. 3591-3601.

Gillingham, A.K. and Munro, S. (2000). The PACT domain, a conserved centrosomal targeting motif in the coiled-coil proteins AKAP450 and pericentrin. *EMBO Rep.* **1**. 524-529.

Hinchcliffe, E.H., Li, C., Thompson, E.A., Maller, J.L., Sluder, G. (1999). Requirement of Cdk2-cyclin E activity for repeated centrosome reproduction in Xenopus egg extracts. *Science* **283**. 851-854.

Hofmann, K. and Bucher, P. (1995). The FHA domain: a putative nuclear signaling domain found in protein kinases and transcription factors. *Trends Biochem. Sci.* **20**. 347-349.

Jackson, M.R., Nilsson, T. and Peterson, P.A. (1990). Identification of a consensus motif for retention of transmembrane proteins in the endoplasmic reticulum. *EMBO J.* **9**. 3153-3162.

Kaiser, B.K., Zimmerman, Z.A., Charbonneau, H. and Jackson, P.K. (2002). Disruption of centrosome structure, chromosome segregation and cytokinesis by misexpression of human Cdc14A phosphatase. *Mol. Biol. Cell* **13**. 2289-2300.

Kimura, M., Kotani, S., Hattori, T., Sumi, N., Yoshioka, T., Todokoro, K. and Okano, Y. (1997). Cell cycle-dependent expression and spindle pole localization of a novel human protein kinase, Aik, related to Aurora of Drosophila and yeast Ipl1. *J. Biol. Chem.* **272**.13766-13771.

Kimura, M., Matsuda, Y., Yoshioka, T. and Okano, Y. (1999). Cell cycle-dependent expression and centrosome localization of a third human aurora/Ipl1-related protein kinase, AIK3. *J. Biol. Chem.* **274**.7334-7340.

Kjer-Nielsen, L., Teasdale, R.D., van Vliet, C. and Gleeson, P.A. (1999). A novel Golgi-localization domain shared by a class of coiled-coil peripheral membrane proteins. *Curr. Biol.* **9**. 385-388.

Laemmli, U.K. (1970). Cleavage of structural proteins during the assembly of the head of bacteriophage T4. *Nature* **227**. 680-685.

Li. Q., Hansen, D., Killilea, A., Joshi, H.C., Palazzo, R.E. and Balczon, R. (2000). Kendrin / pericentrin-B, a centrosomal protein with homology to pericentrin that complexes with PCM-1. *J. Cell Sci.* **114**. 797-809.

Mailand, N., Lukas, C., Kaiser, B.K., Jackson, P.K., Bartek, J. and Lucas, J. (2002). Deregulated human Cdc14A phosphatase disrupts centrosome separation and chromosome segregation. *Nat. Cell Biol.* **4**. 317-322

Mayor, T., Meraldi, P., Stierhof, Y.D., Nigg, E.A. and Fry, A.M. (1999). Protein kinases in control of the centrosome cycle. *FEBS Lett.* **452**. 92-95.

Meraldi, P., Lukas J., Fry A.M., Bartek J. and Nigg E.A. (1999). Centrosome duplication in mammalian somatic cells requires E2F and Cdk2-cyclin A. *Nat. Cell Biol.* **1**. 88-93.

Meraldi, P. and Nigg, E.A. (2002). The centrosome cycle. *FEBS Lett.* **521**. 9-13.

Moudjou, M. and Bornens, M. (1998). Method of Centrosome Isolation from Cultured Animal Cells. In *Cell Biology: A Laboratory Handbook.* (ed. J.E. Celis), 2 pp. 111-119. Toronto: Academic Press.

Mount, S.M. (1982). A catalogue of splice junction sequences. *Nucleic Acids Res.* **10**. 459-472.

Munro, S. and Nichols, B.J. (1999). The GRIP domain – a novel Golgi-targeting domain found in several coiled-coil proteins. *Curr. Biol.* **9**. 377-380.

Nigg, E.A. (2002). Centrosome aberrations: cause or consequence of cancer progression? *Nat. Rev. Cancer* **2**. 815-825.

Pelham, H.R. (1988). Evidence that luminal ER proteins are sorted from secreted proteins in a post-ER compartment. *EMBO J.* **7**. 913-918.

Pestov, D.G., Polonskaia, M. and Lau, L.F. (1999). Flow cytometric analysis of the cell cycle in transfected cells without cell fixation. *Biotechniques* **26**. 102-106.

Pockwinse, S.M., Krockmalnic, G., Doxsey, S.J., Nickerson, J., Lian, J.B., van Wijnen, A.J., Stein, J.L., Stein, G.S. and Penman, S. (1997). Cell cycle independent interaction of CDC2 with the centrosome, which is associated with the nuclear matrix-intermediate filament scaffold. *Proc. Natl. Acad. Sci. U.S.A.* **94**. 3022-3027

Shiebel, E. (2000). Gamma-tubulin complexes: binding to the centrosome, regulation and microtubule nucleation. *Curr. Opin. Cell Biol.* **12**. 113-118.

Sluder G. and Hinchcliffe E.H. (2000). The coordination of centrosome reproduction with nuclear events during the cell cycle. *Curr. Top. Dev. Biol.* **49**. 267-289.

Stearns, T., Evans, L. and Kirschner, M. (1991). Gamma-tubulin is a highly conserved component of the centrosome. *Cell* **65**. 825-836.

Stearns, T. and Kirschner, M. (1994). In vitro reconstitution of centrosome assembly and function: the central role of gamma-tubulin. *Cell* **76**. 623-637.

Sueishi, M., Takagi, M. and Yoneda, Y. (2000). The Forkhead-associated domain of Ki-67 antigen interacts with the novel kinesin-like protein Hklp2. *J. Biol. Chem.* **275**. 28888-28892.

Sun Z, Hsiao J, Fay D.S. and Stern D.F. (1998). Rad53 FHA domain associated with phosphorylated Rad9 in the DNA damage checkpoint. *Science* **281**. 272-274.

Takahashi, M., Shibata, H., Shimakawa, M., Miyamoto, M., Mukai, H., and Ono, Y. (1999). Characterization of a novel giant scaffolding protein, CG-NAP, that anchors multiple signaling enzymes to centrosome and the Golgi apparatus. *J. Biol. Chem.* **274**. 17267-17274.

Takahashi, M., Yamagiwa, A., Nishimura, T., Mukai, H. and Ono, Y. (2002). Centrosomal proteins CG-NAP and kendrin provide microtubule nucleation sites by anchoring γ-tubulin ring complex. *Mol. Biol. Cell* **13**. 3235-3245.

Urbani, L. and Stearns, T. (1999). The centrosome. *Curr. Biol.* **9**. R315-317.

Whitehead, C.M. and Salisbury, J.L. (1999). Regulation and regulatory activities of centrosomes. *J. Cell. Biochem.* **Suppl. *32/33***. 192-199.

Wielowieyski, P.A, Sevinc, S., Guzzo, R., Salih, M., Wigle, J.T. and Tuana, B.S. (2000). Alternative Splicing, Expression, and Genomic Structure of the 3' Region of the Gene Encoding the Sarcolemmal-associated Proteins (SLAPs) Defines a Novel Class of Coiled-coil Tail-anchored Membrane Proteins. *J. Biol. Chem.* **275**. 38474-38481.

Wigle, J.T., Demchyshyn, L., Pratt, M.A., Staines, W.A., Salih, M. and Tuana, B.S. (1997). Molecular cloning, expression, and chromosomal assignment of sarcolemmal-

associated proteins. A family of acidic amphipathic alpha-helical proteins associated with the membrane. *J. Biol. Chem.* **272**. 32384-32394.

Zheng, Y.X., Wong, M.L., Alberts, B. and Mitchison, T. (1995). Nucleation of microtubule assembly by a gamma-tubulin containing ring complex. *Nature* **378**. 578-583.

Table I. Exonic primer sequences used to clone SLMAP genomic fragments.

PRIMER		SEQUENCE
[a]708-F	(22mer)	TTA CCC ATG GGT GTA TTG TTT C
[a]822-R	(28mer)	GCA ACT TTG TCT ACA GGA CTC GGT AAT G
[a]781-F	(24mer)	AGA TGT CAT CCA TGC TCC ATT ACC
[a]829-F	(23mer)	CAC TCC AAG TAT GTA CTC TCA GG
[a]851-R	(23mer)	CCT GAG AGT ACA TAC TTG GAG TG
[a]922-F	(22mer)	CCA CAC TTC AGC GGC TAC TAG C
[a]966-R	(24mer)	GTA TCT GAA CCC TCT TGG GTG ATG
[c]1023-R	(24mer)	CCC ATA ACT TCT AAC CGT GAT AAG
[b]1062-R	(29mer)	TCT TCT GTT TGA TTT TTG GAG CAT GCC TG
[c]1140-R	(22mer)	CGC CTC AGG GAC TCT TTG GCT G
[c]1228-R	(23mer)	CAG GTG GGT ACA TTC ATC TTC AG
[a]1377-R	(24mer)	TTC TCA GCT TGT CCC TTC TGT TGG
[a]Ex1-F	(36mer)	AGA AGC TGA TCG TGG AGG GGC ATC TAA CCA AAG TGG
[b]Ex2-F	(21mer)	AAA ATC AGG CAA AAG CAA AGG
[b]Ex2-R	(18mer)	CTG TAG TGT CGT CGC TGC
[b]Ex3-R	(38mer)	CTT TTA ATA GAG ACA CCT TAG CAA GGG GTT CAT TTA GG
[b]Ex4-F	(32mer)	ACT TAC AGG GTA CCC AGT CAG AAA CTG AGG CC
[c]Ex4-R	(33mer)	CTT GAA GTT CAA AGC ATT TTT GTT TAC TTG TTC
[b]Ex5-F	(19mer)	CTC TTT TGG AAG AAG AAA G
[c]Ex5-R	(19mer)	CTT GAA GAA CCT GTA TTT G
[c]Ex6-R	(33mer)	ACC TTG TTG CCT CCT CCC TTT GCT GGT CTT CAC
[b]Ex7-F	(20mer)	GTG AGC TGG AGA AGT TGA AG
[b]Ex7-R	(22mer)	TTG TGC AAT TCT TTC TCT TGT C
[c]Ex11-R	(25mer)	GGT GCA CTA AGA AGC GTA CTT TAG G
[c]1-15F	(25mer)	CTC CAG CCC AAA ACT GCT TCC AGA G
[c]405-F	(27mer)	ACC CGT TTC AGG AGC GTC ATG TCT ACC

[a]Used for PCR cloning.
[b]Used for internal verification of genomic library clones and/or large PCR clones.
[c]Used to generate SLMAP cDNA probe

Table II. List of genomic clones containing SLMAP exons and the methods of isolation.

Clone (size)	Exons Encompassed	Method Obtained
A (10 kb)	Exon II	direct screening of genomic library[1]
B (3.6 kb)	Exon IV to Exon V	PCR cloning (708-F & 822-R)[2]
C (2.0 kb)	Exon V to Exon VI	PCR cloning (781-F & 851-R)[2]
D (3.0 kb)	Exon VI to Exon II	PCR cloning (829-F & 966-R)[3]
E (6.0 kb)	Exon VII to Exon IX	PCR cloning (922-F & 1377-R)[3]
F (4.0 kb)	Exon XIV to Exon XVI	PCR cloning (Ex1-F & Ex3-R)[3]
G (20 kb)	Exon XV to Exon XXI	direct screening of genomic library[2]
H (4.5kb)	Exon XIII to Exon XV	direct screening of genomic library[2]

[1] λ FIX II mouse genomic library (Stratagene)
[2] λ DASH II mouse genomic library (Stratagene)
[3] Primers used in PCR

Table III. The exon-intron junctions of SLMAP3 and sizes of the respective exons and introns.

Exon No.	Size (bp)	Exon	Intron No.	Size (bp)	Class	Exon	Exon No.
						GGCCCTTGA	I
I	1604	ACGAGCAAG**gt**aatgtcg	1	50542	0	tcctttc**ag**TTCTATCTC	II
II	148	CCCGGAAAG**gt**atgagta	2	8847	1	tttaacc**ag**TTACCCATG	III
III	73	TCGTTCAGA**gt**gagtata	3	3571	2	actttgc**ag**TGTCATCCA	IV
IV	37	GTAGACAAA**gt**aagttgt	4	1818	0	tatttct**ag**GTTGCTGCT	V
V	63	TATCTACAG**gt**aaaagtc	5	2819	0	ttatgtt**ag**GAGGCCTTA	VI
VI	96	AGTTGGCAG**gt**attccat	6	295	0	tttcaac**ag**GCTTTAATA	VII
VII	72	TGCTCCAAA**gt**aggtatt	7	1484	0	ttatcct**ag**AATCAAACA	VIII
VIII	141	GAAGTTGAG**gt**atttcac	8	1178	0	gccttgc**ag**CGAAGTCTG	IX
IX	138	AAATTAAAG**gt**atgtata	9	2050	0	atgcaac**ag**GTAGCAGAG	X
X	169	CTCTGCAAG**gt**aagctgg	10	87	1	ttttac**ag**TACGGTTAG	XI*
XI	51	GCAGCTTAG**gt**aggtgtc	11	443	1	taatcct**ag**GGATACAAG	XII*
XII	51	CAGAAAAAG**gta**gcgtaa	12	5809	0	ctttatt**ag**AGCACTTGC	XIII*
XIII	63	AGTGCCAGA**gt**gagtaca	13	10903	1	ctttggc**ag**AGAAGCTGA	XIV
XIV	60	TTTCAAAAG**gt**tagtttg	14	3546	1	tcctaat**ag**AAAATCAGG	XV
XV	81	ACACTACAG**gt**gagtgcg	15	290	1	cccttat**ag**ACGCCCAGA	XVI
XVI	60	TATTAAAAG**gt**attttaa	16	8768	1	ttttgtc**ag**ATGACTTAC	XVII*
XVII	123	AACTTCAAG**gt**gagatga	17	1471	1	gctttttag**CTCTTTTGG**	XVIII
XVIII	75	TTCTTCAAG**gt**atggggc	18	686	1	cttttac**ag**TCCAGCTGC	XIX
XIX	321	GGTTGCAAG**gt**aagtgag	19	552	1	ctactttag**GTGAGCTGG**	XX
XX	118	ATTGCACAA**gt**atgtgag	20	3974	2	gtgttgc**ag**TTCTCAGAA	XXI
XXI	172	CAGAAAGAG**gt**aaagcgg	21	4243	0	tgcctttag**TATGAAAAG**	XXII
XXII	135	GGAAATAAT**gt**aagtgtt	22	1820	0	cttcttc**ag**CCCTCCATA	XIII*
XXIII	90	TAGAGAAAG**gt**acaagca	23	1214	0	tccacac**ag**AAACCCTGG	XXIV
XXIV	1832	TAATCTCCC					

Notes:
* Alternative exon
Exon-intron boundaries conform to the consensus splice donor and acceptor sites (gt-ag).

Fig. 1. Genomic organization of the SLMAP gene. (A) The schematic illustrates that the SLMAP gene is composed of twenty-four exons and introns spanning over 122 kb of genomic DNA. Exon-exon (exons I-XXIV) boundaries are depicted. Exons XI (red), XII (black), XIII (blue), XVII (orange), XXIII (green) encode alternative exons. Transmembrane domains are encoded by exon XXIII and exon XXIV. Exon XX and exon XXI contain the leucine zipper motifs (*). ATG1 (M1, red arrow) is encoded in exon I whereas ATG2 (M2; green arrow) is present in exon II. **(B)** Amino acid composition of alternative exons XI, XII and XIII. Consensus casein kinase 2 phosphorylation sites are underlined; protein kinase C phosphorylation sites are indicated in blue; N-glycosylation site is in italics; and N-myristolyation site is shown in red.

Figure 1

A.

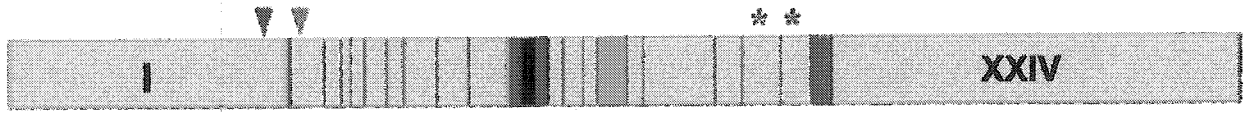

B.

Exon XI:	R L E H L Q E K T L K E C S S L G
Exon XII:	I Q V D D F L P K I *N G S T* E K E
Exon XIII:	H L L S K S G G D C T F I H Q F L E C Q K

Fig. 2. SLMAP3M1 is characterized by a unique N-terminal extension. **(A)** Amino acid composition of the amino-terminal extension identified in SLMAP3. M1 (in red) and M2 (in bold and underlined) represent the two initiating methionines used to generate SLMAPs (Wigle et al., 1997). The consensus fork head associated (FHA) domain is demarcated by bold print. Peptide sequence used to generate anti-SLMAP(N) rabbit antiserum is in italics and underlined (RLSRGEESPPCEI). **(B)** Immunoblot analysis of SLMAP expression in NIH 3T3 cells. NIH 3T3 cells were lysed in RIPA buffer, 15 ug of total protein was separated by 10% SDS-PAGE then electrotransferred to PVDF membranes. Immunoblotting with anti-SLMAP(C) antibody (lane 1) or anti-SLMAP(N) antisera (lane 2) detected a single band at 91 kDa. Prior incubation of the anti-SLMAP(N) with SLMAP peptide abolished the immunoreactivity (lane 3). Positions of molecular mass standards are indicated (BENCHMARK Prestained Protein ladder, Gibco BRL).

Figure 2

A.

```
1   M P S A L A I F T C R P N S H P F Q E R H V Y L D E P
27  P I K I G R S V A R C R P A Q N N A T F D C K V L S R
54  N H A L V W F D H K T G K F Y L Q D T K S S N G T F I
82  N S Q R L S R G S E E S P P C E I L S G D I I Q F G V
109 D V T E N T R K V T H G C I V S T I K L F L P D G M
```

B.

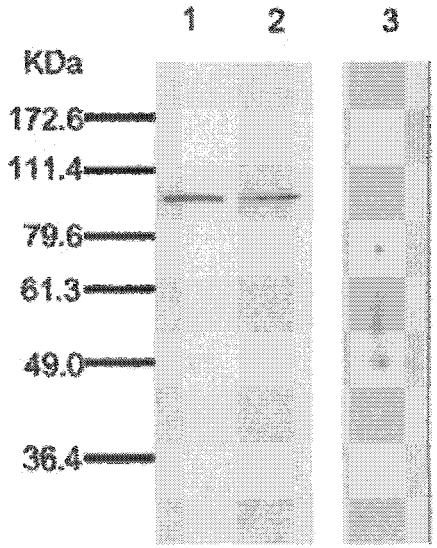

Fig. 3. Subcellular localization of endogenous SLMAP in NIH 3T3 cells. (A) Immuno-fluorescent labeling of SLMAP proteins using anti-SLMAP(C) antiserum revealed staining of reticular formations, the cytosol and perinuclear sites in paraformaldehyde fixed NIH 3T3 cells (a). Reduced cytosolic SLMAP staining and labelling of distinct foci at the perinuclear region was observed in detergent-extracted, paraformaldehyde fixed cells (b). No immunoreactivity was observed with prior incubation of SLMAP(C) antisera with purified SLMAP protein (e) or in cells incubated with the preimmune rabbit serum (f). Staining of foci was also evident in detergent extracted COS-7 cells stained with anti-SLMAP(N) (c). This staining pattern was not observed in COS-7 cells stained with the preimmune serum (d). **(B)** SLMAP co-localizes with ε-tubulin at centrosomes throughout the cell cycle. Paraformaldehyde-fixed NIH 3T3 cells were co-stained with anti-SLMAP (a-e), anti-γ-tubulin (f-j) and DAP1 (k-o). Representative cells in interphase (a, f, k), prophase (b, g, l), metaphase (c, h, m), anaphase (d, i, n) and telophase (e, j, o) are shown. Scale bar = 20 μm.

Figure 3

A.

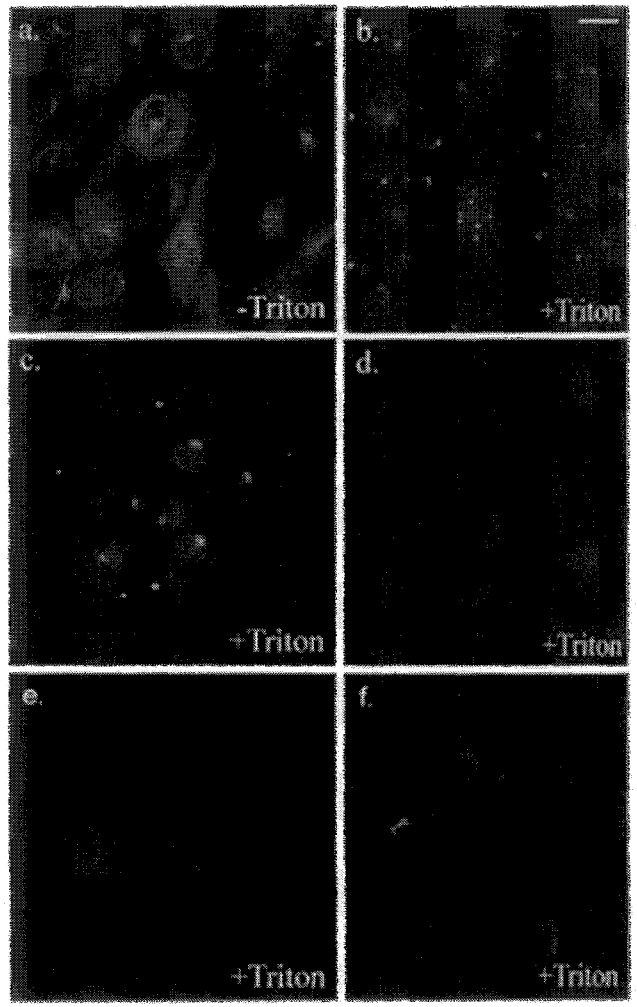

Figure 3

B.

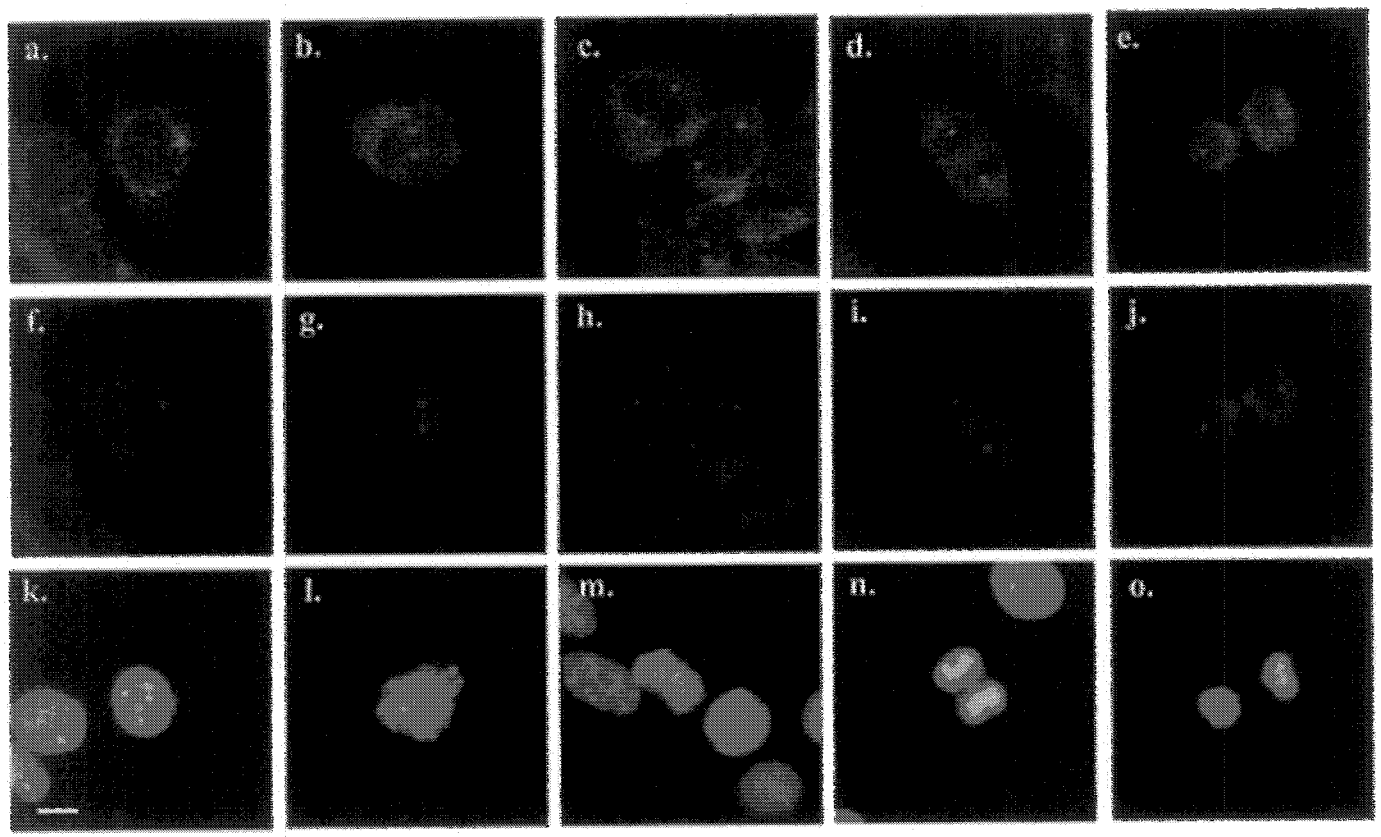

Fig. 4. SLMAP is a component of centrosomes. **(A)** SLMAP localization at centrosomes is not affected by nocodazole or taxol treatment. NIH 3T3 cells were untreated (a, d, g, j) or treated with either taxol (5 uM, 4 hours; b, e, h, k) to stabilize microtubules or nocodazole (6 ug/mL, 4 hours; c, f, i, l) to depolymerize microtubules. Cells were prepared for immunofluorescence microscopy and co-stained with anti-SLMAP (a, b, c), anti-γ-tubulin (d, e, f) and DAPI (g, h, i). To demonstrate that the drugs affected cytoplasmic microtubules, cells were stained with anti-α-tubulin monoclonal antibodies (j, k, l). Scale bar = 25μm. **(B)** Centrosomes were isolated from exponentially growing NIH 3T3 cells by fractionation on a sucrose gradient as described (Moudjou and Bornens, 1998). Equivalent amount (15ug) of each protein fraction was analyzed by SDS-PAGE followed by Western blotting with anti-SLMAP or anti-γ-tubulin. Lane 1 (lysed extract); lane 2 (crude centrosomes); lanes 3-6 represent fractions obtained from sucrose density gradients.

Figure 4

A.

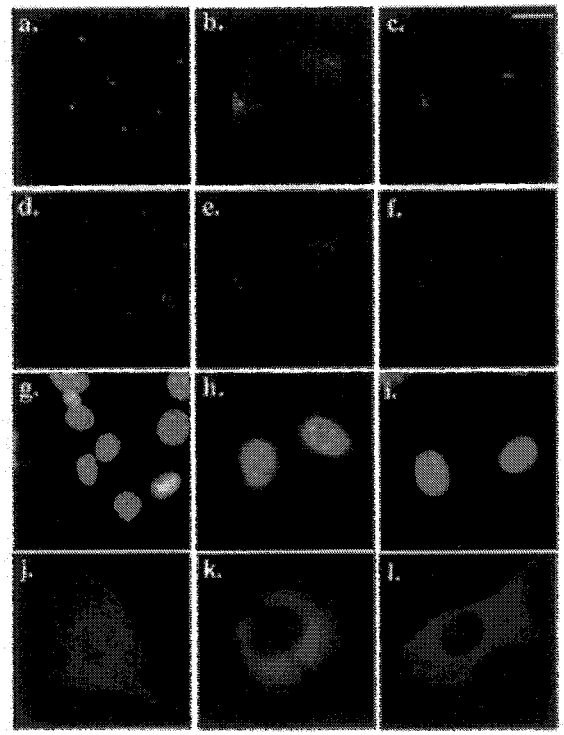

B.

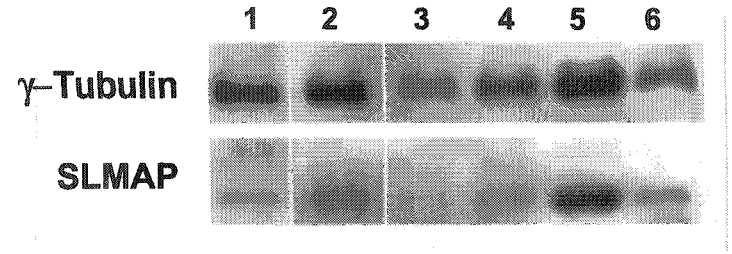

Fig. 5. SLMAP3M1 sequences target GFP to centrosomes. (A) Schematic of the GFP-SLMAPM1 fusion protein used for transient transfection studies. Depicted are the GFP tag, the FHA domain, PEST motif, leucine zippers and the transmembrane domain. **(B)** Localization of GFP-SLMAP fusion proteins transiently expressed in NIH 3T3 was visualized by live microscopy. GFP fluorescence was detected at centrosomes in mitotic cells expressing GFP-SLMAP3M1 (B; a, two closely spaced dots). No green fluorescence was observed at centrosomes in control mitotic cells transfected with GFP-pcDNA alone (B; c). Co-incidence of the γ-tubulin signal (B; d) and GFP fluorescence (B; b) occurred in paraformaldehyde fixed mitotic cells expressing GFP-SLMAP3M1. Scale bar = 25 μm.

Figure 5

A.

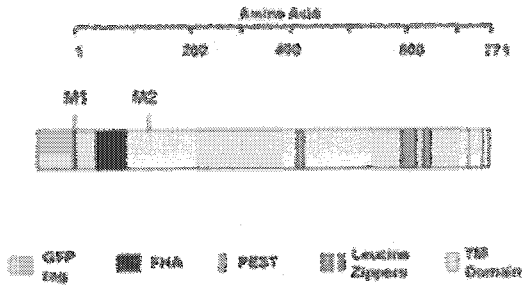
Amino Acids
1
202
400
605
771
M1
M2
GFP
PHA
PEST
Leucine
Zippers
TM
Domain

B.

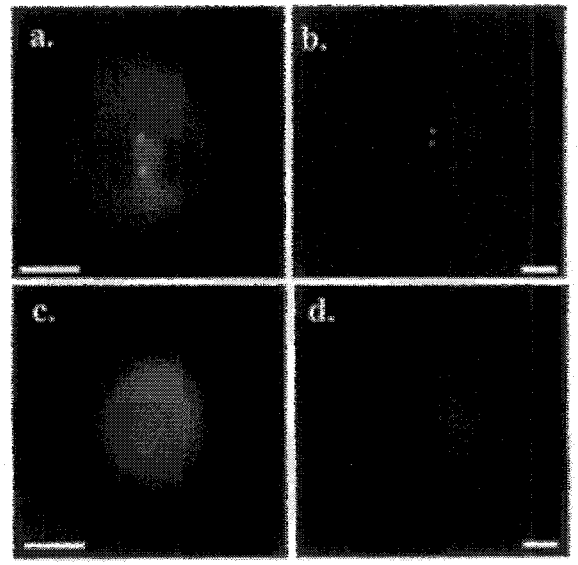
a.
b.
c.
d.

Fig. 6. N-terminal sequences of SLMAP are required for targeting GFP to centrosomes. **(A)** Transient expression of GFP-tagged SLMAP mutants demonstrated that green fluorescence was observed at centrosomes in live cells expressing GFP-SLMAP3M1ΔLZ (A; a) and GFP-SLMAP3M1ΔC (A; b) but not in mitotic cells expressing GFP-SLMAP3M2ΔC (A; c). Corresponding phase contrast images are shown for SLMAP3M1ΔLZ (A; d), GFP-SLAP3M1ΔC (A; e) and GFP-SLMAP3M2ΔC (A; f). Scale bar = 25 μm. **(B)** N-terminal SLMAP3 constructs encoding amino acids 1-163 (B; a), 1-183 (B; b) or 1-201 (B; c) were expressed in fibroblast cells. GFP fluorescence was detected throughout the cell, including the nucleus in (a) or within detergent-insoluble aggregates (b, c). Scale bar = 10 μm. **(C)** Transient expression of the full length GFP-SLMAP fusion protein, GFP-SLMAP3M1 (C; a) was detected at perinuclear sites in interphase cells, indicative of membrane localization. Diffuse cytosolic localization was observed for both carboxyl terminal mutants, GFP-SLMAP3M1ΔC (C;b) and SLMAP3M2ΔC (C; c). Scale bar = 50μm. **(D)** At thirty-six hours post-transfection, cells expressing GFP-SLMAP3M1 were rounded (D; b), whereas those cells expressing either GFP-pcDNA3 (D; a), GFP-SLMAP3M1ΔC (D, c) or GFP-SLMAP3M2ΔC appeared normal. Scale bar = 10 μm.

Figure 6

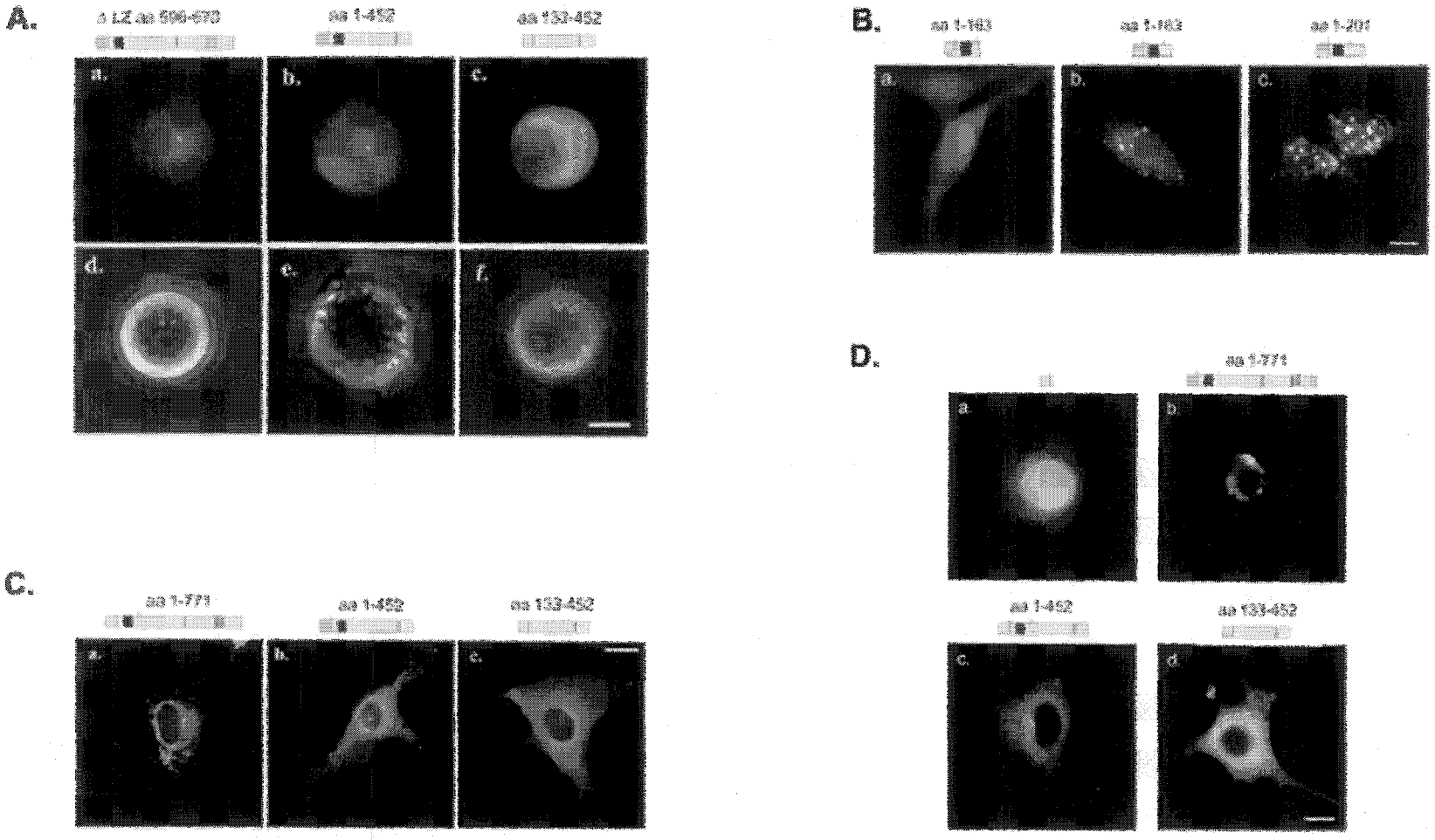
A.
Δ LZ aa 506-670
aa 1-452
aa 133-452
a.
b.
c.
d.
e.
f.
B.
aa 1-163
aa 1-183
aa 1-201
a.
b.
c.
C.
aa 1-771
aa 1-452
aa 133-452
a.
b.
c.
D.
aa 1-771
a.
b.
aa 1-452
aa 133-452
c.
d.

Fig. 7. SLMAP Overexpression Affects Cell Proliferation. **(A)** Overexpression of GFP-tagged SLMAPs inhibits BrdU uptake in NIH 3T3 cells. NIH 3T3 cells were transfected with either GFPpcDNA3 (green bar), GFP-SLMAP3M1 (red bar), GFP-SLMAP3M2 (yellow bar) or GFP-SLMAP3M2ΔC (blue bar). Thirty-six hours post transfection, cells were labeled with BrdU (10 mmol/L) for 2, 8, 12 or 24 hours. Ethanol fixed cells were co-stained with anti-mouse BrdU antibody and anti-rabbit GFP antibody. Transfected cells were identified by their green fluorescence and the number of cells with co-existing nuclear red fluorescence (BrdU positive cells) was determined. The mean results of at least three independent experiments for each labeling period are shown. For each transfectant and condition, a minimum of 200 cells was scored. Error bars represent standard deviations. **(B)** FACS profiles of GFP-pcDNA3 (i) and GFP-SLMAP3M2 (ii) transfected NIH 3T3 cells. At 48 hours post transfection, cells were incubated with propidium iodide to stain DNA (Pestov et al., 1999).

Figure 7

A.

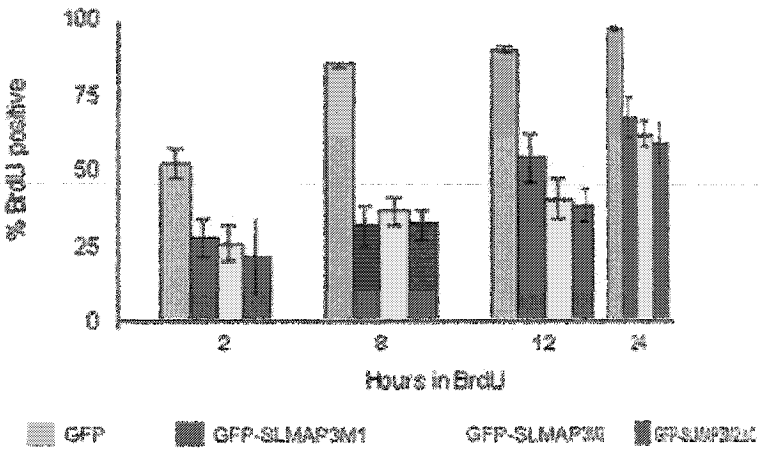
100
75
50
25
0
% BrdU positive
2
8
12
24
Hours in BrdU
GFP
GFP-SLMAP3M1
GFP-SLMAP3W

B.

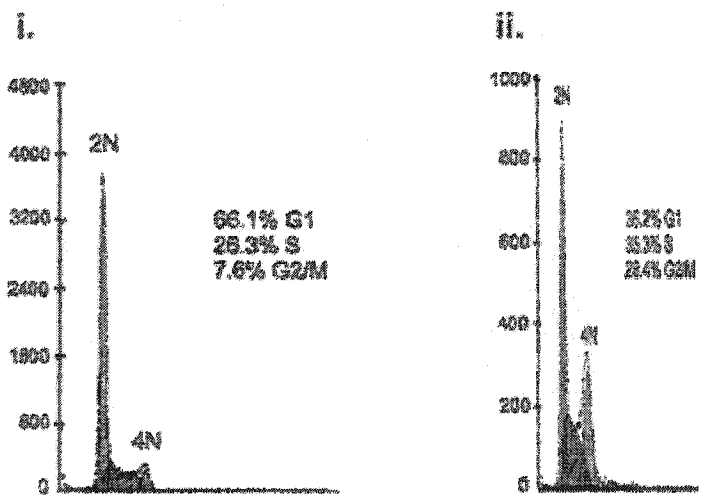
i.
2N
4N
66.1% G1
28.3% S
7.6% G2/M
ii.
2N
4N

Chapter Six.

Discussion and Conclusions.

General Discussion and Conclusions

In era of genomics, large-scale sequencing projects have contributed vast amounts of information to establish the complete genetic profile of organisms from *Drosophila melangaster* to *Homo sapiens*. As a result, molecular biologists are faced with the formidable challenge of assigning function to the proteins encoded by thousands of genes. Experimental approaches for the characterization of protein function have relied upon the amalgamation of applications from various disciplines ranging from cell biology, biochemistry, physiology and genetics to structural biology and computer science (Brent 2000; Pennington et al., 1997). In the studies presented in this thesis, many of the aforementioned approaches have been implemented to gain insight regarding the biological functions of a novel family of sarcolemmal-membrane associated proteins.

Genomic studies have revealed that the complete SLMAP gene is made up of twenty-four exons spanning over 122 kb of DNA, including five alternatively expressed exons (XI, XII, XIII, XVII and XIV). Whereas alternative exons XVII and XIV are present within the genomic sequences encompassing the common core region of the gene, alternative exons XI, XII and XIII are thought to provide diversity to the SLMAP3 and SLMAP2 isoforms. The extensive processing of a common precursor SLMAP mRNA implies that alternative splicing represents a central mechanism for generating structural and functional diversity among SLMAP variants. In this respect, two distinct hydrophobic segments designated TMD1 and TMD2 were shown to be encoded by alternative exon XXIII and exon XXIV, respectively. These transmembrane domains are distinct on the basis of their amino acid composition as well as the type of membrane system with which they associate (further discussed below). Based on the genomic

organization previously reported by Wielowieyski et al. (2000), the two leucine zipper motifs are salient structural features existing in each of the theoretical SLMAP variants and studies presented in this thesis imply that these specialized regions of coiled-coil structure modulate SLMAP function(s) (discussed below). The identification of a forkhead associated domain within the newly identified N-terminal extension of SLMAP3 further suggest that SLMAPs provide functional roles other than those related to membrane biology (discussed below). Overall, the elucidations of the genomic sequences of SLMAPs and their structural elements, combined with the observed tissue distribution have established a significant framework for continued study of protein function (Discussion Figure 1).

To gain insight on function, the distributions of endogenous SLMAPs were analyzed in developing and mature tissue systems, as well as in cultured cells. In vivo analysis of SLMAP expression in mouse embryos indicated that SLMAP expression is induced early in development. SLMAPs were detected in the linear heart tube (9 d.p.c.) as well as in prefusional somites (Chapters 2 and 3). These observations, coupled with the prominent expression profile of SLMAPs in mature striated muscle membranes suggested that these molecules might contribute to structural integrity of the membrane architecture that is necessary for the development, function and maintenance of striated muscle. Confocal imaging further revealed that SLMAPs reside in membrane systems that play a central role in EC coupling mechanisms inherent to both cardiac and skeletal muscle. SLMAP distribution at nonjunctional SR membranes, as well as in junctional membrane structures further supported the hypothesis that divergent transmembrane domains may direct SLMAPs to distinct membrane systems.

Figure 1. Molecular Dissection of SLMAPs.

Overview of the structural features of SLMAPs and the functions ascribed to these features based on results presented in this thesis.

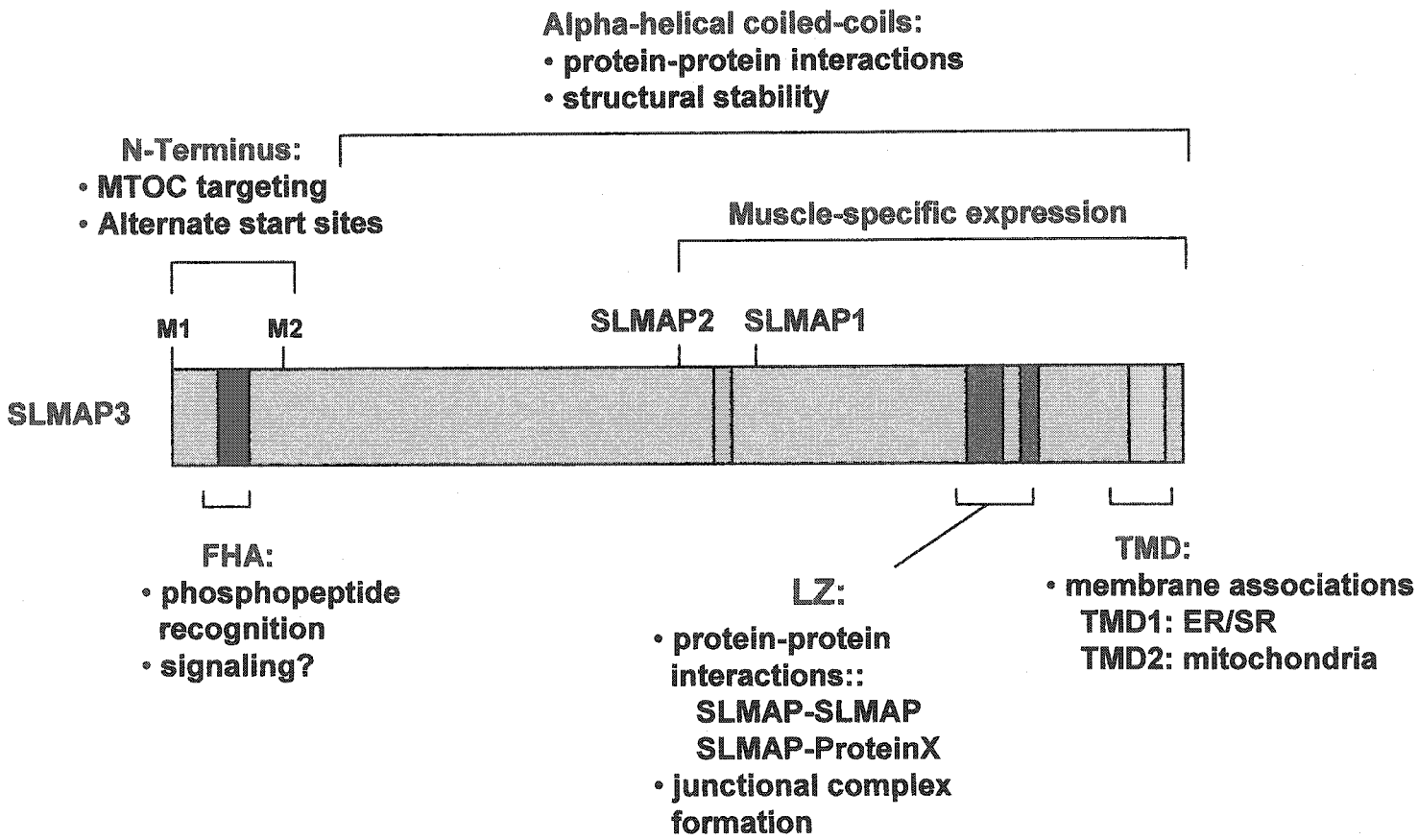
Alpha-helical coiled-coils:
• protein-protein interactions
• structural stability
N-Terminus:
• MTOC targeting
• Alternate start sites
Muscle-specific expression
M1
M2
SLMAP2
SLMAP1
SLMAP3
FHA:
• phosphopeptide recognition
• signaling?
LZ:
• protein-protein interactions::
SLMAP-SLMAP
SLMAP-ProteinX
• junctional complex formation
TMD:
• membrane associations
TMD1: ER/SR
TMD2: mitochondria

The functional role(s) of a protein may also be ascribed based on the identification of associated proteins. Yeast two-hybrid screens, coupled with co-immunoprecipitation assays are frequently used to identify interacting proteins and to characterize the nature of their associations. Such methods have, for instance, been used to identify components associated with the dystrophin-associated glycoprotein complex, which contribute to the maintenance of muscle integrity (Sadoulet-Puccio et al., 1997; Benson et al., 2001; Newey et al., 2001). As a result, these studies have shed light on the organization of dystrophin-associated glycoprotein complex as well as the molecular pathology of muscular dystrophy. Affinity-based methods using recombinant SLMAP fusion proteins were employed to purify biologically relevant protein complexes in tissues and isolated cells. Coupled with mass spectrometric analysis, these studies resulted in the identification of SLMAP-SLMAP interactions (Chapter 3), which were further corroborated by immunoprecipitation experiments and in vitro protein-protein interaction assays (Chapter 2). The ability of SLMAPs to self assemble, by virtue of their leucine zipper motifs, is likely to be highly relevant to the biological activities of this family of proteins. The functional significance of SLMAP-SLMAP assembly may be relevant to the organization of excitatory systems whereby junctional complexes mediate communication between closely apposed membrane systems, such as the T-tubule-SR membranes in striated muscle (Discussion Figure 2). In this respect, SLMAPs anchored in opposing membrane systems by their divergent hydrophobic segments may form homodimers to create junctional membrane complexes that are essential for structural integrity. Furthermore, SLMAP-SLMAP interactions may modulate EC-coupling

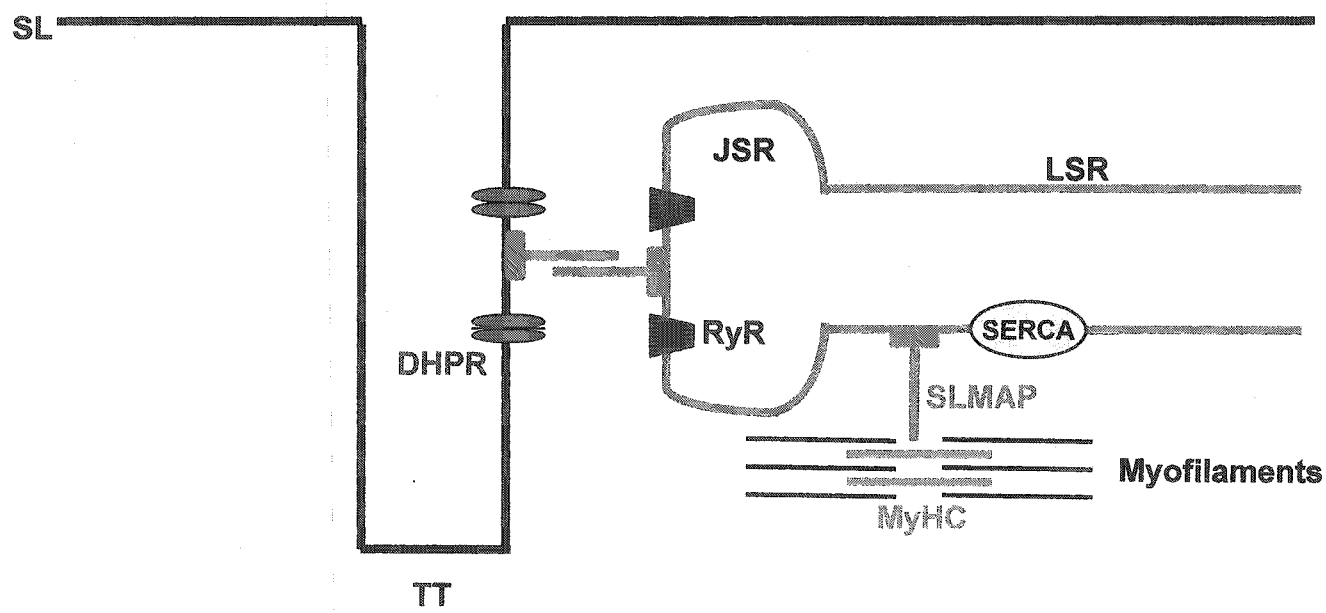
SL
JSR
LSR
RyR
SERCA
DHPR
SLMAP
Myofilaments
MyHC
TT

processes by organizing the assembly of other junctional membrane components or regulatory factors. To further test this possibility, a mouse model may be engineered to specifically ablate the SLMAP leucine zipper motifs in cardiac or skeletal muscles. Examination of the structural organization of muscle membrane systems as well as the process of EC coupling may indicate that SLMAP-SLMAP associations are necessary for the integrity of muscle membrane assembly and activity.

Insight into the functional roles of SLMAPs was further gauged by altering SLMAP protein levels in cultured myogenic cells. This approach is widely used and as such, the overexpression of myogenic regulatory factors has contributed to the understanding of their roles as regulators of skeletal myogenesis. In this respect, seminal studies by Lassar et al. (1989) demonstrated that the forced expression of the MyoD transcription factor in nonmyogenic cells activates skeletal muscle-specific gene expression, thus corroborating a central role for this factor in regulating skeletal myogenesis. Dominant-negative effects are in many circumstances elicited by the overexpression of structural mutants and thus offer valuable insights to structure-function relationships. In view of the abundant SLMAP expression in prefusion myoblasts, various SLMAP structural mutants were expressed in C2C12 myoblasts to assess whether SLMAPs may serve a role in the fusion process. Whereas biochemical differentiation remained unaffected, a significant defect in fusion was observed in cells having altered levels of SLMAP variants. Studies presented in Chapter 2 have indicated that the fusion defective phenotype was not dependent upon either SLMAP-membrane associations or SLMAP-SLMAP interactions. There is evidence supporting the role of protein-protein interactions between cytoskeletal components and the cytosolic portion of

transmembrane domains in the promotion of myoblast fusion. Overexpression of the cytosolic portion of a transmembrane domain metalloprotease, which mediates interactions with α-actinin, resulted in a defect in myoblast fusion (Galliano et al., 2000). We thus speculate that coiled-coil motifs present in SLMAPs may interfere with the fusion process, possibly by associating with structural elements or cytosolic signaling factors regulating the fusion process. Further elucidation of SLMAP-associated proteins may clarify this issue. In addition, Cre-lox technology, coupled with the use of skeletal muscle-specific promoters may be used to generate a SLMAP-deficient mouse. Such a model may then be used to examine the effect of SLMAP deficiency during myoblast fusion in vivo.

The molecular features of SLMAPs indicated that this protein family belongs to a class of carboxyl-terminal tail-anchored membrane proteins with an amino-terminal coiled-coil cytosolic moiety. This topology is ideal for complex association with other cytosolic or cytoskeletal components. Interestingly, the muscle specific SLMAP isoform (SLMAP1) was shown to interact with myosin heavy chain (MyHC). This association between an SR-membrane localized protein and a myofibril component may serve to efficiently transmit the calcium signal to the contractile apparatus during the EC-coupling mechanism in striated muscle (Discussion Figure 2). To further understand the nature of the SLMAP-myofibril association, it is obviously necessary to delineate the sequences that are responsible for directing SLMAP-MyHC associations. In view of the potential SLMAP-myofibril association, animal models that are deficient in SLMAPs are anticipated to have impaired contractile properties.

Immunolocalization studies have revealed that SLMAPs may be differentially targeted to either the ER or the mitochondria by the two divergent carboxyl-terminal transmembrane domains. The transmembrane domain dependent association of SLMAPs with either the ER or the mitochondria is consistent with the localization pattern typically observed for various tail-anchored membrane proteins, including cytochrome b5 (D'Arrigo et al., 1993; Borgese et al., 2001). The differential targeting of SLMAPs to the ER or mitochondria implies that these coiled-coil molecules may serve varied functions, depending on their membrane associations. It is tempting to speculate that SLMAPs may function in calcium regulation as both the ER and mitochondria play central roles in modulating intracellular calcium levels. At the molecular level, the specific amino acids which are necessary for directing SLMAP to the mitochondria versus the ER have not yet been defined. The nature of the amino acids flanking TMD1 and TMD2 may also contain important information necessary for organelle-specific targeting (Kanaji et al., 2000). These issues may be addressed in future studies employing site directed mutagenesis.

As many proteins that are related by function exhibit homology at the amino acid level, the BLAST program is frequently used to identify homologous proteins that may offer insight to some element of protein function. The identification of essential genes in lower organisms (flies, yeast, worms, viruses) has facilitated the identification of mammalian protein orthologues that share analogous functions. For instance, the link between the mammalian inhibitor of apoptosis proteins (IAP's) and their role in impairing cell death responses was first postulated because of the homology shared with proteins encoded by baculoviruses, known to function in inhibiting apoptosis (Huang et al., 2000). Homology searches were periodically performed to identify SLMAP

orthologues of known function. At the amino acid level, SLMAPs were found to share significant homology with a coiled-coil yeast protein, Uso1p, known to function in ER to golgi transport (Sapperstein et al., 1996). This homology, in addition to the presence of an ER exit motif that has been reported to mediate efficient ER to golgi vesicle transport, inspired the studies presented in Chapter three, whereby ER to golgi transport assays were conducted to assess a possible role for SLMAPs in this process. On the basis of these studies, we have concluded that SLMAPs do not provide a role in vesicle transport. These conclusions are further supported by the observation that ectopically expressed SLMAP variants were not distributed to post-ER organelles, such as the ERGIC or the Golgi (Chapter three). Additional studies may be performed to further examine a role for SLMAPs in the intracellular trafficking process. For instance, an inhibition of SLMAP expression may affect the morphology of membrane-bound organelles of the secretory pathway or the mechanism of intracellular trafficking, potentially at the level of vesicle docking or membrane fusion.

Interestingly, the examination of SLMAP distribution in proliferating cells lead to the identification of a centrosome-localized SLMAP variant (Chapter five). Diverse classes of proteins have been shown to localize at the MTOC, and many possess extensive regions of coiled-coil structure (Doxsey et al., 1994; Fry et al., 1998a, 1998b, 1999; Bouckson-Castaing et al., 1996; Takahashi et al., 1999 and 2002; Li et al., 2000; Chevrier et al., 2002). In view of the diverse nature of the classes of proteins localized at the MTOC, the identification of discrete centrosome targeting sequences has posed a considerable challenge. Sequence comparison of the centrosome components pericentrin and A-kinase anchoring protein (AKAP450) revealed that these coiled-coil proteins share

a 90 amino acid motif (PACT motif), which confers centrosome targeting (Gillingham and Munro, 2000). This motif was not identified within the SLMAP sequences necessary for centrosome targeting (Chapter five). Whereas SLMAP localization at the MTOC appears to be dependent upon the presence of amino-terminal sequences, a particular conformational structure is also thought to serve as a determinant for centrosome association. In this respect, the coiled-coil sequences of SLMAPs plus the N-terminal sequences may function to mediate the assembly of cell cycle regulators or other regulatory molecules at the MTOC. Increased synthesis of the centrosome-targeted SLMAP variant in proliferating fibroblast cells compromised cell viability, and this effect may potentially by mediated by affecting the levels of regulatory proteins through protein-protein interactions involving the SLMAP coiled-coil motifs.

Computer-assisted sequence analyses are also common tools used to predict the presence of structural motifs, protein interaction modules, regulatory domains, targeting motifs and consensus post-translational modification sites, such as phosphorylation motifs. The phosphorylation status of proteins provides an additional determinant for the mediation of protein-protein interactions. In this respect, signaling protein modules such as the Src homology 2 (SH2) domain function as discrete phosphopeptide binding motifs. SH2 domains are encoded by several important signaling molecules and serve to mediate interactions with phosphotyrosine peptides present within target substrates (Mayer and Baltimore, 1994). Analysis of SLMAP protein sequences resulted in the identification of an amino-terminal localized forkhead-associated (FHA) domain (Chapter five). Initially identified in forkhead transcription factors, this phosphopeptide recognition motif has since been identified in diverse classes of mammalian and yeast proteins and are thought

to function in DNA damage checkpoint signaling mechanisms as well as in the regulation of mitotic phase progression (Hoffmann and Bucher, 1995; Li et al., 2000b; Durocher and Jackson, 2002; Durocher et al., 2000; Sun et al., 1998; Sueishi et al., 2000). Whereas the functional significance of the FHA domain present in SLMAP is not fully understood, the ectopic expression of the full length SLMAP3M1 encompassing this motif compromised the viability of cultured fibroblasts (Chapter five). Interestingly, SLMAP variants lacking sequences encompassing this motif did not retain the ability to target a heterologous protein to the MTOC. Taken together, these studies suggest that the FHA motif may mediate associations with phosphoproteins that may serve a role in centrosome-mediated functions. This inference may be further explored by identifying the FHA-mediated SLMAP associations.

Inhibition of gene expression represents a powerful tool to examine the function of the encoded protein. At the cellular level, the introduction of antisense oligonucleotides and small interfering RNAs (siRNA) represents an effective method for gene functional analysis (Harborth et al., 2001; Elbashir et al., 2001a and 2001b). In recent years, siRNA-mediated technology has gained popularity for use in cell culture systems. As is the case for any experimental application, there are technical limitations associated with the use of antisense or siRNA technology, and such limitations are attributed to the dilution of the antisense or siRNA effect with increased time in culture as well as the stability of the protein (Elbashir et al., 2001a). During my studies, I have designed and implemented strategies using siRNAs, including commercially synthesized double stranded RNA directed against several regions in SLMAP, as well as a vector siRNA mediated approach (Gou et al., 2003; Miyagishi and Taira, 2002; Yu et al., 2002). When the levels of SLMAP proteins produced in cultured cells (NIH 3T3, C2C12) were

assayed, no apparent inhibition or reduction of SLMAP levels was apparent by immunoblot analysis. These issues may be addressed by designing additional antisense oligonucleotides or siRNA against other regions of SLMAPs. Further insight regarding the role of SLMAPs may be acquired through ongoing studies in our laboratory aimed at generating SLMAP-deficient mice.

Taken together, the original studies described in this thesis support the following conclusions:

(i) Alternative splicing mechanisms generate SLMAP variants that are targeted to multiple subcellular localizations, including membrane bound organelles (ER, SR, mitochondria), junctional membranes (SR,T-tubules) as well as centrosomes. These observations imply that distinct SLMAP variants provide functions specifically related to membrane biology as well as the activity or assembly of the microtubule organizing center.

(ii) The distribution of SLMAPs at the SR and T-tubules membrane systems in striated muscle suggest that SLMAP-SLMAP interactions establish junctional complexes that may be necessary for proper EC coupling mechanisms. Interaction with a myofibril contractile element further suggests a role for SLMAPs in establishing a scaffold that links the SR membrane domains with the contractile cytoskeleton.

(iii) Regulated levels of SLMAPs are critical for developmental processes (myoblast fusion) as well as normal cell proliferation.

Chapter Seven.

Bibliography.

References Cited in Introductory and Summary Chapters

Abmayr, S.M., Balagopalan, L., Galletta, B.J. and Hong, S.J. (2003). Cell and molecular biology of myoblast fusion. International Review in Cytology 225, 33-89.

Adams, B.A., Tanabe, T., Mikami, A., Numa, S. and Beam K.G. (1990). Intramembrane charge movement restored in dysgenic skeletal muscle by injection of dihydropyridine receptor cDNAs. Nature 346, 560-572.

Albrecht-Buehler, G. (1992). Function and formation of centrioles and basal bodies. In: The Centrosome (Kalnins VI, ed). Academic Press, Inc. San Diego, 69-102.

Andersen, S.S.L. (1999). Molecular characteristics of centrosomes. International Reviews in Cytology 187, 51-109.

Andres, V. and Walsh, K. (1996). Myogenin expression, cell cycle withdrawal and phenotypic differentiation are temporally separable events that precede cell fusion upon myogenesis. Journal of Cell Biology 132, 657-666.

Bagnato, P., Barone, V., Giacomello, E., Rossi, D. and Sorrentino. V. (2003). Binding of an ankyrin-1 isoform to obscurin suggests a molecular link between the sarcoplasmic reticulum and myofibrils in striated muscle. Journal of Cell Biology 160, 245-253.

Barnoy, S., Glaser, T. and Kosower, N.S. (1998). The calpain-calpastatin system and protein degradation in fusing myoblasts. Biochimica Biophysica Acta 1402, 52-60.

Benson, M.A., Newey, S.E., Martin-Rendon, E., Hawkes, R. and Blake, D.J. (2001). Dysbindin, a novel coiled-coil-containing protein that interacts with the dystrobrevins in muscle and brain. Journal of Biological Chemistry 276, 24232-24241.

Berridge, M.J. (1998). Neuronal calcium signaling. Neuron 21, 13-26.

Bers, D.M. (2002). Cardiac excitation-contraction coupling. Nature 415, 198-205.

Bers, D.M. and Stiffel, V.M. (1993). Ratio of ryanodine to dihydropyridine receptors in cardiac and skeletal muscle and implications for EC coupling. American Journal of Physiology 264, C1587-C1593.

Biben, C., Weber, R., Kesteven, S., Stanley, E., McDonald, L., Elliott, D.A., Barnett, L, Koentgen, F., Robb, L., Feneley, M., and Harvey R.P. (2000). Cardiac septal and valvular dysmorphogenesis in mice heterozygous for mutations in the homeobox gene Nkx2-5. Circulation Research 87, 888-895.

Blagden, .S. and Hughes, S.M. (1999). Extrinsic influences on limb muscle organization. Cell and Tissue Research 296, 141-150.

Blake, D.J., Wier, A., Newey, S.E. and Davies, K.E. (2002). Function and genetics of dystrophin and dystrophin-related proteins in muscle. Physiological Reviews 82, 291-329.

Block, B.A., Imagawa, T., Campbell, K.P. and Franzini-Armstrong, C., (1988). Structural evidence for direct interaction between the molecular components of the transverse tubule/sarcoplasmic reticulum junction in skeletal muscle. Journal of Cell Biology 107, 2587-2600.

Borgese, N., Gassoni, I., Barberi, M., Solombo, S. and Pedrazzini, E. (2001). Targeting of a tail-anchored protein to the endoplasmic reticulum and mitochondrial outer membrane by independent but competing pathways. Molecular Biology of the Cell 12, 2482-2496.

Bouckson-Castaing, V., Moudjou, M., Ferguson, D.J.P., Mucklow, S., Belkaid, Y., Milon, G. and Crocker, P.R. (1996). Molecular characterization of ninein, a new coiled-coil protein of the centrosome. Journal of Cell Science 109, 179-190.

Boveri, T. (1914). *Zur Frage der Entstehung Maligner Tumoren.* Translation M. Boveri, Jena: Fischer Verlag. 1929 English translation by M. Boveri reprinted as The Origin of malignant tumours. Williams and Wilkins Co, Baltimore, 119.

Brandl, C.J., Green, N.M., Korczak, B., MacLennan, D.H. (1986). Two Ca^{+2}ATPase genes: homologies and mechanistic implications of deduced amino acid sequences. Cell 44, 597-607.

Braun, T. and Arnold, H.H. (1996). Myf-5 and myoD genes are activated in distinct mesenchymal stem cells and determine different skeletal muscle cell lineages. EMBO Journal 15, 310-318.

Brent, R. (2000) Genomic Biology. Cell 100, 169-183.

Brent A.E. and Tabin C.J. (2002). Developmental regulation of somite derivatives: muscle, cartilage and tendon. Current Opinions in Genetic Development 12, 548-557.

Brette, F. and Orchard, C. (2003). T-tubule function in mammalian cardiac myocytes. Circulation Research 92, 1182-1192.

Brinkley, B.R. and Goepfert, T.M. (1998). Supernumerary centrosomes and cancer: Boveri's hypothesis resurrected. Cell Motility and the Cytoskeleton 41, 281-288.

Bruneau, B.G. (2002). Transcriptional regulation of vertebrate cardiac morphogenesis. Circulation Research 90, 509-519.

Buckingham, M. (1994). Molecular biology of muscle development. Cell 78, 15-21.

Buckingham, M. (2001) Skeletal muscle formation in vertebrates. Current Opinions in Genetic Development 11, 440-448.

Burkhard, P., Stetefeld, J. and Stielkov, S.V. (2001). Coiled-coils: a highly versatile protein folding motif. Trends in Cell Biology 11, 82-88.

Buscher, D. and Izpisua Belmonte, J.C. (1999) Muscle development during vertebrate limb outgrowth. Cell and Tissue Research 296, 131-139.

Canaves, J.M. and Montal, M. (1998). Assembly of ternary complex by the predicted minimal coiled-coil-forming domains of syntaxin, SNAP-25 and synaptobrevin. Journal of Biological Chemistry 273, 34214-34221.

Catterall, W.A. (1991a). Structure and function of voltage-gated sodium and calcium channels. Current Opinion in Neurobiology 1, 5-13.

Catterall, W.A. (1991b). Functional subunit structure of voltage-gated calcium channels. Science. 253, 1499-1500.

Catterall, W.A. (1995). Structure and function of voltage-gated ion channels. Annual Review in Biochemistry 64, 493-531.

Chapman, E.R., An, S., Barton, N. and Jahn, R. (1994). SNAP-24, a t-SNARE which binds to both syntaxin and synaptobrevin via domains that may form coiled-coils. Journal of Biological Chemistry 269, 27427-27432.

Charge, S. and Rudnicki, M.A. (2003). Fusion with the fused: a new role for interleukin-4 in the building of muscle. Cell 113, 422-423.

Chevrier, V., Piel, M., Collomb, N., Saoudi, Y., Frank, R., Paintrand, M,, Narumiya, S., Bornens, M. and Job, D. (2002). The Rho-associated protein kinase p160ROCK is required for centrosome positioning. Journal of Cell Biology 157, 807-817.

Crispino, J.D., Lodish, M.B., Thurberg, B.L., Litovsky, S.H., Collins, T., Molkentin, J.D. and Orkin, S.H. (2001). Proper coronary vascular development and heart morphogenesis depend on interaction of GATA-4 with FOG cofactors. Genes and Development 15, 839-844.

Crowe, L.M. and Baskin, R.J. (1977). Stereological analysis of developing sarcotubular membranes. Journal of Ultrastructural Research 58, 10-21.

D'Arrigo, A., Manera, E., Longhi, R. and Borgese, N. (1993). The specific subcellular localization of two isoforms of cytochrome b_5 suggests novel targeting pathways. Journal of Biological Chemistry 268, 2802-2808.

Davis, R.L., Weintraub, H. and Lassar, A.B. (1987). Expression of a single transfected

cDNA converts fibroblasts to myoblasts. Cell 51, 987-1000.

Dictenberg, J.B., Zimmerman, W., Sparks, C.A., Young, A., Vidair, C., Zheng, Y., Carrington, W., Fay, F.S. and Doxsey S.J. (1998). Pericentrin and γ-tubulin form a protein complex and are organized into a novel lattice at the centrosome. Journal of Cell Biology 141, 163-174.

Diviani, D., Langeberg, L.K., Doxsey, S.J. and Scott, J.D. (2000). Pericentrin anchors protein kinase A at the centrosomes through a newly identified RII-binding domain. Current Biology 10, 417-420.

Diviani, D. and Scott, J.D. (2001). AKAP signaling complexes at the cytoplasm. Journal of Cell Science 114, 1431-1437.

Doberstein, S.K., Fetter, R.D., Mehta, A.Y. and Goodman, C.S. (1997) Genetic analysis of myoblast fusion: *blown fuse* is required for progression beyond the prefusion complex. Journal of Cell Biology 136, 1249-1261.

Doxsey, S.J., Stein, P., Evans, L., Calarco, P.D. and Kirschner, M. (1994). Pericentrin, a highly conserved centrosome protein involved in microtubule organization. Cell 76, 639-650.

Doxsey, S. (1998). The centrosomes – a tiny organelle with big potential. Nature Genetics 20, 104-106.

Doxsey, S.J. (2001). Re-evaluating centrosome function. Nature Reviews Molecular Cell Biology 2, 688-698.

Dulhunty, A.F., Haarmann, C.S., Green, D., Laver, D.R., Board, P.G. and Casarotto, M.G. (2002). Interactions between dihydropyridine receptors and ryanodine receptors in striated muscle. Progress in Biophysical and Molecular Biology 79, 45-75.

Durocher, D., Taylor, I.A., Sarbassova, D., Haire, L.F., Westcott, S.L., Jackson, S.P., Smerdon, S.J. and Yaffe, M.B. (2000). The molecular basis of FHA domain: phosphopeptide binding specificity and implications for phospho-dependent signaling mechanisms. Molecular Cell 6, 1169-1182.

Durocher, D and Jackson, S.P. (2002). The FHA domain. FEBS Letters 513, 58-66.

Dworak, H.A. and Fink, H. (2002) Myoblast fusion in Drosophila. *BioEssays* **24**, 591-601.

Edge, M.B. (1970). Development of apposed sarcoplasmic reticulum at the T system and sarcolemma and the change in orientation of triads in rat skeletal muscle. Developmental Biology 23, 634-659.

Edmondson, D.G. and Olson, E.N. (1989). A gene with homology to the myc similarity region of MyoD1 is expressed during myogenesis and is sufficient to activate the muscle differentiation program. Genes and Development 3, 628-640.

Elbashir, S.M., Harborth, J., Lendeckel, W., Yalcin, A., Weber, K. and Tuschl, T. (2001a). Duplexes of 21-nucleotide RNAs mediate RNA interference in mammalian cell culture. Nature 411, 494-498.

Elbashir, S.M., Lendeckel, W. and Tuschl, T. (2001b). RNA interference is mediated by a 21 and 22-nucleotide RNAs. Genes and Development 15, 188-200.

Endo, M., Tanaka, M. and Ogawa, Y. (1970). Calcium induced calcium release of calcium from the sarcoplasmic reticulum of skinned skeletal muscle. Nature 228, 34-36.

Engel, L.C., Egar, M.W. and Przybylski, R.J. (1986). Morphological characterization of actively fusing L6 myoblasts. European Journal of Cell Biology 39, 360-365.

Felix, M.A., Antony, C., Wright, M. and Maro, B. (1994) Centrosome assembly in vitro: role of gamma-tubulin recruitment in Xenopus sperm aster formation. Journal of Cell Biology 124, 19-31.

Fischman, D.A. (1970). The synthesis and assembly of myofibrils in embryonic muscle. Current Topics in Developmental Biology 5:235-280.

Fisk, H.A., Mattison, C.P. and Winey, M. (2002). Centrosomes and tumour suppressors. Current Opinion in Cell Biology. 14, 700-705.

Fleischer, S. and Inui, M. (1989). Biochemistry and biophysics of excitation contraction coupling. Annual Review in Biophysical Chemistry 18, 333-364.

Flucher, B.E. (1992). Structural analysis of muscle development: transverse tubules, sarcoplasmic reticulum and the triad. Developmental Biology 154, 245-260.

Flucher, B.E., Takekura, H. and Franzini-Armstrong, C. (1993) Development of the excitation-contraction coupling apparatus in skeletal muscle: association of sarcoplasmic reticulum and transverse tubules with myofibrils. Developmental Biology 160, 135-147.

Franzini-Armstrong, C. (1991). Simultaneous maturation of transverse tubules and sarcoplasmic reticulum during muscle differentiation in the mouse. Developmental Biology 146, 353-363.

Franzini-Armstrong, C. (1994). The sarcoplasmic reticulum and the transverse tubules. *In* Myology. A.E. Engel and C. Franzini-Armstrong, editors. McGraw-Hill Inc., New York, 176-199.

Franzini-Armstrong, C. and Jorgensen, A.O. (1994). Structure and development of E-C

coupling units in skeletal muscle. Annual Review in Physiology 56, 509-534.

Franzini-Armstrong, C. (1999). The sarcoplasmic reticulum and the control of muscle contraction. FASEB Journal 13, S266-S270.

Freedman S.J., Song H.K., Xu Y., Sun Z.Y. and Eck M.J. (2003). Homotetrameric structure of the SNAP-23 N-terminal coiled-coil domain. Journal of Biological Chemistry 278, 13462-13467.

Fruen, B.R., Bardy, J.M., Byrem, T.M., Strasburg, G.M. and Louis, C.F. (2000). Differential Ca^{+2} sensitivity of skeletal and cardiac muscle ryanodine receptors in the presence of calmodulin. American Journal of Physiology 279, C724-C733.

Fry, A.M., Schultz, S.J., Bartek, J. and Nigg, E.A. (1995). Substrate specificity and cell cycle regulation of the Nek2 protein kinase, a potential human homolog of the mitotic regulator of NIMA of *Aspergillus nidulans*. Journal of Biological Chemistry 2705, 12899-12905.

Fry, A.M., Meraldi, P. and Nigg, E.A. (1998a). A centrosomal function for the human Nek2 protein kinase, a member of the NIMA family of cell cycle regulators. *EMBO J.* **17**, 470-481.

Fry, A.M., Mayor, T., Meraldi, P., Stierhof, Y.D., Tanaka, K. and Nigg, E.A. (1998b). C-Nap1, a novel centrosomal coiled-coil protein and candidate substrate of the cell-cycle regulated protein kinase Nek2. Journal of Cell Biology 141, 1563-1574.

Fry, A.M., Arnaud, L. and Nigg, E.A. (1999). Activity of the human centrosomal kinase, Nek2, depends on an unusual leucine zipper dimerization motif. Journal of Biological Chemistry 274, 16304-16310.

Fuller, S.D., Gowen, B.E., Reinsch, S., Sawyer, A., Buendia, B., Wepf, R. and Karsenti, E. (1995). The core of the mammalian centriole contains gamma-tubulin. Current Biology 5, 1384-1393.

Furst, D.O., Osborn, M. and Weber, K. (1989). Myogenesis in the mouse embryo: differential onset of expression of myogenic proteins and the involvement of titin in myofibril assembly. Journal of Cell Biology 109, 517-527.

Galliano, M.F., Huet, C., Frygelius, J., Polgren, A., Wewer, U.M. and Engvall, E. (2000). Binding of ADAM12, a marker of skeletal muscle regeneration, to the muscle-specific actin-binding protein, α-actinin-2, is required for myoblast fusion. Journal of Biological Chemistry 272, 13933-13939.

Gavanescu, I., Vazquez-Abad, D., McCauley, J., Senecal, J.L. and Doxsey, S. (1999). Centrosome proteins: a major class of autoantigens in scleroderma. Journal of Clinical Immunology 19, 166-171.

Giannini, G., Clementi, E., Ceci, R., Marziali, G. and Sorrentino, V. (1992). Expression of a ryanodine receptor-Ca^{2+} channel that is regulated by TGF-beta. Science. 257, 91-94.

Giet, R. and Prigent, C. (1999). Aurora/Ipl1p-related kinases, a new oncogenic family of mitotic serine-threonine kinases. Journal of Cell Science 112, 3591-35601.

Gillingham, A.K. and Munro, S. (2000). The PACT domain, a conserved centrosomal targeting motif in the coiled-coil proteins AKAP450 and pericentrin. EMBO Reports 1, 524-529.

Gou, D., Jin, N. and Liu, L. (2003). Gene silencing in mammalian cells by PCR-based short hairpin RNA. FEBS Letters 548, 113-118.

Gunderson, G.G., Khawaja, S. and Bulinski, J.C. (1989). Generation of a stable, posttranslationally modified microtubule array is an early event in myogenic differentiation. Journal of Cell Biology 109, 2275-2288.

Guo, W. and Campbell, K.P. (1995). Association of triadin with the ryanodine receptor and calsequestrin in the lumen of the sarcoplasmic reticulum. Journal of Biological Chemistry 270, 9027-9030.

Guo, W., Jorgensen, A.O., Jones, L.R. and Campbell, K.P. (1996). Biochemical characterization and molecular cloning of cardiac triadin. Journal of Biological Chemistry 271, 458-465.

Hakamata, Y., Nakai, J., Takeshima, H. and Imoto, K. (1992). Primary structure and distribution of a novel ryanodine receptor/calcium release channel from rabbit brain. FEBS Letters 312, 229-235.

Harborth, J., Elbashir, S.M., Bechert, K., Tuschl, T. and Weber, K. (2001). Identification of essential genes in cultured mammalian cells using small interfering RNAs. Journal of Cell Science 114, 4557-4565.

Hasty, P., Bradley, A., Morris, J.H., Edmondson, D.G., Venuti, J.M., Olson, E.N. and Klein, W.H. (1993). Muscle deficiency and neonatal death in mice with a targeted mutation in the myogenin gene. Nature 364, 501-506.

Heikinheimo, M., Scandrett, J.M. and Wilson, D.B. (1994). Localization of transcription factor GATA-4 to regions of the mouse embryo involved in cardiac development. Developmental Biology 164, 361-373.

Hoerter, J., Mazet, F. and Vassort, G. (1981). Perinatal growth of the rabbit cardiac cell: possible implications for the mechanism of relaxation. Journal of Molecular and Cellular Cardiology 13, 725-740.

Hofmann, K. and Bucher, P. (1995). The FHA domain: a putative nuclear signaling domain found in protein kinases and transcription factors. Trends in Biochemical Science 20, 347-349.

Holtzer, H., Forry-Schaudie, S., Dlugosz, A., Antin, P. and Dubyak, G. (1985). Interactions between intermediate filaments, microtubules and myofibrils in fibrogenic and myogenic cells. Annals of the New York Academy of Science 455, 106-125.

Hong, Y.R., Chen, C.H., Chang, J.H., Wang, S., Sy, W.D., Chou, C.K. and Howng, S.L. (2000). Cloning and characterization of a novel human ninein protein that interacts with the glycogen synthase kinase 3beta. Biochimica Biophysica Acta 1492(2-3), 513-516.

Horsley, V., Jansen, K.M., Mills, S.T. and Pavlath, G.K. (2003). IL-4 acts as a myoblast recruitment factor during mammalian muscle growth. Cell 113, 483-494.

Huang, Q., Devereaux, Q.L., Meada, S., Salvesen, G.S., Stennicke, H.R., Hammock, B.D. and Reed, J.C. (2000). Evolutionary conservation of apoptosis mechanisms: lepidoperan and baculoviral inhibitor of apoptosis proteins are inhibitors of mammalian caspase-9. Proceedings of the National Academy of Science U.S.A. 97, 1427-1432.

Hulme, J.T., Ahn, J., Hauschka, S.D., Scheuer, T. and Catterall, W.A. (2002). A novel leucine zipper targets AKAP15 and cyclic AMP-dependent protein kinase to the C terminus of the skeletal muscle Ca^{+2} channel and modulates its function. Journal of Biological Chemistry 277, 4079-4087.

Ikemoto, N., Antoniu, R., Kang, J.J., Meszaros, L.G. and Ronjat, M. (1991). Intravesicular calcium transient during calcium release from sarcoplasmic reticulum. Biochemistry 30, 5230-5327.

Ikemoto, T., Komazaki, S., Takeshima, H., Nishi, M., Noda, T., Iino, M. and Endo, M. (1997). Functional and morphological features of skeletal muscle from mutant mice lacking both type 1 and type 3 ryanodine receptors. Journal of Physiology 501, 305-312.

Isenmann, S., Khew-Goodall, Y., Gamble, J., Vadas, M. and Wattenberg, B.W. (1998). A splice isoform of vesicle-associated membrane protein-1 (Vamp-1) contains a mitochondrial targeting signal. Molecular Biology of the Cell 9, 1649-1660.

Ito, K., Komazaki, S., Sasamoto, K., Yoshida, M., Nishi, M. and Kitamura, K. (2001). Deficiency of triad junction and contraction in mutant skeletal muscle lacking junctophilin type I. Journal of Cell Biology 154, 1059-1067.

Johnson, A.E. and van Waes, M.A. (1999). The translocon: a dynamic gateway at the ER membrane. Annual Review in Cell and Developmental Biology 15, 799-842.

Joshi, H.C., Palacios, M.J., McNamara, L. and Cleveland, D.W. (1992). Gamma-tubulin is a centrosomal protein required for cell cycle-dependent microtubule nucleation. Nature

356, 80-83.

Jorgensen, A.O., Broderick, R., Somlyo, A.P. and Somlyo, A.V. (1988). Two structurally distinct calcium storage sites in rat cardiac sarcoplasmic reticulum: an electron microprobe analysis study. Circulation Research 63, 1060-1069.

Kamp, T.J. and Hell, J.W. (2000). Regulation of cardiac L-type calcium channels by protein kinase A and protein kinase C. Circulation Research 87, 1095-1102.

Kanaji, S., Iwahashi, H., Kida, Y., Sakaguchi, M. and Mihara, K. (2000). Characterization of the signal that directs Tom20 to the mitochondrial outer membrane. Journal of Cell Biology 151, 277-288.

Karsenti, E. (1991). Mitotic spindle morphogenesis in animal cells. Seminars in Cell Biology 2, 251-260.

Katz, A.M. and Katz, P.B. (1989). Homogeneity out of heterogeneity. Circulation 79, 712-717.

Katz, A.M. (2001). In: Physiology of the Heart. Third Edition. Lippincott Williams and Wilkins. New York.

Kaufman, M.H. and Navaratnam, V. (1981). Early differentiation of the heart in mouse embryos. Journal of Anatomy 133, 235-246.

Kaufmann, U., Kirsch, M., Irintchev, A., Wernig, A. and Starzinksi-Powitz, A. (1999). The M-cadherin catenin complex interacts with microtubules in skeletal muscle cells: implications for the fusion of myoblasts. Journal of Cell Science 112, 55-67.

Keating, T.J., and Borisy, G.G. (2000). Immunostructural evidence for the template mechanism of microtubule nucleation. Nature Cell Biology 2, 352-357.

Khodjakov, A. and Rieder, C.L. (1999). The sudden recruitment of gamma-tubulin to the centrosome at the onset of mitosis and its dynamic exchange throughout the cell cycle, do not require microtubules. Journal of Cell Biology 146, 585-896.

Klein, P., Kanehisa, M. and DeLisi, C. (1985). The detection and classification of membrane-spanning proteins. Biochimica Biophysica Acta 815, 468-476.

Komazaki, S., Ito, K., Takeshima, H. and Nakamura, H. (2002). Deficiency of triad formation in developing skeletal muscle cells lacking junctophilin type 1. FEBS Letters 524, 225-229.

Komazaki, S., Nishi, M. and Takeshima, H. (2003). Abnormal junctional membrane structures in cardiac myocytes expressing ectopic junctophilin type I. FEBS Letters 542, 69-73.

Kontrogianni-Konstantopoulos, A., Jones, E.M., van Rossum, D.B. and Block, R.J. (2003). Obscurin is a ligand for small ankyrin 1 in skeletal muscle. Molecular Biology of the Cell 14, 1139-1148.

Kostin, S., Scholz, D., Shimada, T., Maeno, Y., Mollnau, H., Hein, S. and Schaper, J. (1998). The internal and external protein scaffold of the T-tubular system in cardiomyocytes. Cell and Tissue Research 294, 449-460.

Kramer, A. and Ho A.D. (2001). Centrosome aberrations and cancer. Onkologie 24, 538-544.

Kuch, C., Winnekendonk, D., Butz, S., Unvericht, U., Kemier, R. and Starzinski-Powitz, A. (1997). M-cadherin-mediated cell adhesion and complex formation with the catenins in myogenic mouse cells. Experimental Cell Research 232, 331-338.

Kuo, H., Chen, J., Ruiz-Lozano, P., Zou, Y., Nemer, M. and Chien, K.R. (1999). Control of segmental expression of the cardiac-restricted ankyrin repeat protein gene by distinct regulatory pathways in murine cardiogenesis. Development 126, 4223-4234.

Kuriyama, R. and Borisy G.G. (1981). Centriole cycle in Chinese hamster ovary cells as determined by whole-mount electron microscopy. Journal of Cell Biology 91, 814-821.

Kuroda, R., Ikenoue, T., Honsho, M., Tsujimoto, S., Mitoma, J.Y. and Ito, A., (1998). Charged amino acids at the carboxyl-terminal portions determine the intracellular location of two isoforms of cytochrome b(5). Journal of Biological Chemistry 273, 31097-31102.

Kutay, U., Hartmann, E. and Rapoport, T.A. (1993). A class of membrane proteins with C-terminal anchor. Trends in Cell Biology 3, 72-75.

Kutay, U., Ahnert-Hilgen, C., Hartmann, E., Wiedenmann, B. and Rapoport, T.A. (1995). Transport routes for synaptobrevin via a novel pathway of insertion into the endoplasmic reticulum membrane. EMBO Journal 14, 224-231.

Landschulz, W.H., Johnson, P.F. and McKnight, S.L. (1988). The leucine zipper: a hypothetical structure common to a new class of DNA binding proteins. Science. 240, 1759-1764.

Lassar, A.B., Buskin, J.N., Lockshon, D., Davis, R.L., Apone, S., Hauschka, S.D. and Weintraub, H. (1989). MyoD is a sequence-specific DNA binding protein requiring a region of myc homology to bind to the muscle creatine kinase enhancer. Cell 58, 823-831.

Lassar, A.B., Skapek, S.X. and Novitch, A.F. (1994). Regulatory mechanisms that coordinate skeletal muscle differentiation and cell cycle withdrawal. Current Opinions in

Cell Biology 6, 788-794.

Lawson, K.A. and Pedersen, R.A. (1992). Clinical analysis of cell fate during gastrulation and early neurulation in the mouse. In: postimplantation Development in the Mouse (Civa Foundation Symposium Vol 165). Chichester: Wiley, 3-26.

Lee, Y., Shioi, T., Kasahara, H., Jobe, S.M., Wiese, R.J., Markham, B.E. and Izumo, S. (1998). The cardiac tissue-restricted homeobox protein Csx/Nkx2.5 physically associates with the zinc finger protein GATA4 and cooperatively activates atrial natriuetic factor gene expression. Molecular and Cellular Biology 18, 3120-3129.

Leong, P. and MacLennan, D.H. (1998a). The cytoplasmic loops between domains II and III and domains III and IV in the skeletal muscle dihydropyridine receptor bind to a contiguous site in the skeletal muscle ryanodine receptor. Journal of Biological Chemistry 273, 29958-29964.

Leong, P. and MacLennan, D.H. (1998b). A 37-amino acid sequence in the skeletal muscle ryanodine receptor interacts with the cytoplasmic loop between domains II and III in the skeletal muscle dihydropyridine receptor. Journal of Biological Chemistry 273, 7791-7794.

Li, J, Lee, G.I., Van Doren, S.R. and Walker, J.C. (2000). The FHA domain mediates phosphoprotein interactions. Journal of Cell Science 113, 4143-4149.

Li, Q., Hansen, D., Killilea, A., Joshi, H.C., Palazzo, R.E. and Balczon, R. (2001). Kendrin/pericentrin-B, a centrosome protein with homology to pericentrin that complexes with PCM-1. Journal of Cell Science 114, 797-809.

Lints, T.J., Parsons, L.M., Hartley, I., Lyons, I. and Harvey, R.P. (1993). Nkx2.5: a novel murine homeobox gene expressed in the early heart progenitor cells and their myogenic descendents. Development 119, 419-431.

Lompre, A.M., Anger, M. and Levitsky, D. (1994). Sarco(endo)plasmic reticulum calcium pumps in the cardiovascular system: function and gene expression. Journal of Molecular and Cellular Cardiology 26, 1109-1121.

Luna, E.J. and Hitt, A.L. (1992). Cytoskeleton-plasma membrane interactions. Science 258, 955-964.

Lupas, A. (1996). Prediction and analysis of coiled-coil structures. Methods in Enzymology 266, 513-525.

Lu, X., Xu, L. and Meissner, G. (1994). Activation of the skeletal muscle calcium release channel by a cytoplasmic loop of the dihydropyridine receptor. Journal of Biological Chemistry 269, 6511-6516.

Lyons, I., Parsons, L.M., Hartely, L., Li, R., Andrews, J.E., Robb, L. and Harvey, R.P. (1995). Myogenic and morphogenic defects in the heart tubes of murine embryos lacking the homeobox gene, Nkx2.5. Genes and Development 9, 1654-1666.

Lyons, G.E. (1996). Vertebrate heart development. Current Opinions in Genetic Development 6, 454-460.

Lytton, J., Zarain-Herzberg, A., Periasamy, M. and MacLennan, D.H. (1989). Molecular cloning of the mammalian smooth muscle sarco(endo)plasmic reticulum Ca^{+2}ATPase. Journal of Biological Chemistry 264, 7059-7065.

Lytton, J., Westlin, M., Burk, S.E., Shull, G.E. and MacLennan, D.H. (1992). Functional comparisons between isoforms of the sarcoplasmic or endoplasmic reticulum family of calcium pumps. Journal of Biological Chemistry 267, 14483-14489.

Mack, G.J., Rees, J., Sandlom, O., Balczon, R., Fritzler, M.J. and Rattner, J.B. (1998). Autoantibodies to a group of centrosomal proteins in human autoimmune sera reactive with the centrosomes. Arthritis and Rheumatism 41, 551-558.

Mahony, L. and Jones, L.R. (1986). Developmental changes in cardiac sarcoplasmic reticulum in sheep. Journal of Biological Chemistry 216, 15257-15265

Marks, A.R., Tempst, P., Hwang, K.S., Taubman, M.B., Inui, M., Chadwick, C., Fleischer, S. and Nadal-Ginard, B. (1989). Molecular cloning and characterization of the ryanodine receptor / junctional channel complex DNA from skeletal muscle sarcoplasmic reticulum. Proceedings of the National Academy of Science U.S.A. 86, 8683-8687.

Marks, A.R., Marx, S.O. and Reiken, S. (2002). Regulation of ryanodine receptors via macromolecular complexes: a novel role for leucine/isoleucine zippers. Trends in Cardiovascular Medicine 12, 166-170.

Martonosi, A.N. (2000). In: The Development of Sarcoplasmic Reticulum. Harwood Academic Publishers Canada.

Marx, S.O., Reiken, S., Hisamatsu, Y., Jayaraman, T., Burkhoff, D., Rosemblit, N. and Marks, A.R. (2000). PKA phosphorylation dissociates FKBP12.6 from the calcium release channel (ryanodine receptor): defective regulation in failing hearts. Cell 101, 365-376

Marx, S.O., Reiken, S., Hisamatsu, Y., Gaburjakova, M., Gaburjakova, J., Yang, Y.M., Rosemblit, N. and Marks, A.R. (2001). Phosphorylation-dependent regulation of ryanodine receptors: a novel role for leucine/isoleucine zippers. Journal of Cell Biology 153, 699-708.

Marziali, G., Rossi, D., Giannini, G., Charlesworth, A. and Sorrentino, V. (1996). cDNA cloning reveals a tissue specific expression of alternatively spliced transcripts of the

ryanodine receptor type 3 (RyR3) calcium release channel. FEBS Letters 394, 76-82.

Matlack, K.E., Mothes, W. and Rapoport, T.A. (1998). Protein translocation: tunnel vision. Cell 92, 381-390.

Mayer, B.J. and Baltimore, D. (1994). Mutagenic analysis of the roles of SH2 and SH3 domains in regulation of the Abl tyrosine kinase. Molecular and Cellular Biology 14, 2883-2894.

Mayor, T., Meraldi, P., Stierhof, Y.D., Nigg, E.A. and Fry, A.M. (1999). Protein kinases in control of the centrosome cycle. FEBS Letters 452, 92-95.

Mayor, T., Hacker, U., Stierhof, Y.D. and Nigg, E.A. (2002). The mechanism regulating the dissociation of the centrosomal protein C-Nap1 from mitotic spindle poles. Journal of Cell Science 115, 3275-3284.

Meacock, S.L., Greenfield, J.J. and High, S. (2000). Protein targeting and translocation at the endoplasmic reticulum membrane--through the eye of a needle? Essays in Biochemistry 36, 1-13.

Miner, J.H. and Wold, B. (1990). Herculin, a fourth member of the MyoD family of myogenic regulatory genes. Proceedings of the National Academy of Science U.S.A. 87, 1089-1093.

Miyagishi, M. and Taira, K. (2002). U6 promoter-driven siRNAs with four uridine 3' overhangs efficiently suppress targeted gene expression in mammalian cells. Nature Biotechnology 20, 497-500.

Molkentin, J.D., Lin, Q., Duncan, S.A. and Olson, E.N. (1997). Requirement of the transcription factor GATA4 for heart tube formation and ventral morphogenesis. Genes and Development 11, 1061-1072.

Moritz, M., Braunfeld, M.B., Guenebaut, V., Heuser, J. and Agard, D.A. (2000). Structure of the γ-tubulin ring complex: a template for microtubule nucleation. Nature Cell Biology 2, 365-370.

Murphy, S.M., Urbani, L. and Stearns, T. (1998). The mammalian gamma-tubulin complex contains homologues of the yeast spindle pole body components spc97p and spc98p. Journal of Cell Biology 141, 663-674.

Nabeshima, Y., Hanaoka, K., Hayasaka, M., Esumi, E., Li, S., Nanaka, I. and Nabeshima, Y. (1993). Myogenin gene disruption results in perinatal lethality because of severe muscle defect. Nature 364, 532-535.

Nakai, K. and Kanehisa, M.A. (1992). A knowledge base for predicting protein localization sites in eukaryotic cells. Genomics 14, 897-911.

Nemer, G. and Nemer, M. (2001). Regulation of heart development and function through combinatorial interactions of transcription factors. Annals of Medicine 33, 604-610.

Newey, S.E., Howman, E.V., Ponting, C.P., Benson, M.A., Nawrotzki, R., Loh, R.U., Davies, K.E. and Blake, D.J. (2001). Syncoilin, a novel member of the intermediate filament superfamily that interacts with alpha-dystrobrevin in skeletal muscle. Journal of Biological Chemistry 276, 6645-6655.

Nigg, E.A. (2002). Centrosome aberrations: cause or consequence of cancer progression? Nature Reviews Cancer 2, 815-825.

Noda, M., Ikeda, T., Suzuki, H., Takeshima, H., Takahashi, T., Kuno, M. and Numa, S. (1986). Expression of functional sodium channels from cloned cDNA. Nature 322, 826-828.

Nomura, T., Sakai, N., Sarai, A., Sudo, T., Kanei-Ishii, C., Ramsay. R.G., Favier, D. Gonda, T.J. and Ishii, S. (1993). Negative autoregulation of c-Myb activity by homodimer formation through the leucine zipper. Journal of Biological Chemistry 268, 21914-21923.

Olson, E.N. and Srivastava, D. (1996). Molecular pathways controlling heart development. Science 272, 671-676.

Opie, L.H., (1991). The heart: physiology and metabolism. Second Edition. Raven Press Ltd. New York.

Otsu, K., Willard, H.F., Khanna, V.K., Zorzato, F., Green, N.M. and MacLennan, D.H. (1990). Molecular cloning of cDNA encoding the Ca^{2+} release channel (ryanodine receptor) of rabbit cardiac muscle sarcoplasmic reticulum. Journal of Biological Chemistry 265, 13472-13483.

Paululat, A., Holz, A. and Renkawitz-Pohl, R. (1999). Essential genes for myoblast fusion in Drosophila embryogenesis. Mechanisms in Development 83, 17-26.

Peachey, L.D. and Franzini-Armstrong, C. (1983). Structure and function of membrane systems of skeletal muscle cells. In: Handbook of Physiology Section 10. Skeletal Muscle. (Peachey,L.D., Adrian, R.H. and Geiger, S.R., eds.) American Physiological Society Bethesda, pp. 23-71.

Pennington. S.R., Wilkins, M.R., Hochstrasser. D.F. and Dunn, M.J. (1997). Proteome analysis: from protein characterization to biological function. Trends in Cell Biology 7, 168-173.

Piel, M., Nordberg, J., Euteneuer, U. and Bornens, M. (2001). Centrosome-dependent exit of cytokinesis in animal cells. Science 291, 1550-1553.

Poirier, M.A., Xiao, W., Macosko, J.C., Chan, C., Shin, Y.K. and Bennett, M.K. (1998). The synaptic SNARE complex is a parallel four-stranded helical bundle. Nature Structural Biology 5, 765-769.

Porter, K.R. and Palade, G.E. (1957). Studies on the endoplasmic reticulum. III Its form and distribution in striated muscle cells. Journal of Biophysical Biochemistry and Cytology 3, 269-300.

Pozzan, T., Rizzuto, R., Volpe, P. and Meldolesi, J. (1994). Molecular and cellular physiology of intracellular calcium stores. Physiological Reviews 74, 595-636.

Purohit, A., Tynan, S.H., Vallee, R. and Doxsey, S.J. (1999). Direct interaction of pericentrin with cytoplasmic dynein light intermediate chain contributes to mitotic spindle organization. Journal of Cell Biology 147, 481-492.

Rawls, A., Valdez, M.R., Zhang, W., Richardson, J., Klein, W.H. and Olson, E.N. (1998). Overlapping functions of the myogenic bHLH genes MRF4 and MyoD revealed in double mutant mice. Development 125, 2349-2358.

Rhodes, S.J. and Konieczny, S.F. (1989). Identification of MRF4: a new member of the muscle regulatory factor gene family. Genes and Development 3, 2050-2061.

Robbins, E., Jentzsch, G. and Micali, A. (1968). The centriole cycle in synchronized HeLa cells. Journal of Cell Biology 36, 329-339.

Robertson, T.A., Grounds, M.D., Mitchell, C.A. and Papadimitriou J.M. (1990). Fusion between myogenic cells in vivo: an ultrastructural study in regenerating murine skeletal muscle. Journal of Structural Biology 105, 170-182.

Rosenquist, G. and DeHaan, R.L. (1966). Migration of precardiac cells in the chick embryo: a radioautographic study. Carnegie Inst. Wash. Contrib. Embryology. 38, 111-121.

Rudnicki, M.A., Schnegelsberg, P.N., Stead, R.H., Braun, T. Arnold, H.H. and Jaenisch, R. (1993). MyoD or Myf-5 is required for the formation of skeletal muscle. Cell 75, 1351-1359.

Rugh, R. (1968). Normal Development. In: the Mouse. Its Reproduction and Development. Minneapolis: Burgess Publishing Company 91-101.

Sabourin, L.A. and Rudnicki, M.A. (2000). The molecular regulation of myogenesis. Clinical Genetics 57, 16-25.

Sadoulet-Puccio, H.M., Rajala, M., and Kunkel, L.M. (1997). Dystrobrevin and dystrophin: an interaction through coiled-coil motifs. Proceedings of the National

Academy of Science U.S.A. 94, 12413-12418.

Salisbury, J.L., Whitehead, C.M., Lingle, W.L. and Barrett, S.L. (1999). Centrosomes and cancer. Biology of the Cell 91, 451-460.

Sapperstein, S.K., Lupashin, V.V., Schmitt, H.D. and Waters, M.G. (1996). Assembly of the ER to golgi SNARE complex requires uso1p. Journal of Cell Biology 132, 755-767.

Schultheiss, T.M., Zydas, S. and Lassar, A.B. (1995). Induction of avian cardiac myogenesis by anterior endoderm. Development 121, 4203-4214.

Scoote, M. and Williams, A.J. (2002). The cardiac ryanodine receptor (calcium release channel): emerging role in heart failure and arrhythmia pathogenesis. Cardiovascular Research 56, 359-372.

Sillibourne, J.E., Milne, D.M., Takahashi, M., Ono, Y. and Meek, D.W. (2002). Centrosomal anchoring of the protein kinase CK1delta mediated by attachment to the large, coiled-coil scaffolding protein CG-NAP/AKAP450. Journal of Molecular Biology 322, 785-797.

Sommer, J.R. and Jennings, R.B. (1992). Ultrastructure of cardiac muscle. New York, NY: Raven Press.

Srivastava, D. and Olson, E.N. (2000). A genetic blueprint for cardiac development. Nature 407, 221-226.

Stearns, T. and Kirschner, M. (1994). In vitro reconstitution of centrosome assembly and function: the central role of gamma-tubulin. Cell 76, 623-637.

Suda, N., Franzius, D., Fleig, A., Nishimura, S., Bodding, M., Hoth, M., Takeshima, H. and Penner, R. (1997). Ca^{2+}-induced Ca^{2+} release in Chinese hamster ovary (CHO) cells co-expressing dihydropyridine and ryanodine receptors. Journal of General Physiology 109, 619-631.

Sueishi, M., Takagi, M. and Yoneda, Y. (2000). The Forkhead-associated domain of Ki-67 antigen interacts with the novel kinesin-like protein Hklp2. Journal of Biological Chemistry 275, 28888-28892.

Sun, X.H., Protasi, F., Takahashi, M., Takeshima, H., Ferguson, D.G. and Franzini-Armstrong, C. (1995). Molecular architecture of membranes involved in excitation-contraction coupling of cardiac muscle. Journal of Cell Biology 129, 659-671.

Sun Z, Hsiao J, Fay D.S. and Stern D.F. (1998). Rad53 FHA domain associated with phosphorylated Rad9 in the DNA damage checkpoint. Science 281, 272-274.

Sutton, R.B., Fasshauer, D., Jahn, R. and Brunger, A.T. (1998). Crystal structure of a SNARE complex involved in synaptic exocytosis at 2.4 A resolution. Nature 395, 347-353.

Tada, M., Yamamoto, T. and Tonomura. Y. (1978). Molecular mechanism of active calcium transport by sarcoplasmic reticulum. Physiological Reviews 58, 1-79

Takahashi, M., Shibata, H., Shimakawa, M., Miyamoto, M., Mukai, H., and Ono, Y. (1999). Characterization of a novel giant scaffolding protein, CG-NAP that anchors multiple signaling enzymes to centrosomes and the Golgi apparatus. Journal of Biological Chemistry 274, 17267-17274.

Takahashi, M., Yamagiwa, A., Nishimura. T., Mukai, H. and Ono, Y. (2002). Centrosomal proteins CG-NAP and kendrin provide microtubule nucleation sites by anchoring γ-tubulin ring complex. Molecular Biology of the Cell 13, 3235-3245.

Takekura, H., Sun, X. and Franzini-Armstrong, C. (1994a). Development of excitation-contraction coupling apparatus in skeletal muscle: peripheral and internal calcium release units are formed sequentially. Journal of Muscle Research and Cell Motility 15, 102-118.

Takekura, H., Bennett, L, Tanabe, T., Beam, K.G. and Franzini-Armstrong, C. (1994b). Restoration of junctional tetrads in dysgenic myotubes by dihydropyridine receptor cDNA. Biophysical Journal 67, 793-803.

Takekura, H., Takeshima, H., Nishimura, S., Takahashi, M., Tanabe, T., Flockerzi, V., Hofmann, F. and Franzini-Armstrong, C. (1995). Co-expression in CHO cells of two muscle proteins involved in excitation-contraction coupling. Journal of Muscle Research and Cell Motility 16, 465-480.

Takekura, H., Flucher, B.E. and Franzini-Armstrong, C. (2001). Sequential docking, molecular differentiation and positioning of T-Tubule / SR junctions in developing mouse skeletal muscle. Developmental Biology 239, 204-214.

Takeshima, H., Nishimura, S., Matsumoto, T., Ishida, H., Kangawa, K., Minamino, N., Matsuo, H., Ueda, M., Hanaoka, M., Hirose, T. and Numa, S. (1989). Primary structure and expression from the complementary cDNA of skeletal muscle ryanodine receptor. Nature 339, 439-445.

Takeshima, Hl, Komazaki, S., Nishi, M., Iino, M. and Kangawa, K. (2000). Junctophilins: a novel family of junctional membrane complex proteins. Molecular Cell. 6, 11-22.

Tanaka, M., Chen, Z., Bartunkova, S., Yamasaki, N. and Izumo, S. (1999). The cardiac homeobox gene Csx/Nkx2.5 lies genetically upstream of multiple genes essential for heart development. Development 126, 1269-1280.

Tanabe, T., Beam, K.G., Powell, I.A. and Numa, S. (1988). Restoration of excitation-contraction coupling and slow calcium current in dysgenic muscle by dihydropyridine receptor complementary DNA. Nature 336. 134-130.

Tanabe, T., Mikami, A., Numa, S. and Beam, K.G. (1990). Cardiac-type excitation-contraction coupling in dysgenic skeletal muscle injected with cardiac dihydropyridine receptor cDNA. Nature 344, 451-453.

Tarroni, P., Rossi, D., Conti, A. and Sorrentino, V. (1997). Expression of the ryanodine receptor type 3 calcium release channel during development and differentiation of mammalian skeletal muscle cells. Journal of Biological Chemistry 272, 19808-19813.

Taylor, M.V. (2000). Muscle development: molecules of myoblast fusion. Current Biology 10, R646-R648.

Taylor, M.V. (2002). Muscle differentiation: how two cells become one. Current Biology 12, R224-R228.

Tuffanelli, D.L., McKeon, F., Kleinsmith, D.M., Burnham, T.K. and Kirschner, M. (1983). Anti-centrosome and anti-centriole antibodies in the scleroderma spectrum. Archives in Dermatology 119, 560-566.

Valdez, M.R., Richardson, J.A., Klein,W.H. and Olson, E.N. (2000). Failure of Myf5 to support myogenic differentiation without myogenin, MyoD, and MRF4. Developmental Biology 219, 287-298.

Vandre, D.D., Davis, F.M., Rao, P.N. and Borisy G.G. (1984). Phosphoproteins are components of mitotic organizing centers. Proceedings of the National Academy of Science U.S.A. 81, 4439-4443.

van Veen, A.A., van Rijen, H.V, and Opthof, T. (2001). Cardiac gap junction channels: modulation of expression and channel properties. Cardiovascular Research 51, 217-229.

Wakelam, M.J. (1985). The fusion of myoblasts. Biochemical Journal 228, 1-12.

Walker, S.M, Schrodt, G.R., and Bingham, M. (1968). Electron microscope study of the sarcoplasmic reticulum at the Z-line level in skeletal muscle fibers of newborn rats. Journal of Cell Biology 39, 469-475.

Walsh, K. and Perlman, H. (1997). Cell cycle exit upon myogenic differentiation. Current Opinions in Genetic Development 7, 597-602.

Walter, P. and Johnson, A.E. (1994). Signal sequence recognition and protein targeting to the endoplasmic reticulum membrane. Annual Review in Cell Biology 10, 87-119.

Wattenberg, G., and Lithgow, T. (2001). Targeting of C-terminal (Tail)-anchored

proteins: understanding how cytoplasmic activities are anchored to intracellular membranes. Traffic 2, 66-71.

Weise, C. and Zheng, Y. (2000). A new function for the gamma-tubulin ring complex as a microtubule minus-end cap. Nature Cell Biology 2, 358-364.

Whitehead, C.M. and Salisbury, J.L. (1999). Regulation and regulatory activities of centrosomes. Journal of Cellular Biochemistry Supplements 32-33, 192-199.

Wielowieyski, P.A, Sevinc, S., Guzzo, R., Salih, M., Wigle, J.T. and Tuana, B.S. (2000). Alternative splicing, expression, and genomic structure of the 3' region of the gene encoding the sarcolemmal-associated proteins (SLAPs) defines a novel class of coiled-coil tail-anchored membrane proteins. Journal of Biological Chemistry 275, 38474-38481.

Wier, W.G. and Balke, C.W. (1999). Ca^{2+} release mechanisms, Ca^{2+} sparks and local control of excitation-contraction coupling in normal heart muscle. Circulation Research 85, 770-776.

Wigge, P.A., Jensen, O.N., Holmes, S., Soues, S., Mann, M. and Kilmartin, J.V. (1998). Analysis of the Saccharomyces spindle poles by matrix-assisted laser absorption/ionization (MALDI) mass spectrometry. Journal of Cell Biology 141, 967-977.

Wigle, J.T., Demchyshyn, L., Pratt, M.A., Staines, W.A., Salih, M. and Tuana, B.S. (1997). Molecular cloning, expression, and chromosomal assignment of sarcolemmal-associated proteins. A family of acidic amphipathic alpha-helical proteins associated with the membrane. Journal of Biological Chemistry 272, 32384-32394.

Wittmann, T., Boleti, H., Antony, C., Karsenti, E. and Vernos, I. (1998). Localization of the kinesin-like protein Xklp2 to spindle poles requires a leucine zipper, a microtubule-associated protein, and dynein. Journal of Cell Biology 143, 673-685.

Wright, W.E., Sassoon, D.A. and Lin, V.K. (1989). Myogenin, a factor regulating myogenesis, has a domain homologous to MyoD. Cell 56, 607-617.

Young, A, Dictenberg, J.B., Purohit, A., Tuft, R. and Doxsey, S.J. (2000). Cytoplasmic dynein mediated assembly of pericentrin and γ-tubulin onto centrosomes. Molecular Biology of the Cell 11, 2047-2056.

Yu, J.Y., DeRuiter, S.L. and Turner, D.L. (2002). RNA interference by expression of short-interfering RNAs and hairpin RNAs in mammalian cells. Proceeding of the National Academy of Science U.S.A. 99, 6047-6052.

Zaffran, S. and Frasch, M. (2002). Early signals in cardiac development. Circulation Research 91, 457-469.

Zarain-Herzberg, A., MacLennan, D.H. and Periasamy, M. (1990). Characterization of rabbit cardiac sarco(endo)plasmic reticulum Ca^{+2}ATPase gene. Journal of Biological Chemistry 264, 4670-4677.

Zeschnigk, M., Kozian, D., Kuch, C., Schmoll, M. and Starzinski-Powitz, A. (1995). Involvement of M-cadherin in fusion and terminal differentiation of myogenic cells. Journal of Cell Science 108, 2973-2981.

Zhang, L, Kelley, J., Schmeisser, G., Kobayashi, Y.M. and Jones, L.R. (1997). Complex formation between junction, triadin, calsequestrin and the ryanodine receptor. Proteins of the cardiac junctional sarcoplasmic reticulum membrane. Journal of Biological Chemistry 272, 23389-23397.

Zheng, Y., Wong, M.L., Alberts, B. and Mitchison, T. (1995). Nucleation of microtubule assembly by a γ-tubulin-containing ring complex. Nature 378, 578-583.

Zorzato, F., Fujii, J., Otsu, K., Phillips, M., Green, N.M., Lai, F.A., Meissner, G. and MacLennan, D.H. (1990). Molecular cloning of cDNA encoding human and rabbit forms of the Ca^{+2} release channel (ryanodine receptor) of skeletal muscle sarcoplasmic reticulum. Journal of Biological Chemistry 265, 2244-2256.

Chapter Eight.

Appendix.

Wielowieyski, P.A, Sevinc, S., Guzzo, R., Salih, M., Wigle, J.T. and Tuana, B.S. (2000). Alternative Splicing, Expression, and Genomic Structure of the 3' Region of the Gene Encoding the Sarcolemmal-associated Proteins (SLAPs) Defines a Novel Class of Coiled-coil Tail-anchored Membrane Proteins. Journal of Biological Chemistry 275, 38474-38481.

Immunocytochemistry studies, microscopy, biochemical fractionations and immunoblot analysis were performed by R. Guzzo.

Department of Cellular and Molecular Medicine
University of Ottawa
451 Smyth Road
Ottawa, ON
K1H 8M5

June 19, 2003

RE: PERMISSIONS

This fax is to request copyright permission to include the following article, in its full form, as an appendix to my Ph.D. thesis:

Paul A. Wielowieyski, Serdal Sevinc, Rosa Guzzo, Maysoon Salih, Jeffrey T. Wigle and Balwant S. Tuana.

Alternative Splicing, Expression and Genomic Structure of the 3' Region of the Gene Encoding the Sarcolemmal-associated Proteins (SLAPs) Defines a Novel Class of Coiled-Coil Tail-anchored membrane proteins.

Journal of Biological Chemistry, Dec 2000;

I would appreciate your response by fax at Please contact me at e if there are any questions regarding this request.

Thank you.

Sincerely

PERMISSION GRANTED

for the copyright owner JUN 20 2003
THE AMERICAN SOCIETY FOR BIOCHEMISTRY
& MOLECULAR BIOLOGY

THE JOURNAL OF BIOLOGICAL CHEMISTRY
Vol. 275, No. 49, Issue of December 8, pp. 38474–38481, 2000
Printed in U.S.A.

Alternative Splicing, Expression, and Genomic Structure of the 3′ Region of the Gene Encoding the Sarcolemmal-associated Proteins (SLAPs) Defines a Novel Class of Coiled-coil Tail-anchored Membrane Proteins*

Received for publication, August 23, 2000
Published, JBC Papers in Press, September 13, 2000, DOI 10.1074/jbc.M007682200

Paul A. Wielowieyski, Serdal Sevinc, Rosa Guzzo, Maysoon Salih, Jeffrey T. Wigle, and Balwant S. Tuana‡

From the Department of Cellular and Molecular Medicine, University of Ottawa, 451 Smyth Road, Ottawa, Ontario K1H 8M5, Canada

The sarcolemmal associated proteins (SLAPs) are encoded by multiple mRNAs that are presumably generated by alternative splicing mechanisms. The amino acid sequence of the SLAP1 isoform exhibited 76% identity with TOP_{AP}, a topographically graded antigen of the chick visual system. The regions of coiled-coil structure including an 11-heptad acidic amphipathic α-helical segment was conserved with a major divergence in sequence noted in the hydrophobic C termini predicted to be transmembrane domains in the two polypeptides. The genomic organization of the 3′ region of the *SLAP* gene indicated that SLAP1 and TOP_{AP} are generated by alternative splicing mechanisms, which are conserved among mammalian and avian species. SLAP1/TOP_{AP} were encoded by 11 exons distributed over a minimum of 35 kilobase pairs of continuous DNA; 9 of the exons were constitutively expressed, and 2 were alternatively spliced. The exons range in size from 60 to 321 base pairs, and the predicted functional domains within the polypeptides were encompassed by single exons. The introns vary from 0.2 to 10 kilobase pairs and conform to consensus dinucleotide splicing signals. Reverse transcriptase-polymerase chain reaction studies demonstrated that alternative exons (IV and X) of SLAP were expressed in a tissue-specific fashion and developmentally regulated. The alternatively spliced exon X, which encodes the putative transmembrane anchor in TOP_{AP}, and a constitutively expressed exon XI, which encodes the putative transmembrane domain in SLAP, were found to target these polypeptides to membrane structures. The presence and conservation of termination codons in exons X and XI render expression of the two SLAP1/TOP_{AP} transmembrane domains mutually exclusive. These data reveal that TOP_{AP} and SLAP are alternatively spliced products of a single gene that encodes a unique class of tail-anchored membrane proteins.

The coiled-coil membrane proteins such as syntaxin, synaptobrevin, and epimorphin are believed to play diverse roles in cell function including membrane fusion, vesicle transport, and neurotransmitter release (1–4). These polypeptides belong to a growing family of membrane proteins that lack a signal sequence and are anchored in the membrane by a hydrophobic segment at the C terminus (5). These tail-anchored proteins can be found at the plasma membrane as well as on intracellular membrane compartments, and evidence suggests that gene families as well as alternative splicing mechanisms may generate products with distinct hydrophobic C-terminal peptides that determine subcellular localizations and hence function (6, 7). The membrane insertion of these polypeptides is believed to be achieved by unique mechanisms that do not require the signal recognition particle (8). An important feature in these polypeptides is an extended coiled-coil structure, believed to be important for their intermolecular interactions (9–11). We have previously defined the cloning of a series of cDNAs that encode polypeptides, which were found to be associated with cardiac membranes, referred to as SLAPs[1] (for sarcolemmal-associated proteins (12)). Three different SLAP transcripts expressed in cardiac tissue were found to contain unique 5′ and common 3′ sequences that encode three SLAP polypeptides (37-kDa SLAP1, 46-kDa SLAP2, and 74-kDa SLAP3). The most noticeable structural features of SLAPs include their predicted ability to form an extended coiled coil over most of their length and a putative transmembrane domain at the extreme C terminus, although there was no consensus signal sequence (12). Our previous studies indicate that SLAPs are integral membrane proteins that localize to the cell membrane as well as intracellular membranes, but it is not known whether the putative transmembrane domain found in the SLAPs is responsible for their membrane integration (12).

Although we do not know the physiological role of the SLAPs, the proteins share common core features with the tail-anchored membrane proteins and hence may play important roles in membrane biology. In this regard, homology searches of the GenBank™ data base revealed that the SLAP1 isoform shares high nucleotide and amino acid sequence identity with TOP_{AP}, a topographically graded antigen of the chick visual system implicated in the neuronal guidance and development of the chick retinotectal map (13). The molecular properties of TOP_{AP} reveal that it is a 35-kDa coiled-coil protein with a putative transmembrane domain at the C terminus, which is believed to be localized at the cell membrane. There was strong identity (76% at the amino acid level) between avian TOP_{AP} and the 37-kDa SLAP1 isoform over most of the coding region, with the differences noted in the predicted transmembrane domains in the two polypeptides. This finding led us to hypothesize that

* This work was supported by a grant from the Heart and Stroke Foundation of Ontario (to B. S. T.). The costs of publication of this article were defrayed in part by the payment of page charges. This article must therefore be hereby marked "*advertisement*" in accordance with 18 U.S.C. Section 1734 solely to indicate this fact.

‡ To whom correspondence should be addressed. Tel.: 613-562-5800 ext. 8355; Fax 613-562-5434; E-mail:BTUANA@UOTTAWA.CA.

[1] The abbreviations used are: SLAP, sarcolemmal-associated protein; TOP_{AP}, topographically graded antigen of the chick visual system; RT-PCR, reverse transcriptase-polymerase chain reaction; TM, transmembrane; bp, base pairs; nt, nucleotide(s).

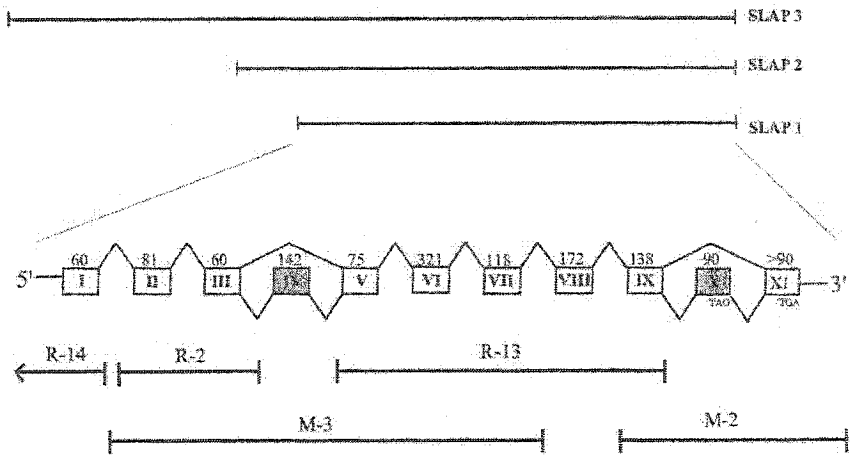

FIG. 1. **Genomic organization of the 3′ region of the *SLAP* gene.** Rabbit and mouse genomic λ DashII DNA libraries were screened with two ^{32}P-radiolabeled SLAP cDNA probes (U21157; nt 1607–1931 and 1–3017) to isolate five positive genomic clones (R-2, R-13, and R-14 from rabbit and M-2 and M-3 from mouse).The DNA was isolated, restriction mapped, and sequenced to elucidate the intron-exon junctions in both the rabbit and mouse *SLAP* genes. Characterization of genomic λ DASHII DNA clones revealed the presence of 11 exons that encode the common C-terminal core of the three isoforms (*SLAP1*, *SLAP2*, and *SLAP3*) (U21157; nt 1560–2675).

A

Exon No.	Exon Size bp	Exon	Intron No.	Intron Size kb	Intron Class	Exon	Exon No.
-	--	.....	1	>3.5	1	tctttggcagAGAAGCTGA	I
I	60	TTGCAAAAGgtcgttttct	2	>2.0	1	ctctctgtagAAAACCAGG	II
II	81	ACACTACGGgtgagtttta	3	0.2	1	cctctcgaagACGCCCAAA	III
III	60	TATTAAAAGgtactttcct	4	>5.0	1	tttttgtcagATGACTTGC	IV
IV	123	AACTTCAAGgtgagatgaa'	5	>3.0	1	ttatttttagCTCTTTTGG	V
V	75	TTCTTCAAGgtatgggaac	6	2.5	1	acttttgtagCCCAACTGC	VI
VI	321	GGCTGCAAGgtgaatgaac	7	0.5	1	actattttagGTGAATTAG	VII
VII	118	ATTGCACAAgtatgcaaga	8	5.0	2	tttgttgcagTTCTCAGAA	VIII
VIII	172	CAAAAAGAGgtaaagcgaa	9	5.5	0	ttgcctttagTATGAAAAG	IX
IX	138	AATAATAATgtaagtcttt	10	>2.0	0	ccttcttcagCCCTCCATA'	X
X	90	TAGAGAAAGgtacaagcac'	11	>1.6	0	ttccacacagAAACCCTGG'	XI
XI	>90	TCTCCATGA.....'	12			....3' UTR	
Consensus		$A_{64}G_{73}\|\|g_{100}t_{100}$.....$a_{100}g_{100}\|\|N$					

B

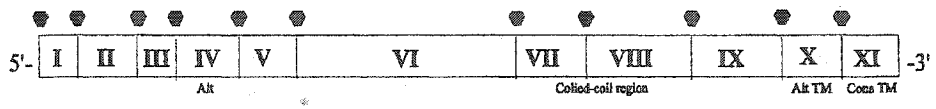

FIG. 2. **Exon/intron organization of the 3′ region of the *SLAP* gene.** *Panel A* summarizes the intron-exon junctions of the common functional core C terminus of SLAP isoforms. All of the exon-intron boundaries encompassing the common 3′ region of the *SLAP* gene conform to the consensus splice donor and acceptor sites (*gt-ag*) (15). *Panel B* is a graphic representation of the exon-exon boundaries of the common core C terminus of the *SLAP* gene. Exon IV encodes an alternative exon, exons VII and VIII encode coiled-coil motifs, and exons X and XI encode mutually exclusive transmembrane domains. ●, denotes conserved exon-exon boundaries between mouse and rabbit *SLAP* genes. All exon-exon boundaries and intron-exon junctions are conserved between rabbit and mouse genes.

avian TOP_{AP} and mammalian SLAP may be derived by alternative splicing mechanisms from a common gene. We therefore undertook studies to determine the genomic organization of the 3′ region of the *SLAP* gene, which revealed that mammalian SLAP1 and avian TOP_{AP} are generated by alternative splicing mechanisms that are highly conserved among mammalian and avian species. In addition, we report that the alternatively spliced products were expressed in a developmental and tissue-specific manner and the putative transmembrane domains were responsible for their membrane integration.

EXPERIMENTAL PROCEDURES

Isolation of Genomic Clones, Southern λ Blot Analysis, and Sequencing—The screening of the rabbit genomic λ DashII library (Stratagene) with a radiolabeled restriction fragment of SLAP3 cDNA (U21157; 324 nt *Ava*I-*Hin*dIII, 1607–1931) led to the isolation of three positive clones (R-2, R-13, R-14). A full-length SLAP3 cDNA probe, *Sal*I-EcoRI (nt 1–3017), was also used to screen a mouse genomic λ DashII library, and two additional clones (M-2 and M-3) were isolated. The genomic clones were digested with *Eco*RI, *Bam*HI, and *Kpn*I, resolved on agarose gels, and blotted onto MCI nylon membranes. The membranes were hybridized at 65 °C for 16 h, with *Ava*I-*Hin*dIII and *Sal*I-EcoRI cDNA radiolabeled probes in 10% polyethylene glycol, 7% SDS and 2.5× saline/sodium phosphate/EDTA. The membranes were then washed at 60 °C for 30 min and using intensifying screens were exposed to Kodak BioMax MR film at −70 °C for 16 to 24 h. The positive restriction fragments of the genomic λ clones were subcloned into pBlueScript KS (Stratagene) and sequenced. Mouse spleen and human cardiac cDNA libraries constructed in λZAP were screened with a *Sal*I-EcoRI restric-

```
      v         v         v         v         v         v         v         v
Rabbit AGAAGCTGATCGTGGAGGGGCATCTAACCAAAGTGGTAGAAGAAACAAAGCTTGCAAAAGAAAACCAGGC   70
Human  AGAAGCTGATCGTcGAaGGGCATCTAACCAAAGcGGTAGAAGAAACAAAGCTTtCAAAAGAAAAtCAGaC   70
Mouse  AGAAGCTGATgGTccAaGGGCATCTAACCAAAGTGGTAGAAGAAAtAAAGCTTtCAAAAGAAAAtCAGGC   70

Rabbit AAGAGCAAAGGAATCTGATTTATCAGATACTCTGAGTCCAAGCAAGGAAAAAAGCAGTGACGACACTACG  140
Human  AAGAGCAAAaGAATCTGATTTtTCAGATACTCTGAGTCCAAGCAAGGAAAAAAGCAGTGACGACACTACa  140
Mouse  AAaAGCAAAGGAATCcGAcTTATCAGAcACTCTGAGTCCAAGCAAGGAAAAAAGCAGcGACGACACTACa  140

Rabbit GACGCCCAAATGGATGAGCAAGACCTGAATGAATCTCTTGCTAAAGTGTCCCTATTAAAAG---------  201
Human  GACGCCCAAATGGATGAGCAAGACCTaAATGAgcCTCTTGCcAAAGTGTCCCTtTTAAAAGatgacttgc  210
Mouse  GACGCCCAgATGGATGAGCAAGACCTaAATGAAcCcCTTGCTAAgGTGTCtCTATTAAAAGatgacttac  210

Rabbit ----------                                                             201
Human  agggtgcacagtcagaaactgaggcaaaacaagaaattcagcatcttcgcaaggaattgatcgaagccca  280
Mouse  agggtacccagtcagaaactgaggccaaacaagacattcagcatcttcgcaaagaattggtggaagccca  280

Rabbit ----------------------------------------CTCTTTTGGAAGAAGAAAGAAAAGCC  227
Human  ggagctagctagagcaagtaaacaaaaatgctttgaacttcaagCTCTTTTGGAAGAAGAAAGAAAAGCC  350
Mouse  ggagctagctagaacaagtaaacaaaaatgctttgaacttcaagCTCTTTTGGAAGAAGAAcGAAAAGCC  350

Rabbit TATCGAAATCAAGTTGAGGAATCCAGTAAACAAATACAGGTTCTTCAAGCCCAACTGCAGAGGTTACACA  297
Human  TATCGAAATCAAGTTGAGGAATCCAcTAAACAAATACAGGTTCTTCAAGCCCAAtTGCAGAGGTTACACA  420
Mouse  TATCGAAATCAAGTTGAaGAATCagcTAAACAAATACAGGTTCTTCAAGtCCAgCTGCAGAaGTTACACA  420

Rabbit TGGACATTGAGAATCTCCGGGAGGAGAAGGACAATGAAATCACAAGCACTAGAGATGAATTGCTTAGTGC  367
Human  TcGAtAcTGAGAATCTCCGGGAGGAGAAGGACAgTGAAATCACAAGtACTAGAGATGAATTGCTTAGTGC  490
Mouse  TGGACATgGAGAATCTCCaGGAGGAaAAGGACAcgGAAATCtCcAGCACaAGAGATaAATTGCTTAGTGC  490

Rabbit CCGAGATGAAATTTTGCTCCTTCATCAAGCAGCAGAAAAGGCTGCCTCTGAGCGGGACACTGACATTGCT  437
Human  CCGAGATGAAATTTTGCTCCTTCATCAAGCAGCAGcAAAGGtTGCCTCTGAGCGGGACACTGACATTGCT  560
Mouse  CCaAGATGAgATTTTGCTCCTTCgTCAAGCAGCAGcAgAGGCTGtgTCTGAGCGGGACACTGACtTTGtT  560

Rabbit TCTTTGCAAGAAGAGCTTAAGAAGGTGAGAGCTGAGCTTGAGCGGTGGCGGAAAGCAGCATCTGAATATG  507
Human  TCTTTaCAAGAAGAGCTTAAGAAGGTGAGAGCTGAGCTTGAGCGGTGGCGGAAAGCAGCgTCTGAATATG  630
Mouse  TCTTTGCAAGAAGAGCTTAAGAAGGTcAGAGCgGAGCTTGAGgGcTGGaGGAAAGCAGCgTCTGAATAcG  630

Rabbit AGAAAGAAGTCACAAGTCTGCAGAGCAGTTTCCAGCTTCGGTGTCAGCAGTGTGAGGACCAGCAGAAAGA  577
Human  AGAAAGAAaTCACAAGTCTGCAaAaCAGTTTtCAGCTTaGaTGTCAaCAGTGTGAGGACCAGCAGAgAGA  700
Mouse  AGAAtGAAaTCAgAAGTCTGCAGAGCAGcTTCCAGCTTaGaTGTCAGCAGTGTGAaGACCAGCAaAggGA  700

Rabbit GGAAGCCACAAGGCTGCAAGGTGAATTAGAGAAGTTGAGAAAGGAATGGAATGTATTGGAAACCGAGTGC  647
Human  aGAAGCaACAAGGtTGCAAGGTGAAcTAGAGAAGTTGAGAAAGGAATGGAATGcATTGGAAACCGAaTGC  770
Mouse  GGAgGCaACAAGGtTGCAAGGTGAgcTgGAGAAGTTGAagAAGGgATGGgATGTAcTGGAAACgGAaTGC  770

Rabbit CATTCTCTAAAAAAGGAAAATGTCTTGTTATCATCAGAACTGCAACGACAGGAAAAAGAATTGCACAATT  717
Human  CATTCTCTAAAAAgGGAAAATGTtTTGcTATCATCAGAACTGCAACGgCAaGAAAAAGAATTGCACAATT  840
Mouse  CATTCTCTAAAAAAGGgAgAcGTgTTGTTgTCtTCAGAACTGCAgCGACAaGAgAAAGAATTGCACAATT  840

Rabbit CTCAGAAGCAGAGTTTAGAGCTTACCAGTGATCTCAGCATCCTTCAGATGACTAGGAAAGAGCTTGAGAA  787
Human  CTCAGAAGCAGAGTTTAGAGCTTACCAGTGATCTCAGCATCCTTCAaATGtCTAGGAAAGAaCTTGAGAA  910
Mouse  CTCAGAAGCAGAGTTTtGAaCTcACgAGTGAcCTCAGCATCCTTCAGATGACTAGGAAAGAGCTgGAGAA  910

Rabbit CCAAATGGGATCCTTGAAAGAACAGCATCTTCGTGATTCAGCTGATTTAAAAATTCTTCTCAGTAAGGCT  857
Human  tCAAgTGGGATCCTTGAAAGAACAGCATCTTCGgGATTCAGCTGATTTAAAAAcTCTTCTCAGTAAGGCa  980
Mouse  gCAAgTGGGATCCTTGAAAGAACAaCAcCTTCGgGATgCAGCTGAccTAAAAAcTCTcCTCAGTAAGGCT  980

Rabbit GAAAACCAAGCAAAGGATGTACAAAAAGAGTATGAAAAGACACAGACTGTACTCTCAGAACTGAAGTTGA  927
Human  GAAAACCAAGCAAAGGATGTgCAgAAAGAGTATGAAAAGACACAGACTGTACTCTCAGAACTGAAGTTGA 1050
Mouse  GAAAACCAAGCAAAGGATGTACAgAAAGAGTATGAAAAGACACAGACTGTtCTCTCAGAACTGAAGTTGA 1050

Rabbit AGTTTGAAATGACTGAGCAGGAAAAGCAATCAATCACAGATGAGCTCAAACAATGTAAAGACAACCTGAA  997
Human  AGTTTGAAATGACTGAGCAGGAAAAGCAgTCAATCACAGATGAGCTCAAACAgTGTAAAaACAACCTGAA 1120
Mouse  AGTTTGAAATGACTGAGCAGGAAAAGCAATCAATCACAGATGAGCTCAAACAgTGTAAAGACAACCTGAA 1120

Rabbit GCTGCTCCAAGAGAAAGGAAATAATAAT---------------------------------------- 1025
Human  GCTGCTCCgAGAGAAAGGAAATAAT---ccttccatattacaacccgtcccagccgtattcatcggccta 1187
Mouse  GCTGCTgCgAGAGAAAGGAAATAAT---ccctccatattacaacctgtcccagccgttttcatcggccta 1187

Rabbit ----------------------------------------------AAACCCTGGCCCTGGATGCCCA 1047
Human  ttsctggctttcctgttttggtgtttcggtccattgtggtagagaaagAAACCCTGGCCCTGGATGCCCA 1257
Mouse  ttcctggctttcctgttttggtgtttcggtccattgtggtagagaaagAAACCCTGGCCCTGGATGCCCA 1257

Rabbit TGTTGGCTGCCCTGGTTGCGGTGACAGCCATCGTGCTGTATGTGCCAGGTCTGGCCAGAGCTTCTCCGTG 1117
Human  TGTTGGCTGCCCTGGTTGCaGTaACAGCCATCGTGCTGTATGTGCCAGGTCTGGCCAGAGCTTCTCCaTG 1327
Mouse  TGTTGGCgGCCCTGGTTGCGGTGACAGCtATgGTGCTGTATGTaCCAGGTCTGGCCAGAGCTTCTCCaTG 1327

Rabbit AGATGT                                                               1123
Human  AGAGcG                                                               1333
Mouse  ACAGTG                                                               1333
```

FIG. 3. **Cloning of SLAP orthologues reveals differential splicing.** Human heart and mouse spleen λZAP cDNA libraries were hybridized with SLAP probes to isolate positive clones. The DNA was isolated, restriction mapped, and subjected to automated sequencing. 55 positive clones from human heart and 43 from mouse spleen were analyzed; the nucleotide sequence alignment of SLAP1 sequences with the previously published rabbit SLAP1 cDNA sequence is presented. The mouse and human SLAP1 cDNAs contain sequence insertions of 142 and 90 nt that are highly

tion fragment of rabbit SLAP3 cDNA encompassing the entire coding region of SLAP3 (U21157, nt 1–3017). Among the various positive clones obtained, mouse spleen clone 15.1 and human cardiac clone 12.3 were *in vivo* excised, and the nucleotide sequences were determined using Ampli*Taq* sequencing methodology (ABI) and analyzed with SeqAidII (University of Kansas), PROSITE, PSORT, and BLAST.

Reverse Transcriptase-Polymerase Chain Reaction—Total RNA was prepared from dissected tissues using the TriPure methodology (Roche Molecular Biochemicals). For developmental expression, RNA was prepared from rat heart, brain, and muscle at fetal (day 18 of gestation), neonatal (day 4), and adult stages. First-strand cDNA synthesis reaction contained 1.0 μg of RNA, 200 units of SuperScript reverse transcriptase (Life Technologies Inc.), and random hexamers. 10 μl of the first-strand product was used as a template in PCR reactions (50 μl total) with a final concentration of 10 mM Tris-HCl, pH 8.3, 50 mM KCl, 0.01% gelatin, 3 mM $MgCl_2$, 400 μM dNTPs, and 0.3 μM primers P1 (5′-ATGGATGAGCAAGACCTG; U21157, nt 1709–1726); P2, (3′-GCTGCTTGATGAAGGAGC; U21157, nt 1942–1956); P3 (5′-TCAATCACAGATGAGC TC; U21157, nt 2516–2533); and P4 (3′-CCTCTTTACAGACAGATAC; U21157, nt 2834–2852). A single round of amplification was initiated by denaturation at 94 °C for 3 min, followed by 94 °C for 45 s, 52 °C for 45 s, and 72 °C for 45 s (30 cycles). The last extension was carried out for 5 min at 72 °C. The amplicons were resolved on a 1% agarose gel and gel-purified, and the DNA was recovered by gel extraction (Qiagen). Following restriction digestion of amplicons with *Eco*RI and *Xho*I restriction enzymes, PCR products were subcloned (pBlueScript KS) and sequenced.

Developmental amplification of the 3′ end of the SLAP was carried out with primers P5 (CAGTGCTCTCAGAACTGAAG; TOP_{AP} U17000, nt 923–942) and P6 (CTTCTAAAGGGAGGAC GGTG; TOP_{AP}, nt 1261–1242) based on the conserved sequences among chicken, rabbit, mouse and human forms. In a series of experiments, the DNA fragments separated on agarose gels were stained with VistraGreen (Molecular Dynamics) and digitalized with the STORM system (Molecular Dynamics) to determine the net intensities of the different size amplicons.

Generation of SLAP Expression Constructs—A Myc-tagged SLAP expression construct in pcDNA3 vectors (Invitrogen) was generated as described previously (12). SLAP lacking both of the putative TM domains (encoded by exons X and XI, respectively), was generated by PCR amplification of Myc-tagged SLAP with the following primers: Myc6 (5′-GAATTCAATGGATGAGCAAG ACCT G-3′) and TM (5′-CCGTCTAGATCATTGGAGCAGCTTCAGGTTGTC-3′). Subsequently, the PCR amplicon was restriction digested with *Eco*RI and *Xba*I and subcloned into the pBlueScript KS vector. The 6-Myc-tagged SLAP cDNA lacking both TM domains was then excised with *KpnI*/*Xba*I, ligated to the pcDNA3 expression vector, and specified as TM−. A SLAP construct containing an alternative TM domain encoded by exon X (TM1) was constructed by digestion of the exon X+ construct with the *Sst*I restriction enzyme and ligated into the *Sst*I predigested 6-Myc-tagged (TM−) pcDNA3 construct lacking both TM domains and specified as TM1. A construct containing a constitutively expressed putative TM domain encoded by exon XI was prepared by restriction digestion of SLAP with *Eco*RI and *Xba*I and ligated in frame to the 6-Myc-tagged pBlueScript KS vector. Following excision of the 6-Myc-SLAP with *Kpn*I and *Xba*I, the insert was ligated to pcDNA3 and specified as TM2.

Immunohistochemistry, Cell Fractionation, and Western Blot Analysis—C2C12 cells were transfected with SLAP plasmids (TM1, TM2, and TM−) using the calcium phosphate method to isolate stable transfectants in G418 antibiotic and processed for immunohistochemistry with anti-Myc antibodies as described previously (12). Subcellular fractionation of C2C12 cells was performed to isolate homogenate, membrane, and cytosoilc fractions (14), and the proteins were analyzed by SDS-polyacrylamide gel electrophoresis followed by Western blotting with anti-Myc as described previously (12).

RESULTS

Genomic Organization of the 3′ Region of the SLAP Gene—Previous studies have identified three SLAP isoforms, SLAP1, SLAP2, and SLAP3, encoded by a single gene mapped to human chromosome 3p14.3–21.2. SLAP isoforms contain common core C-terminal sequences that are highly conserved, with variable N-terminal sequences giving rise to different isoforms. Furthermore, human ESTs (gb N27488) exhibit 100% identity

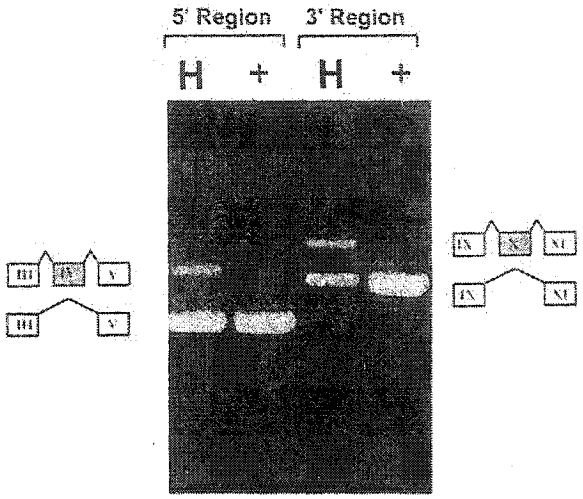

FIG. 4. **RT-PCR of cardiac RNA.** RNA from rabbit heart was reverse-transcribed and subjected to PCR amplification with primers spanning the 5′ and 3′ regions of divergence (primer P1, U21157, nt 1709–1726; primer P2, U21157, nt 1942–1956; primer P3, U21157, nt 2516–2533; primer P4, U21157, nt 2834–2852). The resulting products were resolved by 1% agarose gel-electrophoresis and visualized by ethidium bromide staining. Two distinct fragment are amplified by each set of primers based in the 5′ region (nt 389 and 247) and in the 3′ region (nt 426 and 336) from heart RNA (*lane H*) when compared with amplification from SLAP1 cDNA (*lane* +).

with the C-terminal sequence in rabbit SLAP, suggesting strong conservation and perhaps functional significance of this region of the molecule. To elucidate the genomic organization of the *SLAP* gene encompassing the common core region, rabbit and mouse genomic λ DashII DNA libraries were screened with SLAP cDNA restriction fragments used as hybridization probes (U21157, nt 1607–1931 and 1–3017) A total of five positive genomic clones from rabbit (R-2, R-13, R-14) and mouse (M-2 and M-3) were isolated, and the coding regions and intron-exon junctions of both the rabbit and mouse *SLAP* genes were mapped by restriction endonuclease, Southern blotting, and hybridization analysis. The various fragments were subcloned and partially sequenced to determine exon-exon boundaries. Characterization of genomic λ DASHII DNA clones revealed that they encompass the C-terminal common region of the SLAP isoforms (U21157, nt 1560–2675) and the entire encoding region of the SLAP1 transcript (Fig. 1). The results indicate that the SLAP1 isoform is composed of 11 exons spanning over 35 kilobase pairs of genomic DNA. The identified exons range in size from 60 to 321 bp, where exons I (60 nt) and II (81 nt) were untranslated in SLAP1, whereas they are coding exons in SLAP2 and SLAP3 isoforms. The initiating methionine of the SLAP1 isoform residing in exon III (60 nt) conforms to the Kozak consensus sequence. Utilization of this methionine predicts generation of a 322-amino acid polypeptide of 35.4 kDa as previously shown to be expressed in cardiac muscle. Exons VII (118 nt) and VIII (172 nt) both contain the predicted specialized coiled-coil leucine zippers, whereas exon VIII contains, in addition, a glutamate stretch composed of six glutamate heptad repeats. Exon XI encodes a stretch of hydrophobic residues that potentially represent a transmembrane anchor of SLAPs. Exons IV (142 nt) and X (90 nt) were found to be alternatively spliced (discussed below).

All of the exon-intron boundaries encompassing the common region of SLAP isoforms conform to the consensus splice donor and acceptor sites (Fig. 2*A*) (15). In addition, the exon-exon

conserved between the two species; the sites of the novel sequence inclusions are identical in both cDNAs, *i.e.* after nucleotides 1700 and 2582 of rabbit SLAP cDNA, respectively.

A

```
                                  Alternative Exon IV
SLAP1    VSLLK-------------------------------------------ALLEEERKA
Rabbit   VSLLKDDLQGAQSETEAKQEIQHLRKELIEAQELARASKQKCFELQALLEEERKA
Rat      VSLLKDDLQGTQAETEAKQDTQHLRKELVEAQELAGASKQKCFDLQALLEEERKA
Mouse    VSLLKDDLQGTQSETEAKQDIQHLRKELVEAQELARTSKQKCFELQALLEEERRA
Human    VSLLKDDLQGAQSETEAKQEIQHLRKELIEAQELARASKQKCFELQALLEEERRA
Chicken  VALLKDELQGAQSETEAKQEIQQLHKELIEAQELARTSKQKCFELQALLEEERRA
```

B

```
                    Alternative exon X              Constitutive exon XI
SLAP1    QEKGNNN-----------------------------KPWPWMPMLAALVAVTAIVLYVPGLARASP^ECF
Rabbit   QEKGNNNPSILQPVPAVFIGLFLAFLFWCFGPLW^RKKPWPWMPMLAALVAVTAIVLYVPGLARASP^ECF
Rat      REKGNN-PSILQPVPAVFIGLFLAFLFWCFGPLW^RKKPWPWMPMVAALVAVTAMVLYVPGLARASP^QCV
Mouse    REKGNN-PSILQPVPAVFIGLFLAFLFWCFGPLW^RKKPWPWMPMLAALVAVTAIVLYVPGLARASP^ERS
Human    REKGNN-PSILQPVPAVFIGLFLAFLFWCFGPLW^RKKPWPWMPMLAALVAVTAIVLYVPGLARASP^ERS
Chicken  QEKGNN-PSILQPVPAVFIGLILAFLYWCYGPLW^RKRQWPWMPVMAALVAVTAVVLY-PGLTRASP^ELI
```

FIG. 5. **Alternative splicing is conserved among mammalian and avian species.** RT-PCR of RNA from retina was performed as indicated in the legend to Fig. 4 to amplify the 5′ and 3′ regions of divergence in SLAP1; the PCR fragments were isolated and the DNA sequenced. The deduced amino acid sequence alignments of the 5′ and 3′ regions of SLAP from rabbit heart, rat retina, mouse spleen, human heart and chicken retina indicates that the alternative sequences are in frame with the SLAP1 sequence and highly conserved among species (*panels A* and *B*). Furthermore, the sites of insertion are also conserved among the various species. *Panel A* demonstrates a 43-amino acid sequence that is highly conserved among species. *Panel B* reveals a 30-amino acid peptide that includes a premature in-frame termination that also was conserved among all species analyzed to date. Moreover, sequence alignment reveals that the rabbit sequence contains an additional Asp (asparagine) residue that is absent in other species.

boundaries in mouse and rabbit were also determined to be conserved (Fig. 2*B*).

The size of the SLAP introns range from 0.2 to 5.5 kilobase pairs. All of the identified introns begin with a "gt" and end with an "ag." Introns 1, 2, 3, 4, 5, 6, and 7 represent class 1 introns, where each intron interrupts the coding sequence between the first and second bases of the codon. Intron 8 belongs to class 2 (it interrupts the second and the third bases of the codon), and introns 9, 10, and 11 are class 0 (the intron occurs between codons). As introns 1–7 and 9–11 represent introns of the same class, the open reading frames are good candidates for exon shuffling. Moreover, as the alternative exons IV and X are flanked on either side by class 1 or class 0 introns, respectively, the alternative splicing results in a conservation of the open reading frame of SLAP.

Alternative Splicing of SLAP—To further investigate the molecular nature of SLAP, human cardiac and mouse spleen λZAP cDNA libraries were screened using a rabbit SLAP *SalI-EcoRI* cDNA fragment (U21157, nt 1–3017) as a probe. A total of 55 and 43 positive clones were isolated from the human and mouse libraries, respectively. Following a detailed sequence analysis, the common SLAP regions were found to be highly conserved, although two areas of sequence divergence were identified when compared with the previously published rabbit SLAP1 sequence (Fig. 3). The nucleotide sequence alignment revealed that mouse and human SLAP1 cDNAs contain sequence insertions of 142 and 90 nt that are highly conserved between the two species. Moreover, the sites of the novel sequence inclusions are identical in both human and mouse cDNAs, *i.e.* after nucleotides 1700 and 2582 of rabbit SLAP cDNA, respectively. The open reading frame analysis revealed (see Fig. 5) that both of the novel inserts are in frame with the open reading frame of SLAP cDNA.

To determine whether the identified novel sequences are also present in rabbit SLAP, RT-PCR analysis of RNA from rabbit

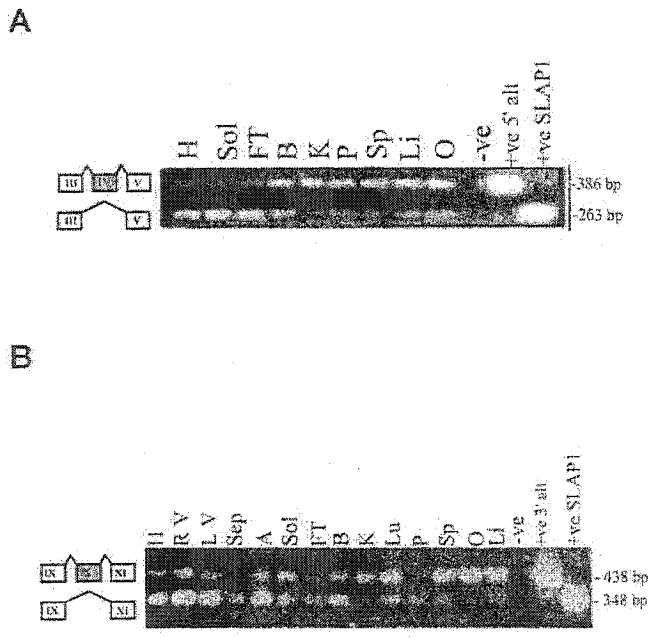

FIG. 6. **Tissue-specific expression of alternative exons IV and X.** RNA was isolated from brain (*B*), heart (*H*), soleus muscle (*S*), fast-twitch muscle (*FT*), lungs (*Lu*), kidneys (*K*), pancreas (*P*), spleen (*Sp*), liver (*Li*), and ovaries (*O*) and subjected to RT-PCR with primers as described in legend to Fig. 4 to amplify exon X (*panel A*) or IV (*panel B*). The PCR products were separated in 1% agarose gels and visualized by ethidium bromide staining. In *panel A*, the amplification of fragments of 389 and 247 nt present SLAP with and without exon IV, respectively. *Panel B* depicts the amplification of fragments of 426 and 336 nt, which represent SLAP products with and without exon X, respectively.

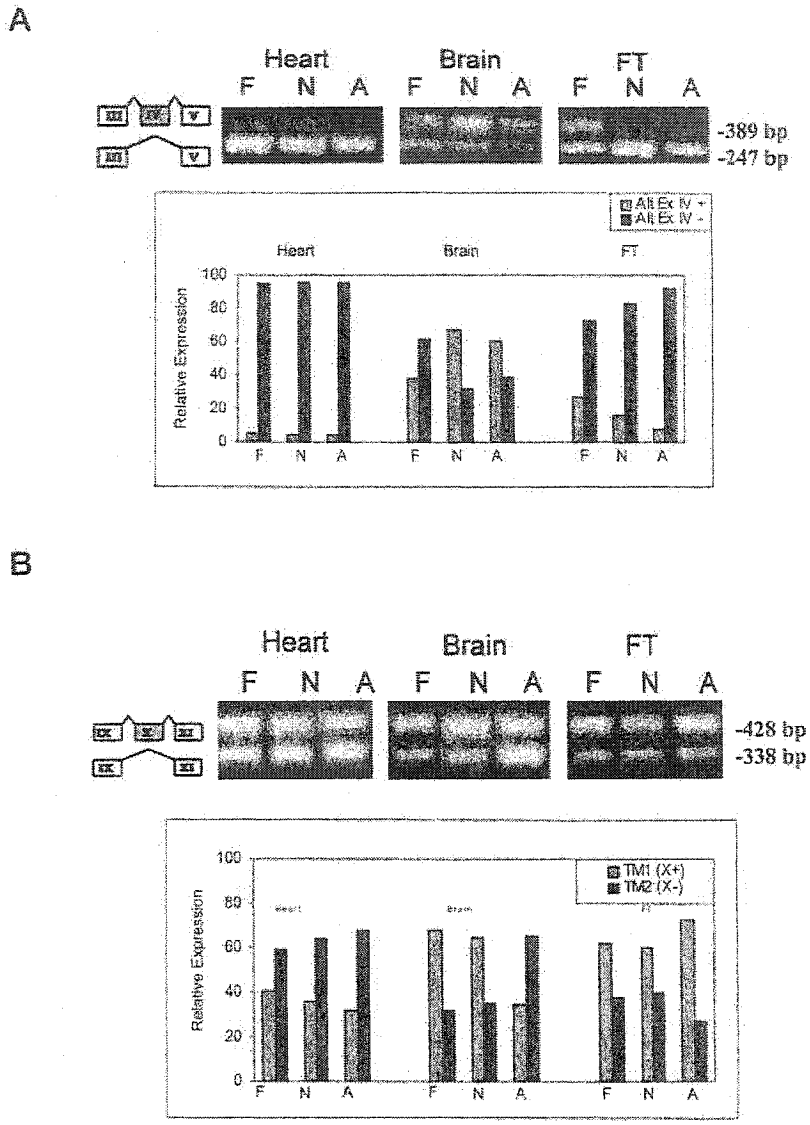

FIG. 7. **Developmental expression of alternative exons IV and X.** RNA from cardiac (*Heart*), brain, and fast-twitch muscle (*FT*) at three distinct stages of rat development, fetal (*F*), neonatal (*N*), and adult (*A*), was subjected to RT-PCR analysis with primers P1 and P2 for the 5′ region of SLAP and P5 and P6 (from avian TOP_{AP} U17000, nt 923–942 and 1261–1242). The amplified PCR products were separated in 1% agarose gels and visualized by ethidium bromide staining. *Panel A* depicts amplification of 389 and 247 nt products with and without exon IV, respectively. *Panel B* depicts amplification of 478 and 358 nt products with and without exon X, respectively. The gels were scanned to determine the relative levels of expression of each variant indicated as *bar graphs* in arbitrary units.

heart was performed with primers (P1 and P2 as well as P3 and P4) designed to amplify SLAP containing the regions of divergence. Rabbit cardiac tissue was selected, as previous studies have shown that the heart is a good expressor of the different SLAP isoforms (12). The results, shown in Fig. 4, indicate that two distinct fragments were amplified by each set of primers based in the 5′ region (P1 and P2) or the 3′ region (P3 and P4) of SLAP from heart RNA (*lane H*). An additional fragment of 389 bp was amplified from heart RNA compared with the 247-bp fragment expected from SLAP1 cDNA (*lane* +) in the 5′ region. A fragment of 426 bp was amplified from heart RNA in addition to the expected 336-bp fragment from SLAP1 cDNA (*lane* +) in the 3′ region. Following subcloning of these fragments, a detailed sequence analysis revealed that the 389-bp fragment contained the 142-nt sequence in the 5′ region of SLAP, and the 426-bp fragment contained the 90-nt sequence at the 3′ region of SLAP. The two rabbit cardiac variants were also generated by the inclusion of 142- and 900-nt sequences after nucleotides 1700 and 2522, respectively, as noted in the human and mouse SLAP variants. It, therefore, appears that inclusion of the 142- and 90-nt sequences could be generated by alternative splicing and are highly conserved regions among various species.

A BLAST search of the SLAP1 sequence indicated that it exhibits 76% identity with avian TOP_{AP} (GenBank™ accession number U17000), a protein expressed in a topographic gradient in the developing chicken retina (13). Further analysis indicated that avian TOP_{AP} also contains the 142- and 90-nt sequences identified in the new SLAP1 splice variants described above. To determine whether the mammalian retina also expresses these SLAP1 splice variants, an RT-PCR of RNA from rat retina was performed with the 5′ and 3′ primers described above, and two fragments were identified that contained the 142- and the 90-nt sequence inserts. The results of the deduced amino acid sequence alignment of rabbit, mouse, rat, and chick SLAP1 variants are summarized in Fig. 5. Fig. 5*A* demonstrates that the 142-nt novel sequence encodes a 43-amino acid peptide sequence that is highly conserved among species. Fig. 5*B* reveals that the 90-nt sequence encoding the C-terminal 30-amino acid peptide includes a premature in-frame termination codon (TGA) that is also conserved among all species analyzed The 3′ alternative sequence would therefore encode an alternative hydrophobic C terminus in SLAP polypeptides. Moreover, sequence alignment reveals that the rabbit sequence contains an additional Asp residue, which is absent in other species. The significance of the extra asparagine remains unclear at present time. Thus, it is clear that the 142- and 90-nt

novel sequences that were identified represent the alternatively spliced exons IV and X of the *SLAP* gene.

Tissue-specific Expression of Alternative Exons IV and X—In view of the strong conservation of sequence and alternative splicing of exons IV and X in mammalian and avian species, studies were carried out to determine the tissue-specific expression of these SLAP variants. RT-PCR analysis was employed to characterize SLAP expression in various rabbit tissues with primers P1 and P2 to amplify the 5′ alternative regions and P3 and P4 for the 3′ alternative variants of SLAP.

The results of RT-PCR analysis of tissue-specific expression of the 5′ region of SLAP reveal that all of the tissues examined express the two variants: a higher molecular size fragment of (389 nt), which encode a variant with the alternative exon IV, and a lower fragment of (247 bp) without the alternative exon (Fig. 6). In heart (*H*), soleus (*Sol*), fast-twitch muscle (*FT*), and lungs (*Lu*), the lower molecular size isoform (without the alternative exon IV) appears to be more predominant. On the other hand, the kidneys (*K*), pancreas (*P*), spleen (*Sp*), liver (*Li*), and ovaries (*O*) express preferentially the higher molecular size isoform encoding the alternative exon IV. In brain (*B*), the expression of both isoforms appear to be similar.

Analysis of the tissue-specific expression pattern of the 3′ alternative exon also utilized the RT-PCR approach using primers P3 and P4, which would amplify two products of 426 and 336 nt. The results of the analysis (Fig. 6*B*) indicate that all of the tissues examined express the two variants, with and without the alternative exon X. However, these variants are expressed at different levels. Heart (*H*), the left and right ventricles (*LV* and *RV*), septum (*Sep*), atria (*A*), and pancreas (*P*) demonstrate a higher expression of the lower molecular size isoform (without the alternative exon X), whereas kidney (*K*), lung (*Lu*), spleen (*Sp*), liver (*Li*), and ovaries (*O*) preferentially express the higher molecular size isoform (with the alternative exon X). None of the tissues examined appears to express exclusively any of the two alternatively spliced transcripts.

Developmental Expression of Alternative Exons IV and X—Alternative splicing represents a fundamental process that generates tissue-specific and developmentally regulated pattern of gene expression. To determine whether the alternatively spliced variants of SLAPs were expressed in a developmentally regulated manner, mRNA from three distinct stages of rat development (fetal (day 18 of gestation), neonatal, and adult tissue) was examined by RT-PCR analysis with primers that would amplify the appropriate regions in SLAP and its variants.

Fig. 7*A* depicts RT-PCR amplification of the 5′ alternative region of SLAP from various developmental stages with the primers P1 and P2, which resulted in amplification of two products of 389 and 247 nt, with and without exon IV, respectively. Quantification of the results by densitometry of the relative level of each variant at each stage of development is indicated (Fig. 7*A, bar graph*). In the heart, the expression of the variant lacking alternative exon IV (IV−) is about 20-fold higher at all stages of development relative to the variant with the alternative exon IV (IV+). In brain, on the other hand the expression of the IV− variant is about 1.5-fold higher at the fetal stage compared with the IV+; this pattern of expression is seen to reverse in the neonatal and adult brain. The level of expression of the IV− variant in fast twitch skeletal muscle was found to increase from 3-fold to about 9-fold during development relative to the IV+ variant.

RT-PCR of the 3′ alternative region of SLAP using primers P5 and P6 and RNA from various developmental stages resulted in amplification of 428- and 338-nt products, with and without exon X, respectively (Fig. 7*B*). In the heart, the expression of the X− variant increases from 1.5-fold at the neonatal stage to about 2.5-fold in the adult myocardium compared with the X+ variant. In brain, on the other hand, the expression of the X+ variant is about 1.5-fold higher at the fetal and neonatal stage compared with the X− variant. Interestingly, the expression of the X− variant in the adult brain was about 2-fold higher then the X+ variant. The relative expression of the X+ variant was about 1.5-fold higher in neonatal and fetal skeletal muscle and increased by twice in adult tissue.

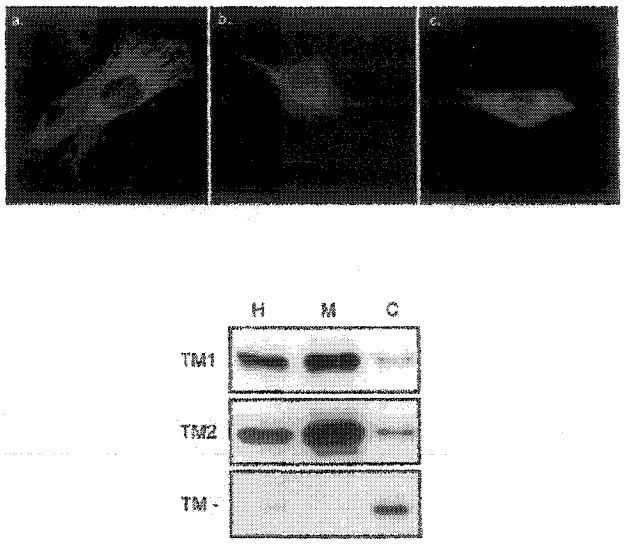

FIG. 8. **Mutually exclusive exons X and XI target SLAP to membranes.** Myc epitope-tagged SLAP expression constructs containing either exon X encoding the putative alternative transmembrane domain (*TM1*) or exon XI encoding the other putative transmembrane domain (*TM2*) or lacking both putative membrane anchors (*TM*−) were transfected in to C2C12 cells, and the localization of expressed SLAP was determined with anti-Myc by immunohistochemistry and Western blot analysis of the subcellular fractionations. *H*, homogenate; *M*, membranes; *C*, cytosol.

Exons X and XI Encode Mutually Exclusive Membrane Anchors—Although both SLAP and TOP_{AP} have been shown to be integral membrane proteins that lack a signal sequence, it remains to be defined whether the hydrophobic C termini direct their membrane integration. Expression constructs of SLAP either lacking the putative TM domains or containing TM1 or TM2 tagged with Myc were transfected into C2C12 myoblasts and the localization studied by immunohistochemistry and subcellular fractionation (Fig. 8). Staining of the C2C12 cells with anti-Myc shows a clear pattern of the perinuclear and reticular membrane networks in cells expressing SLAP constructs containing the putative TM1 or TM2 sequences. Cells expressing SLAP constructs lacking these sequences exhibited a diffuse pattern of staining throughout the cytosol. Subcellular fractionation of these C2C12 cells was performed, and the various fractions were separated by SDS-polyacrylamide gel electrophoresis and immunoblotted with anti-Myc. TM1- and TM2-containing SLAP was found to be enriched in the membrane fractions, whereas the TM− construct (SLAP lacking TM1 and TM2) was enriched in the cytosolic fraction. It therefore appears that hydrophobic sequences encoded in exons X and XI serve to direct the SLAP polypeptide into membrane systems.

DISCUSSION

We have elucidated the genomic organization of the 3′ region of the *SLAP* gene encoding the common C-terminal region of the various SLAP isoforms. The common region (nt 1560–2675 of SLAP3 cDNA U21157) spreads over more than 35 kilobase pairs of continuous DNA and consists of 11 exons. All of the

exon-intron junctions display the consensus splice donor and acceptor sequences. Moreover, rabbit and mouse *SLAP* gene exon-exon boundaries are identical in the common region, indicative of conservation of genomic structure and splicing mechanisms. In addition, the results demonstrates that SLAP isoform heterogeneity, arising because of alternative usage of the N terminus, is further diversified by alternative splicing of a primary transcript in two areas (exons IV and X) of the 3′ region of the *SLAP* gene. The sequence of the alternatively spliced SLAP variant was found to be similar (>90% identity) to TOP_{AP}, a coiled-coil membrane protein thought to be involved in the development of the avian retinotectal map. Thus, avian TOP_{AP} and mammalian SLAP1 are spliced variants, and the observed evolutionary conservation of the alternative splicing in human, rabbit, rat, mouse, and chicken strongly suggests that alternative exons may have functional roles that have been maintained by natural selection.

Alternative splicing of exon IV results in an in-frame inclusion of a 142-nt sequence encoding a 43 amino acid peptide that is predicted to adopt and extend by 11 turns the α-helical secondary structure of SLAP1 (12, 13). Alternative splicing of exon IV also results in the introduction of a putative casein kinase II phosphorylation site ([S/T]xx[D/E]). Casein kinase II represents a ubiquitous kinase found in the nucleus and cytoplasm, which phosphorylates multiple substrates involved in control of cell division and signal transduction (16). This putative phosphorylation site introduced by alternative splicing is not, however, unique, as the SLAP3 isoform polypeptide contains numerous putative phosphorylation sites for casein kinase II (more than 20 sites). Although *in vitro* and *in vivo* phosphorylation studies of this site remain to be performed, its conservation among species strongly suggests a functional role. The alternative exon X, on the other hand, introduces a highly hydrophobic segment containing a premature in-frame termination codon and represents the putative transmembrane domain found in TOP_{AP}. Alternative splicing of exon X, therefore, generates a polypeptide with a putative alternative membrane anchor. Immunocytochemical localization and subcellular fractionation studies of SLAP polypeptides containing either exon X or XI demonstrated that these sequences are necessary for SLAP integration into membranes, because the absence of these exons resulted in exclusion of SLAP from membrane structures. Therefore, mutually exclusive transmembrane domains encoded by exons X and XI, respectively, are responsible for targeting SLAP to membrane systems. Analysis of the alternatively spliced variants of SLAP revealed developmental changes in the expression of the alternative exons IV and X in tissues such as the brain. In addition, expression of the alternative variants was found to be regulated in a tissue-specific manner. The observed developmental and tissue-specific splicing of the alternative exons is indicative of a functional differentiation of the alternative variants. Interestingly, SLAP heterogeneity due to alternative N-terminal usage and diversity due to alternative splicing could together generate up to 12 distinct SLAP variants.

Although the exact functional role of the SLAP variants remains to be defined, it is apparent that several of the splice variants have been localized to the cell membrane as well as to intracellular membranes, suggesting a role in membrane function (12, 13). In this regard, avian TOP_{AP}, which our data reveals to be a SLAP variant, has been proposed to be localized at the cell surface to serve a role in neuronal guidance in the developing chick retina; it is conceivable that the mammalian orthologue would serve a similar function. In this regard, mRNA transcripts for both SLAP1 and the variant TOP_{AP} were found to be expressed in mammalian retina. It is apparent from the results presented that the SLAPs are targeted to the membrane by the alternatively spliced C-terminal hydrophobic domains. In this regard, the SLAPs belong to the emerging family of tail-anchored coiled-coil membrane proteins, which lack a signal sequence and contain a C-terminal transmembrane domain. Several members of the tail-anchored family are involved in diverse and important cellular processes including docking and fusion of synaptic vesicles with plasma membrane (syntaxin 1 and synaptobrevin) and intracellular vesicle trafficking (syntaxins). It has been postulated that the syntaxin family of proteins form intermolecular interactions via their coiled-coil structures with other protein components of the vesicular transport pathway machinery, thus mediating vesicle targeting, membrane fusion, and endocytotic membrane recycling. Syntaxin 1 is a neuronal cell membrane protein that interacts with SNAP-25 (9), synaptobrevin (10), and indirectly with synaptotagmin, a Ca^{2+} sensor of vesicle endocytosis. In addition, syntaxin also interacts with the N-type Ca^{2+} channel (11), thus localizing it to the site of vesicle release. The direct binding between components of exocytotic machinery is mediated by α-helical heptad domains that form intermolecular coiled-coil structures. It is notable that syntaxin 2 is a tail-anchored family member known to contain alternative transmembrane domains generated by splicing mechanisms similar to that described herein for the SLAP isoforms (3). In view of the fact that syntaxin contains different C termini generated by alternative splicing, a specific function for the variants beyond simply anchorage to the membrane is suggested. Thus, the SLAP variants, by virtue of their structural features and cellular locations, are likely to play significant roles in cell function.

REFERENCES

1. Jahn, R., and Sudhof, T. C. (1999) *Annu. Rev. Biochem.* **68,** 863–911
2. Rothman, J. E., and Scheller, R. H. (1994) *Curr. Biol.* **4,** 220–233
3. Bennett, M. K., and Scheller, R. H. (1993) *Proc. Natl. Acad. Sci. U. S. A.* **90,** 2559–2563
4. Sollner, T., Bennett, M. K., Whiteheart, S. W., Scheller, R. H., and Rothman, J. E. (1993) *Cell* **75,** 409–419
5. Kutay, U., Hartmann, E., and Rapoport, T. A. (1993) *Trends. Cell Biol.* **3,** 72–75
6. Bennett, M. K., Calakos, N., and Scheller, R. H. (1992) *Science* **257,** 255–259
7. Spring, J. M., Kato, M., and Bernfield, M. (1993) *Trends. Biochem. Sci.* **18,** 124–125
8. Kutay, U., Ahnert-Hilger, G., Hartmann, E., Wiedenmann, B., and Rapoport, T. A. (1995) *EMBO J.* **14,** 217–223
9. Zhang, P., Chen, Y. A., Tam, D., Chung, D., Scheller, R. H., and Miljanich, G. P. (1997) *Biochemistry* **36,** 4317–4326
10. Chapman, E. R., An, S., Barton, H., and Jahn, R. (1994) *J. Biol. Chem.* **269,** 27427–27432
11. Sheng, Z. H., Rettig, J., Cook, T., and Catterall, W. A. (1996) *Nature* **379,** 451–454
12. Wigle, J. T., Demchyshyn, L., Pratt, M. A. C., Staines, W. A., Salih M., and Tuana, B. S. (1997) *J. Biol. Chem.* **272,** 32384–32394
13. Savitt, J. M., Trisler, D., and Hilt, D. C. (1995) *Neuron* **14,** 253–261
14. Resh, M. D., and Erikson, R. L. (1985) *J. Cell Biol.* **100,** 409–415
15. Mount, S. M. (1982) *Nucleic Acids Res.* **10,** 459–472
16. Allende, J. E., and Allende, C. C.(1995) *FASEB J.* **9,** 313–323